



저작자표시-비영리-변경금지 2.0 대한민국

이용자는 아래의 조건을 따르는 경우에 한하여 자유롭게

- 이 저작물을 복제, 배포, 전송, 전시, 공연 및 방송할 수 있습니다.

다음과 같은 조건을 따라야 합니다:



저작자표시. 귀하는 원저작자를 표시하여야 합니다.



비영리. 귀하는 이 저작물을 영리 목적으로 이용할 수 없습니다.



변경금지. 귀하는 이 저작물을 개작, 변형 또는 가공할 수 없습니다.

- 귀하는, 이 저작물의 재이용이나 배포의 경우, 이 저작물에 적용된 이용허락조건을 명확하게 나타내어야 합니다.
- 저작권자로부터 별도의 허가를 받으면 이러한 조건들은 적용되지 않습니다.

저작권법에 따른 이용자의 권리는 위의 내용에 의하여 영향을 받지 않습니다.

이것은 [이용허락규약\(Legal Code\)](#)을 이해하기 쉽게 요약한 것입니다.

[Disclaimer](#)

**A THESIS FOR THE DEGREE OF DOCTOR OF
PHILOSOPHY**

**MOLECULAR INSIGHTS INTO SELECTIVE
INNATE ANTIVIRAL SIGNALING MECHANISM
IN ROCK BREAM, *Oplegnathus fasciatus***

Saranya Revathy. K

DEPARTMENT OF MARINE LIFE SCIENCES

GRADUATE SCHOOL

JEJU NATIONAL UNIVERSITY

REPUBLIC OF KOREA

2013-06

**MOLECULAR INSIGHTS INTO SELECTIVE INNATE
ANTIVIRAL SIGNALING MECHANISM IN ROCK BREAM,**

Oplegnathus fasciatus

Saranya Revathy. K

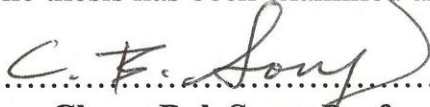
(Supervised by Professor Jehee Lee)

A thesis submitted in partial fulfillment of the requirement for the degree of

DOCTOR OF PHILOSOPHY

2013-06

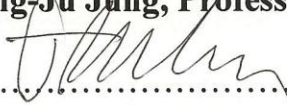
The thesis has been examined and approved by


.....
Thesis Director, Choon Bok Song, Professor of Marine Life Sciences


.....
Joon Bum Jeong, Professor of Marine Life Sciences


.....
Seunghoon Lee, Professor of Marine Life Sciences


.....
Sung-Ju Jung, Professor of Aqualife Medicine


.....
Jehee Lee, Professor of Marine Life Sciences

12.06.2013

Date

**Department of Marine Life Sciences
GRADUATE SCHOOL
JEJU NATIONAL UNIVERSITY
REPUBLIC OF KOREA**

*Dedicated to the almighty, my
beloved parents and my husband*

Acknowledgments

Every PhD thesis could only be perfected with the contribution of other people. I would like to thank everyone who made a contribution to this work. First and foremost, I would like to thank my family for all their love and encouragement. I would not have made it this far without my parents who raised me with unconditional love and care and supported me in all my pursuits. I thank my husband, Dr. S. Purushothaman, for his constant support and encouragement to discover my inner self and capabilities, without whom I would not have crossed my tough times and barriers, with ease. I thank my parents-in-law, brothers, sisters-in-law, brother-in-law for their support and love.

I especially would like to express my heartfelt gratitude to my advisor Prof. Jehee Lee, for providing me the opportunity and the support to pursue my PhD research. I am grateful for his contributions of time, insightful discussions, and funding to make my PhD experience a constructive one. In the past three years, I have adored him as a philosopher, guide and principle centered person who has always brought out the best in me and not less. When I am lost in the fog of my research, his guidance at the prompt time, had built a challenging competency in me. Sans of his guidance and supervision, my enthusiasm and productivity in research would have reduced to a great extent. Last by no means the least, I am really grateful to have Prof. Jehee Lee in my life.

I would also thank the members of my Ph.D. committee, Prof. Choon Bok Song, Prof. Joon Bum Jeong, Prof. Seungheon Lee, Prof. Sung-Ju Jung, who monitored my work and kindly spared their time in reading and providing me with valuable suggestions for making this study an appreciable one. I owe many thanks to Prof. Sung-Ju Jung for kindly providing us with viruses needed for our study. Also, I acknowledge with great thanks to the professors of my department, Gi-Young Kim, and Kwang-Sik Choi for their inspiring and encouraging

guidance for a deeper understanding of knowledge and constructive comments during my course work.

As a vital cog in my research team, Dr. Qiang Wan deserves special thanks for his guidance and inspiring suggestions during my research period.

I thank my lab mates who have constituted the challenging and inspiring research atmosphere that motivated me to strive hard and discover my inner capabilities. I thank my lab mates, Umasuthan, Ajith, Anushka, Gelshan, Thiunuwan, Seung do Lee, and Taesoo Kim. I appreciate the comradeship of Dr. Youngdeuk Lee, MinYoung Oh, Hyowon Kim, and Sukkyoung Lee.

Staying away from home is always challenging and tough and it is true that “A friend in need is a friend in deed”. I have always felt grateful for meeting good people like Niroshana, Bathige Sanjaya, Dr. Anji Reddy, Rajani Reddy and Hamsanandini. I also thank my friends for providing support and friendship that I needed. My heartfelt special thanks to Dr. Gunasekaran, for his immense support. My life in Jeju was blessed with other seniors and friends, Dr. Ganesh Thangaraj, Dr. Sridharan, Dr. Ganesh, Dr. Shrikant, Dr. Gandhi, Dr. Dharaneedharan, Chandran, Navaneethan, Saravanan, Thiyagarajan, Anantha kumar, Sebastian. I thank them all with immense pleasure for making my life in Jeju a beautiful one with cherishable memories. I am indebted to all the members of JISO, for their strength and encouragement.

I am also grateful for the Department of Marine Life Sciences at Jeju National University for providing me an excellent work environment during my study and I appreciate our group's administrative people, Sang Hyuk, and Hee Jung who were always willing to help. I thank Brain Korea 21 which provided the funds for presenting the research work held in

Korea and abroad. I would like to thank all those whom I have not mentioned above but helped me in numerous ways to my success.

Table of Contents

요약	VIII
Summary	XVI
List of Tables	XXI
List of Figures	XXII
1.0 An introduction to innate antiviral signaling mechanisms in fish	2
General introduction	2
1.1 Aquaculture and viruses infecting fish aquaculture	2
1.1.1 Aquaculture	2
1.1.2 Fish viruses	4
1.2 Antiviral immunity in fish	9
1.2.1 Antiviral signaling in mammals	9
1.2.2 Cytosolic sensors and interferon production in mammals	11
1.2.3 Interferon system in mammals	13
1.2.4 Recognition of double stranded (ds) RNA in mammals and IFN induction	14
1.2.5 Antiviral signaling in teleosts	15
1.2.6 Interferon system in teleosts	16
1.2.7 IFN signaling pathways in fish	17
1.3 Aims of this work	19
2.0 Characterization of cytosolic sensor Melanoma Differentiation Associated gene 5 (MDA5)	21
Abstract	21
2.1 Introduction	22
2.2 Materials and methods	24
2.2.1 Animal rearing, cDNA library construction and <i>RbMDA5</i> gene identification	24
2.2.2 BAC library creation and identification of <i>RbMDA5</i> BAC clone	25
2.2.3 Sequence characterization, genome structure and phylogenetic analysis of <i>RbMDA5</i>	26
2.2.4 Transcriptional profile of <i>RbMDA5</i> gene in challenged and normal tissues	27
2.2.4.1 Poly I:C challenge	27
2.2.4.2 RNA isolation and cDNA synthesis	27
2.2.4.3 Tissue distribution	28
2.2.4.4 Temporal <i>RbMDA5</i> mRNA expression analysis post poly I:C challenge	29

2.2.5 Construction of expression vector and antiviral assay.....	29
2.2.5.1 Cell lines and viruses	29
2.2.5.2 Construction of expression vector	30
2.2.5.3 Antiviral assays.....	30
2.3 Results.....	31
2.3.1 RbMDA5 identification, sequence characterization, phylogenetic analysis	31
2.3.2 Genomic characterization of <i>RbMDA5</i>	37
2.3.3 Promoter analysis of <i>RbMDA5</i>	40
2.3.4 Spatial expression analysis of <i>RbMDA5</i>	41
2.3.5 Temporal expression analysis of <i>RbMDA5</i> after poly I:C challenge.....	42
2.3.6 Antiviral activity of RbMDA5.....	44
2.4 Discussion.....	44
3.0 Characterization of the cytosolic sensor Laboratory of Genetics and Physiology 2 (LGP2)	50
.....	50
Abstract.....	50
3.1 Introduction.....	51
3.2 Materials and methods	53
3.2.1 Animal rearing, cDNA library construction and <i>RbLGP2</i> gene identification.....	53
3.2.2 BAC library creation and identification of <i>RbLGP2</i> BAC clone	54
3.2.3 Sequence characterization, genome structure and phylogenetic analysis of RbLGP2	55
.....	55
3.2.4 Transcriptional profile of <i>RbLGP2</i> gene in challenged and normal tissues	56
3.2.4.1 Poly I:C challenge.....	56
3.2.4.2 RNA isolation and cDNA synthesis	56
3.2.4.3 Tissue distribution.....	57
3.2.4.4 Temporal RbLGP2 mRNA expression analysis post poly I:C challenge	58
3.2.5 Construction of expression vector and antiviral assay.....	58
3.2.5.1 Cell lines and viruses	58
3.2.5.2 Construction of expression vector	59
3.2.5.3 Antiviral assays.....	60
3.3 Results.....	60
3.3.1 RbLGP2 identification, sequence characterization and phylogenetic analysis	60
3.3.2 Genomic characterization of <i>RbLGP2</i>	66
3.3.3 Promoter analysis of <i>RbLGP2</i>	68

3.3.4 Spatial expression analysis of <i>RbLGP2</i>	70
3.3.5 <i>RbLGP2</i> temporal expression analysis post poly I:C challenge	70
3.3.6 Antiviral assays	71
3.4 Discussion	72
4.0 Characterization of the signaling adaptor Mitochondrial AntiViral Signaling protein (MAVS)	80
Abstract	80
4.1 Introduction	81
4.2 Materials and methods	83
4.2.1 Animal rearing, cDNA library construction and <i>RbMAVS</i> gene identification	83
4.2.2 Sequence characterization, genome structure and phylogenetic analysis of <i>RbMAVS</i>	84
4.2.3 Transcriptional profile of <i>RbMAVS</i> gene in challenged and normal tissues	84
4.2.3.1 Poly I:C challenge	84
4.2.3.2 RNA isolation and cDNA synthesis	85
4.2.3.3 Tissue distribution	85
4.2.3.4 Temporal <i>RbMAVS</i> mRNA expression analysis post poly I:C challenge	86
4.3 Construction of expression vector and antiviral assay	87
4.3.1 Cell lines and viruses	87
4.3.2 Construction of expression vector	88
4.3.3 Antiviral assays	88
4.4 Results	89
4.4.1 <i>RbMAVS</i> identification, sequence characterization and phylogenetic analysis	89
4.4.2 Spatial expression of <i>RbMAVS</i> in normal tissues	92
4.4.3 Temporal expression of <i>RbMAVS</i> after poly I:C challenge	93
4.4.4 Antiviral activity of <i>RbMAVS</i>	94
4.5 Discussion	94
5.0 Characterization of the non-canonical kinases <i>TBK1</i> and <i>IKKε</i>	100
Abstract	100
5.1 Introduction	101
5.2 Materials and methods	102
5.2.1 Animal rearing, cDNA library construction and <i>RbTBK1</i> and <i>RbIKKε</i> gene identification	102
5.2.2 BAC library creation and identification of <i>RbTBK1</i> BAC clone	103

5.2.3	Sequence characterization and phylogenetic analysis of RbTBK1 and RbIKK ϵ .	104
5.2.4	Transcriptional profile of <i>RbTBK1</i> and <i>RbIKKϵ</i> gene in challenged and normal tissues.....	104
5.2.4.1	Poly I:C challenge.....	104
5.2.4.2	RNA isolation and cDNA synthesis	105
5.2.4.3	Tissue distribution.....	105
5.2.4.4	Temporal RbTBK1 mRNA expression analysis post poly I:C challenge.....	106
5.3	Results.....	107
5.3.1	Sequence characterization of RbTBK1 and RbIKK ϵ	107
5.3.2	Genome characterization of <i>RbTBK1</i>	115
5.3.4	Temporal expression analysis post poly I:C challenge.....	118
5.4	Discussion	119
6.0	Characterization of Interferon Regulatory Factor 3 (IRF3).....	124
	Abstract.....	124
6.1	Introduction.....	125
6.2	Materials and methods	127
6.2.1	Animal rearing, cDNA library construction and RbIRF3 gene identification.....	127
6.2.2	BAC library creation and identification of BAC clone	128
6.2.3	Sequence characterization and phylogenetic analysis of RbIRF3	129
6.2.4	Expression profile of <i>RbIRF3</i> gene in normal and challenged tissues	130
6.2.4.1	Poly I:C challenge.....	130
6.2.4.2	RNA isolation and cDNA synthesis	130
6.2.4.3	Tissue distribution.....	131
6.2.4.4	Temporal RbIRF3 mRNA expression analysis post immune challenges.....	131
6.3	Results.....	132
6.3.1	Sequence characterization and phylogenetic analysis of RbIRF3	132
6.3.2	Genomic characterization of <i>RbIRF3</i>	139
6.3.3	Promoter analysis of <i>RbIRF3</i>	140
6.3.5	Tissue distribution of <i>RbIRF3</i>	142
6.3.6	Temporal expression post immune challenges	143
6.4	Discussion.....	144
7.0	References.....	148

요약

돌돔(영명: Rockbream, 학명: *Oplegnathus fasciatus*)은 한국과 일본에서 중요한 수산 자원 중 하나이다. 그러나 현재 돌돔양식업에서 질병으로 인한 높은 폐사율과 경제적 손실이 일어나고 있기 때문에 이에 대한 대책을 위해서는 어류숙주와 병원균간의 상호작용 및 그에 따른 숙주의 반응에 대한 이해가 절실한 실정이다. 이러한 질병이 없는 상태를 유지하기 위해서는 질병과 스트레스를 관리할 수 있는 기술이 필요하다. 따라서 돌돔의 면역체계를 이해하는 것은 어류질병에 대응하기 위한 새로운 전략의 발전에 도움이 될 것이다.

1 장에서는 dsRNA 바이러스를 인식 할 수 있는 분자인식수용체(pattern recognition protein, PRR) 중 하나인 melanoma differentiation associated 5 (MDA5) 에 대하여 동정 연구에 대해서 논하고자 한다. 유전체 구성과 단백질 구조 분석, 어류의 조직특이적 및 감염과 시간에 따른 유전자 발현양상 및 재조합단백질의 항바이러스 활성에 대해 연구하였다. MDA5 는 세포질에 존재하는 단백질로 retinoic acid inducible gene I (RIG-I)과 같은 다른 PRR 과 유사한 구조를 지녔다. 돌돔의 MDA5 유전자(RbMDA5)의 cDNA 를 분석한 결과, 992 개의 아미노산을 지정하는 2976 bp 의 open reading frame(ORF)을 지닌 분자량 112 kDa 의 단백질로 나타났다. RbMDA5 의

유전체는 16 개의 exon 과 15 의 intron 을 지녔으며 AP-1, AP-4, IRF-1, IRF-2, c-Rel, Lyf-1, Sp1, Oct-1, ISRE 및 AML-1a 과 같은 전사인자결합 부위를 찾아내었다. RbMDA5 단백질은 2 개의 N-말단 CARD domain 과 ResIII site, central DExD/H box RNA helicase domain, MDA5 insert domain, HELIc domain 이 있었고, C-말단 서열에서는 RIG-I_C-RD [(C-terminal repressor domain(RD))]가 조사되었다. 6 개의 helicase motif 와 RNA 결합 loop 또한 존재하는 것으로 나타났다. RbMDA5 는 orange spotted grouper 의 MDA5 와 가장 높은 identity 를 보였다. 다양한 조직에서와 면역원자극실험을 한 후의 정량 RT-PCR 를 수행하여 유전자 발현을 분석한 결과, 조직분석에서는 다양한 조직에서 발현이 됨을 확인하였고 특히 혈구에서 가장 높은 발현을 보였으며 간에서는 그 다음의 높은 발현이 나타나는 것을 확인하였다. Poly I:C 를 주입하여 면역자극을 유도하여 아가미(gill)와 비장(spleen), 두신장(head kidney) 및 혈구(blood)에서 발현량은 상향 발현조절이 이루어짐을 확인하였다. 돌돔의 심장 세포를 이용하여 RbMDA5 유전자의 발현을 유도한 결과 marine birnavirus 의 감염을 억제하는 것으로 나타나 돌돔의 MDA5 는 바이러스 감염에 대한 면역반응에 관여하는 것으로 여겨졌다.

2 장에서는 또 다른 분자인식수용체인 Laboratory of Genetics and Physiology2 (LGP2)에 대해 동정한 연구에 대해 논하고자 한다. LGP2 역시 1 장에서 논한 MDA5 와

마찬가지로 바이러스의 dsRNA 를 인식하는 세포질 내에 존재하는 분자인식수용체로 바이러스의 특이적인 분자를 인식하여 바이러스 감염에 관련된 신호전달에 역할을 수행한다. 돌돔 LGP2(RbLGP2)의 cDNA 를 분석한 결과, 681 개의 아미노산을 지정하는 2043 bp 의 open reading frame(ORF)을 지닌 분자량 77 kDa 의 단백질로 나타났다. RbMDA5 의 유전체는 12 개의 exon 과 11 의 intron 을 지녔으며 AP-1, AP-4, IRF-1, IRF-2, CRE-BP, Oct-1, HSF 및 AML-1a 과 같은 RbLGP2 유전자의 발현에 관여하는 전사인자결합 부위를 찾아내었다. RbLGP2 는 하나의 DExDc(DEAD/DEAH box helicase domain)을 N-말단 서열에서 확인되었으며, RIG-I_C-RD (C-terminal domain of RIG-I/ regulatory domain/ repressor domain) alc ResIII region, MDA4_ID (insert domain of MDA5 helicase and similar proteins) 및 RNA 결합 loop 가 존재함을 확인하였다. 또한 두 개의 zinc binding motif 를 지닌 것으로 나타났다. 또한 단백질 구조 분석 결과 RNA helicase 활성화에 관여하는 DEDxD/H box 와 같은 특징적인 6 개의 motif 가 존재함을 확인하였다. Pairwise alignment 결과 넙치(olive flounder)의 LGP2 와 가장 높은 identity 와 similarity(각각 79 %, 90%)로 나타났다. 정량 RT-PCR 를 이용한 조직별 유전자 발현 분석 결과, RbMDA5 와 유사한 패턴으로 혈구와 간에서 높은 발현을 하는 것으로 나타났다. Poly I:C 를 주입하여 면역자극을 유도하여 아가미(gill)와 비장(spleen), 두신장(head kidney) 및 혈구(blood)에서 발현량은 상향 발현조절이

이루어짐이 나타남에 따라 바이러스감염에 RbLGP2는 바이러스 감염에 따른 활성이 있는 것으로 여겨진다. 재조합단백질을 이용하여 항바이러스 활성을 조사한 실험에서는 marine birnavirus 감염을 억제하는 것으로 나타나 RbLGP2는 돌돔의 선천면역계에 있어 바이러스 감염에 따른 면역활성이 있는 것으로 여겨진다.

3 장에서는 IFN- β promoter stimulator-1(IPS-1) 혹은 VISA, Cardif 라 알려진 Mitochondrial antiviral signaling protein(MAVS)에 대한 동정연구에 대해 논하고자 한다. MAVS 는 RIG-I/MDA5 경로에서 핵심적인 역할을 수행하는 단백질로 interferons(IFNs)와 다른 cytokine 들을 유도한다. 돌돔 MAVS(RbMAVS) cDNA 를 분석한 결과, 586 개의 아미노산을 지정하는 1758 bp 의 open reading frame(ORF)을 지닌 분자량 62 kDa 의 단백질로 나타났다. RbMAVS 의 단백질은 CARD domain 을 지닌 것으로 나타났고, proline rich domain 및 transmembrane domain 을 지닌 것으로 조사되었다. RbMAVS 단백질은 또한 TRAF2 결합 motif 인 PVQDT 가 319-323 사이의 아미노산 잔기서열에 존재함을 확인하였다. RbMAVS 단백질 서열은 전체 단백질 서열과 CARD domain 의 서열을 다른 종의 MAVS 단백질 서열과 비교한 결과 넙치에서 가장 높은 identity 와 similarity 를 공유하는 것으로 조사되었다. 정량 RT-PCR 를 이용한 조직별 유전자 발현 분석 결과, 다양한 조직에서 발현이 되지만 특히

혈구에서 가장 높은 발현이 나타남을 확인하였고 그 다음 간에서 높은 발현을 하는 것으로 나타났다. Poly I:C 를 주입하여 면역자극을 유도하여 아가미(gill)와 비장(spleen), 두신장(head kidney) 및 혈구(blood)에서 발현량은 상항 발현조절이 이루어짐이 나타남에 따라 바이러스감염에 RbMAVS 역시 바이러스 감염에 따른 활성이 있는 것으로 여겨진다. 또한 In vitro 상에서 overexpression 한 결과, 바이러스의 복제를 억제하는 것으로 나타나 돌돔의 항바이러스면역계에 관여하는 단백질임을 추정하였다.

TBK1 과 IKK ϵ 은 비-양이온성 kinase 가계에 속하는 유전자로 특이적인 면역효과 분자들의 전사를 유도하는 인자들의 phosphorylation 에 역할을 함으로써 면역방어기전에 관여하는 것으로 알려져 있다. 돌돔 TBK1(RbTBK1)의 cDNA 를 분석한 결과, 723 개의 아미노산을 지정하는 2169 bp 의 open reading frame(ORF)을 지닌 분자량 83 kDa 의 단백질로 나타났다. RbIKK ϵ 의 cDNA 는 721 개의 아미노산을 지정하는 2169 bp 의 서열을 지닌 것으로 나타났으며 단백질의 분자량은 82 kDa 을 지닌 것으로 조사되었다. RbTBK1 과 RbIKK ϵ 의 단백질은 N-말단 서열에서 보존된 protein kinase(PK), catalytic (c) domain (PKc domain)을 지닌 것으로 나타났다 (RbTBK1: 15-293 아미노산잔기서열, RbIKK ϵ : 19-327 아미노산잔기서열). 두 단백질은 ubiquitin-

like domain (RbTBK1: 297-385 아미노산잔기서열, RbIKK ϵ : 300-388

아미노산잔기서열)이 존재함으로써 kinase 가계에 속하는 단백질임을 확인하였다.

RbTBK1 은 Nile tilapia 와 가장 높은 identity 와 similarity (각각 96% 및 98%)를 지님이

나타났고 또한 인간과 쥐의 TBK1 과 70%의 identity 를 보였다. RbIKK ϵ 은 Nile

tilapia 에서 가장 높은 상동성을 지님이 나타났고(86%) similarity 의 경우 Nile tilapia

뿐만 아니라 Zebra Mbuna 와 함께 높은 값을 나타내었다 (94%). RbTBK1 의 유전체

구조는 21 개의 exon 과 20 개의 intron 이 존재하는 것으로 나타났다. RbTBK1 와

RbIKK ϵ 유전자의 조직별 발현 분석결과 RbTBK1 의 경우 혈구에서 가장 높고 그 다음

간인 반면, RbIKK ϵ 은 간에서 가장 높은 발현이 있었고 그 다음 혈구로 나타났다. Poly

I:C 감염시간에 따른 유전자발현 조사결과 간과 두신장이 현저하게 발현이 되는

것으로 나타나 바이러스 감염에 RbTBK1 와 RbIKK ϵ 는 면역체계에 관여하는 것으로

여겨진다.

전사인자는 IFN 과 IFN-자극유전자의 발현을 조절하는 중심적인 역할을 하는

단백질이다. IRF3 와 IRF7 은 이러한 제 1 형 IFN 과 ISG 유전자의 전사활성에 있어

중요한 역할을 수행한다. IRF3 는 본질적으로 세포질 내에서 비활성화 상태로

존재한다. 그러다 바이러스 감염시에는 조절 부위가 인산화되면서 이형체를

형성한다(dimerization). 돌돔 IRF3(RbIRF3)의 cDNA 를 분석한 결과, 462 개의 아미노산을 지정하는 1368 bp 의 open reading frame(ORF)을 지닌 분자량 51 kDa 의 단백질로 나타났다. *In silico* 를 통한 동정분석에서는 RbIRF3 는 보존된 IRF tryptophan pentad repeat DNA-binding domain(DBD)를 N-말단 서열에 지니고 있음이 조사되었다. 한편 C-말단 서열에서는 다른 종에서 유래한 IRF3 단백질에 존재하는 IRF-associated domain(IAD) 와 serine-rich domain 이 존재함을 확인하였다. Pairwise alignment 결과 *Dicentrarchus labrax* 와 가장 높은 identity 와 similarity 를 가짐을 확인하였다 (각각 87%, 92%). 유전체 구조 분석 결과 11 개의 exon 과 10 개의 intron 의 구조로 이루어진 유전체임을 확인하였고 넙치와 가장 가까운 homology 를 지녔음이 조사되었다. 프로모터 예측 조사 결과 AP-1, AP-4, C/EBP- α , β , Lyf-1, HSF, Sp1, Oct-1, Sox-5, E2F, ROR α , AML-1a, GATA-1 등 다양한 자극에 관여하는 전사인자결합 site 가 발견되었다. 조직에 따른 유전자의 발현양상을 qRT-PCR 을 이용해 조사한 결과 간에서 가장 높은 발현이 나타났고 그 다음은 피부(skin)에서 발현함을 확인하였다. Poly I:C 주입을 통한 감염실험 결과 혈구 및 간, 두신부에서 상향조절이 됨이 나타나, 위의 결과들을 종합하여 RbIRF3 는 숙주의 항바이러스 면역체계에 관여하는 것으로 여겨진다.

이 논문에서는 돌돔의 항바이러스 면역신호체계에 관련하는 몇 가지 유전자와 단백질들에 대해 동정하였다. 유전자 발현양상 조사와 각 분자간의 상호작용에 관한 조사는 바이러스 병원체에 대항하여 어류가 생존할 수 있는 전략을 세우는데 도움이 될 것이다.

Summary

Rock bream (*Oplegnathus fasciatus*), is an important delicacy in Korea and Japan. High mortality rates and economic losses in aquaculture urge the need for understanding fish-pathogen interactions and fish responses against microbes to fight back the diseases. In order to develop a sustained disease free-state of art rock bream aquaculture, techniques are needed to combat disease and stress related mortalities. Immune defense mechanism of rock bream is to be well understood in order to develop novel strategies to prevent diseases and improve the sustainability of rock bream.

In the first part of this study, a pattern recognition receptor, melanoma differentiation associated 5, involved in the recognition of dsRNA viruses, is characterized. The genome organization, protein structure analysis, spatial and temporal expression analysis, and antiviral activity of the recombinant protein have been demonstrated. MDA5 is a cytosol residing protein which is structurally similar to another PRR namely, retinoic acid inducible gene I (RIG-I). Rock bream MDA5 (RbMDA5) cDNA possessed an open reading frame (ORF) of 2976 bp, coding for 992 amino acids with molecular mass of 112 kDa. *RbMDA5* genome possessed 16 exons split by 15 introns and putative promoter analysis revealed significant transcription factor binding sites like AP-1, AP-4, IRF-1 and 2, c-Rel, Lyf-1, Sp1, Oct-1, ISRE and AML-1a. RbMDA5 protein possessed two N-terminal CARD regions, a ResIII site, a central DExD/H box RNA helicase domain, an MDA5 insert domain, a HELIc domain, a RIG-I_C-RD (C-terminal repressor domain (RD) embedded within the C-terminal domain (CTD). There were six helicase motifs and an RNA binding loop present in RbMDA5. RbMDA5 shared highest identity with orange spotted grouper MDA5. Quantitative RT-PCR was employed to analyze the mRNA expression in the normal and challenged tissues. *RbMDA5* mRNA was ubiquitously expressed in all the analyzed tissues obtained from healthy rock bream with the highest expression in blood, followed by liver.

RbMDA5 mRNA expression *in vivo* was elevated upon poly I:C challenge in gill, liver, spleen, head kidney and blood. Overexpression of *RbMDA5* in rock bream heart cells prevented marine birnavirus infection, thus confirming the innate immune antiviral defense role of *MDA5*.

In the second part of the study, a second PRR, Laboratory of Genetics and Physiology 2 (*LGP2*), was characterized. *LGP2* is also a cytosol residing protein involved in both the recognition of viral dsRNA and regulation of the viral PAMP recognition and downstream signaling pathway. Rock bream *LGP2* (*RbLGP2*) cDNA possessed an ORF of 2043 bp coding for 681 amino acids with molecular mass of 77 kDa. *RbLGP2* genome derived from the BAC clone revealed a 12 exon-11 intron structure. Putative promoter analysis revealed various significant transcription factor binding sites like AP-1, AP-4, IRF-1 and 2, CRE-BP, Oct-1, HSF and AML-1a which may play a vital role in the regulation of *RbLGP2* expression. *RbLGP2* possessed one DExDc (DEAD/DEAH box helicase domain) in the N-terminal region, one ResIII region, one HELICc (helicase superfamily c-terminal domain), RIG-I_C-RD (C-terminal domain of RIG-I/ regulatory domain/ repressor domain), one *MDA5_ID* (insert domain of *MDA5* helicase and similar proteins), RNA binding loop. There were two predicted zinc binding motifs. *RbLGP2* protein portrayed the presence of six significant motifs including DEDxD/H box for RNA helicase activity. Pairwise alignment of *RbLGP2* shared highest identity and similarity of 79 and 90%, respectively with the olive flounder *LGP2*. Quantitative RT-PCR analysis of tissues isolated from normal healthy rock bream fish revealed ubiquitous expression of *RbLGP2* with highest expression in blood followed by liver, similar to the rock bream *MDA5* expression. *RbLGP2* expression analysis after poly I:C challenge *in vivo*, revealed significant elevation in tissues including gill, liver, head kidney, spleen and blood, suggesting their activation upon viral encounter. Overexpression of the

recombinant RbLGP2 protein *in vitro* prevented marine birnavirus infection, further affirming the antiviral role of RbLGP2 in rock bream innate immune system.

In the third part of this thesis, Mitochondrial antiviral signaling protein (MAVS), also known as IFN- β promoter stimulator-1 (IPS-1), VISA and Cardif, is a mitochondrial adaptor protein which plays a key role in the signal transduction of the RIG-I/MDA5 pathway to induce the production of interferons (IFNs) and other cytokines was characterized. Rock bream MAVS (RbMAVS) cDNA possessed an ORF of 1758 bp coding for a protein of 586 amino acids with molecular mass of 62 kDa. RbMAVS protein analysis revealed a CARD domain, a proline rich domain and a transmembrane domain. RbMAVS protein also possessed a putative TRAF2 binding motif, ³¹⁹PVQDT³²³. RbMAVS shared the highest identity and similarity with the flounder MAVS homologue when the full protein and CARD region were compared. Spatial expression analysis performed with multiple tissues isolated from healthy rock bream using quantitative RT-PCR revealed ubiquitous expression of *RbMAVS* with maximum level of expression observed in blood, followed by liver. After poly I:C challenge *in vivo*, *RbMAVS* mRNA were elevated in various tissues like blood, liver, spleen and head kidney suggesting their upregulation during a viral attack. *In vitro* overexpression of RbMAVS inhibited viral replication suggesting its function of antiviral defense in rock bream.

TBK1 and IKK ϵ are non-canonical kinase family members involved in immune defense mechanism through phosphorylation of transcription factors which drive the transcription of significant effector molecules. Rock bream (TBK1) cDNA possessed an ORF of 2169 bp coding for 723 amino acids with molecular mass of 83 kDa. *RbIKK ϵ* cDNA possessed an ORF of 2163 bp coding for 721 amino acids with molecular mass of 82 kDa. RbTBK1 and RbIKK ϵ protein revealed the presence of conserved protein kinases (PK),

catalytic (c) domain (PKc domain) in their N-terminal region [(RbTBK1: residues 15-293) and (RbIKK ϵ : residues 19-327)]. Both the protein revealed ubiquitin-like domain [(RbTBK1: residues 297-385) and (RbIKK ϵ : residues 300-388)], characteristic of the similar kinase family proteins. RbTBK1 shared the highest identity with predicted TBK1 protein of Nile tilapia (identity 96% and similarity 98%) and more than 70% identity with that of human and mouse TBK1. RbIKK ϵ shared the highest identity with IKK ϵ homologue of Nile tilapia (86%) and similar percentage of similarity with Zebra Mbuna and Nile tilapia (94%). *RbTBK1* genome possessed 21 exons intervened by 20 introns. Tissue distribution analysis of *RbTBK1* and *RbIKK ϵ* in tissues isolated from normal unchallenged rock bream revealed ubiquitous presence of *RbTBK1* and *RbIKK ϵ* in all the examined tissues. *RbTBK1* was highly expressed in blood followed by liver. *RbIKK ϵ* was detected most in liver followed by blood. Temporal modifications of *RbTBK1* and *RbIKK ϵ* expression could be observed post poly I:C challenge in liver and head kidney, suggesting their significant regulation during a viral encounter.

Transcription factors are a family of proteins which play a pivotal role in the regulation of expression of IFNs and IFN-stimulated genes. IRF3 and IRF7 play a crucial role in the transcriptional activation of type I IFN and ISGs. IRF3 is constitutively expressed in the cytosol in latent form. Upon viral infection, it undergoes phosphorylation at key serine residues in the regulatory domain and dimerization. Rock bream IRF3 (*RbIRF3*) cDNA consists of an ORF of 1386 bp coding for a protein of 462 amino acids with molecular mass of 51 kDa. *In silico* characterization of the RbIRF3 protein revealed the conserved IRF tryptophan pentad repeat DNA-binding domain (DBD) at the N-terminal region, an IRF-associated domain (IAD) and a serine-rich domain at the C-terminal region, similar to the other IRF3 proteins. Pairwise alignment showed that RbIRF3 had the highest identity and similarity of 87 and 92%, respectively with *Dicentrarchus labrax*. The genomic structure of

RbIRF3 derived from the BAC clone revealed 11 exon -10 intron structural organizations, revealing closer homology to Japanese flounder *IRF3*. Putative promoter analysis revealed various transcription factor binding sites namely AP-1, AP-4, C/EBP $-\alpha$ and $-\beta$, Lyf-1, HSF, Sp1, Oct-1 Sox-5, E2F, ROR α , AML-1a, GATA-1, suggesting their regulation upon various stimuli. Tissue distribution profiling of *RbIRF3* performed in 11 different tissues isolated from healthy rock bream maintained under normal conditions using quantitative RT-PCR revealed ubiquitous expression with highest expression in liver, followed by skin. The kinetic transcriptional pattern of *RbIRF3* analyzed by RT-PCR from blood, liver and head kidney isolated from rock bream following *in vivo* challenge with poly I:C revealed up-regulation during different phases of the experiment. The conservation of the domains coupled with the temporal modifications of *RbIRF3* suggests its active involvement in antiviral defense of rock bream.

Finally, the genes involved in selected antiviral signaling pathway of rock bream, *Oplegnathus fasciatus* have been identified and characterized. The modulations of gene expression and their coordinated function together can combat the viral infection and help in the survival of the organism against the pathogenic threats.

List of Tables

Table 1. Families of viruses infecting fish (Derived from (Essbauer and Ahne,2001)).....	7
Table 2. Primers used in RbMDA5 characterization and qRT-PCR.	26
Table 3. Pairwise alignment of RbMDA5	35
Table 4. Conservation of helicase domain motifs in MDA5 orthologues.	36
Table 5. Primers used in RbLGP2 characterization and qRT-PCR.....	55
Table 6. Pairwise alignment of RbLGP2 protein with LGP2 homologues.....	63
Table 7. Percentage of identity and similarity of DExD and HELICc domains of RbLGP2 with that of the other homologues.	64
Table 8. Primers used in RbMAVS characterization and qRT-PCR.....	87
Table 9. Pairwise alignment of RbMAVS protein with MAVS homologues.....	91
Table 10. Primers used in RbTBK1 and RbIKK ϵ characterization and qRT-PCR.	107
Table 11. Pairwise alignment of RbTBK1 protein with TBK1 homologues.....	114
Table 12. Pairwise alignment of RbIKK ϵ protein with IKK ϵ homologues.....	115
Table 13. Primers used in RbIRF3 identification and qRT-PCR.	129
Table 14. Accession numbers of IRF orthologues obtained from NCBI and GenBank.....	138
Table 15. Pairwise alignment of RbIRF3 with full length protein of IRF3 orthologues.	139

List of Figures

Fig. 1. Different families of viruses infecting teleosts.....	6
Fig. 2. Schematic representation of RLR signaling pathway.....	12
Fig. 3. Multiple sequence alignment of RbMDA5 with other homologues.....	34
Fig. 4. Phylogenetic analysis of RbMDA5 with LGP2, RIG-I and MDA5 sequences.....	37
Fig. 5. Genomic structure comparison of <i>RbMDA5</i> with other MDA5 homologues.	39
Fig. 6. Analysis of the <i>RbMDA5</i> gene 5'-flanking region.....	41
Fig. 7. Tissue distribution analysis of <i>RbMDA5</i>	42
Fig. 8. <i>RbMDA5</i> expression analysis after poly I:C challenge.	43
Fig. 9. Antiviral activity of RbMDA5.	44
Fig. 10. Multiple sequence alignment of RbLGP2 with other homologues.	63
Fig. 11. Phylogenetic analysis of RbLGP2 with LGP2, RIG-I and MDA5 sequences.	65
Fig. 12. Genomic structure comparison of <i>RbLGP2</i> with other LGP2 homologues.	67
Fig. 13. Analysis of the <i>RbLGP2</i> gene 5' -flanking region.....	69
Fig. 14. Tissue distribution analysis of <i>RbLGP2</i>	70
Fig. 15. <i>RbLGP2</i> expression analysis after immune challenges.....	71
Fig. 16. Antiviral activity of RbLGP2 against MABV.....	72
Fig. 17. Multiple sequence alignment of RbMAVS with other homologues.	90
Fig. 18. Phylogenetic analysis of RbMAVS with MAVS homologous sequences.	92
Fig. 19. Tissue distribution analysis of <i>RbMAVS</i>	92
Fig. 20. <i>RbMAVS</i> expression analysis after immune challenges.....	93
Fig. 21. Antiviral activity of RbMAVS against MABV.....	94
Fig. 22. Multiple sequence alignment of RbTBK1 with other homologues.....	110
Fig. 23. Multiple sequence alignment of RbIKK ϵ with other homologues.....	112
Fig. 24. Phylogenetic analysis of RbTBK1 and RbIKK ϵ	113

Fig. 25. Genomic structure analysis of <i>RbTBK1</i> with TBK1 orthologues.....	116
Fig. 26. Tissue distribution analysis of <i>RbTBK1</i> and <i>RbIKKε</i>	117
Fig. 27. <i>RbTBK1</i> and <i>RbIKKε</i> expression analysis after poly I:C challenge.....	119
Fig. 28. Multiple sequence alignment of RbIRF3 with other homologues.....	135
Fig. 29. Phylogenetic analysis of RbIRF3 with IRF family proteins.....	137
Fig. 30. Genomic structure analysis of <i>RbIRF3</i>	140
Fig. 31. Promoter analysis of <i>RbIRF3</i>	142
Fig. 32. Tissue distribution analysis of <i>RbIRF3</i>	142
Fig. 33. <i>RbIRF3</i> expression analysis after poly I:C challenge.....	143

CHAPTER I

An introduction to innate antiviral signaling mechanisms in fish

General introduction

1.0 An introduction to innate antiviral signaling mechanisms in fish

General introduction

The overarching goal of this thesis is to explore selected antiviral signaling mechanisms in rock bream, *Oplegnathus fasciatus*. Antiviral defenses in fish are relatively less investigated. Understanding antiviral mechanisms in fish could help us in improving aquaculture and aid in the development of disease free, quality enriched fish. This section of the thesis gives an overall understanding of the antiviral signaling mechanisms, particularly in mammals and a brief introduction about the antiviral signaling molecules characterized from teleosts. The primary objective of this work is described at the end of this introduction.

1.1 Aquaculture and viruses infecting fish aquaculture

1.1.1 Aquaculture

Aquaculture is a fast growing animal husbandry, which provides nutritional security to the food basket. It is a major source of income in many parts of the world, providing a source of living, food security, and poverty alleviation through mechanisms such as income generation, employment, use of local resources, diversified farming practices, and domestic/international trade (Bostock et al., 2010). Like any other farming, aquaculture is plagued with diseases, and a major concern in fish aquaculture is to escort fish from pathogenic microorganisms like virus, bacteria and parasites (Rimstad, 2011; Stewart C. Johnson and Kabata, 2004; Toranzo et al., 2005; Walker and Winton, 2010).

The disease situation in aquaculture can be attributed to various reasons as follows:

- Increased globalization of trade in live aquatic animals and their products.
- Intensification of aquaculture through the translocation of broodstock, post larvae, fry and finger lings.

- Development and expansion of ornamental fish trade.
- Misunderstanding and misuse of specific pathogen free (SPF) stocks.
- Negative interactions between cultured and wild fish populations.
- Poor or lack of biosecurity measures.
- Climate change and slow awareness on emerging diseases (Bondad-Reantaso et al., 2005).

Viruses are obligate parasites which can infect cells of all living organisms. Viral diseases which result in 100% mortality are a primary constraint in aquaculture impeding both economic and social development in many countries. The only recourse is to quarantine and destroy the infected stock. All over the world, viruses belonging to different families including Rhabdoviridae, Iridoviridae, Birnaviridae, Nodaviridae are known to infect different varieties of fish species (Crane and Hyatt, 2011). Viruses belonging to Flaviviridae, Parvoviridae, and Poxviridae families are not known to infect teleost fish (Essbauer and Ahne, 2001). Aquaculture throughout the world encounter challenges of viral infections. South Korean peninsula with a far-stretching coastline is well enriched with natural resources that facilitate aquaculture. South Korea produces 91,123 tons of fish, accounting for 15.2% of the total marine production. In South Korea, viral infections leading to mass mortalities have been reported in rock bream, olive flounder, black rock fish, red and black sea breams and grey mullet (Park, 2009). Mass mortalities in other parts of the world including Europe, United States of America, Indo-Pacific and Mediterranean regions have been reported (Iwamoto et al., 2001; King et al., 2001; Meyers et al., 1999; Mortensen et al., 1999).

High mortality rates and economic losses urge the need for understanding fish-pathogen interactions and fish responses against viruses to combat the diseases. Innate immunity is the antecedent defense weapon present in all forms of life. Lower vertebrates

like fish are like cross roads between the invertebrates which possess only innate immune system and mammals which have well developed adaptive immune system (L. Tort, 2003). Fish rely extensively on innate immune system, for their defense against the pathogens because their adaptive immune system shows poor immunological memory and short-lived secondary response (Du Pasquier, 2001). An added advantage of the innate immune system is that they portray non-specific responses regardless of the type of viruses and quick enough to avoid time lag between infection and immune response. In the war between the virus and the host, the victory of the host lies in combating the infection as quick as possible while the victory of the virus lies in utilizing its virulent factors in replicating faster and or using immune evasion mechanisms that allows replication of virus in the presence of a potent immune response (Yokota et al., 2010). In many fish species, the infected fish would be dead before antibodies specific for the viruses could be produced, if it solely relied on the adaptive immune system. The constitutively expressed innate immune molecules including complement proteins and physical barriers such as mucous and integument play a vital role to combat viral infections. Recent evidences of the fish interferon system, which includes the virus induced type I IFN production and subsequent induction of interferon stimulated genes suggest that it is similar to the mammalian interferon system (Zou and Secombes, 2011). However, studies on the complete antiviral signaling pathways in fish are still lagging. Gaining knowledge on antiviral signaling pathways in fish, type I interferon expression and its effects in fish provides us insights into fish antiviral mechanisms and suggest new avenues to be pursued to combat viral infections.

1.1.2 Fish viruses

Teleost fish are susceptible to a wide variety of viruses, belonging to families of vertebrate viruses that infect humans and livestock (Crane and Hyatt, 2011; Essbauer and

Ahne, 2001). Monitoring mortality in wild stocks is difficult due to insufficient monitoring techniques and practices. Speculations based on declined wild fish harvests than expected or sparse identification of viral symptoms by chance are the opportunities of virus epizootics reports. Unlike the wild stocks, viral diseases and mortality associated with those diseases are more easily monitored in aquaculture, where fish are constantly kept under observation. Viral diseases may result in 100% mortality.

Viral infections are easily spread in aquaculture facilities, because of overcrowding and environmental impacts such as salinity and temperature. Modifications of the temperature play a significant role in spread of viral diseases as it facilitate the infection by decreasing the immune status of fish (Walker and Winton, 2010). Failure to monitor food for viral infections coupled with negligence of hygiene conditions contribute to major outbreaks in hatcheries and fish farms (Munday, 1997). Identification and characterization of the new infectious viral agents has seen a new era after the availability of cell lines for the *in vitro* propagation and isolation of viruses are available. The different viruses infecting fish are tabulated in Table 1 and their families shown in Fig.1.

RNA viruses



DNA viruses



Fig. 1. Different families of viruses infecting teleosts.

Table 1. Families of viruses infecting fish (Derived from (Essbauer and Ahme,2001))

Virus	Abbreviation	Genome	Taxonomic classification	Known geographic distribution	OIE listed
DNA viruses					
Epizootic haematopoietic necrosis virus and other ranaviruses	EHNV	dsDNA	Iridoviridae, Ranavirus	Australia, Europe, Asia, North America, Africa	Yes
Red sea bream iridovirus	RSIV	dsDNA	Iridoviridae, Megalocytivirus	Asia	Yes
Koi herpesvirus	KHV	dsDNA	Alloherpesviridae, Cyprinivirus	Asia, Europe, North America, Israel, Africa	Yes
RNA viruses					
Infectious haematopoietic necrosis virus	IHNV	(-) ssRNA	Mononegavirales, Rhabdoviridae, Novirhabdovirus	Europe, North America, Asia	Yes
Viral haemorrhagic septicaemia virus	VHSV	(-) ssRNA	Mononegavirales, Rhabdoviridae, Novirhabdovirus	Europe, North America, Asia	Yes
Spring viraemia of carp virus	SVCV	(-) ssRNA	Mononegavirales, Rhabdoviridae, Vesiculovirus	Europe, North and South America, Asia	Yes
Infectious salmon anaemia virus	ISAV	(-) ssRNA	Orthomyxoviridae, Isavirus	Europe, North and South America, Asia	Yes
Viral nervous necrosis virus	VNNV	(+) ssRNA	Nodaviridae, Betanodavirus	Australia, Europe, Asia, North America, Africa, South pacific	No

Viruses are unable to replicate on their own and require the host cellular machinery for their replication and survival. Virus entry into the host begins by binding to cellular receptors and penetration of the plasma membrane, to gain access to the cellular synthetic machinery. The mechanism of transfer of genome and accessory proteins across the barrier of the cellular membrane into the cytosol involves membrane fusion in case of enveloped viruses and pore formation or membrane lysis in case of non-enveloped viruses. Inside the host cell, the viral nucleo-protein will be used to transcribe the virus genes for expression of viral proteins. This process of transcription/replication results in the synthesis of viral nucleic acids such as dsRNA and ssRNA. The dsRNA is not a common cellular nucleic acid form; also cellular mRNAs are capped while viral RNAs have a 5' phosphate that can be recognized by cellular PRRs. Thus ssRNA, dsRNA, and viral glycoproteins constitute the basic VAMPs through which PRRs recognize an invading virus. Viruses enter the cells through pH dependent or -independent pathways. Some viruses enter the cell through endosomes, wherein the low pH facilitates viral genome entry into the cell in a pH dependent manner. A few other viruses fuse their membranes with the host cell membrane directly, using a pH independent mechanism (Kielian and Jungerwirth, 1990). Studies have proved ISAV entry into salmon cells via sialoglycoprotein residues present on the cell membrane using a pH-dependent mechanism (Eliassen et al., 2000).

Although many viral diseases result in death, in some cases there occurs a persistent infection, known as a 'carrier state'. Fish in the carrier state neither reveal symptoms of the disease nor detectable virions in their tissues. However, they are capable of shedding high concentrations of viruses into the water, into their ovarian or seminal fluid during spawning, thus infecting other fish (Kocan et al., 1997). This concept of carrier fish can probably explain how geographically distant and separated fish species can be affected by the same virus, through a highly migratory carrier fish species (Curtis et al., 2001).

1.2 Antiviral immunity in fish

Antiviral defenses comprises of a complex signaling network. Antiviral immune defense is activated initially through recognition of virus and signaling by the host cell to ultimately result in the induction of innate defenses that limit virus replication and destruction of the infected cells. These virus-host interactions also determine the extent to which the interferons are produced during the course of infection. The two principal mechanisms of antiviral immune defense are interferon system and apoptosis.

1.2.1 Antiviral signaling in mammals

Antiviral signaling pathways have been extensively characterized in mammals. Nucleic acid-based recognition of viruses can sense either virion-associated viral genome (replication independent) including the whole genome, replication intermediates or replication products, or viral transcripts (Yoneyama and Fujita, 2010). Antiviral signaling primarily included TLRs (2, 3, 4, 7, 8 and 9) which recognize distinct types of virally-derived nucleic acids and activate signaling cascades that result in the induction of type I IFNs. Later, retinoic acid-inducible gene I (RIG-I)-like receptors (RLRs), were identified as a cytosolic receptors for intracellular dsRNA. RIG-I induces IFN in response to intracellular viral dsRNA in a TLR-independent manner. Thus, there are two receptor systems in place to detect the presence of virus and mount an immune response (Takeuchi and Akira, 2009). These receptors are localized to different compartments within a cell and recognize different ligands. TLR 3, 7, 8 and 9 are intracellular and reside in the endosomal compartments inside the cell. TLR 7 and 8 are structurally conserved and are responsible for the recognition of ssRNA, while TLR 3 and 9 are involved in the recognition of dsRNA and CpG DNA, respectively. TLR 2 and 4 reside on the cell surface and are responsible for the recognition of viral envelope components including envelope proteins and hemagglutinin. The RNA PAMP

recognition might be directed by specific stretches of uridine-rich motifs within the RNA molecule. Except for TLR3, all TLRs utilize MyD88 as an adaptor protein to recruit downstream signaling molecules including the protein kinases IRAK4 and IRAK1, and the RING domain ubiquitin ligase TRAF6. TRAF6 functions together with a dimeric ubiquitin conjugating enzyme complex Ubc13-Uev1A to catalyze the synthesis of Lys63-linked polyubiquitin chains that lead to the activation of a protein kinase complex consisting of TAK1, TAB1 and TAB2. The activated TAK1 kinase phosphorylates IKK β in the activation loop, resulting in the activation of IKK and subsequent nuclear translocation of NF- κ B. The TIR domains of TLR3 and TLR4 bind to another adaptor protein TRIF, which binds directly to TRAF6 and RIP1 to activate NF- κ B. TRIF can also bind to TBK1, which phosphorylates and activates IRF3 and IRF7. Recent studies have also shown that TRIF and MyD88 can bind to TRAF3, which activates IRFs to induce type I IFNs, but inhibits NF- κ B to suppress the induction of proinflammatory cytokines. The extracellular, vacuolar and cytosolic compartments of a cell are collectively monitored by these receptors, for infectious signs (Medzhitov, 2001).

The cytosol represents a critical subcellular niche in the life cycle of the majority of RNA viruses and limited number of DNA viruses. Hence intensive investigation has unveiled new receptors that patrol the cytosolic compartment and enlightened their role in antiviral immunity. The cytosolic receptors include RLRs, NLRs, the more recently identified ALRs and an expanding family of DLRs, which together serve as pathogen sensors. RLRs are primarily involved in the recognition of dsRNA. NOD2 identifies ssRNA whereas ALRs and DLRs recognize viral DNAs. During viral infection, viral RNAs or DNAs that arise from the viral genome are accumulated in the cytosol. Hence these viral nucleic acids serve as VAMPs, for the identification by the sensors. The recognition of these VAMPs results in the elaborate program of gene expression like antiviral inflammatory cytokines, interferons and

chemokines. The most extensively studied among these cytokines is the interferon (Yoneyama and Fujita, 2007b).

1.2.2 Cytosolic sensors and interferon production in mammals

RLRs comprising of RIG-I and MDA5 are members DExD/H box-containing RNA helicase family of proteins that unwind dsRNA in an ATPase dependent manner. The helicase domain of RIG-I and MDA5 can bind both synthetic dsRNA [poly (I:C)] and viral dsRNA. RLR activation triggers the formation of an IPS-1 (MAVS) antiviral signaling complex or signalosome anchored at mitochondria-associated membranes, mitochondria, and peroxisomes. MAVS recruits various signaling molecules to transduce downstream signaling. One of the proposed pathway is that MAVS binds to TRAF2 and TRAF3 through TRADD and TANK and promotes phosphorylation of TBK1- and IKK ϵ - mediated phosphorylation of IRF3. MAVS then recruits various signaling molecules to transduce downstream signaling, such as TRAF6 and TRAF5. TRAF6, along with TRADD, activates canonical NF- κ B signaling via RIP1 and FADD. Canonical NF- κ B signaling occurs as the IKK complex consisting of IKK α , IKK β and IKK γ phosphorylates I κ B α , resulting in the proteasomal degradation of I κ B α and thus liberating NF- κ B to translocate into the nucleus and initiate pro-inflammatory cytokine gene expression. These molecules participate in distinct signaling responses which drive the bifurcation of IRF and NF- κ B (Fig. 2). The two distinct pathways of signaling results in the activation of IRFs 3 and 7 or NF- κ B. The activation of IRF pathway is similar to the TLR3 pathway after MAVS activation, whereas the activation of NF- κ B is similar to the other TLR (7, 8) pathways. NF- κ B sequestered inactive in the cytoplasm, after activation migrates to the nucleus and is involved in the regulation of a wide array of genes including proinflammatory cytokines like TNF- α , interleukins and chemokines.

Phosphorylation of inactive IRF3 at conserved serine residues mediated by TBK1 and IKKε, results in nuclear localization and association with the co-activator CBP/p300. Inactive IRF-3 constitutively shuttles into and out of the nucleus, whereas phosphorylation-dependent association with CBP/p300 retains IRF-3 in the nucleus and induces transcription of IFN-β and other genes. The IFN-β gene is activated by the cooperative binding of three transcription factor families (NF-κB, IRFs, and ATF-2/c-Jun) (Baum and Garcia-Sastre, 2011; Kato et al., 2006; Yoneyama and Fujita, 2007b).

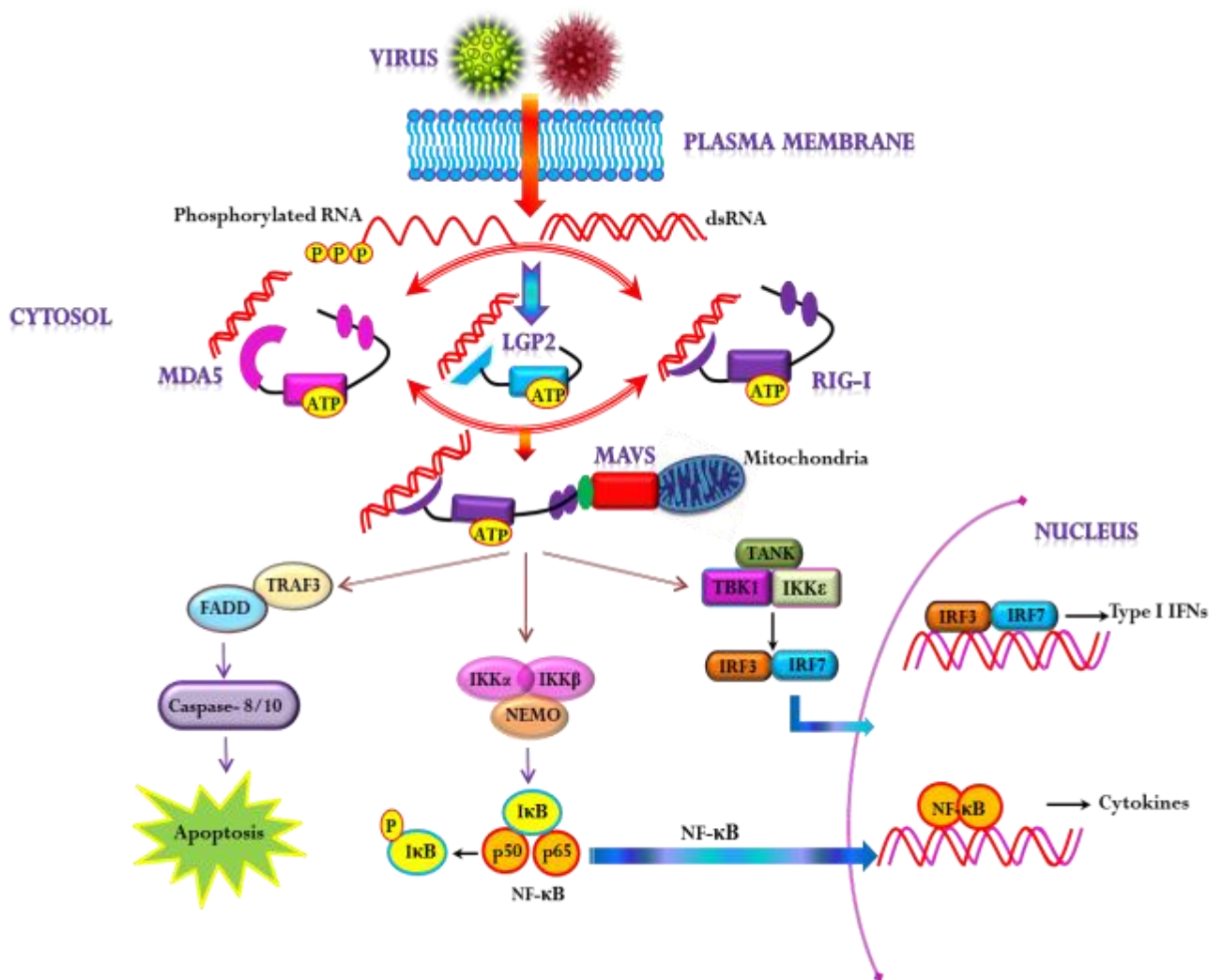


Fig. 2. Schematic representation of RLR signaling pathway.

1.2.3 Interferon system in mammals

Interferons are a class of structurally related cytokines which possess multiple functions like antiviral, antitumor, activity and immunomodulatory effects. The interferon system comprises of interferons (IFNs), the signaling pathways triggered by IFNs by binding to their receptors, the transcription factors activated by the pathways, the genes whose expressions are altered by the transcription factor activation and finally, the change in cellular function (De Andrea et al., 2002; Takaoka and Yanai, 2006). The IFN system triggers the induction of numerous antiviral genes during viral infection and is a formidable barrier against viral multiplication in the infected host.

Type I IFNs (IFN - α , β , ω , κ , δ , τ , ζ , ϵ) are induced in virally infected cells to confer an antiviral state on uninfected cells. Type II IFN comprises solely IFN- γ has antiviral activity and is strongly produced by activated T cells or NK cells but not by virus infected cells (Kontsek et al., 2003). The cellular source of type I interferon is subtype dependent. IFN- β is mostly produced by non-hematopoietic cells namely fibroblasts, while IFN- α and IFN- ω are mainly produced by hematopoietic cells. Pre-implantation embryos of some ruminants produce high amounts of IFN- τ , while IFN- κ is produced by keratinocytes. IFN- ϵ plays a role in the reproductive function of placental mammals, while IFN- δ is associated with porcine trophoblasts (Pestka et al., 2004). All type I IFNs are secreted as monomeric proteins (Sen, 2000). IFN - α and - β are the most extensively studied of the type I IFNs because of their antiviral characteristics.

IFN α/β interact with the same receptor complex, known as IFN- α/β receptor (IFNAR), which consists of two subunits, IFNAR-1 and IFNAR-2. The intracellular domains of these subunits, IFNAR-1 and IFNAR-2, are associated with Janus protein tyrosine kinases (Jak PTKs), Tyk2 and Jak, respectively. In the case of type II IFN, IFN γ binds to IFN- γ

receptor complex (IFNGR), comprising IFNGR-1 and IFNGR-2; the IFNGR1 subunit is constitutively associated with Jak1, whereas IFNGR2 with Jak2. The binding of both types of IFNs to their respective receptor complex results in the cross-activation of these Jak PTKs. The activated Jak PTKs then phosphorylate their downstream Stat substrates, namely Stat1 and Stat2, at tyrosine residues. This phosphorylation of the Stats leads to the formation of transcriptional activator complexes, IFN- α -activated factor [AAF; also termed IFN- γ -activated factor (GAF) and ISGF3. AAF/GAF is a homodimer of tyrosine-phosphorylated Stat1, whereas ISGF3 is a heterotrimeric complex of tyrosine-phosphorylated Stat1, Stat2 and another transcription factor member, IRF-9/p48/ISGF3 γ . Type I IFNs more strongly activate the formation of ISGF3 than type II IFN, whereas type II IFN mainly activates GAF/AAF. The complexes translocate to the nucleus and AAF and ISGF3 bind to their specific DNA sequences containing each of the common motifs, the GAS and the ISRE respectively. The IFN stimulation of promoters containing ISRE and GAS results in the transcriptional induction of a large number of target genes (ISGs) to evoke versatile biological activities (Platanias, 2005; Takaoka and Yanai, 2006). There are other pathways identified in mammals, resulting in the activation of the downstream signaling molecules after IFN binds to their receptors. Type I interferons have been shown to inhibit every stage of viral replication. This includes viral entry and uncoating, transcription, RNA stability, initiation of translation, maturation, assembly and release (Stark et al., 1998).

1.2.4 Recognition of double stranded (ds) RNA in mammals and IFN induction

As described earlier, the expression of type I IFNs is cell type specific. After viral infection, the virus begins replicating its genome, which produces dsRNA during its replicative cycle. In reoviruses, which possess dsRNA genomes, the genomes are protected by the inner viral capsid throughout their cycle and they are never exposed outside. However,

there are instances where small amounts of dsRNA can be incorrectly packaged or uncoated, thus being exposed to dsRNA-sensitive host sensors. In the case of ssRNA viruses, their genomes are transcribed in both sense and antisense directions resulting in a dsRNA replicative intermediate. DNA viruses can produce dsRNA late during infection cycle, where transcription fails to terminate at the end of the gene. Thus mRNAs are produced that contain complementary sequence from incorrectly transcribed gene sequences read in sense and antisense directions. These mRNAs can complex with each other and produce dsRNA (Jacobs and Langland, 1996).

In humans, viral dsRNA has been demonstrated to induce the assembly of an “enhancesome”, composed of transcription factors NF- κ B, IRF3 and the ATF-2/c-Jun heterodimer (Goodbourn et al., 2000). This enhancesome is known to control the transcription of IFN- β and IFN- α 4. However, the mechanism of enhancesome formation by dsRNA is not clear (Goodbourn et al., 2000). The secreted IFN- β functions in autocrine fashion to stimulate the expression of IRF7 and induce IFN- α synthesis. The synthesis of IFN- α requires IFN- α - β expression in fibroblasts (Erlandsson et al., 1998) whereas in human leukocytes IFN- α expression is independent of IFN- β expression. This synthesis of IFNs results in the downstream second wave of cytokines which include TNF α , IL-6, IL-12 and IFN- γ (Sen, 2000).

1.2.5 Antiviral signaling in teleosts

Antiviral signaling in teleosts begins with the pattern recognition of the viruses. Pattern recognition in fish is likely similar to that observed in that of mammals (Zou et al., 2010). Studies related to receptor binding activity and signaling are limited in fish (Takashi Aoki et al., 2008). However, structurally conserved TLR families similar to mammals, together with a set of unique non-mammalian TLR genes and gene variants are observed in

fish. Fish are known to possess orthologues to typical anti-viral TLRs including TLR3, TLR7 and TLR8 (Palti, 2011; Rebl et al., 2010b). In addition to novel TLRs like TLR22, which can bind different forms of RNA, they also have cytosolic sensors like MDA5, LGP2 and the associated signaling MAVS protein. This phenomenon suggests the conservation in the recognition of viral nucleic acids. Most fish lack or possess highly divergent TLR4 genes. Thus, the phenomenon of viral glycoprotein recognition ascribed for TLR4 in mammals may not be conserved among fish species (Purcell et al., 2006). While gene identification and characterization studies in fish are performed based on the studies in mammals, conservation in the structure of the signaling molecules suggests a similar function in fish. Identification of several common sensors like TLRs and cytosolic receptors coupled with the downstream signaling molecules in fish, suggests interferon production mechanism may be similar to that of mammals. Studies of the cytosolic receptors MDA5, LGP2 and MAVS activate the IFN system when overexpressed in fish cells, which correlates protection against several viruses (Biacchesi et al., 2009; Chang et al., 2011; Ohtani et al., 2011; Simora et al., 2010).

1.2.6 Interferon system in teleosts

Interferon was first discovered by Isaacs and Lindemann in 1957 as a non-haemagglutinating molecular particle, interfering with viral infection. Thereafter, various studies in fish were carried out to identify similar genes in fish employing cell lines. The initial studies were based on determining IFN activity *in vitro* following virus infection using cell lines. Later *in vivo* studies were performed and antiviral activity was detected in rainbow trout (de Kinkelin and Dorson, 1973; Dorson et al., 1975). Later, it was determined that the synthetic analog of dsRNA, poly I:C was able to induce an antiviral IFN-like response in fish (Eaton, 1990). Only recently, in 2003, the first fish type I IFN was cloned by independent groups in zebrafish, Atlantic salmon and pufferfish (Zou and Secombes, 2011). IFN genes

have also been reported from different fish species like catfish, common carp, rain-bow trout, sea bass and three spined stickleback, and also elephant shark (Zou and Secombes, 2011). Recently two cysteine duplicated IFN genes were identified from rock bream (Wan et al., 2012). Fish type I genes possess unique genomic organization, consisting of five exons and four introns. Interestingly, all the four introns separating the IFN coding region among fish species are phase 0 introns and presence of multiple AT rich mRNA instability motifs (ATTTA) in the 3' UTR reveals the highly inducible nature of the IFNs. The zebrafish IFN sequence revealed very less similarity to other known mammalian and avian sequences; however zebrafish sequence possessed two cysteine residues and a phenylalanine that are important for IFN function. The identification and characterization of fish IFNs renders us hope in identifying the pathways initiated by this cytokine.

1.2.7 IFN signaling pathways in fish

Unlike the mammalian signaling pathways, IFN signaling pathway is less characterized. The mammalian signaling molecules like janus kinases and STATs have also been identified from fish. Jak1 and Tyk2 have been identified in pufferfish (*T. fluviatilis*) (Leu et al., 2000), and STAT 1 has been cloned from zebrafish and crucian carp (Zhang and Gui, 2004). In rainbow trout, STAT1 was upregulated after IHNV infection (Hansen and La Patra, 2002) and in carp following poly I:C and GCHV infection (Zhang and Gui, 2004). STAT1 gene identified from olive flounder, showed ubiquitous expression in all tissues by real time RT-PCR and ISH, with high expression in gill, spleen, kidney, and heart (Park et al., 2008).

IRFs play a major role in the regulation of IFN expression during viral challenge. A number of IRFs have been characterized from fish species including rainbow trout (Collet et al., 2003; Holland et al., 2010), rock bream (Bathige et al., 2012), Japanese flounder (Hu et

al., 2011b; Hu et al., 2010), crucian carp (Zhang et al., 2003) and pufferfish (Richardson et al., 2001). IRF3 identified from flounder was proven to induce type I IFN promoter and was upregulated upon poly I:C and LCDV treatment (Hu et al., 2011b). IRF7 was identified from turbot and shown to be induced upon infection of turbot with TRBIV (Hu et al., 2011a). IRF3 and 7 was also identified from large yellow croaker. Japanese flounder IRF10 was upregulated by *Edwardsiella tarda*, *Streptococcus iniae* and VHSV infection in kidney (Suzuki et al., 2011). Although a number of IRFs have been identified, it has been only suggested that IRFs in fish function similarly to their mammalian homologues and their exact mechanisms of action needs to be delineated.

Mammalian IFNs are demonstrated to stimulate the expression of ISGs, which in turn confer an antiviral state in uninfected cells. IFNs are known to alter the expression of many genes which tend to constrain virus infection either by limiting virus replication directly or regulate cell cycle and cell death. These ISGs employ programmed cell death as a strategy to control viral replication. The expression of ISGs is dependent on cell and IFN type. They include enzymes, chemokines, antigen presentation proteins, transcription factors, heat shock proteins and apoptotic proteins. Most of them are enzymes which are expressed in an inactive form until exposed to dsRNA, ensuring an antiviral state that remains dormant and harmless until the cell is infected. Among the different ISGs available in mammals, the best characterized are dsRNA-dependent protein kinase (PKR), Mx proteins, and the 2'-5' oligoadenylate synthetase (OAS)/RNaseL pathway.

The probability of similar IFN mechanism in teleosts has brought fish ISGs to limelight only in recent years. The various fish innate immune molecules identified till date include Mx proteins (Das et al., 2007; Leong et al., 1998; Lin et al., 2006; Zenke and Kim, 2009), virus induced gene-1 (vig-1) and vig-2 (Boudinot et al., 1999; Verrier et al., 2011), a host of *vigs* whose functions are yet to be determined (O'Farrell et al., 2002), and PKR,

PKZ(Hu et al., 2004; Rothenburg et al., 2005), ISG-15(Huang et al., 2013; Yasuike et al., 2011; Zhang et al., 2007) , ISG-56(Wan and Chen, 2008).

1.3 Aims of this work

The goal of this thesis is to provide molecular evidence for the existence of selected and conserved antiviral signaling pathways in rock bream, *Oplegnathus fasciatus*. The various innate immune signaling molecules involved in antiviral immunity of rock bream are investigated from the genome to proteome. The thesis will focus on the following works

- Molecular characterization of the genes involved in antiviral defense.
- Genomic structural characterization of the antiviral genes
- Biological activities of the proteins, providing insights into the function of the genes.
- Transcriptional expression analysis of the various genes induced upon immunostimulant challenges.

CHAPTER II

Characterization of cytosolic sensor Melanoma

Differentiation Associated gene 5 (MDA5)

2.0 Characterization of cytosolic sensor Melanoma Differentiation

Associated gene 5 (MDA5)

Abstract

Pattern recognition receptors (PRRs) play a vital role in the recognition of microbial ligands. Melanoma differentiation associated factor 5 is a PRR known to recognize viral RNAs in the cytoplasm and initiate the downstream activation of genes involved in antiviral signaling mechanisms. Rock bream MDA5 designated as RbMDA5 is a highly conserved protein revealing the genome structure with 16 exons similar to that of flounder MDA5. Proximal region of *RbMDA5* revealed the presence of various putative transcription factors involved in the regulation of the gene. RbMDA5 protein possessed the characteristic CARD and helicase domains involved in viral recognition and interaction with the downstream molecules. RbMDA5 protein shared highest identity with the fish homologues while sharing a reasonable range of identity with the mammalian orthologues. Tissue distribution profiling of *RbMDA5* revealed ubiquitous presence with highest expression in blood. Temporal expression analysis *in vivo* post poly I:C challenge showed upregulation in various tissues like gill, liver, spleen, head kidney and blood cells. Finally, the recombinant protein exhibited antiviral activity against marine birnaviruses. Thus, RbMDA5 is an antiviral protein involved in the recognition and signaling of antiviral defense mechanism in rock bream.

2.1 Introduction

Innate immune surveillance for viral infections is primarily performed by germ-line encoded by pattern recognition receptors (PRRs), which comprises of Toll-like receptors, RIG like receptors and NOD-like receptors (Drutskaya et al., 2011; Takeuchi and Akira, 2009). The recognition of viral infections by these sensors initiates various reactions in cells collectively called antiviral innate responses. The production of cytokines like interferons (IFNs) and subsequent synthesis of antiviral enzymes, which are responsible for the impairment of viral replication and promoting adaptive immune responses, are the principal mechanisms of antiviral signaling responses (Takaoka and Yanai, 2006; Yan and Chen, 2012).

RNA viruses generate RNA-RNA strand pairs in the process of RNA-dependent RNA synthesis and some DNA viruses also produce dsRNA during their life cycle. Thus non-self RNA serve as a PAMP for the cytosolic sensors to activate signals against virus infection and elicit a prompt antiviral response (Jensen and Thomsen, 2012). Immune patrolling of the cytoplasm for virus entry is performed by the cytosolic sensors of the RLR-family comprising of three DExD/H box helicases, termed retinoic acid-inducible gene I (RIG-I), melanoma differentiation-associated antigen 5 (MDA5), and laboratory of genetics and physiology 2 (LGP2) (Bruns and Horvath, 2012; Jensen and Thomsen, 2012; Yoneyama and Fujita, 2007b). The three members exhibit primary structure conservation in their helicase domain. The first identified member of this family RIG-I was initially characterized as a dsRNA binding protein which triggered IFN induction and viral signaling as a response to synthetic dsRNA (poly I:C) and was then identified to be involved in antiviral defense against hepatitis C virus (Yoneyama et al., 2004). MDA5 (also known as Helicard and interferon

induced with helicase C domain 1 (IFIH1)) is a structural homologue of RIG-I, involved in viral PAMP recognition (Takeuchi and Akira, 2008).

MDA5 possesses two CARD regions, a helicase domain, a DExD/H box RNA helicase region (consisting of two RecA-like helicase domains, Hel1 and Hel2 and an insert domain, Hel2i), a C-terminal regulatory domain and an RNA binding loop similar to RIG-I. Despite structural conservation between RIG-I and MDA5, each sensor has differential preference for viral recognition (Baum and Garcia-Sastre, 2011; Kato et al., 2006). RIG-I and MDA5 recognize different ligands and distinct viruses. RIG-I receptor limits infection by rhabdoviruses (vesicular stomatitis virus and rabies virus), paramyxoviruses (Sendai virus, respiratory syncytial virus, and Newcastle disease virus), orthomyxoviruses (influenza A and B) and filoviruses (Ebola virus and Marburg virus), whereas MDA5 preferably recognizes picornaviruses (EMCV, coronavirus, and murine hepatitis virus, and murine norovirus-1 type I). Flaviviruses (Dengue virus and West Nile viruses) and reoviruses (rotavirus) can signal through both RIG-I and MDA5 (Kato et al., 2006; Loo and Gale, 2011). These variations could be attributed to the differences in dsRNA recognition as MDA5 can be activated by long dsRNA, whilst RIG-I could be activated by RNA containing 5'ppp and shorter dsRNAs. Comparative studies of ligand recognition by MDA5 and RIG-I suggests that MDA5 preferentially recognizes high molecular weight poly I:C fragments, while RIG-I exhibits a preference for shorter RNA fragments and can also bind to ssRNA (Kato et al., 2008).

In normal uninfected cells, RIG-I adopts a “closed” inactive conformation in the absence of RNA and the CARD is masked (Kowalinski et al., 2011). The binding of virus specific RNA species (dsRNA or 5'-triphosphate ssRNA) to the RNA binding domain and ATP to the helicase domain change RIG-I conformation and release CARD (Jiang et al., 2011; Luo et al., 2011). The CARDS relay signals to the downstream CARD containing molecule IPS-1 [alternatively termed MAVS, VISA, and Cardif] (Berke et al., 2013; Kowalinski et al.,

2011). Contrastingly, MDA5 does not sequester its CARDs and are not likely to interact with the HEL2i or other domains within MDA5. MDA5 cooperatively forms dimers and ATP-sensitive filaments on dsRNA. Moreover, MDA5 CTD/RD is required for filament assembly but not for RNA binding (Berke and Modis, 2012; Berke et al., 2012; Li et al., 2009a; Peisley et al., 2011; Takahasi et al., 2009a). The CARDs on MDA5 have also been proposed to nucleate the assembly of MAVS into its active polymeric form. The self-propagating ‘prion-like or amyloid-like’ properties of MAVS polymers amplify signaling. These findings suggest that MDA5 and RIG-I may be regulated in different ways (Hou et al., 2011; Jiang et al., 2011; Jiang et al., 2012).

Although extensive studies have been performed on human MDA5, teleost MDA5 have been of focus in the recent years. MDA5 have been identified and characterized from grass carp (Su et al., 2010; Wang et al., 2012), Japanese flounder (Ohtani et al., 2011), Rainbow trout (Chang et al., 2011). In this study, an MDA5 gene has been identified from rock bream *Oplegnathus fasciatus* and designated as *RbMDA5*. The genome structure, transcriptional expression analysis and antiviral function of *RbMDA5* have been investigated.

2.2 Materials and methods

2.2.1 Animal rearing, cDNA library construction and *RbMDA5* gene identification

Healthy rock bream fish with average weight of ~50 g, procured from the Ocean and fisheries Research institute (Jeju, Republic of Korea) were adapted to the laboratory conditions (salinity $34 \pm 1\%$, pH 7.6 ± 0.5 at 24 ± 1 °C) in 400 L tanks. Blood samples were harvested from the caudal fin of healthy, unchallenged fish using a 22 gauge needle and centrifuged immediately for 10 min at $3000 \times g$ at 4 °C, to collect the hematic cells. Gill, liver, brain, kidney, head kidney, spleen, intestine, muscle, heart and skin tissues were

harvested on ice from three healthy animals and immediately flash-frozen in liquid nitrogen and stored in -80 °C, until RNA extraction. Tri Reagent™ (Sigma, USA) was employed to obtain total RNA from tissues. The concentration and purity of RNA were evaluated using a UV-spectrophotometer (BioRad, USA) at 260 and 280 nm. Purified total RNA samples were subjected to mRNA purification using Micro-FastTrack 2.0 mRNA isolation kit (Invitrogen). First strand cDNA was synthesized from 1.5 µg of mRNA using Creator™ SMART™ cDNA library construction kit (Clontech, USA); amplification was performed with Advantage 2 polymerase mix (Clontech) under conditions of 95 °C for 7 s, 66 °C for 30 min and 72 °C for 6 min. Over-representation of the most commonly expressed transcripts was excluded by normalizing the synthesized cDNA using Trimmer-Direct cDNA normalization kit (Evrogen, Russia). A cDNA GS-FLX shotgun library was created from the sequencing data obtained by using the GS-FLX titanium system (DNA Link, Republic of Korea). A cDNA contig showing high homology to the earlier identified MDA5 homologues was identified using BLAST and designated as *RbMDA5*.

2.2.2 BAC library creation and identification of *RbMDA5* BAC clone

Rock bream obtained from the Jeju Special Self-Governing Province Ocean and Fisheries Research Institute (Jeju, Republic of Korea) were accustomed to the laboratory conditions. Blood was harvested aseptically from the caudal fin using a sterile 1 mL syringe with 22 gauge needles, and a BAC library was constructed from the isolated blood cells (Lucigen Corp., USA). Briefly, genomic DNA obtained from blood cells was randomly sheared and the blunt ends of large inserts (>100 kb) were ligated to pSMART BAC vector to obtain an unbiased, full coverage library. Around 92160 clones, possessing an average insert size of 110 kb, were arrayed in 240 microtiter plates with 384 wells.

A two-step PCR based screening method was used to identify the clone of interest based on manufacturer's instructions. Primers were designed based on the cDNA sequence identified from the cDNA database. A gene specific clone was isolated and purified using Qiagen Plasmid Midi Kit (Hidden, Germany). The sequence was confirmed by pyrosequencing (GS-FLX titanium sequencing, Macrogen, Republic of Korea). The gene specific primers employed in the identification of the clone from the BAC library are tabulated in Table 2.

Table 2. Primers used in RbMDA5 characterization and qRT-PCR.

The restriction sites are in small letters.

Gene	Purpose	Orientation	Primer sequences (5'-3')
RbMDA5	BAC screening & qRT-PCR	Forward	ATCAAGCGGACTACGACAAACGGA
RbMDA5	BAC screening & qRT-PCR	Reverse	TCTCGCTCTTCAAGCCTTTCTGCT
RbMDA5	pcDNA cloning	Forward	GAGAGaGaattcTATGGCGTCCGATAACGATGACGAAAA
RbMDA5	pcDNA cloning	Reverse	GAGAGActcgagCTACGTAGTTGACGTTGATTCTGTTTCATCATCATCAT
β -actin	qRT-PCR amplification	Forward	TCATCACCATCGGCAATGAGAGGT
β -actin	qRT-PCR amplification	Reverse	TGATGCTGTTGTAGGTGGTCTCGT

2.2.3 Sequence characterization, genome structure and phylogenetic analysis of

RbMDA5

A cDNA sequence portraying domain similarity with the MDA5 homologues available in NCBI, was identified by BLAST and was subjected to DNAssist2.2 to predict the open reading frame (ORF) and translate nucleotide to protein. The conserved domains were identified using Expasy (<http://www.expasy.org/>), SMART (<http://smart.embl-heidelberg.de/>) and conserved domain database search (CDD). Pairwise alignment and multiple sequence alignment were executed using ClustalW (Thompson et al., 1994). A phylogenetic tree was reconstructed using minimum evolution method available in MEGA 5.0, with bootstrap values calculated with 5000 replications to estimate the robustness of internal branches

(Tamura et al., 2011). The amino acid identity percentages were calculated by MatGAT program using default parameters (Campanella et al., 2003). The exon-intron structure was determined by aligning mRNA to the genomic sequence of *RbMDA5* using Spidey available on NCBI (<http://www.ncbi.nlm.nih.gov/spidey/>) (Wheelan et al., 2001). The complete genomic structure and putative promoter region were determined from the BAC sequencing data. The genomic structures used for comparison were obtained from exon view of Ensembl genome database. The transcription factor binding sites (TFBS) in the promoter region were predicted using TFSEARCH, TESS and TRANSFAC.

2.2.4 Transcriptional profile of *RbMDA5* gene in challenged and normal tissues

2.2.4.1 Poly I:C challenge

In order to monitor the transcriptional changes of *RbMDA5* post dsRNA injection *in vivo*, poly I:C was employed as an immunostimulant. Sterile poly I:C stock was prepared by dissolving poly I:C at the rate of 1.5 mg/ml in PBS and filtered through a 0.2 μ m filter. A time course experiment was performed by intraperitoneally injecting the animals with 100 μ L suspension of poly I:C stock. The control animals were injected with an equal volume of PBS. Liver, gill, spleen, head kidney tissues and whole blood cells were harvested from the un-injected, PBS-injected and immune challenged animals at time points of 3, 6, 12, 24, and 48 h post injection/infection (p.i.).

2.2.4.2 RNA isolation and cDNA synthesis

In order to perform the tissue distribution profiling of *RbMDA5*, gills, liver, brain, kidney, head kidney, spleen, intestine, muscle, heart and skin tissues and whole blood cells were harvested from un-injected fish. After challenge with PBS and poly I:C, gill, liver, spleen, head kidney tissues and whole blood cells were harvested from challenged animals at

the corresponding time points. Total RNA was obtained from tissues using Tri Reagent™ (Sigma, USA). The concentration and purity of RNA were evaluated using a UV-spectrophotometer (BioRad, USA) at 260 and 280 nm. The RNA was diluted to 1 µg/µL and cDNA was transcribed from 2.5 µg of RNA from each tissue using a PrimeScript™ first strand cDNA synthesis kit (TaKaRa). Concisely, RNA was incubated with 1 µL of 50 µM oligo(dT)₂₀ and 1 µL of 10 mM dNTPs for 5 min at 65 °C. After incubation, 4 µL of 5× PrimeScript™ buffer, 0.5 µL of RNase inhibitor (20 U), 1 µL of PrimeScript™ RTase (200 U), were added and incubated for 1 h at 42 °C. The reaction was terminated by adjusting the temperature to 70 °C for 15 min. Finally, synthesized cDNA was diluted 40-fold before storing at -20 °C for further use.

2.2.4.3 Tissue distribution

Quantitative reverse transcription polymerase chain reaction (qRT-PCR) was used to examine tissue distribution of *RbMDA5* mRNAs in various tissues of healthy fish. qRT-PCR was performed in a 15 µL reaction volume containing 4 µL of diluted cDNA, 7.5 µL of 2× SYBR Green Master Mix, 0.6 µL of each primer (10 pmol/µL) and 2.3 µL of PCR grade water and subjected to the following conditions: one cycle of 95 °C for 3 min, amplification for 40 cycles of 95 °C for 20 sec, 58 °C for 20 sec, 72 °C for 30 sec. The baseline was automatically set by the Thermal Cycler Dice™ Real Time System software (version 2). In order to confirm that a single product was amplified by the primer pair used in the reaction, a dissociation curve was generated at the end of the reaction by heating from 60 °C to 90 °C, with a continuous registration of changes in fluorescent emission intensity. The Ct for the *RbMDA5* (target gene) and *β-actin* (internal control) were determined for each sample. *RbMDA5* gene expression was determined by Livak comparative Ct method. The relative

expression level calculated in each tissue was compared with respective expression level in muscle.

2.2.4.4 Temporal RbMDA5 mRNA expression analysis post poly I:C challenge

qRT-PCR was performed with cDNA prepared from RNA obtained from gill, liver, spleen, head kidney tissues and whole blood cells isolated from PBS and poly I:C challenged animals. qRT-PCR conditions were the same as used for tissue distribution profiling. The ΔCt for each sample was determined by the method described above. The relative expression of *RbMDA5* was determined by the Livak method. The relative fold change in expression after immune challenges was obtained by comparing the expression to corresponding PBS-injected controls. The expression normalized to PBS-injected controls is represented in the figures.

All experiments were performed in triplicate. All data have been presented in terms of relative mRNA expressed as means \pm standard deviation (S.D.). Statistical analysis was performed using un-paired two-tailed Student's t-Test. Statistical significance was accepted at a P-value below 0.01.

2.2.5 Construction of expression vector and antiviral assay

2.2.5.1 Cell lines and viruses

Rock bream heart cells were established as previously described (Wan et al., 2012). Concisely, heart tissue was aseptically isolated from healthy rock bream fish (n=3). The tissue was minced into small pieces (approximately 1 mm³ in size) and washed thrice with HBSS (Sigma) containing antibiotics (400 IU/mL penicillin and 400 μ g/mL streptomycin). Then, the tissue was digested in 0.2% collagenase II (Sigma) solution for 2 hours at 20 °C. The digestion mixture was filtered through a cell strainer (70 μ m mesh size), centrifuged at 1000 rpm for 10 min. The cells were resuspended in Leibovitz's L-15 medium supplemented

with 20% FBS, 100IU/mL penicillin and 100µg/mL streptomycin, and inoculated into 75 cm² cell culture flask. The cells were sub-cultured more than three times and adapted to growth medium containing 10% FBS. Cells' susceptibility to marine birnavirus (MABV) infection was tested. The 80% confluent monolayer cells were treated with serially diluted MABV and the plates were kept at room temperature (RT) for 2 h for adsorption and facilitate viral infection. The plates were then incubated at 24 °C for 72 h. The susceptibility of rock bream heart cells for MABV infection was confirmed by observing the cytopathic effect (CPE) and the maximal non-cytotoxic concentration was determined and used for the subsequent antiviral activity assay. MABV was kindly provided by Prof. Sung-Ju Jung (Department of Aqualife Medicine, Chonnam National University, and Republic of Korea).

2.2.5.2 Construction of expression vector

The full length ORF of *RbMDA5* (2979 bp) was amplified from liver cDNA using gene specific primers (Table 2.) and PCR and cloned into TA vector (Takara, Japan). The orientation and sequence was confirmed by restriction digestion and sequencing, respectively. The *RbMDA5* ORF cloned into TA vector was used as the template and the amplified PCR product was digested with *EcoRI* and *XhoI*. The digested PCR products were purified using Gel purification kit (Bioneer) and ligated overnight at 4 °C with *EcoRI* and *XhoI* digested pcDNATM 3.1/His B vector (Life Technologies). The ligation mixture was transformed into *E. coli* DH5α cells and the clone harboring the recombinant plasmid was sequenced. The affirmed clone harboring the recombinant RbMDA5 was selected and named as pcDNA3.1-RbMDA5.

2.2.5.3 Antiviral assays

A monolayer of rock bream heart cells were cultured in 24 well plates at 24 °C, 24 h prior to transfection. Before transfection, cells were washed once with sterile PBS, and then

replaced with Opti-MEM (Life technologies). The transfection procedure was performed with Lipofectamine™2000 (Life technologies), as per manufacturer's instructions. Briefly, 1.5 µg of pcDNA vectors (empty pcDNA3.1 and pcDNA3.1-RbMDA5) were mixed with 1µL of Lipofectamine™2000 and transfected into the heart cells in 100 µL Opti-MEM, and then cultured at 24 °C for 48 h. After 48 h, cells were infected with MABV and left at RT for 1 h for adsorption. The cells were then cultured with Leibovitz's L-15 medium and observed for the appearance of CPE. The cells transfected with empty pcDNA3.1 and pcDNA3.1-RbMDA5, but not infected with virus served as the mock infection control. After 7 days of MABV infection, the cells were washed once with PBS, fixed with 4% paraformaldehyde (PFA) and stained with 3% crystal violet for visualizing live cells.

2.3 Results

2.3.1 RbMDA5 identification, sequence characterization, phylogenetic analysis

A cDNA sequence portraying similarity to the MDA5 homologues submitted in NCBI was identified while delving our rock bream cDNA library for genes involved in antiviral immunity. *RbMDA5* cDNA was 3379 bp with ORF of 2976 bp, 5' untranslated region (UTR) of 6 bp and 3' UTR of 397 bp. There were two mRNA instability motifs (³¹³¹ATTTA³¹³⁵ and ³²⁷²ATTTA³²⁷⁶) present in the 3' UTR. The ORF coded for a protein of 992 amino acids with molecular mass of 112 kDa and isoelectric point of 5.6. Protein motif analysis of RbMDA5 protein through conserved domain database and SMART, revealed conserved structures including two N-terminal CARDS (residues 10-95 and 108-189), a ResIII site (residues 284-477), a central DExD/H box RNA helicase domain (DEAD/DEAH box helicase domain; residues 302-392), an MDA5 insert domain (residues 522-647), a HELIc domain (helicase superfamily c-terminal domain; residues 644-786) and a RIG-I_C-RD (C-terminal repressor domain (RD) embedded within the C-terminal domain (CTD) (residues 854-973)). ATP

binding site ³¹¹GSGKT³¹⁵ was found in the DExD helicase domain. There were six helicase domain motifs (I: ³⁰⁸LPTGSGKTRV³¹⁷, II: ⁴²⁰IIDECHHT⁴²⁷; III: ⁴⁶⁵GLTAS⁴⁶⁹; IV: ⁶⁷⁴IIFTKTRR⁶⁸¹; V: ⁷⁴¹TTVAEEGLDI⁷⁵⁰; VI: ⁷⁷⁰QALGRGRA⁷⁷⁷) and an RNA binding loop (⁸⁹⁸TSPPERLLDY⁹⁰⁷) present in RbMDA5 (**Fig. 3**). In order to study molecular evolution and compare the sequence identities, MDA5, LGP2 and RIG-I sequences were obtained from NCBI and aligned using clustalW and phylogenetic tree was constructed (**Fig. 4**). RbMDA5 was placed contiguous to orange spotted grouper MDA5, with which it shared the highest identity and similarity (full protein: 74 and 84% and CARD region: 64 and 75%, respectively) (**Table 3. and 4**). Multiple sequence alignment of RbMDA5 with other MDA5 proteins revealed conservation explicitly in the domain regions, sharing moderate conservation in the domain flanking regions (**Fig. 3**).

Rock bream -MASDNDDE-N[RFTEENFRPRLRACIEVEFVLDYMPFIETDDKERIROKARTECNSTAVGVLDITVLT-K-PHTLGFRAFV]
Rainbow trout -MAADKNDTNTNISLIEDFRPRLRLKIIIEFVLDLHNFLDNDNDKDLIRTKARKESNLKAVDLDLIDTIIIRIRLPKQWFREFV
Gold fish -MSSDQDAE-TRHILDCFRDLRLKRIIEVEFVLDLHLFLEPDRKDIRAKLRRLDGGIDSAALLIDEIKLT--HDKGWSRELI
Mouse MSIVCSAEDSFRNLISIFRPRVKMYIQVEFVLDHLIFLSAETKEQILKIKKINTCGNTSAAELLSTLEQG-QWPLGWTQMFV
Rat MSTVCSAEDSFRNLISIFRPRVKMYIQVEFVLDYLVFLPAETKEQILKIKKINTCGNTSAAELLSTLEQG-QWPLGWTQMFV
Human MSNGYSTDENFRYLISCFRFRVVKMYIQVEFVLDYLVFLPAEVEKEQIQRTVATSGNQAVELLSTLEKQ-VVHLLGWTREFV
Chicken MSEECR-DERFLYMISCFRFRRLKRCIRVQFVLDLWPLSLSAEKKDKVRAAALQRGEVEGAELLCAVERG-RRDPGWTFEFL
Frog MPQNSEDARGIYLIIECFRFRRLVRYIQAVPVLDHLTWLGRDIREQVVSKAQNGEQDAARLLDRIVRG-PRPWFEEAFV

:: ** * : * : ** : : : : : : : : . . * : : : ** :

Rock bream [DALVOSGSDRAADYMQT]--NLPEPEVEEAEND[SCVRLIELLSPTLVD-MOTAEVCMHCVSEGLLTPDDSEI IK]----NOQG
Rainbow trout DALSAAGCKHAATYVED---SPPCPALEAENDNCVRLIELLSRLLG-MKTTDVCWDCFSKGI LTAEDREII LAEQNRGN
Gold fish TALETVGCTNAVNYVLN---SPNPTEEAENDSCVRLIDLMLQSLIN-MKTGDVCAHCF SQGLLTQEDHENI TKATENHGN
Mouse EALEHSGNPLAARYVKPTLTLDPSPSETAHDECLHLLTLLOPTLVDKLLINDVLDTCFEKGLLTVEDRNRI SAAGNS-GN
Rat EALEHSGNPLAARYVKPSLTDLPSPSETAHDECLHLLNLLQPTLVGKLLINDVLDTCSEKGLVTVEDRNRI SAAGNS-GN
Human EALRRTGSPLAARYMPELTDLPSPFENAHDEYLQLLNLLQPTLVDKLLVLDVLDKCMEEELTIEDRNRIAAAENN-GN
Chicken LALKKGGCDLAACYVNP--SQLPSQEEHDLVHVLQHLGLHGTLDVNMQTRQVAEKLELGI FQEDLDVGIETVIESRGN
Frog RALKDSHTQAAAAYLSE---GRPTPSLEATWYDYEQLLIVLYPELIIKIDPKETAPLCRREEICSDDEDVNVISNVTDQHGN

** * : * : ** : : : : : : : : . . * : : : ** * : *

Rock bream [RAGARELLRRIVRGRHGFWSKFLNIIHETGHOHLYLE]FGGSPDCDKLGSDEKLSSMKDEP----AGSEAAAAEEAESCVD
Rainbow trout MGGARELPRRIVRFPFPGWFSTFLKALQVTEHNDLCKELTSGSPGDNLIDEPGVLMAVNEAPGNVYPMVEEGPVEAAGSKFL
Gold fish IKGARVLLKRLVKNEAGWFSKFLQALEDEHHELVRELGRPEONKDESMSVETHEFKTVEEGEQMCLAAEKEADSVNSSLL
Mouse ESGVRELLRRIVQKEN-WFSTFLDVLVRLQGTGNDALFQELTGGGCPEDNTDLANS SHRDGPAANECLLPAVDES-SLETEAWN
Rat ESGVRELLRRIVQKEN-WFSTFLDVLVRLQGTGNDALVQELTGVSCPEESTDLDNASHKDRPAANEPLIPALD-LSETEAWT
Human ESGVRELLRRIVQKEN-WFSAFLNLRVQTNELVQELTGVSCPEESNAEINLSQVDGQVBEQLLSTTVQF-NLEKEVWG
Chicken RDGARELLSRIVQKQD-WFSQFLVALRETQHESLADDLGSNTGGTEDKDYELKNN-TGKKTEAASQFVYVTE-DLKQQENL
Frog QQGSRELLNRI IKKQD-WFSKFLTVLRTMGQNSLADYLTGSNNDENAE SSGARPTVEGADSSSVADIKMHHELGS HDVK

** * : * : ** : : * : * : * : * : * : * : * : * : * : * : * : * : * : * : * : * : * : * : *

Rock bream PEF-----MHISITEDPQSEATDLYQSGASPQRSQPDSSEPSQPDGTDVSA---AAAARGPENGDIIVLRDYQMEVAR
Rainbow trout PEQETLDSSVNTMHLDEPSEADSEADLYLQGT--EPMENKGPENSLLDLSMSGCI---APAAESPPKAVIVLRDYQMDVAR
Gold fish SED-----LNSVDSSVLSVSAENE-DVDMYNGKEEEKGLTEDDDP---PVSKR-----EIVLRDYQMEVAR
Mouse VDDILPEASCTDSSVTTESDTSLAEGSVSCFDES LG-HNSNMGRDSTGMSGSDSE-SVIQTKRVSPEPELQLRPYQMEVAQ
Rat IEDTSPSASFADSSVTTESDTSLAEGSVSCFDES LG-HNSNMGRDSTGMSGSDSEDTIMGTRKASPKPELQLRPYQMEVAQ
Human MENNSSESSFADSSVSES DTS LAEGSVSCFDES LG-HNSNMGRDSTGMSGSDSE--ENVAAASPEPELQLRPYQMEVAQ
Chicken DDSFVRESSVLETSVGK--NSVISESVAVGDASVSNENLQSSSTSDSGEDE---AEGRASPEPDLTLR DYQMEVAK
Frog CENNLAE S S F A G S N A T S D L D T S S P E L Y C S A D I E S L E I S D S D E Q E T T A S -----R A S P V P Q I T L R N Y Q M E V A K

1

Rock bream [PALEGKNIIVCLPTGSGKTRVAVYITKHLDSRREEGRSGKVVLVNVKPLVEQHLYSEFSFPLKRAYKLERVSGDCQLKI]
Rainbow trout PALEGKNI IICLPTGSGKTRVAVYITKEHLDSRREGRPGKVVLVNVKPLVEQHLYSTEFWKFLNKYKVERVSGDSQLKI
Gold fish PALEEKNI IICLPTGSGKTRVAVYITKEHLERKQMGQPGKVVLVNVKPLVEQHLYKAEFGFLKHQYSVERVSGASQLKI
Mouse PALDGNKI IICLPTGSGKTRVAVYITKDHLDKKQASESGKVI VLNVKMLAEQLFRKEFNPKYKWRVIGLSGDTQLKI
Rat PALDGNKI IICLPTGSGKTRVAVYITKDHLDKKQASESGKVI VLNVKMLAEQLFRKEFNPKYKWRVIGLSGDTQLKI
Human PALEGKNI IICLPTGSGKTRVAVYIAKDLHLDKKQASEPGKVI VLNVKMLAEQLFRKEFQPFLLKWRVIGLSGDTQLKI
Chicken PALNGENI IICLPTGSGKTRVAVYITKDHLDKKQASEQKVI VLNVKPLVEQHLRKEFNPKYKWRVIGLSGDESELKI
Frog PALEGKNI IICLPTGSGKTRVAVYITREHLCKRREEGRLAKAIVLVNVKPLVEQHLYRREFFYFPLKDYHVTIKISGDSQLKN

*** : .*** : ***** : . : * : * : * : * : * : * : * : * : * : * : * : * : * : * : * : * : * : * : *

2

Rock bream [SFTEIVKKNVDVICTAQI LENYLERFNKGEDEGVNLSDLTLIIIDECHHTQKGGVYNHIMRYLQKHKNKRLKKEQKEPM
Rainbow trout SFTDIVQKNDVICTAQI LENYLERAHSGDDGKLSDLSLIVIDECHHTQKGGVYNHIMIRYLQKHKNAKLKKEQKQDTP
Gold fish SLPQIIEQNDDI IICTAQI LENYLERAHSGDDGKLSDLSLIVIDECHHTQKGGVYNHIMIRYLQKHKNAKLKKEQKQDTP
Mouse SFPEVVKSYDVI IICTAQI LENYLERAHSGDDGKLSDLSLIVIDECHHTNKEAVYNNIMRRLYKQLKLNHLKKNKPAI
Rat SFPEVVKSYDVI IICTAQI LENYLERAHSGDDGKLSDLSLIVIDECHHTNKEAVYNNIMRRLYKQLKLNHLKKNKPAI
Human SFPEVVKSYDVI IICTAQI LENYLERAHSGDDGKLSDLSLIVIDECHHTNKEAVYNNIMRRLYKQLKLNHLKKNKPAI
Chicken SFPEVVKRYDVI IICTAQI LENYLERAHSGDDGKLSDLSLIVIDECHHTQKGGVYNHIMIRYLKKEIKNRKQAKENKPLI
Frog SFHKVQEHVDVICTAQI LENYLERAHSGDDGKLSDLSLIVIDECHHTQKDAVYNNIMIRYLKKNKRNKRNKMEKAQV

* : . : : *

3

Rock bream [SIPQIILGLTASPGVGATKMEKAEHILRICANLDASKIMTR----SLGEY-KKEQRKMTVTVEDRKEPDPGDVIKIKIMHA
Rainbow trout AIPQIILGLTASPGVGAKKIEKAEEHILRICANLDAYKIMTG----NLGEN-KKEPHKKIATAEERKEDPFGDVLKGVNNA
Gold fish PIPQIILGLTASPGVGAMQMAEQHILQICANLDAFTIKTK----TFEEEEAKTPYKRIARAEERKEDPFGDVIKIKIMDE
Mouse PLPQIILGLTASPGVGAACKQSEAEKHILNICANLDAFTIKTVKENLGQLKHQIKEPCKKFIADDTRENPFKEKLEIMAS
Rat HLPQIILGLTASPGVGAACKQSEAEKHILNICANLDAFTIKTVKENLSQLKHQIKEPCKKFIADDTRENPFKEKLEIMAS
Human PLPQIILGLTASPGVGATKQAKAEHILKICANLDAFTIKTVKENLSQLKHQIKEPCKKFIADDTRENPFKEKLEIMTR
Chicken PQPQIILGLTASPGVGARSNSKAEHILKICANLDAFTIKTVKENLSQLKHQIKEPCKKFIADDTRENPFKEKLEIMQD
Frog PLPQIILGLTASPGVGAKNIKKSEHILRICANMDFKIMTVQENAEQLRQVQKDPYKEVKISDEKKNPFGDKLEIMGK

***** : *

Rock bream [IHTHAGLSPICDLGSQNYEQWVQKREKAAAEQKVRVCAEHLROYSEGLNLSNTIRMRDFAFSLNKYHMEFIRKRTTPD
Rainbow trout IHIHAE LNPTCDLGTQNYEQWVQKREKAAAEQKVRVCAEHLRQYNEALYLGKTI RMDFAFSLNKYHMEFIRKRTTPD
Gold fish IHTHAGLLPLCEPQTQNYEQWVQKREKAAAEQKVRVCAEHLRHYNEALHQSNTIRMSDAFRFLDRYHSEELKTKSSPD
Mouse IQTYCQKSPMSDFGTQHYEQWAIQMEKKAADGNRKRDRVCAEHLRKYNEALQINDTIRMIDAYSHLEAFYDEKEKFFAVL
Rat IQTYCQKSPMSDFGTQHYEQWAIQMEKKAADGNRKRDRVCAEHLRKYNEALQINDTIRMIDAYSHLEAFYDEKEKFFAVL
Human IQTYCQKSPMSDFGTQHYEQWAIQMEKKAADGNRKRDRVCAEHLRKYNEALQINDTIRMIDAYSHLEAFYDEKEKFFAVI
Chicken IQKYCQLYPKSEFSGPYEQWVIREERRAAEKERKERVCAEHLKKNYNDALQINDTIRMVDAYNHLLNFKYELKRRKTAES
Frog IEEYSKLYPTSDHGSQSYEQWVIQTDKTAKEGKRKEHVCAEHLRKYNDALQINDTIRMTDSLIHLRKFYEEKRRKIKLLN

* : . . * : *

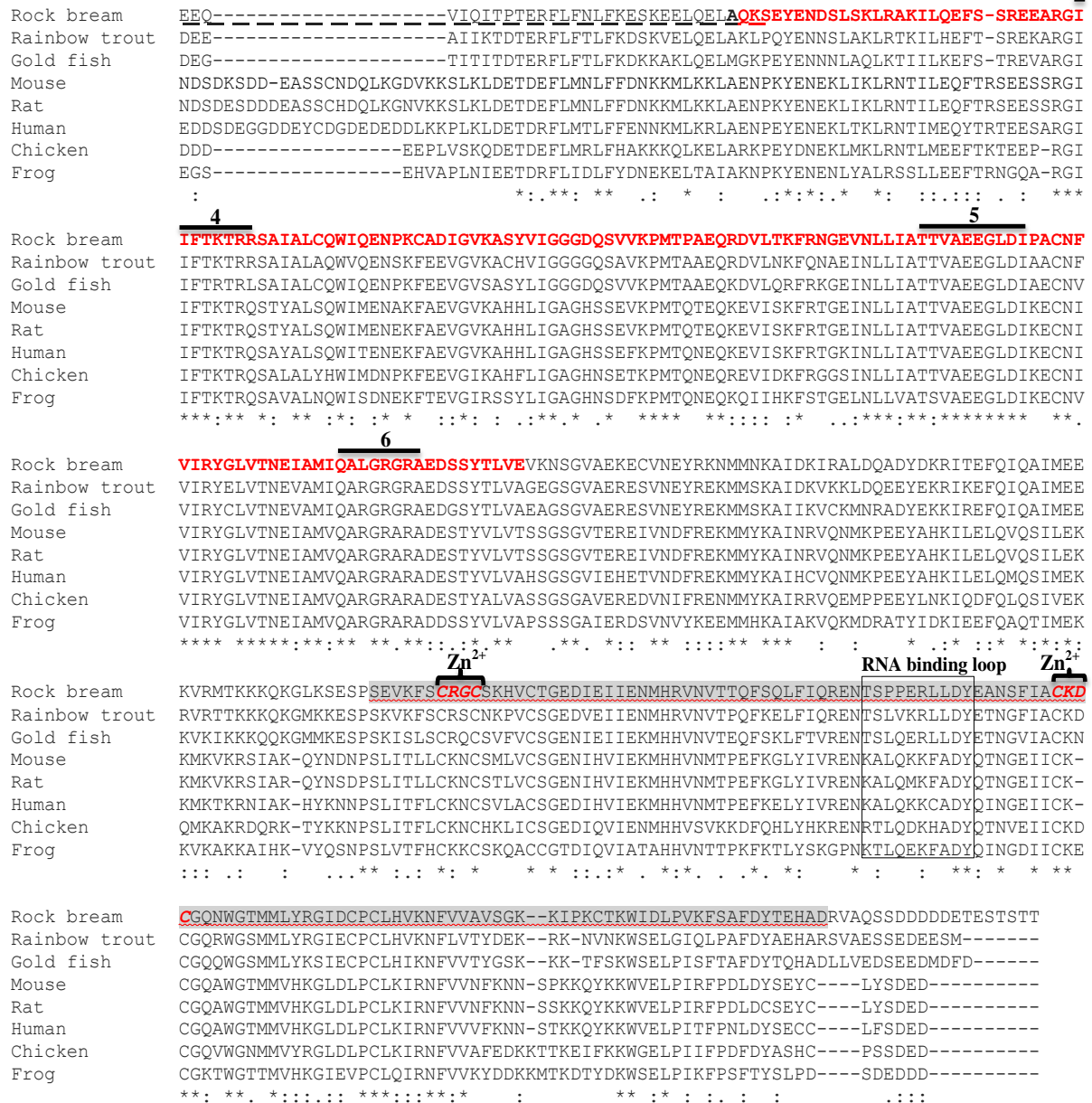


Fig. 3. Multiple sequence alignment of RbMDA5 with other homologues.

The amino acid sequence derived from RbMDA5 was submitted to GenBank under the accession ID. KF267452). The rock bream species name is written on the top of all sequences. The homologous MDA5 sequences were obtained from NCBI and GenBank and the accession numbers are given in Table 3.. Identical residues are indicated by “*”. Highly conserved and semi-conserved residues are indicated by “:” and “.”, respectively. The CARD regions are boxed. The Res III domain (284-477) is red underlined. The DExDc helicase

domain (302-392) is grey shaded and the helicase motifs (I: ³⁰⁸LPTGSGKTRV³¹⁷, II: ⁴²⁰IIIDECHHT⁴²⁷; III: ⁴⁶⁵GLTAS⁴⁶⁹; IV: ⁶⁷⁴IIFTKTRR⁶⁸¹; V: ⁷⁴¹TTVAEEGLDI⁷⁵⁰; VI: ⁷⁷⁰QALGRGRA⁷⁷⁷) are indicated by a black bar with the corresponding numbers written on it. ATP binding site ³¹¹GSGKT³¹⁵ is red, bold and grey shaded. MDA5 insert domain (residues 522-647) is split underlined. The HELIc domain (residues 644-786) is red and bold. RNA binding loop (⁸⁹⁸TSPPERLLDY⁹⁰⁷) is boxed. RIG-I_C-RD (residues 854-973) is grey shaded, red wave underlined. The Zn²⁺ motifs (⁸⁶⁰CRGC⁸⁶³ and ⁹¹⁵CKDC⁹¹⁸) indicated with a black bracket and name written on the top.

Table 3. Pairwise alignment of RbMDA5

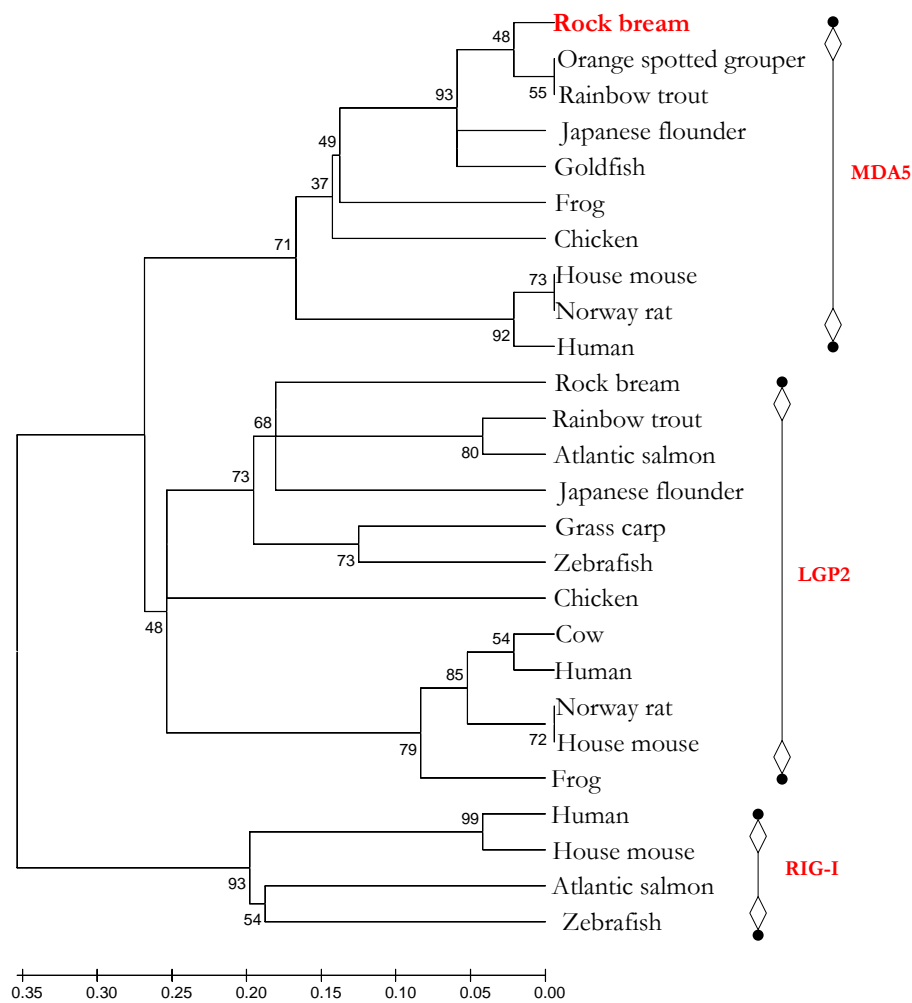
Pairwise alignment of RbMDA5, accomplished using MatGat program with complete amino acid and CARD region sequences of MDA5 homologues obtained from different organism.

Identity percentage is denoted by “I” and similarity by “S”.

Species	Taxonomy	Full protein		CARD region		Accession No.	Database
		I	S	I	S		
Rock bream	Actinopterygii	100	100	100	100	KF267452	
Orange spotted grouper	Actinopterygii	74	84	64	75	AEX01716	GenBank
Olive flounder	Actinopterygii	72	83	61	74	ADU87114	GenBank
Rainbow trout	Actinopterygii	65	78	53	67	NP_001182108	NCBI
Gold fish	Actinopterygii	58	75	46	64	AEN04473	GenBank
Grass carp	Actinopterygii	56	72	45	62	FJ542045	GenBank
Human	Mammalia	47	65	42	60	AAG34368	GenBank
Chicken	Aves	48	66	39	59	BAJ14020	GenBank
House mouse	Mammalia	47	67	42	62	AAM21359	GenBank
Frog	Amphibia	46	66	34	54	XP_002933320	NCBI
Norway Rat	Mammalia	46	66	40	60	NP_001102669	NCBI
Pacific oyster	Bivalvia	25	43	16	33	EKC38304	GenBank

Table 4. Conservation of helicase domain motifs in MDA5 orthologues.

Species	Helicase domain motifs					
	I	II	III	IV	V	VI
Rock bream	LPTGSGKTRV	IIIIDECHHT	GLTAS	IIFTKTRR	TTVAEEGLDI	QALGRGRA
Orange spotted grouper	LPTGSGKTRV	IVIDECHHT	GLTAS	IIFTKTRR	TTVAEEGLDI	QARGRGRA
Olive flounder	LPTGSGKTRV	IIDECHHT	GLTAS	IIFTKTRR	TTVAEEGLDI	QARGRGRA
Rainbow trout	LPTGSGKTRV	IVIDECHHT	GLTAS	IIFTKTRR	TTVAEEGLDI	QARGRGRA
Gold fish	LPTGSGKTRV	MVIDECHHT	GLTAS	IIFTRTRL	TTVAEEGLDI	QARGRGRA
Grass carp	LPTGSGKTRV	MVIDECHH	GLTAS	IIFTRTRL	TTVAEEGLDI	QARGRGRA
Human	LPTGSGKTRV	IIIIDECHHT	GLTAS	IIFTKTRQ	TTVAEEGLDI	QARGRGRA
Chicken	LPTGSGKTRV	IIIIDECHHT	GLTAS	IIFTKTRQ	TTVAEEGLDI	QARGRGRA
House mouse	LPTGSGKTRV	IIIIDECHHT	GLTAS	IIFTKTRQ	TTVAEEGLDI	QARGRGRA
Frog	LPTGSGKTRV	IIIIDECHHT	GLTAS	IIFTKTRQ	TSVAEEGLDI	QARGRGRA
Norway Rat	LPTGSGKTRV	IIIIDECHHT	GLTAS	IIFTKTRQ	TTVAEEGLDI	QARGRGRA
Consensus %	100%	96%	100%	97%	99%	99%



1

Fig. 4. Phylogenetic analysis of RbMDA5 with LGP2, RIG-I and MDA5 sequences.

The tree was constructed by the minimum evolution method in MEGA 5.0 using the full-length amino acid sequences. The RIG-I and LGP2 sequences were obtained from GenBank. The accession numbers of LGP2 sequences are Rainbow trout: CAZ27718, Japanese flounder: ADI75503, Atlantic salmon: NP_001133649, Grass carp: ACY78116, Zebrafish: NP_001244086; Chicken: AEK21509, Cow: NP_001015545, Human: NP_077024, Norway rat: NP_001092258, House mouse: NP_084426, Frog: NP_001085915. The accession numbers of the RIG sequences are Human: AF038963, House mouse: AY553221, Atlantic salmon: NP_001157171, zebrafish: ENSDART00000058176. The accession numbers of the MDA5 sequences are tabulated in Table 3.. Numbers above the line indicate percent bootstrap confidence values derived from 5000 replications.

2.3.2 Genomic characterization of *RbMDA5*

The BAC PCR using cDNA specific oligos yielded a clone that spanned the entire MDA5 genome with additional 5' and 3' flanking sequences. The genome of *RbMDA5* (10689 bp) possessed 16 exons split by 15 introns (**Fig. 5**). The exon-intron junctions were consistent with the GT/AG rule. The *RbMDA5* genome size was nearly similar to that of flounder *MDA5*, with shorter introns compared to the human *MDA5*. Although the number of exons (16) and introns (15) were similar to those present in other vertebrates, variations could be observed in the sizes of coding exons. The domain distribution among the exons was similar to that of flounder and human *MDA5*. The two CARDS were coded by 1st exon and 2nd exon. The helicase domains and RD were coded by nucleotides in exons 5 to 13 and 14 to 16, respectively. The nucleotides present in exons 5 and 7 codes for the ATPase A motif (³¹⁰TGSGK³¹⁵) and ATPase B motif (⁴²²DECH⁴²⁵), respectively. The RNA destabilizing motif

(⁴⁶⁵GLTAS⁴⁶⁹) locates to 7th exon and positive charge cluster for potential RNA binding
(⁷⁷⁰QALGRGRA⁷⁷⁷) to 13th exon.

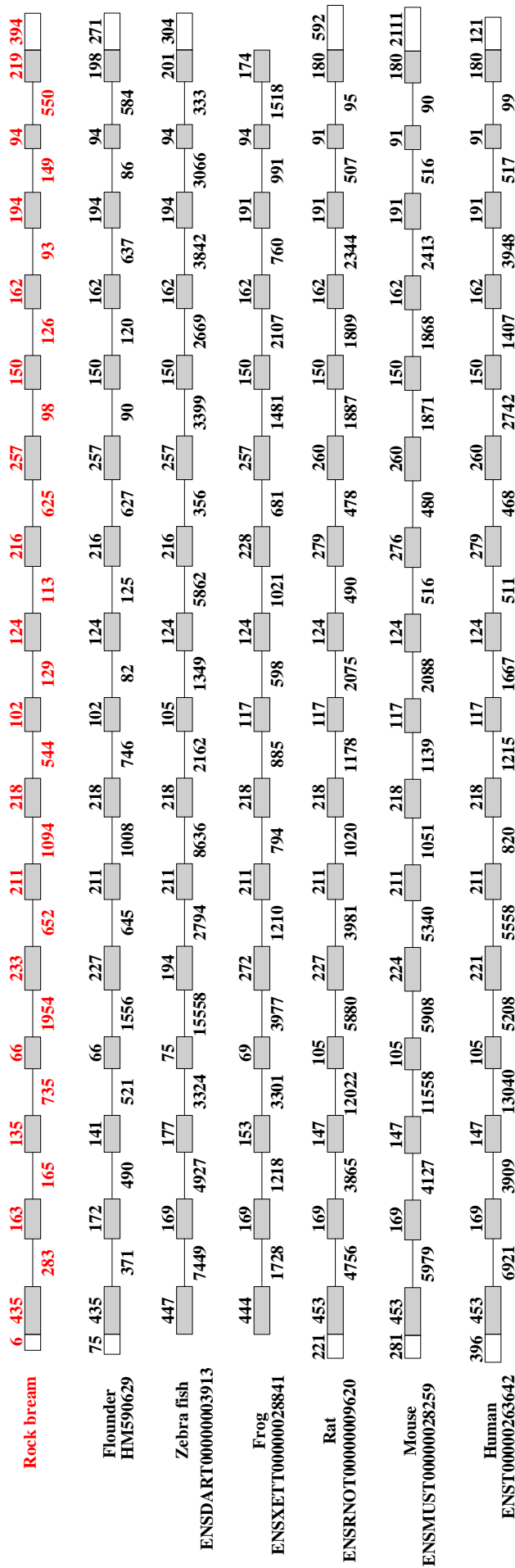


Fig. 5. Genomic structure comparison of *RbMDA5* with other *MDA5* homologues.

The exon-intron structures were derived from exon-view of Ensembl. The ensemble ids are indicated in brackets. The translated/coding regions are denoted by dark shaded boxes and the introns are denoted by lines. Exon sizes are indicated above the exon boxes and intron lengths are shown below the intron lines. Untranslated regions at the 5'- and 3'-ends are denoted by empty boxes.

2.3.3 Promoter analysis of *RbMDA5*

The putative promoter and 5' flanking region analysis revealed the presence of putative binding sites for various transcription factors. Proximal region revealed the presence of activator protein-1 and -4 (AP-1 and -4), interferon regulatory factor-1 and -2 (IRF-1 and -2), c-Rel, Lyf-1, Sp1, cAMP response element binding protein (CREB), Interferon-sensitive response element (ISRE), Oct-1, AML-1a and heat shock factor 2 (HSF2) while CCAAT-enhancer binding protein- α , - β (C/EBP α and β), HNF-3b, and P300 could be observed distantly (**Fig. 6**).

AGTTGTGTCA **CTGGATTT** **CCCTTTTT** AAGTCCATATAGGTGTGTTTACAATGAAAACAC -1500
 c-Rel IRF-2
 TGTGGTACTTCTGCAGTATGTACGGACTAAGAGAGACATGATGATGTGAATTGTCCAGG -1440
 CGATGAAAGGCCAGGTATCATTATATTGTACATACTTTGTTGCTGGTGTAGTAGCAGTA -1380
 GAGTTGTTGGGTGGGTTTGG **GGGATGAGCTGTGTTCAG** GGAGCCCAGAAACCACACTTG -1320
 AP-4
 AATGAAACTATGCTGTAGTATGAATTGAGAGAATAA **TGTGGGATA** CTCATGTGAAGGACA -1260
 Lyf-1
 GGGGATATAAATTAGGCCAT **GTATAGTGTAATATC** AATAAAAATAACATATATTTTATACT -1200
 C/EBP β
 TAGCTTT **TGAGG** TGATTATGTATATACCATTGACTGGCAAATGTAGTTTTGATTGTT **GTCT** -1140
 AML-1a
TAGGAAAAAC AGAACTAGGCATTCACTACACATTACTAAGCAGTGGTAAAAGGAGGATAG -1080
 C/EBP β
 AAATCCTAGT **GGCAAACCCA** CAATCA **GAAGATACT** CCAATCAAAGTAATCTCGCACTGA -1020
 c-Rel HSF2
 CAATTTTACTCAGATAAGTAAAAAAA **CACATATATAT** GTATTTGCATAAAAACATTCTTA -960
 HNF-3b
 CAATAAGTATCAACAGTGGCGTTTTTTTTCCCTTTCATAGTCTTAAA **TTATTGATAAAC** TA -900
 C/EBP α
 ATCCTAACCCATTGTA **ATGTTGT** AGGGATCCATGTCTGACTACTGC **CTCACGTT** GCTGGG -840
 AML-1a AP-1
 TGTCCATGGCAATATATCAT **ATTTTCATGAGTT** TTCAGTTCATCTCACTGGCATGTCTTGA -780
 C/EBP β
 TCTGCAAAGTAACTACAGTTGTTGATAAATGTAATGGA **GTAGGGAGTATGATAT** TTCCCT -720
 P300
 CTCAGTGGAGTATTTCTGCTCCTGCACAAAATAAAAAAAAAAAGAACGGTACTTAAAGG **CC** -660
CTGCCC TGCTACCAACACAAGTGTTTTTAAATACTCTGGCTGATATGAGCTATGCTGGG -600
 Sp1
 AATTTAAAT **GAGGTC** ACCAAAGTCAGTGTACCAATAACAATGGTAGAGGTGCAAGTTGTCC -540
 CREB
 CGCCTTTACAG **CTGAGACAG** TGAGAGTGAGGGAGGTGTCAATCAAATGGTCTGCACACGC -480
 AP-1
CACACCC TCCTAATCAGAAAACGTGTGTAGGGCCTTTAACTAA **ATGTGC** TGACACTCAC -420
 AML-1a AML-1a
 CTCTAAATAAAGTACCTAAATACTTTTATAATCATTTTTT **ATAATTATTGCACAA** ATGCA -360
 Oct-1
 ACGCCCTATTAACAGCTGAATACTCAGTCC **TTATGG** TTCACTGTT **GGAATATTA** GAA -300
 AML-1a HSF2
 GCATGTGCTTTTAAAAATAGAAAACAGCTGTAATGCCTCTGTCACCGGTGTACGTGCAG -240
 AGACCTACTCACTATGCTCCAAT **ACTGACACCT** AGCGGTCACTTTAATTGTTAAAGAGTT -180
 AP-1
 TT **GGAAAAACGAAAG** TAAAA **GAGTTTCTTTTTCC** TCCACACA **GTGAATCATC** GTTTTTATT -120
 IRF-1/IRF-2 ISRE AP-1
 CTGCCAGTAAGTTGCACTACGCA **GGAGTCAGC** CATCATCAGTGT **ATTGATAA** GGTGG -060
 AP-1 AP-1
 GTCGTAATG
 ↑ *M

Fig. 6. Analysis of the *RbMDA5* gene 5'-flanking region.

The transcription factor binding sites are red colored, bold, underlined and denoted with the corresponding name below. The transcription initiation site (G) is denoted by an upward-facing arrow. The start codon is purple colored and indicated by a “*” with a methionine residue written below.

2.3.4 Spatial expression analysis of *RbMDA5*

RbMDA5 mRNA was analyzed in various tissues to understand its physiological significance. *RbMDA5* was observed to be ubiquitously expressed in all the examined tissues. Highest level of expression could be found in blood. Relatively similar levels of expression could be observed in liver and heart. Moderate level of expression could be observed in spleen and gill (Fig. 7).

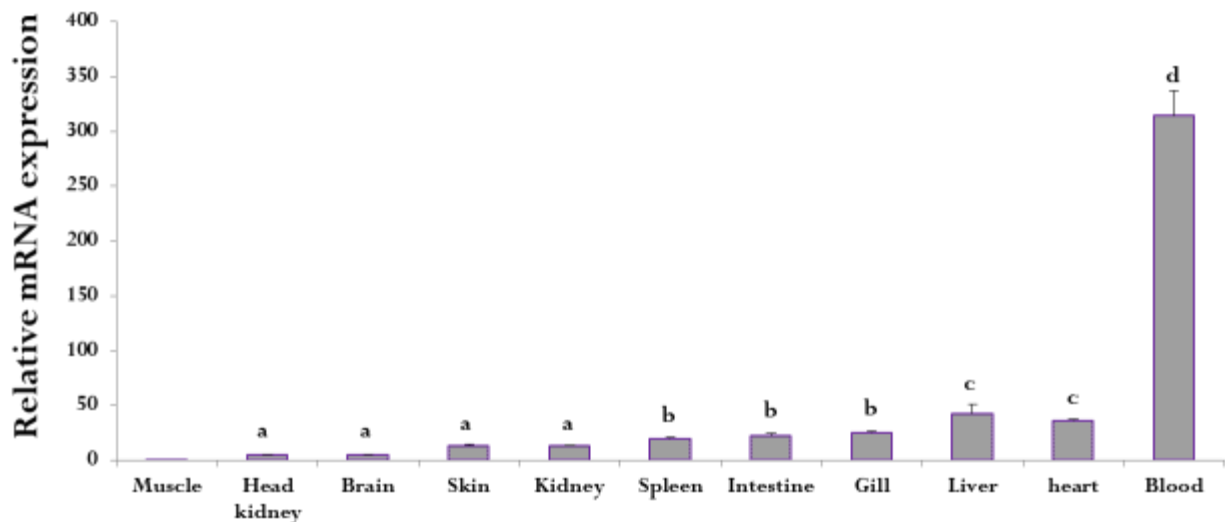


Fig. 7. Tissue distribution analysis of *RbMDA5*.

RbMDA5 tissue-specific expression in muscle, head kidney, brain, skin, kidney, spleen, intestine, gill, liver, heart tissues, and blood collected from unchallenged rock bream was analyzed using quantitative RT-PCR. Relative mRNA expression was calculated using the $2^{-\Delta\Delta Ct}$ method, with β -actin as the invariant control gene. In order to determine the tissue-specific expression, the relative mRNA level was compared with muscle expression. Data are presented as mean values (n=3) with error bars representing SD. Data shown with “*” indicates significant expression levels at $P < 0.01$.

2.3.5 Temporal expression analysis of *RbMDA5* after poly I:C challenge

In vivo modulation of *RbMDA5* mRNA after poly I:C challenge was detected in blood, gill, liver, spleen and head kidney. In blood and head kidney, induction of *RbMDA5* could be

observed from early 3 h to 12 h p.i., with highest level of modulation at 12 h (blood: 7.6-fold and head kidney: 6.1-fold). In blood, upregulation could be observed at 24 h p.i, whereas in head kidney, expression reached the basal level at 24 h p.i. In gill and spleen, similar pattern of expression could be observed from 6 h to 24 h p.i., with highest transcriptional change at 6 h p.i. (gill:2.8-fold and head kidney: 6- fold). However, in spleen upregulation was seen till 24 h p.i. In liver, up-regulation was observed from 3 h p.i. which existed till 12 h p.i, revealing highest expression at 6 h p.i. (6.4-fold) (Fig. 8).

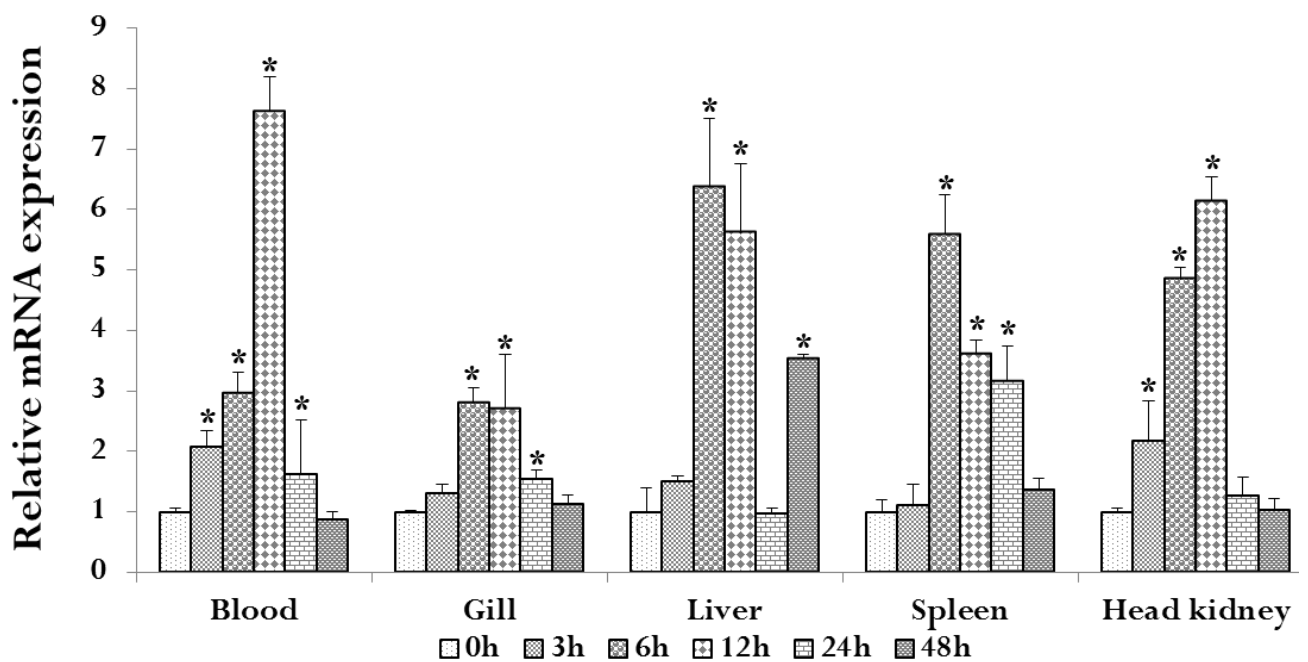


Fig. 8. *RbMDA5* expression analysis after poly I:C challenge.

RbMDA5 expression was analyzed in liver, blood, spleen, gill and head kidney post poly I:C challenge. Relative mRNA expression was calculated by the $2^{-\Delta\Delta C_t}$ method relative to PBS-injected controls and normalized with the same, with β -actin as the reference gene. Data are presented as mean values (n=3) with error bars representing SD. Data shown with “*” indicates significant expression levels at $P < 0.01$.

2.3.6 Antiviral activity of RbMDA5

In order to demonstrate the antiviral function of the *RbMDA5*, rock bream heart cells were transiently transfected with either the empty vector (pcDNATM 3.1/His B vector) or the pcDNA3.1-RbMDA5 and then infected with MABV. Infection of heart cells transfected with empty vector did not show any inhibition of virus similar to the virus infected control, where more than 90% of the cells showed CPE and were killed. Cells transfected with pcDNA3.1-RbMDA5 revealed strong inhibition of virus infection and cell protection. These results suggest the antiviral defense role of RbMDA5 against MABV (Fig. 9).

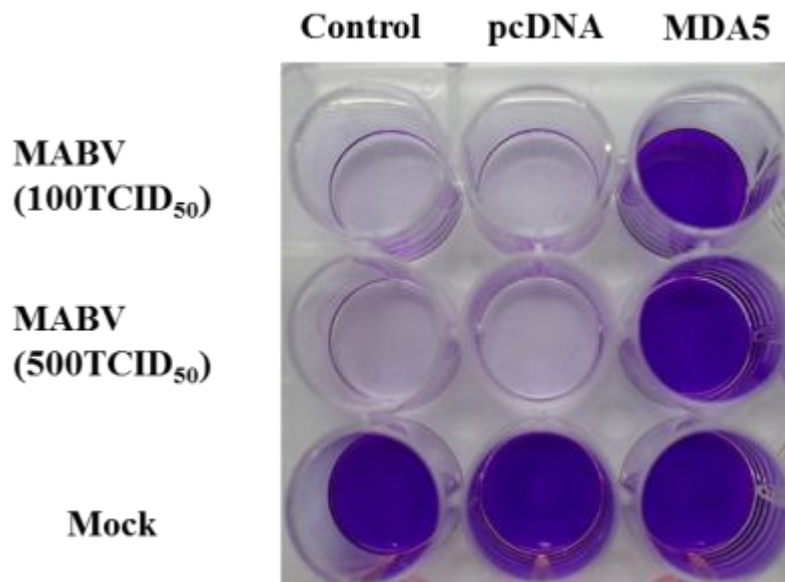


Fig. 9. Antiviral activity of RbMDA5.

The empty pcDNA 3.1 vector and pcDNA3.1-RbMDA5 were transfected into rock bream heart cells. After 48 h of transfection, at 24 °C, the cells were infected with MABV at indicated densities. After 7 days of infection, cells were fixed with 4% PFA and stained with 3% crystal violet.

2.4 Discussion

Innate immune defense against pathogenic infections commences with the identification of pathogen conserved non-self-molecular patterns named PAMPs. The extracellular, vacuolar and cytosolic compartments are under continuous screening for signs of infection. Viruses in particular accumulate viral RNAs or DNAs in the cytoplasm that originates from the incoming viral genome, viral transcripts, or transcription and replication intermediates (Thompson and Locarnini, 2007). Consequently, the viral nucleic acids become the major PAMPs for the cytosolic sensors. This recognition of viral PAMPs by the cytosolic sensors leads to the downstream activation of a robust program of gene expression that includes antiviral inflammatory cytokines, chemokines and IFNs. The early synthesis of IFNs not only prevents viral infection but also primes the subsequent development of antigen-specific T cell and antibody responses (Takaoka and Yanai, 2006).

RbMDA5 protein characterization revealed conserved motifs including CARDs, helicase domains, and RD. In mammals, RIG-I activation is initiated by binding of RNA to the RD, after which it attains the “active open” conformation and the CARDs interact with the CARDs of MAVS to induce the signaling cascade for IFN synthesis. According to this model, initiation of RIG-I signaling in part is controlled through a combination of RNA binding which initiates conformational changes that alter self-interactions, leading to signaling induction or suppression. Unlike RIG-I where the CARDs are sequestered before RNA binding, MDA5 does not sequester CARDs and MDA5 CARDs are involved in cooperatively assembling sensitive filaments on dsRNA and nucleate the assembly of MAVS into its active polymeric form (Berke et al., 2013). These data suggest that RIG-I and MDA5 may be regulated through different mechanisms, which needs further investigation in teleosts. MDA5 possesses a central DExD/H box RNA helicase domain (consisting of two RecA-like helicase domains, Hel1 and Hel2 and an insert domain, Hel2i) to bind and possibly unwind RNA with the energy generated by ATP hydrolysis. The RNA helicases belong to helicase

superfamily II, which is divided into three subfamilies DEAD, DEAH and DExH box containing helicases. MDA5 possesses conserved signatures belonging to the DExH subfamily of RNA helicases (Kang et al., 2004; Kang et al., 2002). MDA5 contain a C-terminal domain (CTD) which is proposed to be involved in autoregulation in RIG-I, but MDA5 CTD is not required for RNA binding but for assembling filaments (Berke et al., 2013). RbMDA5 revealed conservation in the functional domains with other homologues suggesting a similar function and regulatory mechanism in rock bream. The phylogenetic analysis revealed closer association of RbMDA5 with the fish homologues. Contrary to the presence of RIG-I only in Atlantic salmon and zebrafish, MDA5 is found in many fish species indicating that MDA5 might have evolved before RIG-I (Zou et al., 2009).

The genome of *RbMDA5* comprising 16 exons and 15 introns was similar to that of other vertebrates. However, the length of *RbMDA5* genome was similar to that of Japanese flounder *MDA5* while shorter than that of human (Ohtani et al., 2011). The coding region of *RbMDA5* was also highly similar to that of flounder *MDA5*, while little variation could be observed in the first four coding exons of zebrafish. The promoter analysis of *RbMDA5* revealed putative IRF and ISRE binding sites. MDA5 is an early response gene whose expression requires JAK/STAT signaling of the IFN pathway and is induced by IFN and TNF α (Gitlin et al., 2006; Kang et al., 2004). IRF-1 plays a vital role in controlling RIG-I expression (Su et al., 2007). MDA5 and RIG-I are IFN-inducible genes, creating a positive feedback-loop generating a potent anti-viral state (Kang et al., 2002). This suggests that MDA5 may be a target of regulation at the transcriptional level by the ISGF3 complex and presence of IRF and ISRE binding sites in the promoter of *RbMDA5* suggests a similar mechanism in rock bream.

Spatial expression analysis revealed ubiquitous expression in all the analyzed tissues with highest expression in blood, followed by liver and heart. Japanese flounder *MDA5* was

strongly detected in kidney, heart and muscle (Ohtani et al., 2011). Northern blot analysis employed to determine the human *MDA5* expression revealed high expression in spleen and placenta, while low levels of expression was determined in other tissues (Kang et al., 2004). Rainbow trout *MDA5* was constitutively produced in fibroblast and macrophage cell lines (Chang et al., 2011). *MDA5* from grass carp was highly expressed in gill, skin and spleen of healthy fish (Su et al., 2010). The ubiquitous and continuous expression in all the tissues suggests their constant role of surveillance for viral infections.

DsRNA is the genetic component of viruses with double stranded genomes and part of ssRNA with secondary structures. It can be generated during viral replication and RNA metabolism, making it the primary target for host PRRs. The synthetic analog of viral dsRNA, poly I:C triggers the innate immune system to secrete antiviral cytokines like IFN α/β and inflammatory cytokines. Temporal modulations of *RbMDA5* expression *in vivo* after poly I:C challenge revealed up-regulation mostly in the early phase of infection, in all the examined immune related tissues. Japanese flounder *MDA5* was induced in kidney and peripheral blood leukocytes after treatment with lipopolysaccharide (LPS) and poly I:C (Ohtani et al., 2011). Rainbow trout *MDA5* was also upregulated in fibroblast and macrophage cell lines post poly I:C treatment (Chang et al., 2011). Grass carp *MDA5* was induced in liver and spleen after Grass Carp Reovirus (GCRV with dsRNA as genome) administration (Su et al., 2010; Wang et al., 2012). Recently identified RIG-I homologue from grass carp also revealed upregulation post bacterial and viral stimulations (Chen et al., 2012). These data together with our results suggests that *MDA5* expression is induced by virus and viral mimics like poly I:C like the mammalian *MDA5* and play a defensive role against viral infections.

In vitro antiviral assays revealed that the rock bream heart cells transfected with *RbMDA5* and infected with MABV show delay in the appearance of CPE compared to the empty controls. *MDA5* portrayed potential antiviral activity against a variety of viruses

including ss(+)RNA viruses (*Picornaviridae*, *Caliciviridae* and *Flaviviridae*), ss(-)RNA viruses (*Paramyxoviridae*, *Orthomyxoviridae* and *Rhabdoviridae*), and dsRNA virus (*Reoviridae*) (Kato et al., 2006; McCartney et al., 2008; Siren et al., 2006). RIG-I and MDA5 shows preferential inhibition of viruses in mice (Kato et al., 2006). Japanese flounder MDA5 exhibited inhibition against both ssRNA (VHSV, HIRRV) and dsRNA viruses (IPNV). Our results suggest that RbMDA5 inhibits the replication of a dsRNA virus MABV, and stands as an affirmation for the RLR pathway in rock bream, with RbMDA5 added as a new member of the teleost RLR family.

In conclusion, this study affirmed the existence of an ancestral PAMP recognition receptor: MDA5 in rock bream through genomic and functional characterization. Our results demonstrate the induction of MDA5 by poly I:C and MDA5 inhibits the MABV infection. This study stands as an averment for the positive regulatory role of MDA5 in teleosts.

CHAPTER III

Characterization of the cytosolic sensor Laboratory of Genetics and Physiology 2 (LGP2)

3.0 Characterization of the cytosolic sensor Laboratory of Genetics and Physiology 2 (LGP2)

Abstract

Innate cytosolic surveillance for viral pathogen associated molecular patterns is performed by cytosolic receptors comprising of Laboratory of Genetics and Physiology 2 (LGP2) as one of the receptors. Rock bream LGP2 (*RbLGP2*) genome possessed 12 exons intervened by 11 introns. Putative promoter analysis revealed the presence of significant transcription factor binding sites. RbLGP2 protein revealed the conserved domains like DExD domain, regulatory domain and helicase domain. RbLGP2 did not possess CARD similar to the other LGP2 orthologues. RbLGP2 shared its highest with a teleost homologue, Olive flounder. Phylogenetic analysis revealed its closer association with fish homologues. Spatial expression analysis revealed ubiquitous presence in all the examined tissues with highest expression in blood. Temporal expression analysis post poly I:C challenge, revealed upregulation in various immune related tissues like gill, liver, spleen, head kidney and blood cells. Recombinant RbLGP2 protein prevented rock bream cells from infection against marine birnavirus revealing its antiviral activity. Thus, RbLGP2 is an evolutionarily conserved protein involved in defense against viruses in rock bream.

3.1 Introduction

Innate immunity is the primitive defense barrier against pathogenic invasion in all organisms, ranging from invertebrates to vertebrates. The initiation of anti-pathogenic responses begins with the recognition of conserved pathogen associated molecular patterns (PAMPs) including proteins, lipids and nucleotides characteristic of the pathogens but not the host, by pattern recognition receptors (PRRs) (Kawai and Akira, 2010; Kumar et al., 2011; Rathinam and Fitzgerald, 2011). The extracellular and cytoplasmic surveillance of pathogen invasion is executed by PRRs including Toll-like receptors (TLRs), retinoic acid induced RIG-like receptors and nucleotide oligomerization domain containing (NOD-like) receptors (Rathinam and Fitzgerald, 2011). Inside the cell, TLRs 3, 7, 8 and 9 localize to the endocytic compartments, where TLRs 3, 7, and 8 scan for the presence of double stranded (ds) RNA and single stranded (ss) RNA viruses, while TLR9 is involved in non-methylated CpG DNA recognition. The RIG-I like receptors (RLRs), comprising of three members, retinoic acid-inducible gene I (RIG-I, also called DEAD (Asp-Glu-Ala-Asp) box polypeptide 58 (DDX58)), melanoma differentiation-associated gene 5 (MDA5, also called interferon induced with helicase C domain 1 (IFIH1)), and laboratory of genetics and physiology 2 (LGP2, also called DExH (Asp-Glu-X-His) box polypeptide 58 (DHX58)), are crucial in triggering interferon (IFN) response against intracellular RNA virus (Rathinam and Fitzgerald, 2011; Yoneyama and Fujita, 2007a). NLRs are primarily involved in bacterial detection (Rosenstiel et al., 2007).

The members of RLR family are structurally conserved in sharing a common functional RNA helicase domain near the C terminus (HELICc) which specifically binds to the RNA molecules of viral origin. The members of this family also hold a distinct core ATP dependent DExD/H domain, containing a conserved motif Asp-Glu-X-Asp/His (DExD/H),

involved in ATP-dependent RNA or DNA unwinding. RIG-I and MDA5 proteins possess two tandem arranged caspase activation and recruitment domains (CARDs) involved in protein-protein interactions, at the N terminal region, while CARD domain is absent in LGP2. Regarding the specificity of viral detection, RIG-I is sensitive to a wide range of viruses including paramyxoviruses, orthomyxoviruses, and the rhabdovirus *vesicular stomatitis virus* (Hornung et al., 2006; Kato et al., 2005; Kato et al., 2006; Pichlmair et al., 2006) whilst MDA5 is evoked by picornaviruses (Gitlin et al., 2006; Kato et al., 2006). RLRs recognize distinct patterns of viruses (Loo et al., 2008). MDA5 exclusively binds long, capped di- or mono-5' phosphate dsRNAs whilst RIG-I possesses high binding affinity for short dsRNA or 5'ppp uncapped ssRNA (Kato et al., 2006).

The viral nucleic acids accumulated in the cytosol during viral infection, serve as potential PAMPs recognized by the cytosolic sensors like RLRs. Specific binding of the virus specific RNA species (dsRNA or 5'-triphosphate ssRNA) to the RNA binding domain in the sensors RIG-I/MDA5 change their “closed” structure confirmation, releasing the CARD. The CARD relays signals to the downstream signaling molecule MAVS present on the outer membrane of mitochondria, through CARD-CARD interactions. The signaling bifurcates at MAVS, resulting in the activation of NF- κ B and IRF3/IRF7. The latter pathway involves the TNF (tumor necrosis factor) receptor-associating factor 3 (TRAF3) and the protein kinases, I κ B kinase-I (IKK-i (ϵ)) or TANK-binding kinase-1 (TBK-1), responsible for the phosphorylation and activation of latent IRF-3 and -7. IRF3, essential for the primary activation of IFN genes is phosphorylated at specific serine residues by two members of the I κ B kinase (IKK) family, TANK-binding kinase 1 (TBK1) and IKKi/IKK ϵ culminating in the induction of IFN and other antiviral effector genes in the nucleus. IRF7 is also known to be regulated by these kinases and is involved in the secondary induction of IFN genes (Matsui et al., 2006; Pichlmair and Reis e Sousa, 2007; Yoneyama and Fujita, 2007a).

LGP2 is a virus inducible gene belonging to the RLR family and sharing structural similarity of 30-40% with RIG-I and MDA5, except for the CARD domain. Its role in antiviral defense is contradictory as it was first discovered that RIG-I/MDA5 directed IFN response was negatively regulated by LGP2 (LGP2 lack CARD domain and hence unable to interact with MAVS) (Diperna, 2005) and later additional evidence indicated that LGP2 is required for virus recognition by RIG-I and MDA5 (Sato et al., 2010). The negative regulation of LGP2 is performed either by binding of LGP2 to dsRNA and preventing RIG-I and MDA5-mediated recognition or by inhibiting multimerization of RIG-I and its interaction with MAVS via the RD of LGP2 or by competing with IKK- ϵ for a common interaction site on MAVS (Komuro and Horvath, 2006; Vitour and Meurs, 2007; Zou et al., 2009). In teleosts, LGP2 homologue has been identified and demonstrated to play a significant role in antiviral defense in rainbow trout (Chang et al., 2011), grass carp (Huang et al., 2010b), Atlantic cod (Seppola et al., 2009), and Olive flounder (Hikima et al., 2012; Ohtani et al., 2010).

In this study, we have identified an LGP2 homologue from rock bream (designated as RbLGP2) and characterized from the genomic to proteome level. We have demonstrated the antiviral activity of the *RbLGP2* gene using rock bream cells and analyzed the transcriptional modifications *in vivo* after poly I:C challenge.

3.2 Materials and methods

3.2.1 Animal rearing, cDNA library construction and *RbLGP2* gene identification

Healthy rock bream fish with average weight of ~50 g, procured from the Ocean and fisheries Research institute (Jeju, Republic of Korea) were adapted to the laboratory conditions (salinity $34 \pm 1\%$, pH 7.6 ± 0.5 at 24 ± 1 °C) in 400 L tanks. Blood samples were harvested from the caudal fin of healthy, unchallenged fish using a 22 gauge needle and

centrifuged immediately for 10 min at $3000 \times g$ at $4\text{ }^{\circ}\text{C}$, to collect the hematic cells. Gill, liver, brain, kidney, head kidney, spleen, intestine, muscle and skin tissues were harvested on ice from three healthy animals and immediately flash-frozen in liquid nitrogen and stored in $-80\text{ }^{\circ}\text{C}$, until RNA extraction. Tri Reagent[™] (Sigma, USA) was employed to obtain total RNA from tissues. The concentration and purity of RNA were evaluated using a UV-spectrophotometer (BioRad, USA) at 260 and 280 nm. Purified total RNA samples were subjected to mRNA purification using Micro-FastTrack 2.0 mRNA isolation kit (Invitrogen). First strand cDNA was synthesized from 1.5 μg of mRNA using Creator[™] SMART[™] cDNA library construction kit (Clontech, USA); amplification was performed with Advantage 2 polymerase mix (Clontech) under conditions of $95\text{ }^{\circ}\text{C}$ for 7 s, $66\text{ }^{\circ}\text{C}$ for 30 min and $72\text{ }^{\circ}\text{C}$ for 6 min. Over-representation of the most commonly expressed transcripts was excluded by normalizing the synthesized cDNA using Trimmer-Direct cDNA normalization kit (Evrogen, Russia).

A cDNA GS-FLX shotgun library was created from the sequencing data obtained by using the GS-FLX titanium system (DNA Link, Republic of Korea). A cDNA contig showing high homology to the earlier identified LGP2 homologues was identified using BLAST and designated as *RbLGP2*.

3.2.2 BAC library creation and identification of *RbLGP2* BAC clone

Rock bream obtained from the Jeju Special Self-Governing Province Ocean and Fisheries Research Institute (Jeju, Republic of Korea) were accustomed to the laboratory conditions. Blood was harvested aseptically from the caudal fin using a sterile 1 mL syringe with 22 gauge needles, and a BAC library was constructed from the isolated blood cells (Lucigen Corp., USA). Briefly, genomic DNA obtained from blood cells was randomly sheared and the blunt ends of large inserts ($>100\text{ kb}$) were ligated to pSMART BAC vector to

obtain an unbiased, full coverage library. Around 92160 clones, possessing an average insert size of 110 kb, were arrayed in 240 microtiter plates with 384 wells.

A two-step PCR based screening method was used to identify the clone of interest based on manufacturer's instructions. Primers were designed based on the cDNA sequence identified from the cDNA database. A gene specific clone was isolated and purified using Qiagen Plasmid Midi Kit (Hidden, Germany). The sequence was confirmed by pyrosequencing (GS-FLX titanium sequencing, Macrogen, Republic of Korea). The gene specific primers employed in the identification of the clone from the BAC library are tabulated in Table 5..

Table 5. Primers used in RbLGP2 characterization and qRT-PCR.

The restriction sites are in small letters.

Gene	Purpose	Orientation	Primer sequences (5'-3')
RbLGP2	BAC screening & qRT-PCR	Forward	TCGATGAGTGTCCACCACACCAACA
RbLGP2	BAC screening & qRT-PCR	Reverse	TGACTGAATCCAGGTTGGCACAGA
RbLGP2	pcDNA cloning	Forward	GAGAGaattcTATGGCAGAATTTGAACTGTACGCATACCA
RbLGP2	pcDNA cloning	Reverse	GAGAGActcgagTTAGTCGAAGATGTTAGGGAAGTGGTCTTGG
β -actin	qRT-PCR amplification	Forward	TCATCACCATCGGCAATGAGAGGT
β -actin	qRT-PCR amplification	Reverse	TGATGCTGTTGTAGGTGGTCTCGT

3.2.3 Sequence characterization, genome structure and phylogenetic analysis of RbLGP2

A cDNA sequence homologous to earlier identified LGP2 sequences in NCBI was identified by BLAST and was subjected to DNAssist2.2 to predict the open reading frame (ORF) and translate nucleotide to protein. The conserved domains were identified using Expasy (<http://www.expasy.org/>), SMART (<http://smart.embl-heidelberg.de/>) and conserved domain database search (CDD). Pairwise alignment and multiple sequence alignment were executed using ClustalW (Thompson et al., 1994). A phylogenetic tree was reconstructed

using minimum evolution method available in MEGA 5.0, with bootstrap values calculated with 5000 replications to estimate the robustness of internal branches (Tamura et al., 2011). The amino acid identity percentages were calculated by MatGAT program using default parameters (Campanella et al., 2003). The exon-intron structure was determined by aligning mRNA to the genomic sequence of *RbLGP2* using Spidey available on NCBI (<http://www.ncbi.nlm.nih.gov/spidey/>) (Wheelan et al., 2001). The complete genomic structure and putative promoter region were determined from the BAC sequencing data. The genomic structures used for comparison were obtained from exon view of Ensembl genome database. The transcription factor binding sites (TFBS) in the promoter region were predicted using TFSEARCH, TESS and TRANSFAC.

3.2.4 Transcriptional profile of *RbLGP2* gene in challenged and normal tissues

3.2.4.1 Poly I:C challenge

In order to monitor the transcriptional changes of *RbLGP2* post dsRNA injection *in vivo*, poly I:C was employed as an immunostimulant. Sterile poly I:C stock was prepared by dissolving poly I:C at the rate of 1.5 mg/ml in PBS and filtered through a 0.2µm filter. A time course experiment was performed by intraperitoneally injecting the animals with 100 µL suspension of poly I:C stock. The control animals were injected with an equal volume of PBS. Liver, gill, spleen, head kidney tissues and whole blood cells were harvested from the un-injected, PBS-injected and immune challenged animals at time points of 3, 6, 12, 24, and 48 h post injection/infection (p.i.).

3.2.4.2 RNA isolation and cDNA synthesis

In order to perform the tissue distribution profiling of *RbLGP2*, gills, liver, brain, kidney, head kidney, spleen, intestine, muscle and skin tissues and whole blood cells were

harvested from un-injected fish. After challenge with PBS and poly I:C, gill, liver, spleen, head kidney tissues and whole blood cells were harvested from challenged animals at the corresponding time points. Total RNA was obtained from tissues using Tri Reagent™ (Sigma, USA). The concentration and purity of RNA were evaluated using a UV-spectrophotometer (BioRad, USA) at 260 and 280 nm. The RNA was diluted to 1 µg/µL and cDNA was transcribed from 2.5 µg of RNA from each tissue using a PrimeScript™ first strand cDNA synthesis kit (TaKaRa). Concisely, RNA was incubated with 1 µL of 50 µM oligo(dT)₂₀ and 1 µL of 10 mM dNTPs for 5 min at 65 °C. After incubation, 4 µL of 5× PrimeScript™ buffer, 0.5 µL of RNase inhibitor (20 U), 1 µL of PrimeScript™ RTase (200 U), were added and incubated for 1 h at 42 °C. The reaction was terminated by adjusting the temperature to 70 °C for 15 min. Finally, synthesized cDNA was diluted 40-fold before storing at -20 °C for further use.

3.2.4.3 Tissue distribution

Quantitative reverse transcription polymerase chain reaction (qRT-PCR) was used to examine tissue distribution of *RbLGP2* mRNAs in various tissues of healthy fish. qRT-PCR was performed in a 15 µL reaction volume containing 4 µL of diluted cDNA, 7.5 µL of 2× SYBR Green Master Mix, 0.6 µL of each primer (10 pmol/µL) and 2.3 µL of PCR grade water and subjected to the following conditions: one cycle of 95 °C for 3 min, amplification for 40 cycles of 95 °C for 20 sec, 58 °C for 20 sec, 72 °C for 30 sec. The baseline was automatically set by the Thermal Cycler Dice™ Real Time System software (version 2). In order to confirm that a single product was amplified by the primer pair used in the reaction, a dissociation curve was generated at the end of the reaction by heating from 60 °C to 90 °C, with a continuous registration of changes in fluorescent emission intensity. The Ct for the *RbLGP2* (target gene) and *β-actin* (internal control) were determined for each sample. The

differences between the target and internal control Ct, called Δ Ct were calculated to normalize the differences in the amount of total cDNA added to each reaction and the efficiency of the RT-PCR. The Δ Ct for each sample was subtracted from Δ Ct of the calibrator and this difference was called $\Delta\Delta$ Ct and the *RbLGP2* gene expression was determined by Livak comparative Ct method. The relative expression level calculated in each tissue was compared with respective expression level in muscle.

3.2.4.4 Temporal RbLGP2 mRNA expression analysis post poly I:C challenge

qRT-PCR was performed with cDNA prepared from RNA obtained from gill, liver, spleen, head kidney tissues and whole blood cells isolated from PBS and poly I:C challenged animals. qRT-PCR conditions were the same as used for tissue distribution profiling. The Δ Ct for each sample was determined by the method described above and subtracted from Δ Ct of the un-injected control and this difference was called $\Delta\Delta$ Ct. The relative expression of *RbLGP2* was determined by the Livak method. The relative fold change in expression after immune challenges was obtained by comparing the relative expression to corresponding PBS-injected controls. The expression normalized to PBS-injected controls is represented in the figures.

All experiments were performed in triplicate. All data have been presented in terms of relative mRNA expressed as means \pm standard deviation (S.D.). Statistical analysis was performed using un-paired two-tailed Student's t-Test. *P*-values of less than 0.01 were considered to indicate statistical significance.

3.2.5 Construction of expression vector and antiviral assay

3.2.5.1 Cell lines and viruses

Rock bream heart cells were established as previously described (Wan et al., 2012). Concisely, heart tissue was aseptically isolated from healthy rock bream fish (n=3). The tissue was minced into small pieces (approximately 1 mm³ in size) and washed thrice with HBSS (Sigma) containing antibiotics (400 IU/ml penicillin and 400 µg/ml streptomycin). Then, the tissue was digested in 0.2% collagenase II (Sigma) solution for 2 hours at 20 °C. The digestion mixture was filtered through a cell strainer (70 µm mesh size), centrifuged at 1000 rpm for 10 min. The cells were resuspended in Leibovitz's L-15 medium supplemented with 20% FBS, 100IU/ml penicillin and 100µg/ml streptomycin, and inoculated into 75 cm² cell culture flask. The cells were sub-cultured more than three times and adapted to 15% FBS. Cells' susceptibility to MABV infection was tested. The 80% confluent monolayer cells were treated with serially diluted MABV and the plates were kept at room temperature (RT) for 2 h for adsorption and facilitate viral infection. The plates were then incubated at 24 °C for 72 h. The susceptibility of rock bream heart cells for MABV infection was confirmed by observing the cytopathic effect (CPE) and the maximal non-cytotoxic concentration was determined and used for the subsequent antiviral activity assay. MABV was kindly provided by Prof. Sung-Ju Jung (Department of Aqualife Medicine, Chonnam National University, Republic of Korea).

3.2.5.2 Construction of expression vector

The full length ORF of *RbLGP2* (2046 bp) was amplified from liver cDNA using gene specific primers (Table 5.) and PCR and cloned into TA vector (Takara, Japan). The orientation and sequence was confirmed by restriction digestion and sequencing, respectively. The *RbLGP2* ORF cloned into TA vector was used as the template and the amplified PCR product was digested with *EcoRI* and *XhoI*. The digested PCR products were purified using Gel purification kit (Bioneer) and ligated overnight at 4 °C with *EcoRI* and *XhoI* digested

pcDNA™ 3.1/His B vector (Life Technologies). The ligation mixture was transformed into *E. coli* DH5 α cells and the clone harboring the recombinant plasmid was sequenced. The affirmed clone harboring the *rRbLGP2* was selected and named as pcDNA3.1-RbLGP2.

3.2.5.3 Antiviral assays

A monolayer of rock bream heart cells were cultured in 24 well plates at 24 °C, 24 h prior to transfection. Before transfection, cells were washed once with sterile PBS, and then replaced with Opti-MEM (Life technologies). The transfection procedure was performed with Lipofectamine™2000 (Life technologies), as per manufacturer's instructions. Briefly, 1.5 μ g of pcDNA vectors (empty pcDNA3.1 and pcDNA3.1-RbLGP2) were mixed with 1 μ L of Lipofectamine™ 2000 and transfected into the heart cells in 100 μ L Opti-MEM, and then cultured at 24 °C for 48 h. After 48 h, cells were infected with MABV and left at RT for 1 h for adsorption. The cells were then cultured with Leibovitz's L-15 medium and observed for the appearance of CPE. The cells transfected with empty pcDNA3.1 and pcDNA3.1-RbLGP2, but not infected with virus served as the mock infection control. After 7 days of MABV infection, the cells were washed once with PBS, fixed with 4% paraformaldehyde (PFA) and stained with 3% crystal violet for visualizing live cells.

3.3 Results

3.3.1 RbLGP2 identification, sequence characterization and phylogenetic analysis

A search of rock bream cDNA library for genes involved in antiviral immunity resulted in a cDNA contig which when subjected to BLASTX shared highest homology with the Olive flounder LGP2 and revealed conserved DEXDc and HELICc domains. The identified cDNA sequence was named as *RbLGP2*. The cDNA comprised of a 5' untranslated region (UTR) of 105 bp, coding region of 2046 bp and 3' UTR of 718 bp. The ORF encoded for a protein of 681 amino acids with a molecular mass of 77 kDa and isoelectric point of 6.7.

The 3' UTR revealed two mRNA instability motifs. The RbLGP2 protein length was three amino acids excess than the human and mouse homologues. Subjecting the derived RbLGP2 protein to the CDD in NCBI revealed several conserved motifs common among the other homologues. RbLGP2 possessed one DEXDc (DEAD/DEAH box helicase domain) (residues 1-174) in the N-terminal region, one ResIII (conserved restriction domain of bacterial type III restriction enzyme; residues 3-223), one HELICc (helicase superfamily c-terminal domain; residues 339-507), RIG-I_C-RD (C-terminal domain of RIG-I/ regulatory domain/ repressor domain; residues 552-675), one MDA5_ID (insert domain of MDA5 helicase and similar proteins; residues 230-309), RNA binding loop (residues 596-607). There were two predicted zinc binding motifs (residues 556-561 and 610-618). RbLGP2 protein portrayed the presence of six significant motifs including DEXD/H box for RNA helicase activity (**Fig. 10**). Pairwise alignment of RbLGP2 shared highest identity and similarity of 79 and 90%, respectively with the olive flounder LGP2. RbLGP2 shared more than 60% of identity with fish homologues while 46 to 51% identity with the other vertebrates. However, RbLGP2 DEXD/H (69-85% identity) and HELICc domains (68-80% identity) possessed high percentage of identity with the respective domains of fish homologues (**Table 6. and 3.3**). Multiple sequence alignment showed high degree of conservation in the domain specific regions. In particular, the DEXDc and HELICc domains showed higher conservation with the vertebrate homologues. The cysteine residues forming a disulfide-bond in the C-terminal portion were evolutionarily preserved in all the analyzed species (**Fig. 10**). The phylogenetic analysis performed to unravel the evolutionary relationship of RbLGP2 revealed its closer homology and association with the fish homologues with the other vertebrates forming a separate cluster and the MDA5 homologues separated as a distinct branch and grouped together. Owing to the highest identity shared, rock bream associated closer with that of olive flounder (**Fig. 11**).

Fig. 10. Multiple sequence alignment of RbLGP2 with other homologues.

The amino acid sequence derived from RbLGP2 was submitted to GenBank under the accession ID. KF267451). The rock bream species name is bold and red wave underlined. The homologous LGP2 sequences were obtained from NCBI and GenBank and the accession numbers are given in Table 6. Identical residues are indicated by “*”. Highly conserved and semi-conserved residues are indicated by “:” and “.”, respectively. The DExDc helicase domain (1-174) and DExDc helicase motifs are grey and blue shaded (with numbers on the top), respectively. The Res III domain (3-223) was red underlined. The MDA5_ID (230-309) is indicated by purple residues which are pink wave underlined. The HELICc domain (339-507) was red bold and double underlined. The RIG-I_C_RD (RD domain: 552-675) is indicated in a pink dash lined box. The RNA binding loop is denoted by a red box. The Zn²⁺ binding motifs are enclosed in a black box and the cysteine residues forming a disulfide-bond are indicated as purple colored bold residues.

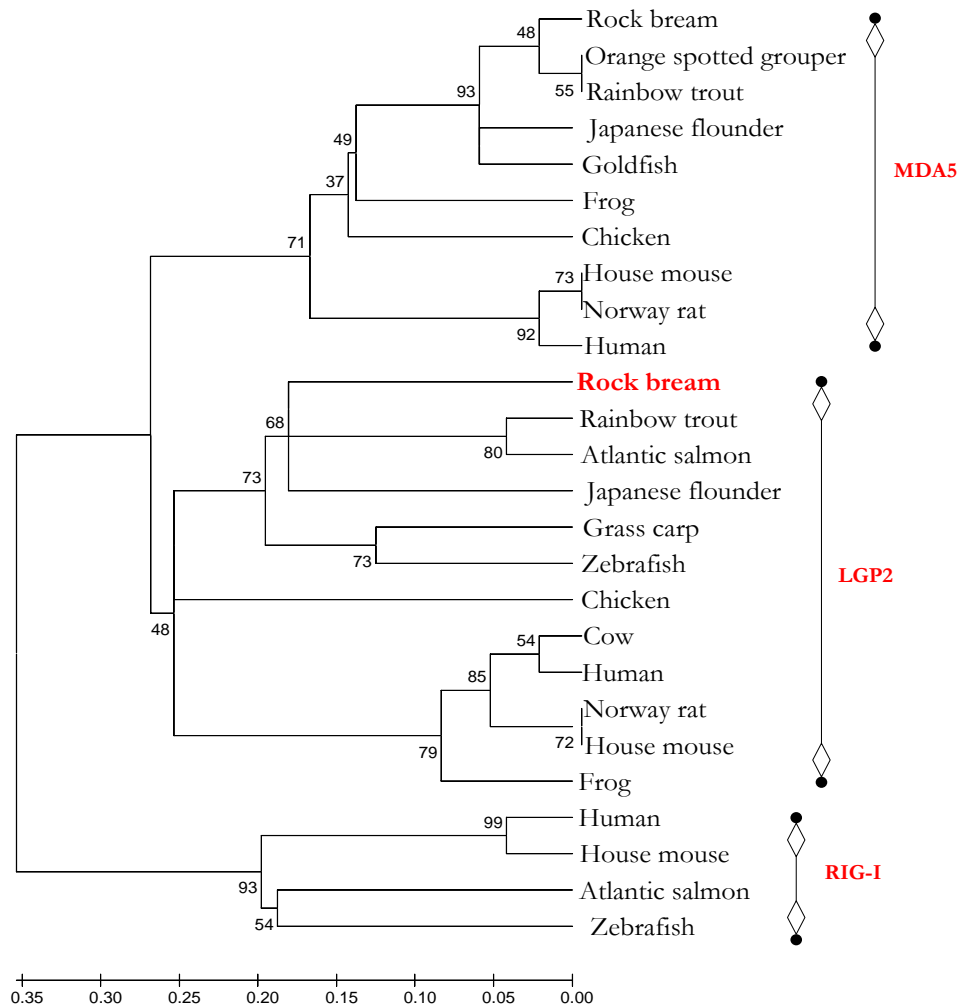
Table 6. Pairwise alignment of RbLGP2 protein with LGP2 homologues.

Identity and similarity percentages were derived using the whole protein sequence of RbLGP2 and homologues.

Species	Taxonomy	Identity	Similarity	Length	Accession No.	Database
Rock bream	Actinopterygii	100	100	681	KF267451	
Olive flounder	Actinopterygii	79	90	682	ADI75503	GenBank
Rainbow trout	Actinopterygii	71	84	677	CAZ27718	GenBank
Atlantic salmon	Actinopterygii	71	84	678	NP_001133649	NCBI
Grass carp	Actinopterygii	64	78	680	ACY78116	GenBank
Zebrafish	Actinopterygii	64	77	679	NP_001244086	NCBI
Frog	Amphibia	51	71	682	NP_001085915	NCBI
Chicken	Aves	52	67	674	AEK21509	GenBank
Cow	Mammalia	49	67	680	NP_001015545	NCBI
Human	Mammalia	47	67	678	NP_077024	NCBI
Norway Rat	Mammalia	46	68	678	NP_001092258	NCBI
House mouse	Mammalia	46	67	678	NP_084426	NCBI

Table 7. Percentage of identity and similarity of DExD and HELICc domains of RbLGP2 with that of the other homologues.

Species	DExD domain (Identity %)	DExD domain (Similarity %)	HELICc domain (Identity %)	HELICc domain (Similarity %)
Rock bream	100	100	100	100
Olive flounder	85	92.5	79.5	88.8
Rainbow trout	74.5	83.7	78.8	87
Atlantic salmon	76.7	85.1	78.1	86.4
Grass carp	71.8	83.7	73.1	40.8
Zebrafish	69.4	80.9	68.4	78.1
Frog	58.3	76.7	57.9	72.2
Chicken	58	72.6	53.7	65.7
Cow	52.8	72.9	52.9	66.9
Human	52.1	73	50.3	66.3
Norway Rat	49.8	74	51.7	68.8
House mouse	50.2	74	51.1	68.8



1

Fig. 11. Phylogenetic analysis of RbLGP2 with LGP2, RIG-I and MDA5 sequences.

The tree was constructed by the minimum evolution method in MEGA 5.0 using the full-length amino acid sequences. The RIG-I and MDA5 sequences were obtained from GenBank. The accession numbers of MDA5 sequences are Orange spotted grouper: AEX01716, Rainbow trout: NP_001182108, Japanese flounder: ADU87114, Goldfish: AEN04473, Frog: XP_002933320, Chicken: BAJ14020, House mouse: AAM21359, Norway rat: NP_001102669, Human: AAG34368. The accession numbers of the RIG sequences are Human: AF038963, House mouse: AY553221, Atlantic salmon: NP_001157171, zebrafish: ENSDART00000058176. The accession numbers of the LGP2 sequences are tabulated in

Table 6.. Numbers above the line indicate percent bootstrap confidence values derived from 5000 replications.

3.3.2 Genomic characterization of *RbLGP2*

The genome of *RbLGP2* was derived from the BAC clone using gene specific primers. *RbLGP2* genome possessed 12 exons intervened by 11 introns (**Fig. 12**). Exons 2 to 12 comprised the coding region while the first exon contained untranslated nucleotides in its entirety. The exon 12 harbored the 3' untranslated nucleotides. The DExDc domain was distributed in the 2nd, 3rd and a part of 4th exon. The coding part for the HELICc domain was present in the 8th and 9th exon. The *RbLGP2* genome shared its high similarity with that of olive flounder, except for the 6th exon where olive flounder *LGP2* showed three nucleotides in excess, accounting for the extra amino acid than that of *RbLGP2*. Next to flounder, *RbLGP2* shared high similarity with the genome of stickleback. Both olive flounder and stickleback had the first exon with untranslated region in its entirety.

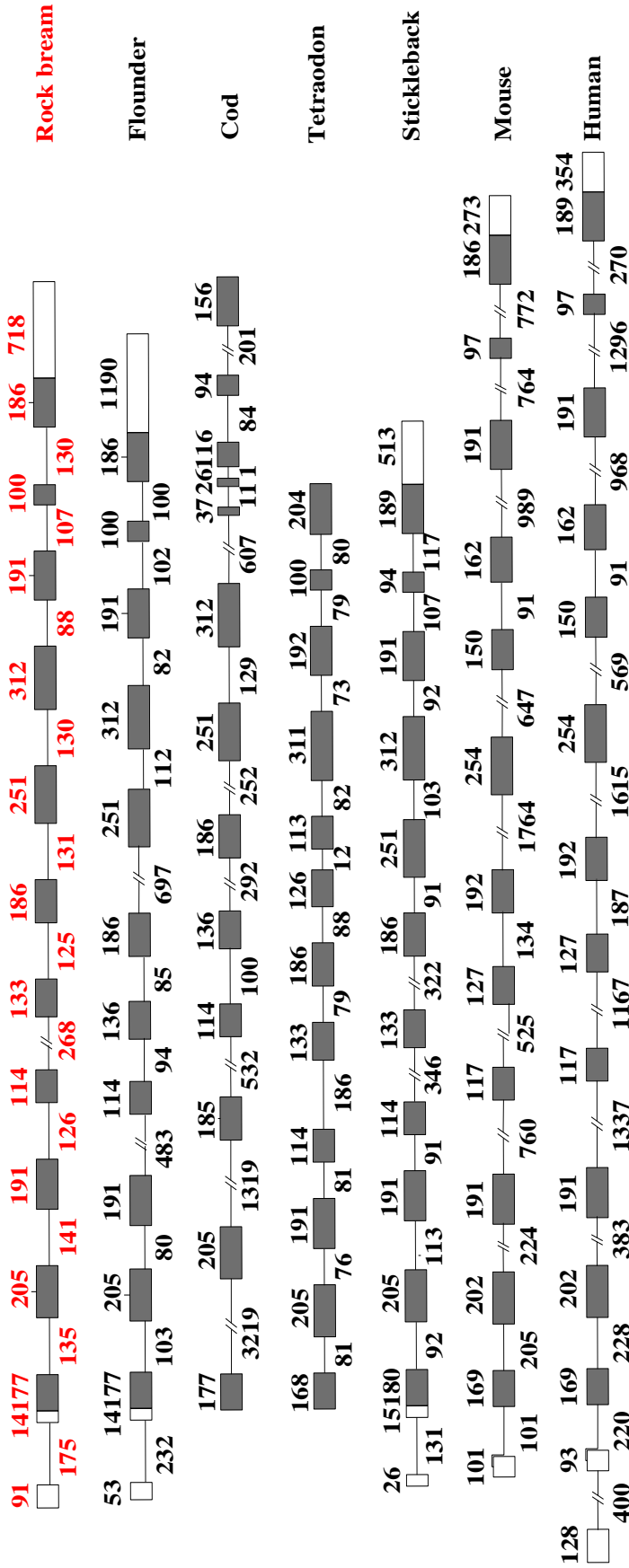


Fig. 12. Genomic structure comparison of *RbLGP2* with other LGP2 homologues.

The exon-intron structures were derived from exon-view of Ensembl. The ensemble ids are Japanese flounder: HMI100666,

Cod: ENSGMOT00000016632, Tetraodon: ENSTNIT00000014864, Stickleback: ENSGACT00000011575, House mouse:

ENSMUST00000017974, and Human: NT_010783. The translated/coding regions are denoted by dark shaded boxes and the

introns are denoted by lines. Exon sizes are indicated above the exon boxes and intron lengths are shown below the intron lines.

Untranslated regions at the 5'- and 3'-ends are denoted by empty boxes.

3.3.3 Promoter analysis of *RbLGP2*

The putative promoter and 5' flanking region analysis revealed the presence of several TFBS common to that of olive flounder. Proximal region revealed the presence of activator protein-1 and -4 (AP-1 and -4), CCAAT-enhancer binding protein- α , - β (C/EBP - α and - β), interferon regulatory factor-1 and -2 (IRF-1 and -2), nuclear factor-kappa (NF-kappa), cAMP response element binding protein (CRE-BP/CREB), Oct-1, AML-1a, heat shock factor (HSF), Brn-2, Sterol Regulatory Element-Binding Protein (SREBP), and CdxA (**Fig. 13**).

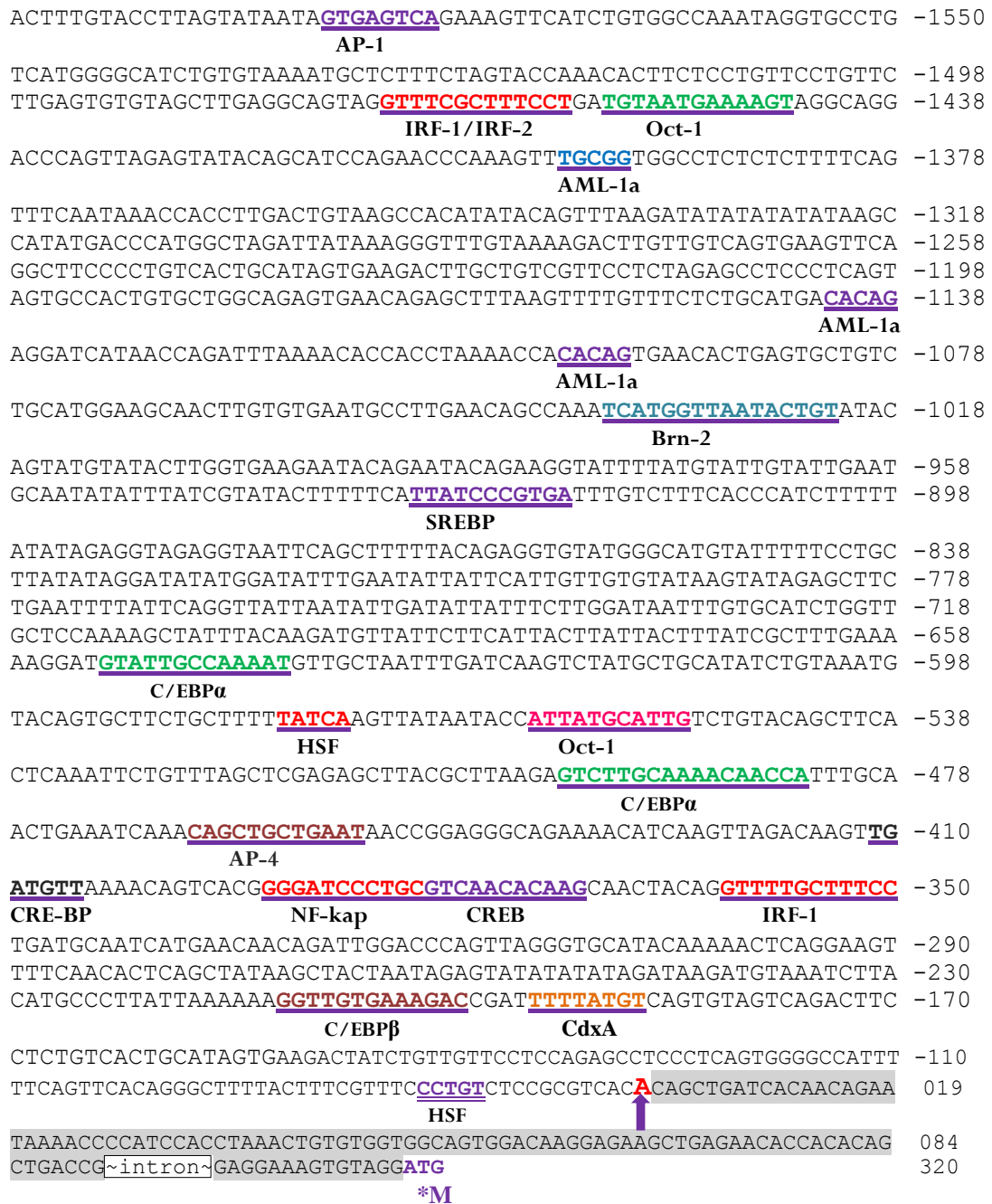


Fig. 13. Analysis of the *RbLGP2* gene 5' -flanking region.

The transcription factor binding sites are colored, bold, underlined and denoted with the corresponding name below. The transcription initiation site is bold, red and denoted by an upward-facing arrow. The intron between the UTR and the start codon is denoted by a box. The start codon is indicated by a “*” with a methionine residue written below.

3.3.4 Spatial expression analysis of *RbLGP2*

In order to delineate the physiological distribution of *RbLGP2* mRNA, various tissues from healthy rock bream were isolated and analyzed using RT-PCR. Although ubiquitous expression was found in all the examined tissues, *RbLGP2* mRNA was highly detected in blood, followed by liver. Gill showed almost half the expression as detected in liver (Fig. 14).

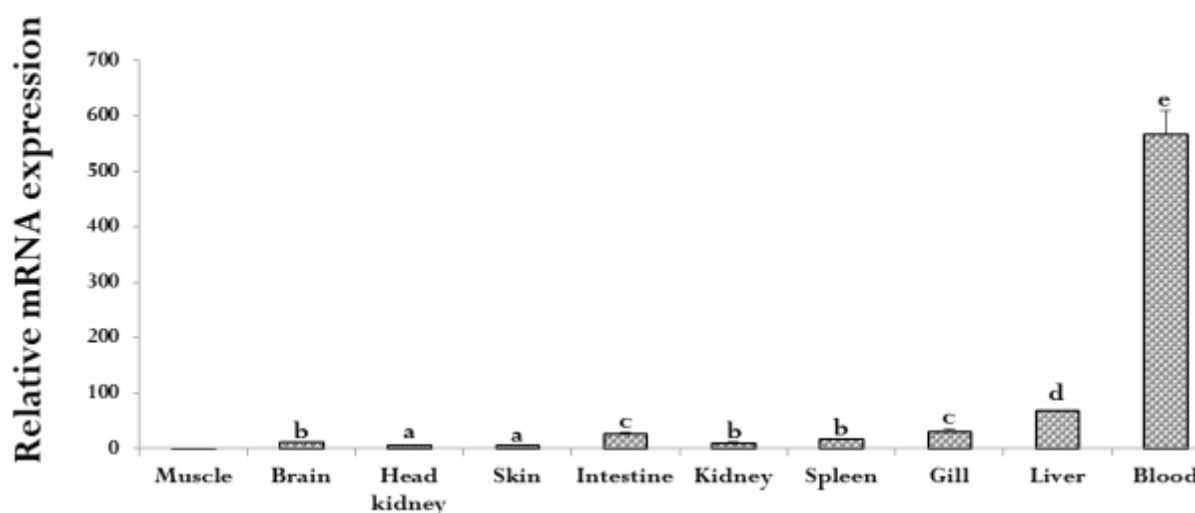


Fig. 14. Tissue distribution analysis of *RbLGP2*.

RbLGP2 tissue-specific expression in muscle, intestine, skin, kidney, head kidney, spleen, gill, brain, liver tissues, and blood, collected from unchallenged rock bream was analyzed using quantitative RT-PCR. Relative mRNA expression was calculated using the $2^{-\Delta\Delta Ct}$ method, with β -actin as the invariant control gene. In order to determine the tissue-specific expression, the relative mRNA level was compared with muscle expression. Data are presented as mean values (n=3) with error bars representing SD. Data shown with “*” indicates significant expression levels at $P < 0.01$.

3.3.5 *RbLGP2* temporal expression analysis post poly I:C challenge

Since LGP2 is known to recognize dsRNA, poly I:C which is a synthetic analog of dsRNA was employed to understand the modifications of the *RbLGP2* mRNA level in rock bream. Poly I:C administered *in vivo* altered the *RbLGP2* expression in the major immune organs including blood, gill, liver, spleen and head kidney. In gill, liver and spleen, modulations of expression could be observed at all time-points of study, whereas in blood, changes could be observed from 6 h to 24 h. In head kidney, stimulation could be observed from 3 h to 12 h p.i. In gill (12-fold), liver (9-fold), spleen (14-fold) and head kidney (13-fold), maximum level of expression was observed at 6 h p.i, whereas in blood, highest expression was observed a little later at 12 h (4.4-fold) p.i. (Fig. 15).

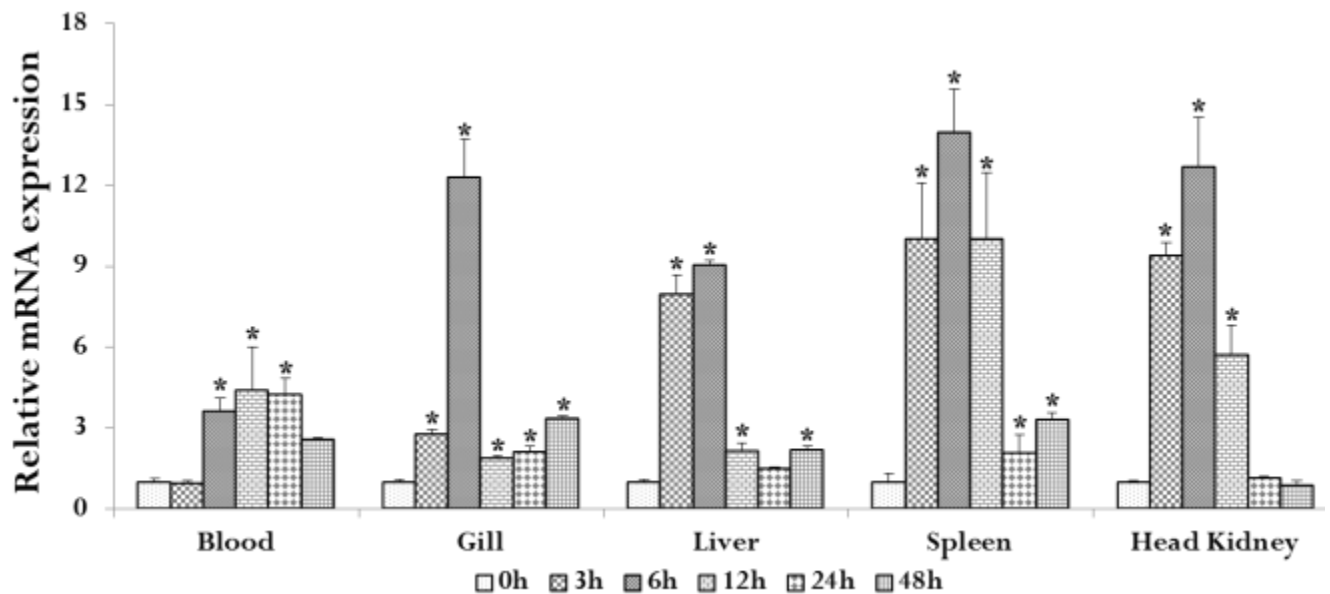


Fig. 15. *RbLGP2* expression analysis after immune challenges.

RbLGP2 expression was analyzed in liver, blood, spleen, gill and head kidney post poly I:C challenge. Relative mRNA expression was calculated by the $2^{-\Delta\Delta Ct}$ method relative to PBS-injected controls and normalized with the same, with β -actin as the reference gene. Data are presented as mean values (n=3) with error bars representing SD. Data shown with “*” indicates significant expression levels at $P < 0.01$.

3.3.6 Antiviral assays

In order to demonstrate the antiviral function of the *RbLGP2*, rock bream heart cells were transiently transfected with either the empty vector (pcDNA™ 3.1/His B vector) or the pcDNA3.1-RbLGP2 and then infected with marine birnavirus. After 7 days post infection of the cells with the virus, CPE could be observed followed by cell death. The cells transfected with empty vector were completely killed while the cells transfected with pcDNA3.1-RbLGP2 revealed complete protection against infection. The cells in which the RbLGP2 was overexpressed led to the activation of the downstream signaling pathways and synthesis of IFNs and ISGs. These results affirmed the antiviral function of *RbLGP2* and the existence of RLR signaling pathway in teleosts (Fig. 16).

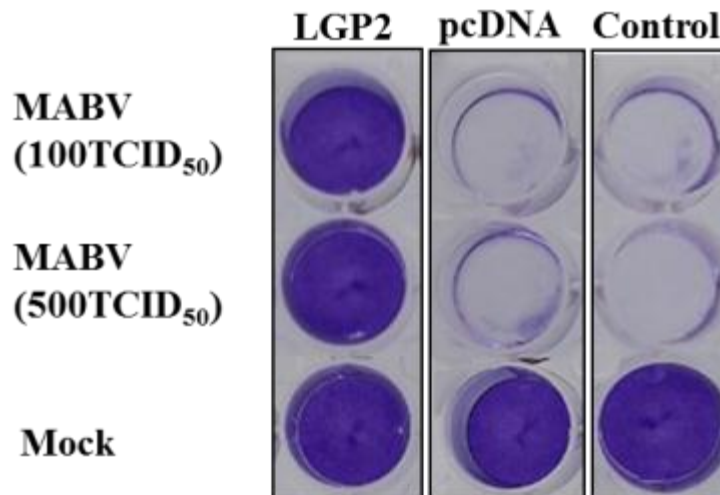


Fig. 16. Antiviral activity of RbLGP2 against MABV.

The empty pcDNA 3.1 vector and pcDNA3.1-RbLGP2 were transfected into rock bream heart cells. After 48 h of transfection, at 24 °C, the cells were infected with MABV at indicated densities. After 7 days of infection, cells were fixed with 4% PFA and stained with 3% crystal violet.

3.4 Discussion

Innate immune recognition of viruses is the preliminary step in the initiation of innate immunity/cell protection against infection and triggering of adaptive immunity. Multitude of

signal transduction events are involved in the activation and production of proinflammatory cytokines with IFN being the hallmark of antiviral responses. The cytosolic surveillance and induction of antiviral immunity is exclusively performed by cytosolic receptors of the RLR family, comprising of RIG-I, LGP2 and MDA5. LGP2 was first described as gene neighboring the STAT3 and STAT5 loci on 11th chromosome of mouse, by Laboratory of genetics and Physiology (Cui et al., 2001). LGP2 is a virus inducible protein, first identified to be a negative regulator of RIG-mediated dsRNA recognition (Diperna, 2005; Rothenfusser et al., 2005).

Unlike the grass carp LGP2, *RbLGP2* sequence possessed only two mRNA instability motifs (Huang et al., 2010b). *In silico* characterization of RbLGP2 protein revealed the presence of an N-terminal DExD/H-box helicase domain and a C-terminal RD but lacked any CARD, similar to the other LGP2 members (Yoneyama et al., 2005). RbLGP2 possessed conserved domains including DExD/H-box helicase domain, RD, ResIII domain, and HELICc domain similar to other fish species (Chang et al., 2011; Huang et al., 2010b; Ohtani et al., 2010). The RLRs (RIG-I, MDA5 and LGP2) are members of large helicase superfamily II (SFII), which participate as ubiquitous group of energy-dependent, nucleic acid remodeling proteins in many cellular pathways involving nucleic acids. Similar to the other SF2 members, the RLRs harbor a catalytic core comprising of two RecA-like domains which contains eight helicase domain motifs. The highly conserved helicase domain sequence motifs, motif I-VI function to co-ordinate RNA binding and ATP hydrolysis. The DExD/H box, alternatively called as Walker B motif corresponds to “DECH” in the RLR proteins. Mutations in these motifs of RLR proteins resulted in defective ATP hydrolysis activity and hence antiviral signaling (Bruns and Horvath, 2012). The regulatory domain was identified as an auto-inhibitory domain for RIG-I. Deletion of RD in RIG-I increased basal signaling activity. This auto-inhibition plays a vital role in RIG-I regulation, which is generally inactive in the

absence of an activating ligand. Mammalian LGP2 is known to bind (+) ssRNA, ssRNA(-) and dsRNA viruses (Sato et al., 2010). The mammalian RD with two Zn²⁺ binding motifs and an RNA-binding loop plays a significant role in binding to viral RNAs (Li et al., 2009b; Takahasi et al., 2009b). The RD of LGP2 was also shown to interact with the RD of RIG-I and suppress its self-association (Venkataraman et al., 2007). LGP2 RD possess higher affinity for RNA compared to the RIG-I RD and MDA5 RD (Takahasi et al., 2009a). The lysine and phenyl alanine residues are determined to be significant in RNA binding (Takahasi et al., 2009b). In RbLGP2, although the phenyl alanine (F) residue was present, the lysine residue (K) was replaced by arginine (R). The two cysteines in the Zn²⁺ binding motif (CxxC motif) are required for LGP2 binding of RNA (Cui et al., 2008). Similar to the second flounder CxxxxxC motif, RbLGP2 also revealed an extra residue forming a CxxxxC motif, instead of the conserved CxxC motif. RD in flounder was proven to be necessary for antiviral activity (Ohtani et al., 2010). The structural conservation of RbLGP2 RD suggests that RbLGP2 may recognize ds-and ss-RNA viruses in a similar fashion. CARD domain hidden in the inactive conformation of RIG-I is activated upon the recognition of viral ligands by RD (Bruns and Horvath, 2012). CARD proteins are involved in protein-protein interactions. The tandem CARDS located in the N-termini of RIG-I and MDA5 are the primary effector domains in transducing signals to MAVS. The absence of CARDS in LGP2 determined it to have an alternative role in antiviral signaling as a negative regulator of RIG-I mediated IFN response (Diperna, 2005). However, later it was dissolved to be a positive regulator of viral signaling upstream of RIG-I and MDA5. The common structural features among the RLR family members reveal functional similarity, yet a controversial view persists on exact function of LGP2. However, in teleosts, LGP2 homologues had been proven to induce IFN signaling and possess antiviral functions (Chang et al., 2011; Huang et al., 2010b; Ohtani et al., 2010). The multiple sequence alignment and phylogenetic analysis, revealing

conservation and closer relationship of *RbLGP2* with the teleost and human homologues are expected to possess similar antiviral functions.

The genomic structure of *RbLGP2* composed of 12 exons is similar to that of flounder and stickleback. Tetraodon genome revealed 12 coding exons, contrary to the 11 coding exons in *RbLGP2* and flounder *LGP2*. The 7th coding exon in *RbLGP2* was split into two exons in Tetraodon. Although a few coding exons seemed to be conserved with the human and mouse homologues, certain degree of variation could be observed. Similar to the flounder *LGP2*, the 9th exon in *RbLGP2* corresponded to two exons (10th and 11th exons) in human *LGP2*. The two exons at the 5' end of human *LGP2* were composed of only untranslated regions, making the number of exons higher than the teleosts. The functional significance of intron insertion between the UTRs and coding exons needs to be delineated. The structural conservation of *RbLGP2* with the teleosts suggests that the separation of the coding exons and insertion of introns would have happened later in evolution whose significance is still not understood.

The promoter and 5' flanking region analysis revealed the presence of several canonical motifs that bind transcription factors. However, *RbLGP2* did not possess any TATA box upstream of the transcription initiation site. A comparative computational analysis performed with the upstream sequence of humans, medaka and Tetraodon revealed that human sequence possessed very few motifs significant for binding of transcription factors, compared to teleosts. The presence of IRF-motifs signifies their regulation during viral infection. However, *RbLGP2* flanking region revealed only six IRF binding sites compared to flounder *LGP2* which possessed 12 IRF motifs (Hikima et al., 2012). Earlier studies on the putative *cis* regulatory elements suggested that although the disposition and clustering of the motif elements were not conserved in the promoter structure among teleosts and human, the types of canonical motifs including IRFs were conserved. The presence of IRF and NF-kappa

binding sites in the promoter of *RbLGP2*, similar to those present in the type I IFN and IFN inducible proteins (like Mx and ISG15), which are regulated by TLRs and RLRs suggests *RbLGP2* regulation by similar factors.

Spatial expression analysis of *RbLGP2* showed constitutive expression in all the examined tissues with highest expression level in blood and liver. Constitutive expression in all the tissues signifies the immunosurveillance function of *RbLGP2*. Blood is a major immune organ and recently the significance of liver as an immune organ is being highlighted (Gao et al., 2008; Nakashima et al., 2012; Seki et al., 2012). Gill is a mucosa-associated lymphoid tissue, under constant exposure to the environment is always under threat of infection. However, the low levels of *RbLGP2* in immune tissues like head kidney, skin, and spleen suggest their tight regulation. Flounder and grass carp *LGP2* were also highly expressed in immune related tissues (Huang et al., 2010b; Ohtani et al., 2010).

Poly I:C and RNA viruses are known to induce *LGP2* expression (Kato et al., 2008; Rothenfusser et al., 2005). In this study, *in vivo* poly I:C challenge modulated the expression of *RbLGP2* at the early phase suggesting its involvement in innate antiviral immune defense against RNA viruses. Further, similar to the grass carp *LGP2* which was stimulated after GCRV infection, up-regulation of *RbLGP2* transcripts could be observed during the early phase in spleen. However, *RbLGP2* showed different pattern of expression in liver. Grass carp *LGP2* was elevated to the maximum at 48 h p.i. whereas *RbLGP2* showed highest expression level at 6 h p.i. (Huang et al., 2010b). Atlantic cod *LGP2* was induced at 6 h in spleen after poly I:C stimulation, similar to *RbLGP2* (Rise et al., 2008). *LGP2* is known to exert a feedback control at the early steps of IFN synthesis (Vitour and Meurs, 2007). In mammals, under different experimental conditions, contrary roles had been expressed on the function of *LGP2* as both a negative and positive regulator (Bruns and Horvath, 2012). *LGP2* may play both roles in IFN induction and there may be distinct effects depending on the type

of virus and whether it is recognized by RIG-I or MDA-5 (Childs et al., 2012). LGP2 is proposed to work upstream of RIG-I and MDA5 and helps in RNA recognition by unwinding or stripping nucleoproteins of viral RNA, thereby making the nucleic acid PAMP accessible for binding (Schmidt et al., 2012). LGP2 sequesters RNA and prevents its binding to MDA5 or RIG-I and hence controlling the IFN level when viral infection diminishes. However, in teleosts, LGP2 has been demonstrated to be positively involved in antiviral immunity (Chang et al., 2011; Hikima et al., 2012; Ohtani et al., 2010). The high expression of immune genes resulting in synthesis of proinflammatory cytokines and apoptotic related proteins is normally kept under low level to prevent host damage because of excessive inflammatory responses. The induction of *RbLGP2* after poly I:C injection suggests its activation after viral stimulation and its role in antiviral defense.

In mammals, both positive and negative regulatory aspects of RIG-I/MDA5 signaling have been attributed for LGP2. Studies with *LGP2* deficient mice showed impaired IFN production in dendritic cells and embryonic fibroblasts against RNA viruses recognized by MDA5 (e.g., picornaviruses), but not for influenza virus RNAs recognized by RIG-I. However, LGP2 was necessary for IFN β production against Sendai virus, Japanese encephalitis virus, and reo viruses, which are recognized by RIG-I, providing evidence for LGP2 as a positive regulator of both RIG-I and MDA5 mediated antiviral responses. In teleosts, LGP2 has been demonstrated to enhance antiviral immunity and play a positive regulatory role in RLR signaling cascade (Chang et al., 2011; Hikima et al., 2012; Ohtani et al., 2010). This study revealed the antiviral protection activity of *RbLGP2* against an ssRNA virus, MABV, thus expanding the family of viruses which could be recognized by the RLR family proteins and confer protection.

In conclusion, this study affirmed the existence of an ancestral PAMP recognition receptor: LGP2 in rock bream through genomic and functional characterization. Our results

demonstrate the induction of LGP2 by poly I:C and LGP2 inhibits the MABV infection. This study stands as an averment for the positive regulatory role of LGP2 in teleosts.

CHAPTER IV

Characterization of the signaling adaptor Mitochondrial AntiViral Signaling protein (MAVS)

4.0 Characterization of the signaling adaptor Mitochondrial AntiViral Signaling protein (MAVS)

Abstract

Mitochondrial antiviral signaling protein (MAVS), also termed as VISA (virus-induced signaling adapter), IPS-1 and Cardif, is a mitochondrial resident protein involved in the activation of downstream signaling molecules after recognition of viruses by cytosolic receptors. Aggregated MAVS form protease resistant prion-like aggregates that activate IRF3 dimerization. Rock bream MAVS (RbMAVS) protein harbored a CARD and a transmembrane domain. Pairwise alignment and phylogenetic analysis revealed the closer relationship of RbMAVS with the fish homologues. RbMAVS tissue distribution analysis showed ubiquitous presence with maximum level of expression being determined in blood and transcriptional modulations analyzed in immune related tissues like liver, spleen, head kidney and blood cells revealed upregulation after poly I:C challenge. The recombinant RbMAVS protein showed protection of cells against marine birnavirus infection. Thus RbMAVS is a new member of the MAVS family of proteins playing a significant role in the defense of rock bream against viruses.

4.1 Introduction

Innate immune recognition of the viral PAMPs through the germ-line encoded pattern recognition receptors (PRRs) activates multiple signaling cascades resulting in the induction of interferons (IFNs) and several other cytokines. The innate immune system plays a vital role in the early control of infection and induction of adaptive immunity. The three main families of PRRs involved in PAMP detection are toll-like receptors (TLRs), retinoic acid inducible gene I (RIG-I)-like receptors (RLRs), and nucleotide oligomerization domain-like receptors (NLRs) (Hayashi et al., 2011; Kumagai and Akira, 2010). The TLR orthologues have been characterized from teleosts. A few orthologues which were identified from teleosts need to be characterized from humans (Rebl et al., 2010a; Rebl et al., 2010b).

The RLR family comprises of three structurally homologous members namely, retinoic acid-inducible gene I (RIG-I, also called DEAD (Asp-Glu-Ala-Asp) box polypeptide 58 (DDX58)), melanoma differentiation-associated gene 5 (MDA5, also called interferon induced with helicase C domain 1 (IFIH1)), and laboratory of genetics and physiology 2 (LGP2, also called DExH (Asp-Glu-X-His) box polypeptide 58 (DHX58)) (Loo and Gale, 2011). Ever since the recognition of RIG-I's role in antiviral immunity, studies on structural and regulatory aspects of these receptors have burgeoned in recent years (Yoneyama and Fujita, 2007b; Yoneyama et al., 2004). RIG-I and MDA5 possess a helicase and CARD domains. LGP2 harbors a helicase domain while it differs from RIG-I and MDA5 in lacking a CARD domain (Leung and Amarasinghe, 2012). This structural variation confers LGP2 a controversial role in antiviral immunity (Diperna, 2005; Satoh et al., 2010). RIG-I and MDA5 show variation in viral PAMP recognition; while RIG-I binds preferentially to ssRNA phosphorylated at the 5' end, MDA5 recognizes long dsRNA that do not require 5' phosphorylation (Yoneyama et al., 2005). The difference in the ligand specificity of the

receptors determines the type of viruses being recognized. Studies from knock-out mice provided evidence for the RLR pathway being the central innate immune pathway against viral infection (Kato et al., 2006; Kumar et al., 2006). IFN signaling has been understood to induce an amplification loop in the innate immune response that further increases immune activation (Foy et al., 2005). In addition to that, IFN- α/β signaling drives the maturation of dendritic cells and other antigen presenting cells, supports the differentiation of specific immune effector cells as well as induces the production of localized proinflammatory cytokines, which together serve to control cell-mediated defenses and modulate the adaptive immune response to virus infection (Biron, 1999). Fish are also determined to have virus induced receptors like RIG-I, MDA5 and LGP2 and also downstream signaling molecules like IFNs, interferon stimulated genes (ISGs), suggesting the conservation of the RLR system in vertebrates (Robertsen, 2006; Zou et al., 2010; Zou and Secombes, 2011).

The RIG-I and MDA5 signaling bifurcates in the cytosol at a mitochondrial resident protein, called mitochondrial antiviral signaling protein (MAVS), also known as IFN- β promoter stimulator 1 (IPS-1), virus-induced signaling adaptor (VISA), and CARD adaptor inducing IFN- β (Cardif) (Kumar et al., 2006). The recognition of virus by RIG-I results in an ATP-dependent conformational change, exposing its two N-terminal CARDS and induces oligomerization. The exposed CARD domains of RIG-I interact with the CARD domain of the MAVS, and subsequently activate inhibitors of κ B kinase (IKK)- α , - β , - ϵ , and TANK binding kinase 1 (TBK1) resulting in the phosphorylation and activation of NF- κ B and IRF3/IRF7. The signaling process culminates in the induction of IFN promoters and synthesis of IFNs and inflammatory cytokines (Loo and Gale, 2011).

Human MAVS possesses an N-terminal CARD, a proline-rich (Pro) region, and a C-terminal mitochondrial transmembrane (TM) sequence. Extensive studies about location, structure, functions, enhancer, inhibitor and other mechanisms have been performed on

human MAVS (Jia et al., 2009; Onoguchi et al., 2010; Tang and Wang, 2009). Teleosts MAVS have been identified from grass carp (Su et al., 2011), green-spotted pufferfish (Xiang et al., 2011), Atlantic salmon and zebrafish (Biacchesi et al., 2009). Functional characterization of fish MAVS has proven it to be a mediator for IFN gene activation and plays a major role in innate immune response against viruses (Biacchesi et al., 2009; Simora et al., 2010; Xiang et al., 2011). In this study, we have cloned MAVS gene from rock bream and proven to possess antiviral function against an RNA virus, marine birnavirus (MABV).

4.2 Materials and methods

4.2.1 Animal rearing, cDNA library construction and *RbMAVS* gene identification

Healthy rock bream fish with average weight of ~50 g, procured from the Ocean and fisheries Research institute (Jeju, Republic of Korea) were adapted to the laboratory conditions (salinity $34 \pm 1\text{‰}$, pH 7.6 ± 0.5 at 24 ± 1 °C) in 400 L tanks. Blood samples were aseptically harvested from the caudal fin of healthy, unchallenged fish using a 22 gauge needle and centrifuged immediately for 10 min at $3000 \times g$ at 4 °C, to collect the hematic cells. Gill, liver, brain, kidney, head kidney, spleen, intestine, muscle and skin tissues were harvested on ice from three healthy animals and immediately flash-frozen in liquid nitrogen and stored in -80 °C, until RNA extraction. Tri Reagent™ (Sigma, USA) was employed to obtain total RNA from tissues. The concentration and purity of RNA were evaluated using a UV-spectrophotometer (BioRad, USA) at 260 and 280 nm. Purified total RNA samples were subjected to mRNA purification using Micro-FastTrack 2.0 mRNA isolation kit (Invitrogen). First strand cDNA was synthesized from 1.5 µg of mRNA using Creator™ SMART™ cDNA library construction kit (Clontech, USA); amplification was performed with Advantage 2 polymerase mix (Clontech) under conditions of 95 °C for 7 s, 66 °C for 30 min and 72 °C for 6 min. Over-representation of the most commonly expressed transcripts was excluded by

normalizing the synthesized cDNA using Trimmer-Direct cDNA normalization kit (Evrogen, Russia).

A cDNA GS-FLX shotgun library was created from the sequencing data obtained by using the GS-FLX titanium system (DNA Link, Republic of Korea). The cDNA library was searched for genes involved in antiviral immunity using BLASTX. A cDNA contig when subjected to BLASTX was identified to reveal high homology to *Tetraodon nigroviridis* and was found to contain the conserved domains present in the other homologues. The cDNA was named *RbMAVS* and taken for further work.

4.2.2 Sequence characterization, genome structure and phylogenetic analysis of RbMAVS

The *RbMAVS* cDNA sequence identified by BLAST was subjected to DNAssist2.2 to predict the open reading frame (ORF) and translate nucleotide to protein. The conserved domains were identified using Expasy (<http://www.expasy.org/>), SMART (<http://smart.embl-heidelberg.de/>) and conserved domain database search (CDD). ClustalW was employed to execute pairwise and multiple sequence alignment (Thompson et al., 1994). A phylogenetic tree was reconstructed using minimum evolution method available in MEGA 5.0, with bootstrap values calculated with 5000 replications to estimate the robustness of internal branches (Tamura et al., 2011). The complete amino acid and CARD region identity and similarity percentages were calculated by MatGAT program using default parameters (Campanella et al., 2003).

4.2.3 Transcriptional profile of *RbMAVS* gene in challenged and normal tissues

4.2.3.1 Poly I:C challenge

In order to understand the transcriptional modifications of *RbMAVS* *in vivo* after dsRNA administration, poly I:C which is a viral mimic was employed. Sterile poly I:C stock was

prepared by dissolving poly I:C at the rate of 1.5 mg/ml in PBS and filtered through a 0.2 μ m filter. A time course experiment was designed, wherein 100 μ L of the poly I:C stock was intraperitoneally administered to the fish. The control animals were injected with an equal volume of PBS. Liver, spleen, head kidney tissues and whole blood cells were harvested from the un-injected, PBS-injected and immune challenged animals at time points of 3, 6, 12, 24, and 48 h post injection/infection (p.i.).

4.2.3.2 RNA isolation and cDNA synthesis

In order to perform the tissue distribution profiling of *RbMAVS*, gills, liver, brain, kidney, head kidney, spleen, intestine, muscle and skin tissues and whole blood cells were harvested from un-injected fish. After challenge with PBS and poly I:C, liver, spleen, head kidney tissues and whole blood cells were harvested from challenged animals at the corresponding time points. Total RNA was obtained from tissues using Tri ReagentTM (Sigma, USA). The concentration and purity of RNA were evaluated using a UV-spectrophotometer (BioRad, USA) at 260 and 280 nm. The RNA was diluted to 1 μ g/ μ L and cDNA was transcribed from 2.5 μ g of RNA from each tissue using a PrimeScriptTM first strand cDNA synthesis kit (TaKaRa). Concisely, RNA was incubated with 1 μ L of 50 μ M oligo(dT)₂₀ and 1 μ L of 10 mM dNTPs for 5 min at 65 °C. After incubation, 4 μ L of 5 \times PrimeScriptTM buffer, 0.5 μ L of RNase inhibitor (20 U), 1 μ L of PrimeScriptTM RTase (200 U), were added and incubated for 1 h at 42 °C. The reaction was terminated by adjusting the temperature to 70 °C for 15 min. Finally, synthesized cDNA was diluted 40-fold before storing at -20 °C for further use.

4.2.3.3 Tissue distribution

Quantitative reverse transcription polymerase chain reaction (qRT-PCR) was used to examine tissue distribution of *RbMAVS* mRNAs in various tissues of healthy fish using gene

specific primers (Table 8.). qRT-PCR was performed in a 15 μ L reaction volume containing 4 μ L of diluted cDNA, 7.5 μ L of 2 \times SYBR Green Master Mix, 0.6 μ L of each primer (10 pmol/ μ L) and 2.3 μ L of PCR grade water and subjected to the following conditions: one cycle of 95 $^{\circ}$ C for 3 min, amplification for 40 cycles of 95 $^{\circ}$ C for 20 sec, 58 $^{\circ}$ C for 20 sec, 72 $^{\circ}$ C for 30 sec. The baseline was automatically set by the Thermal Cycler Dice[™] Real Time System software (version 2). In order to confirm that a single product was amplified by the primer pair used in the reaction, a dissociation curve was generated at the end of the reaction by heating from 60 $^{\circ}$ C to 90 $^{\circ}$ C, with a continuous registration of changes in fluorescent emission intensity. The *RbMAVS* gene expression was determined by Livak comparative Ct method. The relative expression level calculated in each tissue was compared with respective expression level in muscle.

4.2.3.4 Temporal RbMAVS mRNA expression analysis post poly I:C challenge

qRT-PCR was performed with cDNA prepared from RNA obtained from gill, liver, spleen, head kidney tissues and whole blood cells isolated from PBS and poly I:C challenged animals. qRT-PCR conditions were the same as used for tissue distribution profiling. The relative expression of *RbMAVS* with respect to the un-injected controls was determined by the Livak method. The relative fold change in expression after immune challenges was obtained by comparing the relative expression to corresponding PBS-injected controls. The expression normalized to PBS-injected controls is represented in the figures.

All experiments were performed in triplicate. All data have been presented in terms of relative mRNA expressed as means \pm standard deviation (S.D.). Statistical analysis was performed using un-paired two-tailed Student's t-Test. *P*-values of less than 0.01 were considered to indicate statistical significance.

Table 8. Primers used in RbMAVS characterization and qRT-PCR.

The restriction sites are in small letters.

Gene	Purpose	Orientation	Primer sequences (5'-3')
RbMAVS	BAC screening & qRT-PCR	Forward	TAATGGTCCATCTGCCTTGCCTGA
RbMAVS	BAC screening & qRT-PCR	Reverse	TGTTCACACGCCTCAAGTGCTTTG
RbMAVS	pcDNA cloning	Forward	GAGAGAgaaattcTATGTCTGTTTGCCAGTGACAAACTGTACA
RbMAVS	pcDNA cloning	Reverse	GAGAGActcgagTTAATTCTTAAACTTCCACGCCATCAGCAGTG
β -actin	qRT-PCR amplification	Forward	TCATCACCATCGGCAATGAGAGGT
β -actin	qRT-PCR amplification	Reverse	TGATGCTGTTGTAGGTGGTCTCGT

4.3 Construction of expression vector and antiviral assay

4.3.1 Cell lines and viruses

Rock bream heart cells were established as previously described (Wan et al., 2012). Concisely, heart tissue was aseptically isolated from healthy rock bream fish (n=3). The tissues were minced into small pieces (approximately 1 mm³ in size) and washed thrice with HBSS (Sigma) containing antibiotics (400 IU/ml penicillin and 400 μ g/ml streptomycin). Then, the tissue was digested in 0.2% collagenase II (Sigma) solution for 2 hours at 20 °C. The digestion mixture was filtered through a cell strainer (70 μ m mesh size), centrifuged at 1000 rpm for 10 min. The cells were resuspended in Leibovitz's L-15 medium supplemented with 20% FBS, 100IU/ml penicillin and 100 μ g/mL streptomycin, and inoculated into 75 cm² cell culture flask. The cells were sub-cultured more than three times and adapted to 15% FBS. Cells' susceptibility to MABV infection was tested. The 80% confluent monolayer cells were treated with serially diluted MABV and the plates were kept at room temperature (RT) for 2 h for adsorption and facilitate viral infection. The plates were then incubated at 24 °C for 72 h. The susceptibility of rock bream heart cells for MABV infection was confirmed by observing the cytopathic effect (CPE) and the maximal non-cytotoxic concentration was determined and used for the subsequent antiviral activity assay. MABV was kindly provided

by Prof. Sung-Ju Jung (Department of Aqualife Medicine, Chonnam National University, Republic of Korea).

4.3.2 Construction of expression vector

The full length ORF of *RbMAVS* (1761 bp) was amplified from liver cDNA using gene specific primers (Table: 4.1) and PCR and cloned into TA vector (Takara, Japan). The orientation and sequence was confirmed by restriction digestion and sequencing. The *RbMAVS* ORF cloned into TA vector was used as the template and the amplified PCR product was digested with *EcoRI* and *XhoI*. The digested PCR products were purified using Gel purification kit (Bioneer) and ligated overnight at 4 °C with *EcoRI* and *XhoI* digested pcDNA™ 3.1/His B vector (Life Technologies). The ligation mixture was transformed into *E. coli* DH5 α cells and the clone harboring the recombinant plasmid was sequenced. The affirmed clone harboring the rRbMAVS was selected and named as pcDNA3.1-RbMAVS.

4.3.3 Antiviral assays

A monolayer of rock bream heart cells were cultured in 24 well plates at 24 °C, 24 h prior to transfection. Before transfection, cells were washed once with sterile PBS, and then replaced with Opti-MEM (Life technologies). The transfection procedure was performed with Lipofectamine™2000 (Life technologies), as per manufacturer's instructions. Briefly, 1.5 μ g of pcDNA vectors (empty pcDNA3.1 and pcDNA3.1-RbMAVS) were mixed with 1 μ L of Lipofectamine™ 2000 and transfected into the heart cells in 100 μ L Opti-MEM, and then cultured at 24 °C for 48 h. After 48 h, the expression of transfected *RbMAVS* was assessed by RT-PCR. The cells were then infected with MABV and left at RT for 1 h for adsorption. The cells were then cultured with Leibovitz's L-15 medium and observed for the appearance of CPE. After 7 days of MABV infection, the cells were washed once with PBS, fixed with 4% paraformaldehyde (PFA) and stained with 3% crystal violet for visualizing live cells.

4.4 Results

4.4.1 RbMAVS identification, sequence characterization and phylogenetic analysis

A 2281bp cDNA contig was identified as a homologue of MAVS when subjected to BLASTX. The *RbMAVS* cDNA possessed an ORF of 1758 bp coding for a protein of 586 amino acids with molecular mass of 62 kDa and isoelectric point of 4.6. *RbMAVS* possessed a 5' untranslated region (UTR) of 5 bp and 3' UTR of 518 bp, which harbored two mRNA instability motifs ¹⁷⁷¹ATTTA¹⁷⁷⁵ and ²⁰⁶⁹ATTTA²⁰⁷³. RbMAVS protein analysis revealed a CARD domain (residues 5-90), a proline rich domain (residues 119-216) and a transmembrane domain (residues 566-582). RbMAVS protein also possessed a putative TRAF2 binding motif, ³¹⁹PVQDT³²³ (**Fig. 17**). Multiple sequence alignment showed conservation in the CARD region. The human and mouse homologues were 46 and 83 amino acids shorter than the RbMAVS, respectively. Even among the teleost MAVS sequences, only limited conservation could be observed (**Fig. 17**). Pairwise alignment of RbMAVS with 11 other MAVS members comprising of 6 sequences from fish and 5 sequences from other vertebrates revealed that RbMAVS shared the highest identity and similarity with the flounder MAVS homologues (60-61 and 70-71% identity and similarity, respectively) (**Table 9**). Alignment of the CARD regions of the homo- and orthologues revealed that the identity and similarity is primarily because of the conservation in the CARD region. RbMAVS CARD domain shared the maximum identity with the flounder CARD region. However, when only the fish sequences were aligned, they revealed a reasonably higher degree of similarity (figure not shown). The phylogenetic analysis stood as an averment with the closer relationship of RbMAVS with the flounder homologue. It clustered among the teleost MAVS group, particularly closer to the flounder homologue. The high bootstrap values confirmed the robustness and reliability of the tree (**Fig. 18**).



Fig. 17. Multiple sequence alignment of RbMAVS with other homologues.

The rock bream species name is bold and red wave underlined. The homologous MAVS sequences were obtained from NCBI and GenBank and the accession numbers are given in Table 9. The N-terminal CARD domain is grey shaded. The proline rich domain is enclosed in a box. The TRAF2 binding motifs are red and bold. The transmembrane helix is underlined. The length of amino acids is denoted at the end.

Table 9. Pairwise alignment of RbMAVS protein with MAVS homologues.

Identity (I) and similarity (S) percentages were derived using the whole protein and CARD sequence of RbMAVS and homologues.

Common name	Scientific name	Full Protein		CARD		Length	Mass (Da)	Source/Accession#
		I	S	I	S			
Rock bream	<i>Oplegnathus fasciatus</i>	100	100	100	100	586	61868	
Japanese flounder 1	<i>Paralichthys olivaceus</i>	61	71	78	88	671	68620	GenBank: ADI48370
Japanese flounder 2	<i>Paralichthys olivaceus</i>	60	71	78	88	673	68918	GenBank: ADI49715
Green spotted pufferfish	<i>Tetraodon nigroviridis</i>	51	67	69	80	578	58142	GenBank: ADL16494
Atlantic salmon	<i>Salmo salar</i>	33	52	47	72	636	64826	NCBI: NP_001161824
Rainbow trout	<i>Oncorhynchus mykiss</i>	25	40	51	73	422	43480	NCBI: NP_001182110
Common carp	<i>Cyprinus carpio</i>	33	50	53	70	612	62810	GenBank: ADZ55453
Zebra fish	<i>Danio rerio</i>	30	49	38	57	612	63490	GenBank: CAX48608
Human	<i>Homo sapiens</i>	24	39	34	47	564	56589	GenBank: AAH44952
Cow	<i>Bos taurus</i>	26	40	40	58	544	55170	NCBI: NP_001040085
House mouse	<i>Mus musculus</i>	24	39	39	55	527	53398	NCBI: NP_659137
Pig	<i>Sus scrofa</i>	26	41	40	53	548	55105	GenBank: BAF42542
Chicken	<i>Gallus gallus</i>	24	39	30	46	671	67748	NCBI:NP_001012911

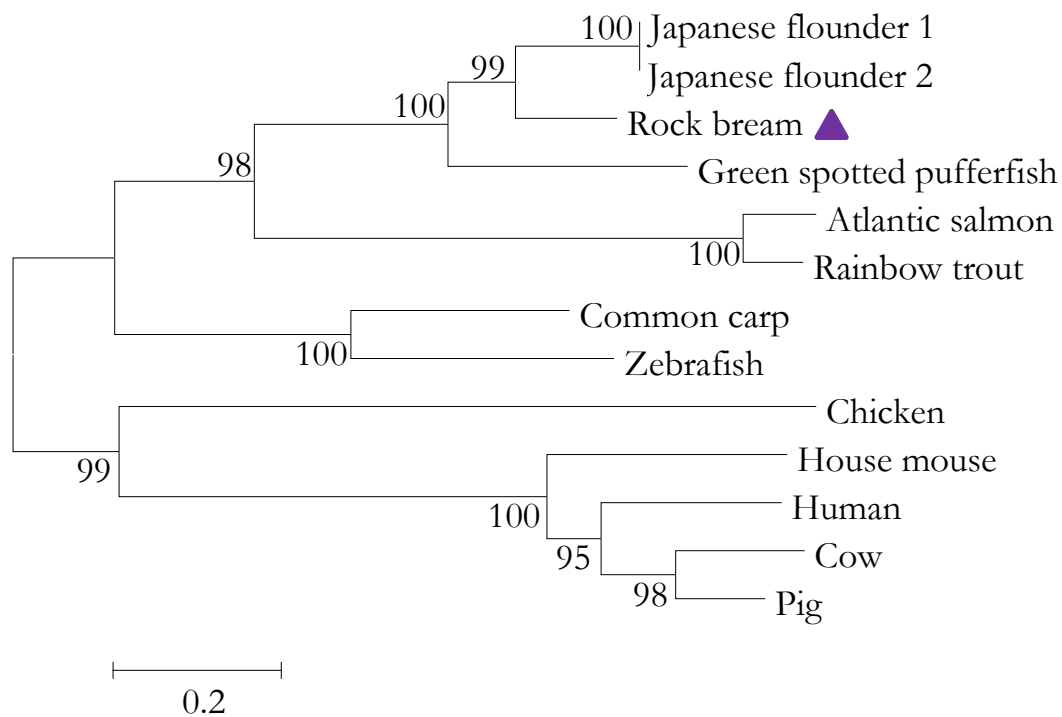


Fig. 18. Phylogenetic analysis of RbMAVS with MAVS homologous sequences.

The tree was constructed by the minimum evolution method in MEGA 5.0 using the full-length amino acid sequences. The accession numbers are denoted in Table 9.

4.4.2 Spatial expression of RbMAVS in normal tissues

Spatial expression analysis of *RbMAVS* in normal tissues revealed ubiquitous presence, with the maximum level of expression in blood (278-fold), followed by liver and kidney. Gill, intestine and brain shared similar levels of expression. Head kidney and spleen showed slightly lower levels of expression (Fig. 19).

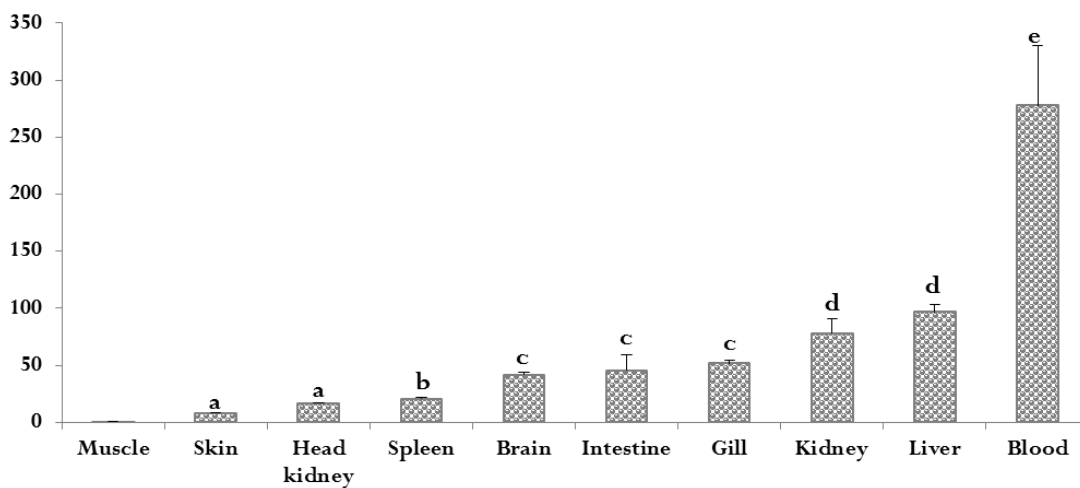


Fig. 19. Tissue distribution analysis of RbMAVS.

RbMAVS tissue-specific expression in muscle, intestine, skin, kidney, head kidney, spleen, gill, brain, liver tissues, and blood, collected from unchallenged rock bream was analyzed using quantitative RT-PCR. Relative mRNA expression was calculated using the $2^{-\Delta\Delta Ct}$ method, with β -actin as the invariant control gene. In order to determine the tissue-specific expression, the relative mRNA level was compared with muscle expression. Data are presented as mean values (n=3) with error bars representing SD. Data shown with “*” indicates significant expression levels at $P < 0.01$.

4.4.3 Temporal expression of RbMAVS after poly I:C challenge

RbMAVS expression was analyzed in blood, liver, spleen and head kidney isolated at different time points from fish challenged with poly I:C. In blood, alternative upregulation could be observed from 3 h p.i to 24 h p.i, with maximum level of expression at 12 h (1.9-fold). In liver, spleen and head kidney, elevation in the transcript level could be observed from 3 h p.i. In all these three tissues, maximum expression could be observed at 6 h p.i. (liver: 4-fold; spleen: 3.8-fold; head kidney: 2.4-fold). In head kidney, almost equal level of expression could be observed at 3 h p.i. (Fig. 20).

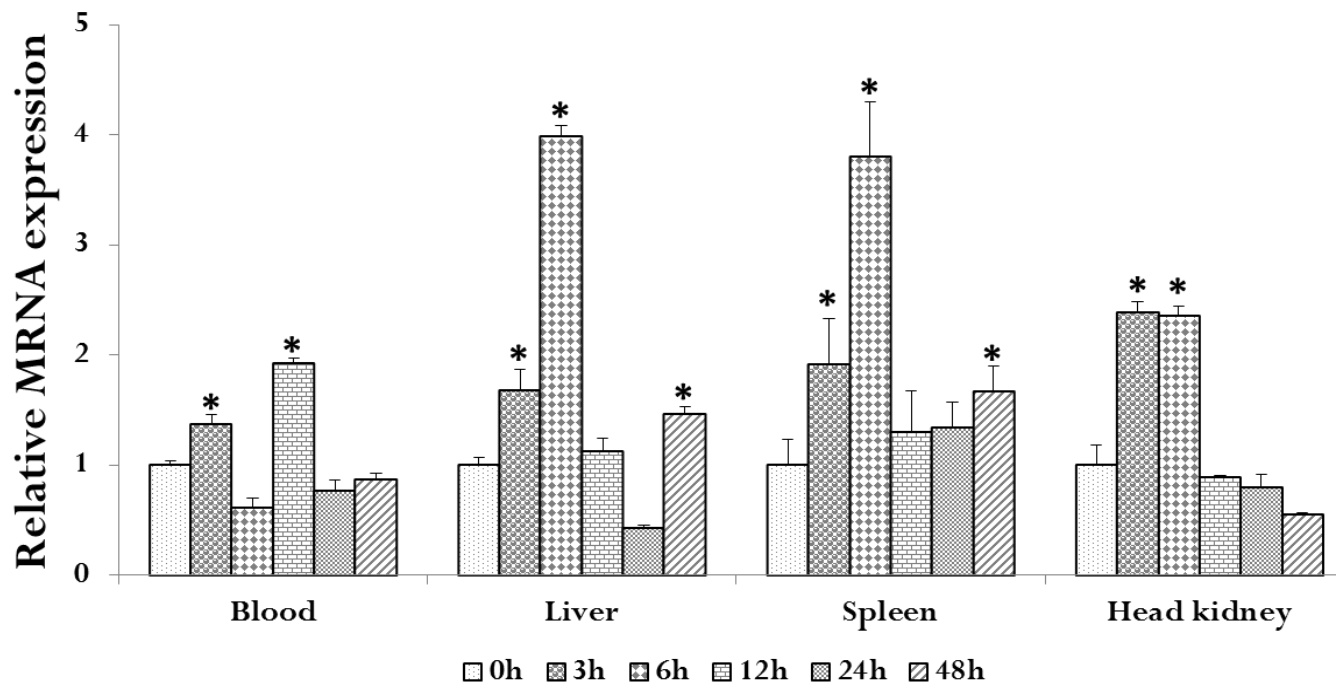


Fig. 20. *RbMAVS* expression analysis after immune challenges.

RbMAVS expression was analyzed in liver, blood, spleen, and head kidney post poly I:C challenge. Relative mRNA expression was calculated by the $2^{-\Delta\Delta C_t}$ method relative to PBS-injected controls and normalized with the same, with β -actin as the reference gene. Data are presented as mean values (n=3) with error bars representing SD. Data shown with “*” indicates significant expression levels at $P < 0.01$.

4.4.4 Antiviral activity of RbMAVS

In order to evaluate the antiviral activity of the rock bream MAVS, rock bream heart cells were transfected with either the empty vector (pcDNA™ 3.1/His B vector) or the pcDNA3.1-RbMAVS and then infected with marine birnavirus. As described earlier, the optimum amount of virus necessary to infect the cells and form CPE was identified earlier (data not shown). When two different viral titers were employed, more than 90% of the cells transfected with the empty vector showed CPE and were completely killed. Contrastingly, cells transiently transfected with the recombinant pcDNA3.1-RbMAVS inhibited the replication of the virus and protected the cells from infection. More than 90% of the cells were protected against infection compared with the control (**Fig. 21**).

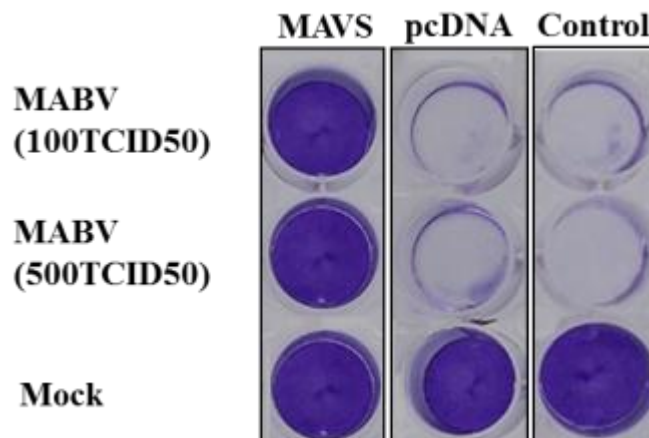


Fig. 21. Antiviral activity of RbMAVS against MABV.

The empty pcDNA 3.1 vector and pcDNA3.1-RbMAVS were transfected into rock bream heart cells. After 48 h of transfection, at 24 °C, the cells were infected with MABV at indicated densities. After 7 days of infection, cells were fixed with 4% PFA and stained with 3% crystal violet.

4.5 Discussion

Antiviral signaling pathways including the TLR and RLR cascades have been well documented in mammals. However, new facts about the regulation and signaling molecules

involved in viral defense are still emerging (Eisenacher and Krug, 2012; Li et al., 2012). In uninfected cells, the intramolecular interactions between the CARD and C-terminal regulatory domain hold the cytosolic helicases RIG-I/MDA5 in a closed, inactive conformation. The recognition of viral nucleic acids by RIG-I/MDA5 coupled with ATPase activity induces conformational changes that relieve the repression induced by the C-terminal regulatory domain, required to initiate the downstream signaling. The released CARD domains of RIG-I/MDA5 interact with the CARD domain of MAVS (Zemirli and Arnoult, 2012). Although, it is known that this interaction leads to the downstream activation of the signaling cascade, the mechanism by which MAVS plays a central role in regulating the complex events is still not fully elucidated. However, MAVS-deficient mice could not mount a proper IFN response to poly I:C stimulation and against RNA virus infection; thus standing as an evidence for the essential role of MAVS in antiviral innate immunity (Kumar et al., 2006; Sun et al., 2006). MAVS is known to interact with various proteins which either positively or negatively regulate various processes like antiviral, inflammatory responses, or cell death (Belgnaoui et al., 2011). It is also known to interact with mitochondrial proteins, kinases and E3 ubiquitin ligases that promote MAVS post-translational modifications (Belgnaoui et al., 2011).

In silico characterization of *RbMAVS* deduced protein revealed the presence of a MAVS-domain arrangement (CARD- Pro rich region- TM domain) with a conserved N-terminal CARD, a proline rich region, a putative TRAF2 binding motif and a transmembrane helix in the C-terminal region similar to the mammalian counterparts (Kawai et al., 2005; Meylan et al., 2005; Seth et al., 2005a). The CARD of MAVS is significant in interacting with the CARD of the active RIG-I/MDA5 and signaling the downstream cascade; and constructs lacking this evolutionarily conserved signatures have dominant negative effects and abolished activation of IFN β /NF- κ B in mammals (Seth et al., 2005a) and antiviral

function in fish (Biacchesi et al., 2009). Point mutations in CARD region inactivated the MAVS, signifying the conservation of the residues in accordance with their function (Seth et al., 2005a). Recent studies have demonstrated that MAVS forms detergent- and protease-resistant prion-like aggregates which induced IRF3 activation. The aggregate formation was solely dependent on CARD (Moresco et al., 2011). The C-terminal TM domain resembling the TM of several other tail-anchored mitochondrial proteins is essential for the antiviral function of MAVS and its localization to the outer mitochondrial membrane to exert its function (Seth et al., 2005a). A similar phenomenon had been demonstrated in fish MAVS where the truncated MAVS lacking TM domain revealed impaired activity (Biacchesi et al., 2009). A putative TRAF2 binding motif with a consensus sequence (PVQ/RD/ET) was observed in RbMAVS suggesting its interaction with the TRAF2. TRAF2 is required for IRF3 and NF- κ B induction (Sasai et al., 2010). The interaction of TRAF domain of TRAF3 and TRAF binding motif of MAVS is significant for antiviral response (Saha et al., 2006; Xu et al., 2005). MAVS is known to interact with the TRAF3/TRAF6 molecules which lead to IRF3 and NF- κ B activation in mammals (Zemirli and Arnoult, 2012). However, further studies are required to elucidate its interaction with TRAF2 and activation. Thus, the presence of evolutionarily conserved and functionally significant domains in RbMAVS portrays similar function like mammalian orthologues and fish homologues. Finally, the data obtained by pairwise alignment and phylogenetic analysis which shows the closer relationship of RbMAVS with the fish homologues (whose function has already been demonstrated) together with the earlier synteny associated studies of salmon MAVS (Biacchesi et al., 2009) confirms the expression of MAVS gene by a common ancestor of fish and mammals and RbMAVS as a new member of the MAVS family.

The ubiquitous expression of *RbMAVS* is not surprising since the protein is crucial in antiviral defense of the organism. The highest expression of *RbMAVS* was detected in the

immune organs of fish including blood and liver (Gao et al., 2008; Seki et al., 2012). Flounder *MAVS* was also highly expressed in immune organs like head and trunk kidney and spleen. Human IPS-1 showed ubiquitous expression including interferon-relevant tissues such as spleen, lung and peripheral blood leukocytes (Kawai et al., 2005). Atlantic salmon and carp *MAVS* also revealed high levels of expression in immune related tissues like spleen, trunk and head kidney (Lauksund et al., 2009; Su et al., 2011). *RbMAVS* expression was similar to that of green spotted pufferfish, where high expression was observed in liver (Xiang et al., 2011). A basal expression level is necessary for viral surveillance while induction of expression after viral entry provides protection from infection. The temporal expression of *RbMAVS* was significantly upregulated in the immune related tissues like blood, liver, and lymphoid organs like spleen and head kidney after poly I:C injection. The common carp *MAVS* which was significantly upregulated in spleen at 12 h after GCRV injection and at 48 h p.i. in liver. When the common carp cells were stimulated with poly I:C, *MAVS* transcripts were rapidly upregulated and recovered to control level. *RbMAVS* was rapidly stimulated in the major immune organs upon poly I:C injection. The results could not be comparatively discussed either with that of common carp or Atlantic salmon since those studies reported the expressional modulation of *MAVS* homologues after poly I:C treatment in cells. Fish *MAVS* plays a vital role in antiviral signaling against both RNA and DNA viruses (Biacchesi et al., 2009). Since the viral RNA recognition by the cytosolic sensors RIG/MDA5 bifurcate at the point of *MAVS*, upregulation of *RbMAVS* after poly I:C challenge, suggests its potential involvement in antiviral defense.

Overexpression of *RbMAVS* in rock bream heart cells provoked an antiviral state against the dsRNA virus, MABV. Rock bream fingerlings were determined to be infected by MABV (Kim et al., 2007). Mammalian *MAVS* provides potential antiviral effects against various viruses (Kawai et al., 2005; Kumar et al., 2006; Seth et al., 2005b). The teleost and

mammalian MAVS are effective against different viruses harboring ssRNA, dsRNA and DNA genomes (Biacchesi et al., 2009; Kumar et al., 2006; Lauksund et al., 2009). Our results demonstrate the antiviral potential of RbMAVS against MABV, further standing as an averment for the diversified viruses being recognized by the RLR system and protection conferred by the activation of downstream signaling molecules.

The molecular and functional evidences for the existence of RLR surveillance system and interferon system in teleost fish (Robertson, 2006; Zhang and Gui, 2012; Zou and Secombes, 2011) provide affirmation of the antiviral signaling pathway similar to that present in mammals (Eisenacher and Krug, 2012) and other vertebrates (Schultz et al., 2004). Furthermore, functional aspects of new genes/proteins involved in these pathways are still emerging in teleosts and mammals, making this long road of innate immunity a never ending one. A lot about ways could be understood from the mechanism of teleost fish to prevent viral infection and exert its potential therapeutic applications (Ireton and Gale, 2011).

Conclusively, in this study, we have affirmed the molecular existence of MAVS gene in rock bream, its transcriptional modulations post immunostimulant challenge and demonstrated its antiviral signaling role against marine birnavirus.

CHAPTER V

Characterization of the non-canonical kinases TBK1 and IKK ϵ

5.0 Characterization of the non-canonical kinases TBK1 and IKKε

Abstract

Tank-binding kinase 1 (TBK1) and I-κB kinase ε (IKK-ε, also called IKK-i) are non-canonical kinases which are determined to be pivotal regulators of type-I interferon production. RbTBK1 genome possessed 21 exons interrupted by 20 introns. RbTBK1 and RbIKKε proteins possessed the conserved catalytic kinase and ubiquitin like domain involved in phosphorylation and protein-protein interaction, respectively. RbTBK1 and RbIKKε showed higher conservation with the other orthologues. Phylogenetic analysis revealed that RbTBK1 and RbIKKε could have evolved from a common ancestor. Tissues distribution profiling of RbTBK1 and RbIKKε revealed highest expression in immune related tissues like liver and blood. Temporal expression analysis showed upregulation in liver and head kidney post poly I:C challenge. The conservation of structure at the protein level, its common ancestral origin and upregulation of RbTBK1 and RbIKKε upon immunostimulant challenge like poly I:C together suggests the pivotal role of RbTBK1 and RbIKKε in antiviral defense in rock bream, similar to the other orthologues.

5.1 Introduction

Innate immune system relies on multitude of signaling molecules for an efficient execution of defense against the invading microorganisms. The preliminary detection of bacterial and viral components by the pattern recognition receptors including Toll-like receptors, RIG like receptors triggers the assembly of signaling complexes that activate the inhibitor of κ B kinase (IKK) family of kinases. The defense function is accomplished through the activation of transcription factors which induce the activation/synthesis of effector molecules including interferons ($\text{IFN}\alpha/\beta$), chemokines (Interleukin-8 (IL-8), monocyte chemoattractant protein-1 (MCP-1), and proinflammatory cytokines (tumor necrosis factor- α (TNF- α) and interleukin-1 β (IL-1 β)) (Dinarello, 2007). The activation of transcription factors is primarily performed by kinases. The human kinome possesses an extensive group of intracellular signaling molecules involved in multiple cellular functions like metabolism, transcription, cell cycle progression, cytoskeletal rearrangement and cell movement, apoptosis, immunity and differentiation (Nousiainen et al., 2013; Pines, 1994). The conserved reaction mechanism of catalysis and their involvement in multiple processes makes them the potential targets for therapeutic applications in acute and chronic inflammation and cancer (Zhang and Daly, 2012).

TNF-receptor-associated factor (TRAF) family member-associated NF- κ B activator (TANK)-binding kinase 1 [TBK1, also referred to as NF- κ B-Activating Kinase (NAK) and TRAF2-associated kinase (T2K)] and I-kappa-B kinase epsilon [IKK ϵ ; also called as IKK-related kinase epsilon; Inducible I kappa-B kinase (IKKi)] are serine/threonine kinases that play important roles in regulation of inflammatory responses against foreign molecules. TBK1 and IKK ϵ belonging to the I κ B kinase (IKK)-activating kinase family are essentially involved in innate immunity through signal-induced activation of NF- κ B, IRF3 and IRF7. TBK1 was first identified as a TNF (tumor necrosis factors) receptor associated factor (TRAF)

binding protein functioning upstream of NF- κ B-inducing kinase (NIK) and IKK in the activation of NF- κ B. Initially, TBK1 was identified to be NF- κ B activating kinase, based on the death observed in mice deficient for *TBK1* because of massive liver apoptosis *in vitro*. The characterization of *TBK1*- deficient cells highlighted the crucial role of TBK1 in IFN gene induction, through signal-induced phosphorylation of IRF3 and IRF7. IKK ϵ was originally discovered on the basis of its structural similarity to the I κ B kinases (IKK α and IKK β) and transcriptional induction in response to lipopolysaccharide (Peters et al., 2000; Peters and Maniatis, 2001; Shimada et al., 1999). TBK1 and IKK ϵ phosphorylate IRF3 and IRF7 specific serine residues in the transcription factors IRF3 and IRF7 in response to virus infection. This phosphorylation of IRF3 and IRF7 induces a conformational change, promotes homodimerization and subsequent nuclear translocation where the factors bind to the IFN β gene enhancer along with NF- κ B and ATF2/cJUN to form the IFN β enhanceosome (Fitzgerald et al., 2003; Hemmi et al., 2004; Perry et al., 2004; Sharma et al., 2003).

5.2 Materials and methods

5.2.1 Animal rearing, cDNA library construction and *RbTBK1* and *RbIKK ϵ* gene identification

Healthy rock bream fish with average weight of ~50 g, procured from the Ocean and fisheries Research institute (Jeju, Republic of Korea) were adapted to the laboratory conditions (salinity $34 \pm 1\%$, pH 7.6 ± 0.5 at 24 ± 1 °C) in 400 L tanks. Blood samples were harvested from the caudal fin of healthy, unchallenged fish using a 22 gauge needle and centrifuged immediately for 10 min at $3000 \times g$ at 4 °C, to collect the hematic cells. Gill, liver, brain, kidney, head kidney, spleen, intestine, muscle, heart and skin tissues were harvested on ice from three healthy animals and immediately flash-frozen in liquid nitrogen and stored in -80 °C, until RNA extraction. Tri Reagent™ (Sigma, USA) was employed to

obtain total RNA from tissues. The concentration and purity of RNA were evaluated using a UV-spectrophotometer (BioRad, USA) at 260 and 280 nm. Purified total RNA samples were subjected to mRNA purification using Micro-FastTrack 2.0 mRNA isolation kit (Invitrogen). First strand cDNA was synthesized from 1.5 µg of mRNA using Creator™ SMART™ cDNA library construction kit (Clontech, USA); amplification was performed with Advantage 2 polymerase mix (Clontech) under conditions of 95 °C for 7 s, 66 °C for 30 min and 72 °C for 6 min. Over-representation of the most commonly expressed transcripts was excluded by normalizing the synthesized cDNA using Trimmer-Direct cDNA normalization kit (Evrogen, Russia). A cDNA GS-FLX shotgun library was created from the sequencing data obtained by using the GS-FLX titanium system (DNA Link, Republic of Korea). A cDNA contig showing high homology to the earlier identified TBK1 homologues was identified using BLAST and designated as *RbTBK1*.

5.2.2 BAC library creation and identification of *RbTBK1* BAC clone

Rock bream obtained from the Jeju Special Self-Governing Province Ocean and Fisheries Research Institute (Jeju, Republic of Korea) were accustomed to the laboratory conditions. Blood was harvested aseptically from the caudal fin using a sterile 1 mL syringe with 22 gauge needles, and a BAC library was constructed from the isolated blood cells (Lucigen Corp., USA). Briefly, genomic DNA obtained from blood cells was randomly sheared and the blunt ends of large inserts (>100 kb) were ligated to pSMART BAC vector to obtain an unbiased, full coverage library. Around 92160 clones, possessing an average insert size of 110 kb, were arrayed in 240 microtiter plates with 384 wells.

A two-step PCR based screening method was used to identify the clone of interest based on manufacturer's instructions. Primers were designed based on the cDNA sequence identified from the cDNA database. A gene specific clone was isolated and purified using Qiagen Plasmid Midi Kit (Hidden, Germany). The sequence was confirmed by pyro-

sequencing (GS-FLX titanium sequencing, Macrogen, Republic of Korea). The gene specific primers employed in the identification of the clone from the BAC library are tabulated in Table 10..

5.2.3 Sequence characterization and phylogenetic analysis of *RbTBK1* and *RbIKKε*

A cDNA sequence portraying domain similarity with the TBK1 homologues available in NCBI, was identified by BLAST and was subjected to DNAssist2.2 to predict the open reading frame (ORF) and translate nucleotide to protein. The conserved domains were identified using Expasy (<http://www.expasy.org/>), SMART (<http://smart.embl-heidelberg.de/>) and conserved domain database search (CDD). Pairwise alignment and multiple sequence alignment were executed using ClustalW (Thompson et al., 1994). A phylogenetic tree was reconstructed using minimum evolution method available in MEGA 5.0, with bootstrap values calculated with 5000 replications to estimate the robustness of internal branches (Tamura et al., 2011). The amino acid identity percentages were calculated by MatGAT program using default parameters (Campanella et al., 2003). The exon-intron structure was determined by aligning mRNA to the genomic sequence of *RbTBK1* using Spidey available on NCBI (<http://www.ncbi.nlm.nih.gov/spidey/>) (Wheelan et al., 2001). The complete genomic structure and putative promoter region were determined from the BAC sequencing data. The genomic structures used for comparison were obtained from exon view of Ensembl genome database.

5.2.4 Transcriptional profile of *RbTBK1* and *RbIKKε* gene in challenged and normal tissues

5.2.4.1 Poly I:C challenge

In order to monitor the transcriptional changes of *RbTBK1* and *RbIKKε* post dsRNA injection *in vivo*, poly I:C was employed as an immunostimulant. Sterile poly I:C stock was

prepared by dissolving poly I:C at the rate of 1.5 mg/ml in PBS and filtered through a 0.2 μ m filter. A time course experiment was performed by intraperitoneally injecting the animals with 100 μ L suspension of poly I:C stock. The control animals were injected with an equal volume of PBS. Liver and head kidney tissues were harvested from the un-injected, PBS-injected and immune challenged animals at time points of 3, 6, 12, 24, and 48 h post injection/infection (p.i.).

5.2.4.2 RNA isolation and cDNA synthesis

In order to perform the tissue distribution profiling of *RbTBK1* and *RbIKK ϵ* , gills, liver, brain, kidney, head kidney, spleen, intestine, muscle, heart and skin tissues and whole blood cells were harvested from un-injected fish. After challenge with PBS and poly I:C, liver, and head kidney tissues were harvested from challenged animals at the corresponding time points. Total RNA was obtained from tissues using Tri Reagent[™] (Sigma, USA). The concentration and purity of RNA were evaluated using a UV-spectrophotometer (BioRad, USA) at 260 and 280 nm. The RNA was diluted to 1 μ g/ μ L and cDNA was transcribed from 2.5 μ g of RNA from each tissue using a PrimeScript[™] first strand cDNA synthesis kit (TaKaRa). Concisely, RNA was incubated with 1 μ L of 50 μ M oligo(dT)₂₀ and 1 μ L of 10 mM dNTPs for 5 min at 65 °C. After incubation, 4 μ L of 5 \times PrimeScript[™] buffer, 0.5 μ L of RNase inhibitor (20 U), 1 μ L of PrimeScript[™] RTase (200 U), were added and incubated for 1 h at 42 °C. The reaction was terminated by adjusting the temperature to 70 °C for 15 min. Finally, synthesized cDNA was diluted 40-fold before storing at -20 °C for further use.

5.2.4.3 Tissue distribution

Quantitative reverse transcription polymerase chain reaction (qRT-PCR) was used to examine tissue distribution of *RbTBK1* and *RbIKK ϵ* mRNAs in various tissues of healthy fish. qRT-PCR was performed in a 15 μ L reaction volume containing 4 μ L of diluted cDNA,

7.5 μL of 2 \times SYBR Green Master Mix, 0.6 μL of each primer (10 pmol/ μL) and 2.3 μL of PCR grade water and subjected to the following conditions: one cycle of 95 $^{\circ}\text{C}$ for 3 min, amplification for 40 cycles of 95 $^{\circ}\text{C}$ for 20 sec, 58 $^{\circ}\text{C}$ for 20 sec, 72 $^{\circ}\text{C}$ for 30 sec. The baseline was automatically set by the Thermal Cycler DiceTM Real Time System software (version 2). In order to confirm that a single product was amplified by the primer pair used in the reaction, a dissociation curve was generated at the end of the reaction by heating from 60 $^{\circ}\text{C}$ to 90 $^{\circ}\text{C}$, with a continuous registration of changes in fluorescent emission intensity. The Ct for the *RbTBK1* and *RbIKK ϵ* (target genes) and *β -actin* (internal control) were determined for each sample. *RbTBK1* and *RbIKK ϵ* gene expression was determined by Livak comparative Ct method. The relative expression level calculated in each tissue was compared with respective expression level in muscle.

5.2.4.4 Temporal RbTBK1 mRNA expression analysis post poly I:C challenge

qRT-PCR was performed with cDNA prepared from RNA obtained from liver, and head kidney tissues isolated from PBS and poly I:C challenged animals. qRT-PCR conditions were the same as used for tissue distribution profiling. The ΔCt for each sample was determined by the method described above. The relative expression of *RbTBK1* and *RbIKK ϵ* were determined by the Livak method. The relative fold change in expression after immune challenges was obtained by comparing the relative expression to corresponding PBS-injected controls. The expression normalized to PBS-injected controls is represented in the figures.

All experiments were performed in triplicate. All data have been presented in terms of relative mRNA expressed as means \pm standard deviation (S.D.). Statistical analysis was performed using un-paired two-tailed Student's t-Test. Statistical significance was accepted at a P-value below 0.01.

Table 10. Primers used in RbTBK1 and RbIKKε characterization and qRT-PCR.

Gene	Purpose	Orientation	Primer sequences (5'-3')
RbTBK1	BAC screening & qRT-PCR	Forward	ACAGAGACACAAACTGCTCGTCGT
RbTBK1	BAC screening & qRT-PCR	Reverse	ACGGTATTGTTACCGGGACATCA
RbIKKε	qRT-PCR amplification	Forward	TGCCCTCTAAGCAGAAGGTGCT
RbIKKε	qRT-PCR amplification	Reverse	CTATAAACAGACTTGCCGTCCTCCCC
β-actin	qRT-PCR amplification	Forward	TCATCACCATCGGCAATGAGAGGT
β-actin	qRT-PCR amplification	Reverse	TGATGCTGTTGTAGGTGGTCTCGT

5.3 Results

5.3.1 Sequence characterization of RbTBK1 and RbIKKε

The partial cDNA sequences obtained from the rock bream cDNA library were determined using BLASTX and were assembled to obtain the complete open reading frame (ORF) and was further verified by sequencing. The 2169 bp ORF of *RbTBK1* cDNA (3130 bp) coded for a protein of 723 amino acids with molecular mass of 83 kDa and isoelectric point of 6.6. The *RbTBK1* cDNA possessed two mRNA instability motifs (²⁴⁷⁰ATTTA²⁴⁷⁴ and ²⁶⁹⁵ATTTA²⁶⁹⁹) and a poly adenylation signal 13 bp upstream of the poly-A tail. *RbIKKε* cDNA (3361 bp) possessed an ORF of 2163 bp coding for 721 amino acids with molecular mass of 82 kDa and isoelectric point of 6.9. *RbIKKε* cDNA possessed two mRNA instability motifs ²⁵⁸⁵ATTTA²⁵⁸⁹ and ²⁸⁷⁶ATTTA²⁸⁸⁰ in the 3' UTR. RbTBK1 and RbIKKε protein revealed the presence of conserved protein kinases (PK), catalytic (c) domain (PKc domain) in their N-terminal region [(RbTBK1: residues 15-293) and (RbIKKε: residues 19-327)]. Both the protein revealed ubiquitin-like domain [(RbTBK1: residues 297-385) and (RbIKKε: residues 300-388)], characteristic of the similar kinase family proteins (Fig. 22). The pairwise alignment performed with the predicted and characterized TBK1 proteins available in NCBI, revealed that RbTBK1 shared the highest identity with the predicted TBK1 protein of Nile tilapia (identity 96% and similarity 98%) and more than 70% identity with that of human and mouse TBK1 (Table 11.). RbIKKε shared the highest identity with IKKε homologue of Nile

tilapia (86%) and similar percentage of similarity with Zebra Mbuna and Nile tilapia (94%) (**Table 12**). The multiple sequence alignment of both RbTBK1 (**Fig. 22**) and RbIKK ϵ protein (**Fig. 23**) sequence with the orthologous proteins revealed high conservation in the domain regions, compared to the C-terminal region. Phylogenetic analysis performed to reveal the evolutionary ancestral relationship of RbTBK1 and RbIKK ϵ revealed that the kinase orthologues originated from a common ancestor and RbTBK1 and RbIKK ϵ were placed closer to the fish homologues that formed a separate cluster with the mammalian orthologues forming a distinct cluster (**Fig. 24**).

Rock bream MQSTNYLWLISDLGOGATANVYRGRHKKTGDLAYAVKVFNNLSFLRPLDVQMREFEVLKK 61
 Tilapia MQSTANYLWLISDLGOGATANVYRGRHKKTGDLAYAVKVFNNLSFLRPLDVQMREFEVLKK 61
 Zebrafish MQSTANYLWMSDLLGOGATANVYRGRHKKTGDLAYAVKVFNNLSFLRPLDVQMREFEVLKK 61
 House mouse MQSTSNHLWLLSDILGOGATANVFRGRHKKTGDLAYAVKVFNNISFLRPLDVQMREFEVLKK 61
 Human MQSTSNHLWLLSDILGOGATANVFRGRHKKTGDLFAIKVFNNISFLRPLDVQMREFEVLKK 61
 *****:***:*****:*****:*****:*****:*****:*****:*****:*****:*****

Rock bream LNHNKIVKLFAVEEESNTRHKVLMVEYCPGSLYTVLEESSNAYGLPEDEFLIVLHDVVAG 122
 Tilapia LNHNKIVKLFAVEEESNTRHKVLMVEYCPGSLYTVLEESSNAYGLPEDEFLIVLHDVVAG 122
 Zebrafish LNHNKIVKLFAVEEESNTRHKVLMVEYCPGSLYTVLEEPSNAYGLPEDEFLIVLQDVVAG 122
 House mouse LNHNKIVKLFADIEEETTRHKVLMVEYCPGSLYTVLEEPSNAYGLPESEFLIVLRDQVVG 122
 Human LNHNKIVKLFADIEEETTRHKVLMVEYCPGSLYTVLEEPSNAYGLPESEFLIVLRDQVVG 122
 *****:***:*****:*****:*****:*****:*****:*****:*****:*****:*****

Rock bream MNHLREYGIHVHRDIKPGNIMRVIGEDGRSVYKLTDFGAARELEDDEQFVSLYGTTEYLHPD 183
 Tilapia MNHLREYGIHVHRDIKPGNIMRVIGEDGRSVYKLTDFGAARELEDDEQFVSLYGTTEYLHPD 183
 Zebrafish MNHLREYGIHVHRDIKPGNIMRVIGEDGQSVYKLTDFGAARELEDDEQFVSLYGTTEYLHPD 183
 House mouse MNHLREYGIHVHRDIKPGNIMRVIGEDGQSVYKLTDFGAARELEDDEQFVSLYGTTEYLHPD 183
 Human MNHLREYGIHVHRDIKPGNIMRVIGEDGQSVYKLTDFGAARELEDDEQFVSLYGTTEYLHPD 183
 ***** *****:*** *****

Rock bream MYERAVLRKDHQKYGATVDLWSIGVTFYHAATGSLPFRPFEGPRRNKEVYKIITEKPSG 244
 Tilapia MYERAVLRKDHQKYGATVDLWSIGVTFYHAATGSLPFRPFEGPRRNKEVYKIITEKPSG 244
 Zebrafish MYERAVLRKDHQKYGATVDLWSIGVTFYHAATGSLPFRPFEGPRRNKEVYKIITEKPPG 244
 House mouse MYERAVLRKDHQKYGATVDLWSIGVTFYHAATGSLPFRPFEGPRRNKEVYKIITEKPSG 244
 Human MYERAVLRKDHQKYGATVDLWSIGVTFYHAATGSLPFRPFEGPRRNKEVYKIITEKPSG 244
 *****:*****:***** *****

Rock bream TISGHQKCENGKIEWSTEMPVSCSLSKGLQSLTLPVLANILEADQEKCWGFDQFFAETNDI 300
 Tilapia TISGHQKCENGKIEWSTEMPVSCSLSKGLQSLTLPVLANILEADQEKCWGFDQFFAETNDI 300
 Zebrafish AISGHQKFENGKIEWSSEMPVSCSLSKGLQSLTLPVLANILEADQEKCWGFDQFFAETSDI 300
 House mouse AISGVQKAENGPIDWSGDMPLSCSLSQGLQALLTPVLANILEADQEKCWGFDQFFAETSDV 300
 Human AISGVQKAENGPIDWSGDMPLSCSLSRGLQVLLTPVLANILEADQEKCWGFDQFFAETSDI 300
 :*** ** * ** * ** * :***:*****:*** *****

Rock bream LHRTVVYVFSLQOATLHHVYIHEYNTAALFOELLSRRTSIPLHNQELLYEGRRLLVDPNRQ 366
 Tilapia LHRTVVYVFSLQOATLHHVYIHEYNTAALFOELLSRRTSIPLHNQELLYEGRRLLVDPNRQ 366
 Zebrafish LHRIVVYVFSLQOATLHHVYIHTYNTANLFOELLSRRTSIPLHNQELLYEGRRLLVDPNRQ 366
 House mouse LHRMVIHVFSLQOATLHHVYIHTYNTAALFOELLSRRTSIPLHNQELLYEGRRLLVDPNRQ 366
 Human LHRMVIHVFSLQOATLHHVYIHTYNTATIFHELVIYKQTKIISNQELLYEGRRLLVDPNRQ 366
 ** * :*****: * * : * * * * * : * * * * * : * * * * * : * * * * * : * * * * * : * * * * *

Rock bream AKTFPKTSRDNPIMLVSRRESVATVGLIFEDPSPPKVQPRYDLDDLASAYAKTFAGDVGHVWK 427
 Tilapia AKTFPKTSRDNPIMLVSRRESVATVGLIFEDPSPPKVQPRYDLDDLASAYAKTFAGDVGHVWK 427
 Zebrafish AQTFPKTSRDNPIMLLCRDPVNTVGLLIFEDPSPPKVQPRYDLDDLASAYAKTFAGDVGHVWK 427
 House mouse AQHFPKTTEENPIFVTSREQLNTVGLRYEKISLPKIHPRYDLDDLASAYAKTFAGDVGHVWK 427
 Human AQHFPKTTEENPIFVTSREQLNTVGLRYEKISLPKIHPRYDLDDLASAYAKTFAGDVGHVWK 427
 * : * * * * * : * * * * * : * * * * * : * * * * * : * * * * * : * * * * * : * * * * *

Rock bream TSESLVYQELVVRKGVRLIELMKEDYSEILHKKSEVFHLCNFCQILEKTEQLFEVMMRA 488
 Tilapia TSESLVYQELVVRKGVRLIELMKEDYSEILHKKSEVFHLCNFCQILEKTEQLFEVMMRA 488
 Zebrafish TSDSLVYQELVVRKGVRLIELMKEDYSEILHKKSEVFHLCNFCQILEKTEQLFEVMMRA 488
 House mouse TASTLLVYQELVVRKGVRLIELMKEDYSEILHKKSEVFHLCNFCQILEKTEQLFEVMMRA 488
 Human IASTLLVYQELVVRKGVRLIELMKEDYSEILHKKSEVFHLCNFCQILEKTEQLFEVMMRA 488
 :.***:*****:***: * * * * * : * * * * * : * * * * * : * * * * * : * * * * * : * * * * *

Rock bream NMQSSEYDEISDMHKKVLRISGSLEPIERTTQDVKSKFLSGGLTDTGWTQVVGTHPEDRNV 549
 Tilapia NMLSSEYDEISDMHKKVLRISGSLEPIERTTQDVKSKFLSGGLTDTGWTQVVGTHPEDRNV 549
 Zebrafish NILSSEYDEIRDRKVKVLRISGSLEPIERTTQDVKSKFLSGGLTDTGWTQVVGTHPEDRNV 549
 House mouse NLEAAELGEISDIHTKLLRLSSSQGTIETSQDIDSRSLPGLLADTWAHQEGTHPKDRNV 549
 Human NLEAAELGEISDIHTKLLRLSSSQGTIETSQDIDSRSLPGLLADTWAHQEGTHPKDRNV 549
 * : * * * * * : * * * * * : * * * * * : * * * * * : * * * * * : * * * * * : * * * * *

Rock bream EKIKVLLDAITAIYQFQKDKAERRLPYNEEQIHKFDKQKLVHASKARSLFTEECAMKYR 600
 Tilapia EKIKVLLDAITAIYQFQKDKAERRLPYNEEQIHKFDKQKLVHASKARSLFTEECAMKYR 600
 Zebrafish EKIKVLLDAIGAIYQFQKDKAERRLPYNEEQIHKFDKQKLVHASKARSLFTEECAMKYR 600
 House mouse EKLQVLLNCITEIYQFQKDKAERRLPYNEEQIHKFDKQKLVHASKARSLFTEECAMKYR 600
 Human EKLQVLLNCMTEIYQFQKDKAERRLPYNEEQIHKFDKQKLVHASKARSLFTEECAMKYR 600
 :: : * * * * * : * * * * * : * * * * * : * * * * * : * * * * * : * * * * *

Rock bream LFISKSEEWMRKVHVRKQLLGLSGQLISIEKEVTMLMERAIKLQEQPLQKVLPLVSSGMK 671
 Tilapia LFISKSEEWMRKVHVRKQLLGLSGQLISIEKEVTMLMERAIKLQEQPLQKVLPLVSSGMK 671
 Zebrafish LFISKSEEWMRKVHVRKQLLGLSGQLISIEKEVTMLMERAIKLQEQPLQKVLPLVSSGMK 671
 House mouse AFKDKSEEWMRKMLHLRKLQSLTQCFDIEEEVSKYQDYTNELQETLPQKMLAASGGVKH 671
 Human AFLNKSEEWIRKMLHLRKLQSLTQCFDIEEEVSKYQDYTNELQETLPQKMLAASGGVKH 671
 * : * * * * * : * * * * * : * * * * * : * * * * * : * * * * * : * * * * * : * * * * *

Rock bream PQA--YLSQNTLVEMTLGMKKLKEEMEGVVKELAENNHFLERFGTLTLDGGLRG---- 723
 Tilapia PQA--YLSQNTLVEMTLGMKKLKEEMEGVVKELAENNHFLERFGTLTLDGGLRG---- 723
 Zebrafish PQA--YLSQNTLVEMTLGMKKLKEEMEGVVKELAENNHFLERFGTLTLDGGLRG---- 723
 House mouse AMAPIYSSNTLVEMTLGMKKLKEEMEGVVKELAENNHFLERFGTLTLDGGLRG---- 729
 Human TMTPIYSSNTLVEMTLGMKKLKEEMEGVVKELAENNHFLERFGTLTLDGGLRG---- 729
 . : * * * * * : * * * * * : * * * * * : * * * * * : * * * * * : * * * * * : * * * * *

Fig. 22. Multiple sequence alignment of RbTBK1 with other homologues.

TBK1 homologues were obtained from GenBank. Rock bream species name is inclined. The accession numbers of the TBK1 is tabulated in Table 11. The protein kinase domain is grey shaded and the active site residues are bold and underlined. The ubiquitin-like domain is underlined and the hydrophobic patch (polypeptide binding sites) is grey shaded.

Rock bream MSGMTASTTNYLWSLQDV **LQGGATASVYKARNKKSSELVAVKVFNMVSYNRPHEVQVQVREF** 60
Zebra Mbuna MSGITASTISYLWSVDDVVLQGGATASVYKARHKRSSELVAVKVFNIMSYNRPHQVQVQVREF 60
Zebrafish ---MTSTANYLWSQEDILQGGATANVYKARNKKTGELVAVKVFNLVSYNRPYEVQVQVREF 56
Human ---MQSTANYLWHTDDLLQGGATASVYKARNKKSSELVAVKVFNTTSYLRPREVQVQVREF 56
House mouse ---MQSTTNYLWHTDDLLQGGATASVYKARNKKSSELVAVKVFNSASYRRPPEVQVQVREF 56
* * * * * : * : * * * * * . * * * * * : * : * * * * * * * * * * * : * : * * * * *

Rock bream **EMLRKLNHSNIVRLYTVVEELPS--KQKVLVMEYCSGGSLLSVLEEPENAFGLPETEFLTV** 118
Zebra Mbuna EMLRKLNHSNIVRLYTVVEELPS--KQKVLVMEYCSGGSLLSVLEEPENAFGLPETEFLTV 118
Zebrafish EVLQQLNHNIVKLVFAVEEIIISNPQKILVMEYCSGGSLNMLEQPEHAFGLPESEFLIV 116
Human EVLRLNHNQIVKLVFAVEETGGS-RQKVLVMEYCSGGSLLSVLESPENAFGLPEDEFLV 115
House mouse EVLRLNHNQIVKLVFAVEETGGS-RQKVLVMEYCSGGSLLSVLEDPENTFGLSEEEFLV 115
* : * : * * * * * : * : * * * * * . * * * * * : * : * * * * * * * * * * * : * : * * * * *

Rock bream **LQCVVQGMNHLRENGVVRDIPKPGNIMROVGEDGKSVYKLTDFGAARELEDDDEKFMFSIYG** 178
Zebra Mbuna LQCVVQGMNHLRENGVVRDIPKPGNIMROVGEDGKSVYKLTDFGAARELEDDDEKFMFSIYG 178
Zebrafish LHCVAHGMNHLRENSVVRDIPKPGNIMROVGEDGKSVYKLTDFGAARELEDDDEKFMFSIYG 176
Human LRCVVAGMNHLRENGIVHRDIPKPGNIMRLVGEEGQSIYKLTDFGAARELEDDDEKFMFSIYG 175
House mouse LRCVVAGMNHLRENGIVHRDIPKPGNIMRLVGEEGQSIYKLSDFGAARKLDDDEKFMFSIYG 175
* : * : * * * * * : * : * * * * * . * * * * * : * : * * * * * * * * * * * : * : * * * * *

Rock bream **TEEYLHPDMYERAVLRKPKHKSIVGVSVDLWSIGVTLYHAATGSLPFTPYGGPRNKPTMF** 238
Zebra Mbuna TEEYLHPDMYERAVLRKPKHKSIVGVSVDLWSIGVTLYHAATGSLPFTPYGGPRNKPTMF 238
Zebrafish TEEYLHPDMYERAVLRSPQKAYGVSVDLWSIGVTIYHMATGSLPFRPFGGPRNKPKMMH 236
Human TEEYLHPDMYERAVLRKPKQKAFGVTVDLWSIGVTLYHAATGSLPFTPYGGPRNKPTMF 235
House mouse TEEYLHPDMYERAVLRKPKQKAFGVTVDLWSIGVTLYHAATGSLPFTPYGGPRNKPTMF 235
* * * * * * * * * * * . * : * : * * * * * : * * * * * * * * * * * * * : * * * * * * * .

Rock bream **KITTEKPMGAIAGIQRVADGPIEWSYHLPHSCQLSQGLMVQLVPLVLAGILEADQERCWGF** 298
Zebra Mbuna KITTEKPMGAIAGIQRRREGPIDWSYHLPHSCQLSQGLRVQLVPLVLAGIMEADQERCWGF 298
Zebrafish KITTEKPMGAIAGIQKEDGPIEWRDKLPLSCQLSEGLKTLVPLVLANILLADDEKCKWKF 296
Human RITTEKPMGAIAGAQRRRENGPLEWSYTLPIITCQLSLGQLVPLVLANILLEVEQAKCWGF 295
House mouse RITTEKPMGAIAGISGTQKQENGPLEWSYSLPITCRLSMGLQNLVPLVLANILLEVEQAKCWGF 295
* * * * * * * * * * * . * : * : * * * * * : * * * * * * * * * * * * * : * * * * * * * .

Rock bream **DQFFATATDILQROPIHLSLQQAAMACIYIHHYNTVSLFFEEVASOTGIGVQLQHL** 358
Zebra Mbuna DQFFATATDILQROPIHLSLQQAAMACIYIHHYNTVSLFFEEVASOTGIGVQLQHL 358
Zebrafish QPFFATNDILNRITIIYIFSLQATYYSIYIQFHNTVSIFFEDVQAQTGIEPAAQQYLFQ 356
Human DQFFAETSDDLQRVVHVFLSQAVALHHIYIHAHNTIAIFQEAHVKTQSVAPRHQYLFQ 355
House mouse DQFFAETSDDLQRTVIHVFLSQAVALHHVYIHAHNTIAIFLEAVYEQTNVTPKHQYLFQ 355
* * * : * : * * * * * : * : * * * * * . * * * * * : * : * * * * * * * * * * * : * : * * * * *

Rock bream **GHELPLEGNMKVVNLPRTSPARPLIILSHG--PEANTSLPFREPESPGISRFVDMADYN** 416
Zebra Mbuna GHDLLEGSMMKVVNLPRTSPSQPLIILSYAT--DEANTSLPFREPESPIPARFVDMADYN 417
Zebrafish GHPLLDPSMKVVNIPHTSSDKPMILISRR--LERIIGYPFEPESPPMPGKFDVADVF 414
Human GHLCVLEPSVSAQHIAHTTASSPLTLFSTA--IPKGLAFRDPALDVPKFPKVDLQADYN 413
House mouse GHPCVLEPSLSAQHIAHTAASSPLTLFMSSDTPKGLAFRDPALDVPKFPKVDLQADYS 415
* * * : * : * * * * * : * : * * * * * . * * * * * : * : * * * * * * * * * * * : * : * * * * *

Rock bream **FSKVIQVGVHQLRIVRLLHTRHRELLQGYYSYMMRLRRECCEAMHSIAMTIRLQACLN** 476
Zebra Mbuna FSKVIQVGVHQLRIVRLLHTRHRELLQGYYSYIMKLRNECREALHSIAMTIRLQACLN 477
Zebrafish FTKTIVKVIHQYLRVIAIYSLQYRQFQILQGFNSYIEQTSSEVIDVAHRISKVKMKLHSSIS 474
Human TAKGVLGAGYQALRLARALLDQQLMFRGLHWVMEVLQATCRRTLEVARTSLLYLSSSLG 473
House mouse TAKGVLGAGYQALWLRVLLDQALMLRGLHWVLEVLQDTCQOTLEVTRTALLYLSSSLG 475
* * : * : * * * * * : * : * * * * * . * * * * * : * : * * * * * * * * * * * : * : * * * * *

Rock bream **IEHRIHTLGH-FPSENQGSADNSQKLQVHEHLP-IYAAGIQEFQNRDLHLQIEQAKLAE** 534
Zebra Mbuna AEHGIRTLDP-YTSENQGSAAANGRLRQVHQLP-LYSAGIQEFQNRDLHLQIEQAKLAE 535
Zebrafish TEKTLHVFTQTFAHEFPDFIDSKKPLIEAELQHMCGRGIREFQNLQYLRVTLKSHSE 534
Human TERFSSVAGTPEIQELKAAELRSRLRTLAEVLS-RCSQNTTETQESLSSLNRELVKSRD 532
House mouse TERFSSGAGMPDVQERKEATELRLRQLTLEILS-KCSHNVTETQRSLSLQELGELLKNRD 534
* : * : * * * * * : * : * * * * * . * * * * * : * : * * * * * * * * * * * : * : * * * * *

Rock bream **TLAND-KSCQKMEMLQOKIMAIHQYRKDRDLTGKLAYNDEQIHKFEKIHLSCHIKRVKSL** 593
Zebra Mbuna TLAND-KSCQKMEMLQOKITAIHQYRKDRDLTGKLAYNDEQIHKFEKIHLSCHIKRVKSL 594
Zebrafish TLAND-KSIQKMEVLLSQVVDVHFQYFRDRQTRKLGYNDEQIHKFEKLNLSYLLKFKFSL 593
Human QVHED-RSIQIQIQCCLDKMNFYKQFKKSRMRPGLGYNEEQIHKLKDKNVFNHSLAKRLLQV 591
House mouse QIHEDNKSQKIQCCLDKMHFIYKQFKKSRMRPGLSYNEEQIHKLKDKNVFNHSLAKRLLQV 594
: * : * * * * * : * : * * * * * . * * * * * : * : * * * * * * * * * * * : * : * * * * *

Rock bream **CREDCVQRYKELLASTRTWSSVLEMQTRLQDFSSFSTGLLADLEMSEQRHNKALDRILF** 653
Zebra Mbuna FREDCVQRYKEVLDSTRWNSLMLQLQDFSSFSAGLIADLEMSEQCQNKVMDRILY 654
Zebrafish FKDDCFQKYLDVLTNTDRCRSALYDMQTHLDFRDTLLQRIQDLKAHEILQNKVLERVVH 653
Human FQEECVQRYKQASLVTHGKRMVHETRNHLRLVGCVAACNTEAQGVQESLSKLEELSH 651
House mouse FQEECVQRYQVSLVTHGKRMVQVQRAQNHHLIGHSVATCNSEARGAQESLNKIFDQLL 654
: * : * * * * * : * : * * * * * . * * * * * : * : * * * * * * * * * * * : * : * * * * *

Rock bream **SLQSKRAGQQPGITP-----RDQDMVSRMHLKEEMEILVRELQCNNIIIESLGAAN** 706
Zebra Mbuna TLQSKRPEQQSAVIP-----KDNDQDMVSRMHLKEEMEILVRELQCNNIIIESLGAAN 707
Zebrafish RAVQFPVKAQEVVDGK-----KKEEHMILKMTLRLKSEMAVAVELQKNNNMIESLSVVT 706
Human QLLQDRAKGAQASPPPIAPYPSPTKDLLLHMQLCEGMKLLASDLDNRIIERLNRVP 711
House mouse DRASE--QGAEVSPQPMAPHPGDPKDLVFMHQLCNDMKLLAFDLQDNNRIIERLNRVP 712
. : * : * * * * * : * : * * * * * . * * * * * : * : * * * * * * * * * * * : * : * * * * *

Rock bream SPAALEPSLARPSTL 721
Zebra Mbuna SPAALEPTLARPSTL 722
Zebrafish PTMPVEKKNPQTRNP 721
Human APPDV----- 716
House mouse SAPDV----- 717
. : * : * * * * * : * : * * * * * . * * * * * : * : * * * * * * * * * * * : * : * * * * *

Fig. 23. Multiple sequence alignment of RbIKK ϵ with other homologues.

IKK ϵ homologues were obtained from GenBank and the accession numbers are tabulated in Table 12. Rock bream species name is inclined. The protein kinase domain is grey shaded with the active site residues are bold and underlined. The ubiquitin-like domain is wave underlined and the polypeptide binding sites are marked in red and circled.

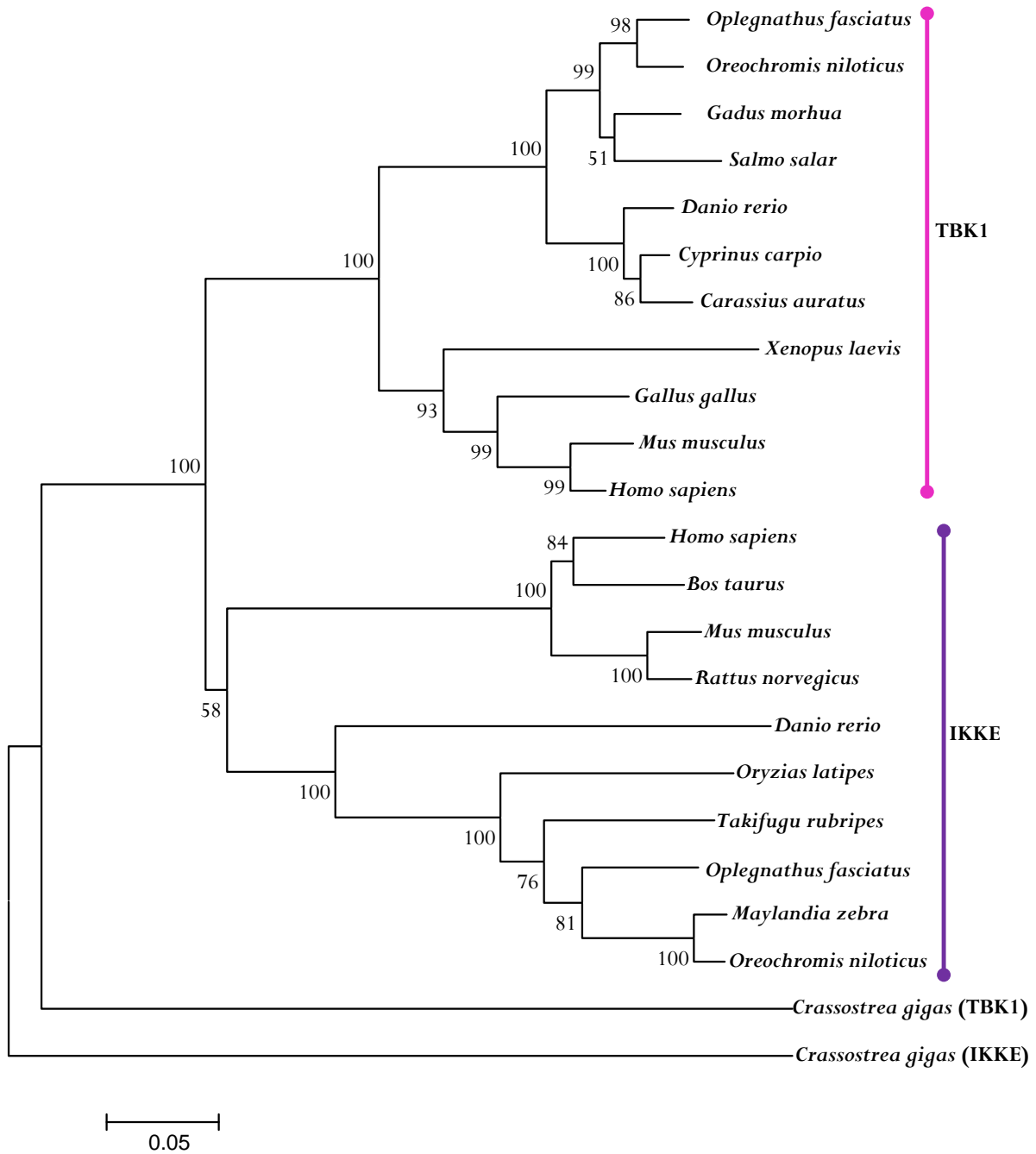


Fig. 24. Phylogenetic analysis of RbTBK1 and RbIKKε.

The TBK1 and IKKε homologues were obtained from GenBank and tabulated in tables 5.2 and 5.3, respectively. The tree was constructed by the minimum evolution method in MEGA 5.0 using the full-length amino acid sequences.

Table 11. Pairwise alignment of RbTBK1 protein with TBK1 homologues.

Identity (I) and similarity (S) percentages were derived using the whole protein sequence of RbTBK1 and homologues.

| Species | Common name | Taxonomy | I % | S % | Source and accession no. |
|------------------------------|---------------------|-----------------|------------|------------|---------------------------------|
| <i>Oplegnathus fasciatus</i> | Rock bream | Actinopterygii | 100 | 100 | NCBI: KF267454 |
| <i>Oreochromis niloticus</i> | Nile tilapia | Actinopterygii | 96 | 98 | NCBI: XP_003458486 |
| <i>Gadus morhua</i> | Atlantic cod | Actinopterygii | 90 | 94 | GenBank: ADL60136 |
| <i>Salmo salar</i> | Atlantic salmon | Actinopterygii | 88 | 95 | NCBI: NP_001243651 |
| <i>Cyprinus carpio</i> | Common carp | Actinopterygii | 84 | 92 | GenBank: ADZ55455 |
| <i>Danio rerio</i> | Zebrafish | Actinopterygii | 85 | 92 | NCBI: NP_001038213 |
| <i>Carassius auratus</i> | Goldfish | Actinopterygii | 84 | 92 | GenBank: AEN04475 |
| <i>Gallus gallus</i> | Chicken | Aves | 71 | 83 | NCBI: NP_001186487 |
| <i>Mus musculus</i> | House mouse | Mammalia | 71 | 83 | NCBI: NP_062760 |
| <i>Homo sapiens</i> | Human | Mammalia | 71 | 83 | NCBI: NP_037386 |
| <i>Xenopus laevis</i> | African clawed frog | Amphibia | 64 | 78 | NCBI: NP_001086516 |
| <i>Crassostrea gigas</i> | Pacific oyster | Bivalvia | 29 | 49 | GenBank: EKC41453 |

Table 12. Pairwise alignment of RbIKKε protein with IKKε homologues.

Identity (I) and similarity (S) percentages were derived using the whole protein sequence of RbIKKε and homologues.

| Species | Common name | Taxonomy | I % | S% | Source & accession no. |
|------------------------------|--------------------|----------------|-----|-----|------------------------|
| <i>Oplegnathus fasciatus</i> | Rock bream | Actinopterygii | 100 | 100 | NCBI |
| <i>Maylandia zebra</i> | Zebra Mbuna | Actinopterygii | 85 | 94 | NCBI: XP_004545132 |
| <i>Oreochromis niloticus</i> | Nile tilapia | Actinopterygii | 86 | 94 | NCBI: XP_003441417 |
| <i>Takifugu rubripes</i> | Pufferfish | Actinopterygii | 83 | 90 | NCBI: XP_003973740 |
| <i>Oryzias latipes</i> | Japanese rice fish | Actinopterygii | 75 | 85 | NCBI: XP_004069314 |
| <i>Danio rerio</i> | Zebrafish | Actinopterygii | 57 | 75 | NCBI: NP_001002751 |
| <i>Homo sapiens</i> | Human | Mammalia | 50 | 67 | NCBI: NP_054721 |
| <i>Mus musculus</i> | House mouse | Mammalia | 48 | 68 | NCBI: NP_062751 |
| <i>Rattus norvegicus</i> | Norway Rat | Mammalia | 48 | 67 | NCBI: NP_001102324 |
| <i>Bos taurus</i> | Cow | Mammalia | 50 | 67 | NCBI: NP_001039810 |
| <i>Crassostrea gigas</i> | Pacific oyster | Bivalvia | 30 | 53 | GenBank: EKC36402 |

5.3.2 Genome characterization of *RbTBK1*

RbTBK1 genome possessed 21 exons intervened by 20 introns. The first exon composed of untranslated region in its entirety, similar to the other compared orthologues. *RbTBK1* genomic structure was similar to that of human and mouse genes in the number of exons, while a little variation could be observed in the 19th and 21st exons, resulting in the excess 6 amino acids in human and mouse TBK1 proteins. The genome size of *RbTBK1* (13668 bp) was less than that of human *TBK1* genome (50060 bp). The coding exons of *RbTBK1* were exactly similar to that of tilapia, with which it shared the highest level of identity at the protein level as well (**Fig. 25**).

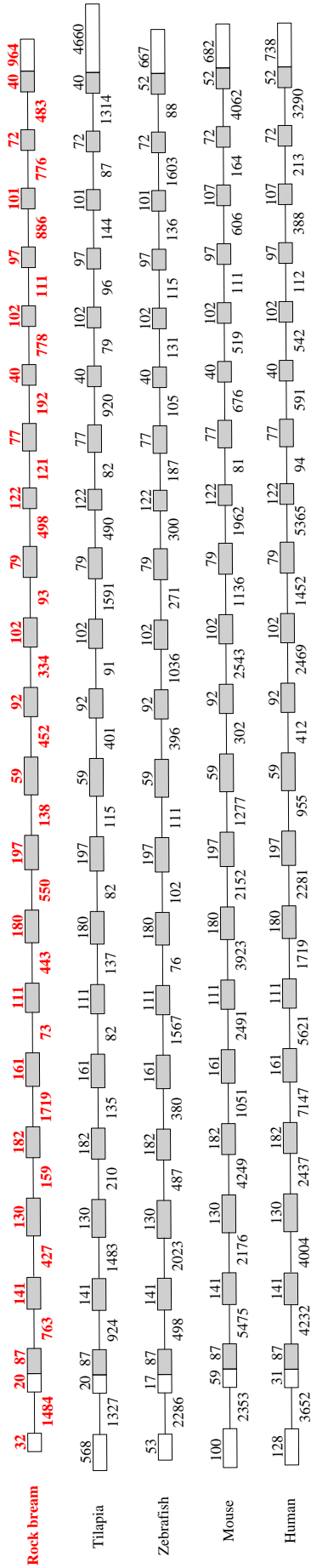


Fig. 25. Genomic structure analysis of *RbTBK1* with *TBK1* orthologues.

The exon-intron structures of few orthologues were derived from the exon view of Ensembl and human *TBK1* structure was derived from NCBI. The ensemble ids are Tilapia: ENSTNIT00000006093, Zebrafish: ENSDART00000150097, Mouse: ENSMUST00000020316 and the NCBI reference id of Human: NC_000012 (gene ID: 29110). The translated/coding regions are denoted by dark shaded boxes and the introns are denoted by lines. Exon sizes are indicated above the exon boxes and intron lengths are shown below the intron lines. Untranslated regions at the 5'- and 3'-ends are denoted by empty boxes.

5.3.3 Tissue distribution profiling of *RbTBK1* and *RbIKKε*

Tissue distribution analysis of *RbTBK1* and *RbIKKε* in tissues isolated from normal unchallenged rock bream revealed ubiquitous presence of *RbTBK1* and *RbIKKε* in all the examined tissues. *RbTBK1* was highly expressed in blood (175-fold) followed by liver (74-fold). *RbIKKε* was detected most in liver (155-fold) followed by blood (125-fold). Gill, spleen, intestine and kidney showed relatively similar levels of expression of both *RbTBK1* and *RbIKKε* (Fig. 26)

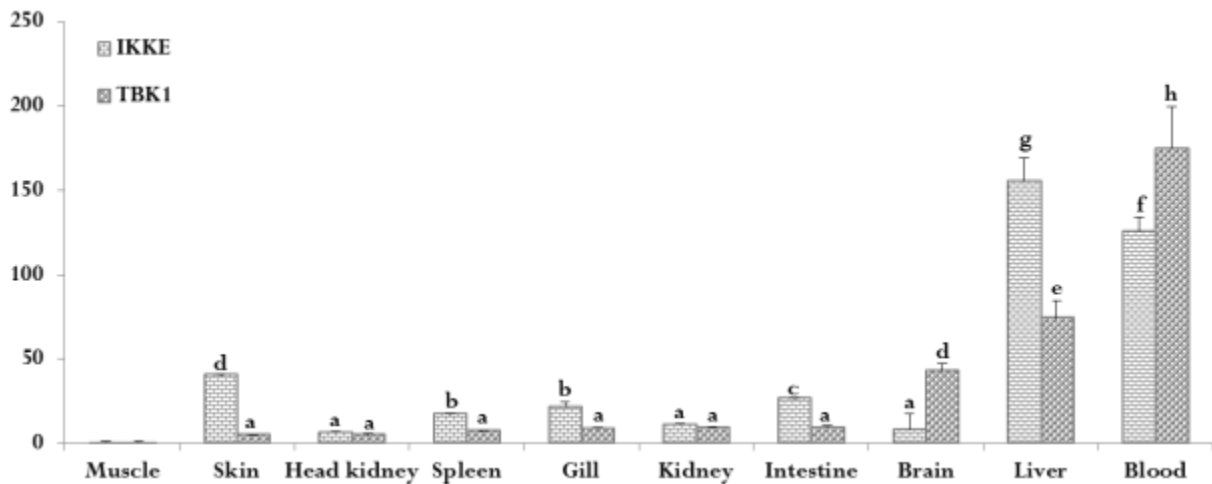
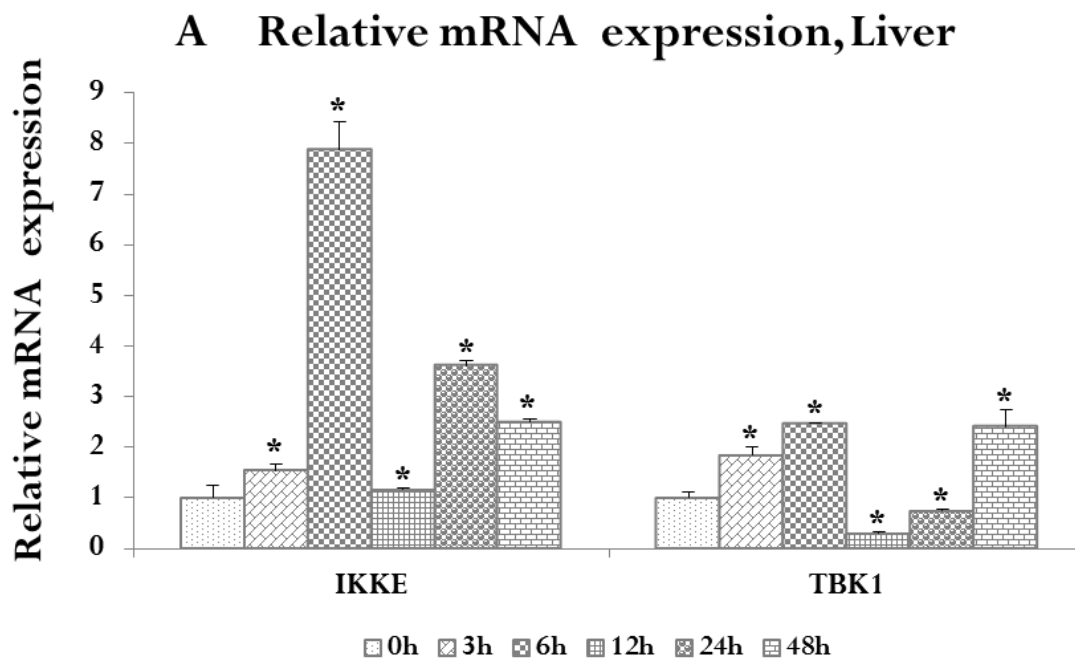


Fig. 26. Tissue distribution analysis of *RbTBK1* and *RbIKKε*

RbTBK1 and *RbIKKε* tissue-specific expression in muscle, intestine, skin, kidney, head kidney, spleen, gill, brain, liver tissues, and blood, collected from unchallenged rock bream was analyzed using quantitative RT-PCR. Relative mRNA expression was calculated using the $2^{-\Delta\Delta C_t}$ method, with β -actin as the invariant control gene. In order to determine the tissue-specific expression, the relative mRNA level was compared with muscle expression. Data are presented as mean values (n=3) with error bars representing SD. Data shown with “*” indicates significant expression levels at $P < 0.01$.

5.3.4 Temporal expression analysis post poly I:C challenge

Temporal modifications of *RbTBK1* and *RbIKKε* expression post poly I:C challenge was analyzed in different tissues including liver and head kidney tissues. In liver and head kidney, early phase induction of *RbTBK1* could be observed. In head kidney, highest level of expression could be observed at 3 h (2.1-fold), while in liver, highest level of induction could be observed at 6 h p.i. (2.5-fold). It is noteworthy to note that down regulation of *RbTBK1* could be observed at 12 h p.i. in liver and also a second upregulation equivalent to 6 h was seen at 48 h p.i. (2.4-fold) (**Fig. 27A**). *RbIKKε* revealed induction at all-time points in liver except 12 h p.i. Maximum level of expression could be observed at 6 h (7.9-fold), while in head kidney significant upregulation could be determined at 3 h p.i. (2-fold). In head kidney, similar to *RbTBK1*, *RbIKKε* also showed down regulation revealing similar transcriptional expression pattern of both kinases (**Fig. 27B**).



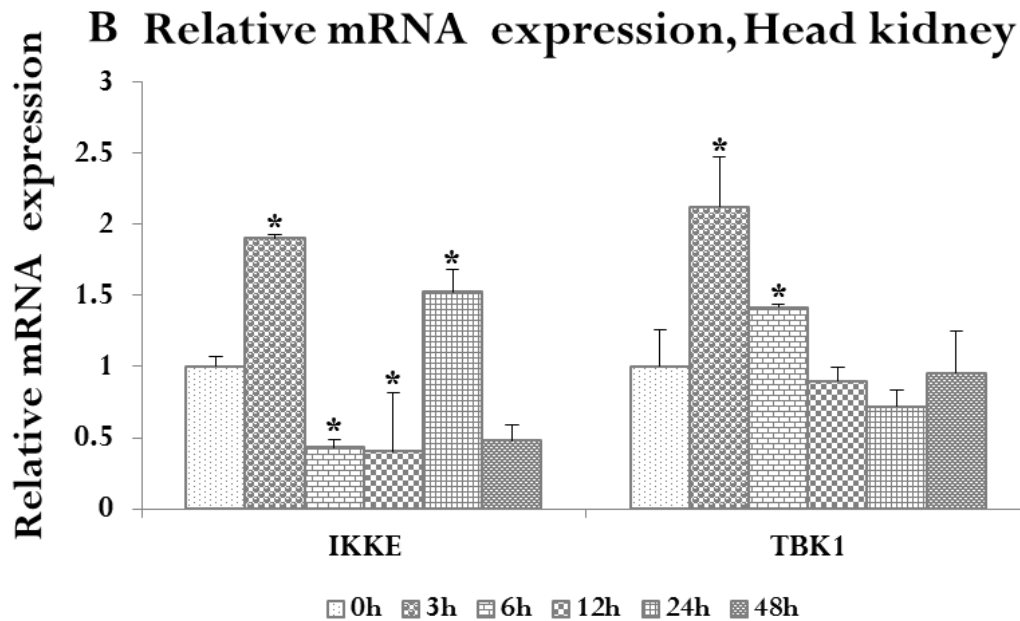


Fig. 27. *RbTBK1* and *RbIKKε* expression analysis after poly I:C challenge.

RbTBK1 and *RbIKKε* expression was analyzed in liver (A) and head kidney (B) post poly I:C challenge. Relative mRNA expression was calculated by the $2^{-\Delta\Delta Ct}$ method relative to PBS-injected controls and normalized with the same, with β -actin as the reference gene. Data are presented as mean values (n=3) with error bars representing SD. Data shown with “*” indicates significant expression levels at $P < 0.01$.

5.4 Discussion

Protein kinases are a large superfamily of homologous proteins related by virtue of their kinases/catalytic domains and are key regulators of major cell functions. They act by adding phosphate groups to substrate proteins and direct their activity and orchestrate the activity of all cellular processes. Kinases are particularly in signal transduction and coordination of complex cellular functions.

TBK1 and IKKε are non-canonical kinase family members involved in immune defense mechanism through phosphorylation of transcription factors which drive the

transcription of significant effector molecules. In this study, TBK1 and IKK ϵ orthologues isolated from rock bream was characterized. Eukaryotic TBK1 and IKK ϵ have been characterized from mammalian species including human, mouse and from zebrafish in teleosts. The RbTBK1 and RbIKK ϵ proteins shared a high conservation of the kinase domain with their respective orthologous proteins. Pairwise and multiple sequence alignment revealed higher identity and conservation at the amino acid level portraying the conservation of function in all the species. The protein kinase domain, sharing the catalytic function of kinases was conserved around 90% in all the orthologues. The glycine residues in the vicinity of the lysine residue and aspartic residue significant for the protein kinase activity were found to be conserved in RbTBK1 and RbIKK ϵ (Yu et al., 2012b).

The genome of *RbTBK1* revealed 21exon/ 20 intron structures consistent with other fish homologues and mammalian orthologues. The structural similarity observed in the orthologues suggested a much conserved function of RbTBK1 like the other TBK1. The cod promoter analysis has stood as an affirmation for the induction of TBK1 and involvement in immune defense (Chi et al., 2011). IKK ϵ have not been characterized from any teleost except zebrafish. However, detailed characterization of the teleost IKK ϵ has not been performed to avail a comparative understanding.

Tissue distribution profiling of both the kinases revealed high expression in immune related tissues like blood and liver. Cod *TBK1* was highly expressed in spleen, followed by liver, gill, head kidney (Chi et al., 2011). Mouse TBK1 is ubiquitously expressed in stomach, small intestine, lung, skin, brain, heart, kidney, spleen, thymus, and liver, and at especially high levels in testis (Pomerantz and Baltimore, 1999; Tojima et al., 2000), whereas IKK ϵ exhibit differential expression patterns. IKK ϵ expression is restricted to particular tissue compartments, with higher levels detected in lymphoid tissues, peripheral blood lymphocytes,

and the pancreas (Hammaker et al., 2012; Tojima et al., 2000). The ubiquitous presence of *RbTBK1* and *RbIKKε*, suggests their involvement in various physiological functions. Liver and blood are major immune organs involved in multiple functions (Gao et al., 2008; Seki et al., 2012). The abundant presence of *RbTBK1* and *RbIKKε* in immune related tissues strongly suggests their immune related functions.

Inflammation is the immune response of organisms to pathogens, or cell damage and it is a protective mechanism to remove injurious stimuli (Ferrero-Miliani et al., 2007). During an immune response against pathogens, inflammation that occurs is driven by immunopathological events such as the overproduction of various proinflammatory cytokines, including tumor necrosis factor (TNF- α), interleukin (IL-1 β), interferon (IFN- β) (Qureshi et al., 2005). The production of inflammatory mediators is dependent on the activation of pattern recognition receptors PRRs like TLRs, RLRs and NLRs, which can recognize various microbial ligands including lipopolysaccharide and poly I:C. The recognition of PAMPs by these receptors leads to the activation of several intracellular proteins followed by the activation of transcription factors such as nuclear factor (NF- κ B), activator protein (AP)-1, and interferon regulatory factors (IRF-3 and IRF-7) (Batbayar et al., 2012; Butchar et al., 2006; Lee et al., 2011). TBK1 and IKK ϵ are intracellular proteins which initiate the induction of inflammatory responses. TBK1 and IKK ϵ play vital roles in in the regulation of immune response to bacterial and viral challenges and regulate the expression of inflammatory mediators such as IL-6, TNF- α , and IFN- β (Marchlik et al., 2010; Perry et al., 2004; Solis et al., 2007; Xie et al., 2012; Yu et al., 2012a). Both TBK1 and IKK ϵ are essential in the activation of IRF3 signaling pathway (Fitzgerald et al., 2003). The significance of TBk1 in antiviral immunity came into limelight when the viral mechanisms developed to raget or hijack this enzyme was understood (Alff et al., 2008; Ma et al., 2012; Otsuka et al., 2005). These studies from mammals suggest that TBK1 and IKK ϵ are critical players in various

immuno-biological and immuno-pathological events. Atlantic cod TBK1 was induced upon the various immuno stimulations inclusive of poly I:C (Chi et al., 2011). Our investigation on the expression pattern of *RbTBK1* and *RbIKKε* post poly I:C challenge revealed up-regulation suggesting their activation and involvement in antiviral defense.

In conclusion, the structural conservation and induction upon viral ligand challenge suggests the involvement of *RbTBK1* and *RbIKKε* in the immune defense pathway of rock bream.

CHAPTER VI

Characterization of Interferon Regulatory Factor 3 (IRF3)

6.0 Characterization of Interferon Regulatory Factor 3 (IRF3)

Abstract

Transcription factors are evolutionarily conserved DNA-binding proteins that bind to DNA sequences and drive the transcription of genes involved in various physiological processes including cell cycle, immunity, apoptosis, inflammation, differentiation and metabolism. Interferon regulatory factor 3 (IRF3) is a significant transcription factor involved in the regulation of interferon expression. *RbIRF3* genome possessed 11 exon- 10 intron structural organizations. RbIRF3 protein possessed a DNA-binding domain, IRF-associated domain and serine rich domain. The DNA binding domain harbored the tryptophan repeats characteristic of the IRF family proteins. Pairwise alignment and phylogenetic analysis showed higher identity and closer relationship of RbIRF3 with the fish homologues, also sharing reasonable identity with the mammalian orthologues. Tissue distribution analysis of RbIRF3 showed ubiquitous expression with highest transcript level in liver, followed by skin. Transcriptional modulations performed in liver, head kidney tissues and blood cells revealed upregulation post poly I:C challenge, suggesting its activation upon viral challenge and its regulation upon infection. Thus, RbIRF3 is a significant transcription factor involved in antiviral defense of rock bream.

6.1 Introduction

Interferons (IFNs) are cytokines, which are so called because of their ability to interfere (inhibit) virus replication in a cell (Isaacs and Lindenmann, 1957; Isaacs et al., 1957). IFNs are classified into three distinct types namely type I, II and III. Type I IFNs comprises of IFN- α , - β , - ϵ , - κ , - ω , - δ , - τ , - ζ , of which IFN- α and - β , are extensively investigated because of their antiviral characteristics. Human and mice possess multifunctional IFN- α gene subtypes, whereas for IFN- β exists as a single gene (Weissmann and Weber, 1986). Type II IFN is referred to as IFN- γ , which exists as a single copy and is primarily induced in cells of the immune system such as T cells or natural killer cells (NK cells). Recently, new IFN family members namely, IFN- λ 1, - λ 2, and - λ 3 (also known as interleukin-29 (IL-29), IL-28A, and IL-28B, respectively) have been identified (Pestka et al., 2004). The type III IFNs are also induced in virally infected cells and the mechanism of signal transduction may be similar to those of type I IFNs. The IFN expression is primarily controlled at the transcriptional level and it occurs as a highly ordered process, regulated by multiple transcription factors (Honda et al., 2006).

Interferon regulatory factors (IRFs) are a family of transcription factors, known to play a pivotal role in the regulation of expression of IFNs and IFN-stimulated genes (ISGs). IRF family in vertebrates comprises of 10 members, IRF-1 to -10. IRF1, IRF2, IRF3, IRF4 [also known as LSIRF (**L**ymphocyte-**S**pecific **I**nterferon **R**esponse **F**actor), PIP (**P**U.1 **I**nteraction **P**artner) or ICSAT (**I**FN **C**onsensus **S**equences-binding protein in **A**dult **T**-cell leukemia cell line or **A**ctivated **T** cells)], IRF5, IRF6, IRF7, IRF8 [also known as ICSBP (**I**nterferon **C**onsensus **S**equences-**B**inding **P**rotein)] and IRF9 [also known as ISGF3 γ (**I**nterferon-**S**timulated transcription **F**actor 3, **G**amma or **I**nterferon-**S**timulated **G**ene **F**actor 3 **g**amma)] (Honda and Taniguchi, 2006). IFN- β gene promoter possesses at least four regulatory cis elements, namely, the positive regulatory domains (PRDs) I, II, III, and IV,

whereas IFN- α gene promoter contain PRD I- and PRD III-like elements (PRD-LEs). PRD I and PRD III are the binding sites for IRF family members, whereas PRD II and PRD IV elements are for NF- κ B and AP-1 (Honda et al., 2005). IRF family members are characterized by well conserved N-terminal DNA binding domain (DBD) with five tryptophan repeats, similar to the DBD of myb transcription factors. The DBD forms a helix-turn-helix domain and recognizes similar DNA sequences. The helix-turn-helix domain of IRFs bind to the consensus sequence 5'-AANNGAAA-3' present in the PRDI and PRDIII domains of the promoter region of the IFNs. The 5' flanking AA sequence was found to be essential for the recognition by IRFs and, therefore, IRFs do not bind to the NF- κ B binding site, which contains the GAAA core sequence but no 5' flanking AA sequence (Honda et al., 2006). In addition to the DBD, all IRFs (except IRF1 and IRF2) contains a unique C-terminal domain, termed the IRF association domain (IAD), which enables the formation of homodimers and interaction with other members of the IRF family and also recruitment of other transcription factors to target promoters.

IRF3 and IRF7 play a crucial role in the transcriptional activation of type I IFN and ISGs in mammals. Their regulatory role has a major impact on understanding the molecular mechanism behind pathogen induced innate immune response against viruses. IRF3 is constitutively expressed in the cytosol in latent form. Upon viral infection, it undergoes phosphorylation at key serine residues in the regulatory domain and dimerization (Lin et al., 1998). IRF3 as a homodimer or heterodimer with IRF7 translocate to the nucleus and forms a complex with the co-activators CBP and/or p300. The complex then binds to its target DNA sequence in type I IFN genes and certain cytokine and chemokine genes to alter the local chromatin structure and switch on the gene expression. Inactive IRF3 is found to constitutively shuttle in and out of the nucleus, whereas IRF3 and CBP/p300 complex is

retained in the nucleus and engaged in the transcription induction of IFNs and other genes (Kumar et al., 2000; Lin et al., 1999; Sato et al., 2000).

Identification of numerous genes involved in antiviral signaling pathways, including PRRs (TLRs and cytosolic receptors), IFNs (Robertson, 2006), ISGs, transcription factors, kinases like TBK1 and IKKs (Zou et al., 2010), suggests a similar mechanism of IFN induction in teleosts as in mammals. IRF3 has been identified and characterized from large yellow croaker, rainbow trout and Japanese flounder.

6.2 Materials and methods

6.2.1 Animal rearing, cDNA library construction and RbIRF3 gene identification

Healthy rock bream fish with average weight of ~50 g were obtained from the Ocean and fisheries Research institute (Jeju, Republic of Korea). The animals were reconciled to the laboratory conditions (salinity $34 \pm 1\%$, pH 7.6 ± 0.5 at 24 ± 1 °C) in 400 L tanks. Blood samples were harvested from the caudal fin of healthy, unchallenged fish using a 22 gauge needle and centrifuged immediately for 10 min at $3000 \times g$ at 4 °C, to collect the hematic cells. Tissues from gills, liver, heart, brain, kidney, head kidney, spleen, intestine, muscle and skin were harvested on ice from three healthy animals and immediately snap-frozen in liquid nitrogen and stored in -80 °C, until RNA extraction. Total RNA was obtained from tissues using Tri Reagent™ (Sigma, USA). The concentration and purity of RNA were evaluated using a UV-spectrophotometer (BioRad, USA) at 260 and 280 nm. Purified total RNA samples were subjected to mRNA purification (Micro-FastTrack 2.0 mRNA isolation kit, invitrogen). First strand cDNA was synthesized from 1.5 µg of mRNA using Creator™ SMART™ cDNA library construction kit (Clontech, USA); amplification was performed with Advantage 2 polymerase mix (Clontech) under conditions of 95 °C for 7 s, 66 °C for 30 min and 72 °C for 6 min. In order to exclude the over-representation of the most commonly

expressed transcripts, synthesized cDNA was normalized using Trimmer-Direct cDNA normalization kit (Evrogen, Russia).

A cDNA GS-FLX shotgun library was created from the sequencing data obtained by using the GS-FLX titanium system (DNA Link, Republic of Korea). A cDNA contig showing high homology to the earlier identified IRF3 homologues was identified using BLAST and designated as RbIRF3.

6.2.2 BAC library creation and identification of BAC clone

Rock bream were obtained from the Jeju Special Self-Governing Province Ocean and Fisheries Research Institute (Jeju, Republic of Korea). Blood was harvested aseptically from the caudal fin using a sterile 1 mL syringe with 22 gauge needles, and a BAC library was constructed from the isolated blood cells (Lucigen Corp., USA). Briefly, genomic DNA obtained from blood cells was randomly sheared and the blunt ends of large inserts (>100 kb) were ligated to pSMART BAC vector to obtain an unbiased, full coverage library. Around 92160 clones, possessing an average insert size of 110 kb, were arrayed in 240 microtiter plates with 384 wells.

A two-step PCR based screening method was used to identify the clone of interest based on manufacturer's instructions. Primers were designed based on the cDNA sequence obtained from the cDNA database. A gene specific clone was isolated and purified using Qiagen Plasmid Midi Kit (Hidden, Germany). The sequence was confirmed by pyrosequencing (GS-FLX titanium sequencing, Macrogen, Republic of Korea). The genomic sequence of RbIRF3 was determined by aligning the available cDNA sequence using the Spidey program available on NCBI (<http://www.ncbi.nlm.nih.gov/spidey/>). The complete genomic structure and putative promoter region were determined from the sequencing data. The gene specific primers employed in the identification of the clone from the BAC library are tabulated in Table 6. 1.

Table 13. Primers used in RbIRF3 identification and qRT-PCR.

| Gene | Purpose | Orientation | Primer sequences (5'-3') |
|----------------|-------------------------|-------------|--------------------------|
| RbIRF3 | BAC screening & qRT-PCR | Forward | ATGTCTCATTCCAAACCGCTGCTC |
| RbTBK1 | BAC screening & qRT-PCR | Reverse | ATGGGATGGAGAACTCTGTTCGCT |
| β -actin | qRT-PCR amplification | Forward | TCATCACCATCGGCAATGAGAGGT |
| β -actin | qRT-PCR amplification | Reverse | TGATGCTGTTGTAGGTGGTCTCGT |

6.2.3 Sequence characterization and phylogenetic analysis of RbIRF3

The cDNA sequence of *RbIRF3* was analyzed using BLAST and confirmed by comparing with IRF3 homologues reported in other organisms. DNAssist2.2 was used to predict the open reading frame (ORF) and translate nucleotide to protein. The conserved domains were identified using ExPasy (<http://www.expasy.org/>) and SMART (<http://smart.embl-heidelberg.de/>). ClustalW was used to perform pairwise alignment and multiple sequence alignment (Thompson et al., 1994). Phylogenetic analysis was performed using minimum evolution method in MEGA 5.0, with bootstrap values calculated with 5000 replications to estimate the robustness of internal branches (Tamura et al., 2011). The amino acid identity percentages were calculated by MatGAT program using default parameters (Campanella et al., 2003). The transcription factor binding sites (TFBS) in the promoter region were predicted using TFSEARCH, TESS and TRANSFAC. The exon-intron structure was determined by aligning mRNA to the genomic sequence of *RbIRF3* obtained from the BAC library using Spidey available on NCBI (<http://www.ncbi.nlm.nih.gov/spidey/>) (Wheelan et al., 2001). The mRNA and genomic sequences used for the comparison of the genome structures were evaluated from the sequences obtained from GenBank.

6.2.4 Expression profile of *RbIRF3* gene in normal and challenged tissues

6.2.4.1 Poly I:C challenge

In order to evaluate the defense responses of *RbIRF3*, a time course experiment was performed with immunostimulants like poly I:C. For poly I:C challenge, animals were intraperitoneally injected with a 100 μ L suspension of poly I:C in PBS (1.5 μ g/ μ L; Sigma).

For the above challenge, PBS-injected animals were used as controls. Liver, head kidney tissues and blood from the un-injected, PBS-injected and immune challenged animals were collected at time points of 3, 6, 12, 24, and 48 h post injection/infection (p.i.).

6.2.4.2 RNA isolation and cDNA synthesis

To determine the expression pattern of *RbIRF3* gene, gills, liver, heart, brain, kidney, head kidney, spleen, intestine, muscle and skin tissues and blood cells, from un-injected fish were harvested. After challenge with PBS, and poly I:C, liver, blood and head kidney tissues were harvested from challenged animals at the corresponding time points. Total RNA was obtained from tissues using Tri Reagent[™] (Sigma, USA). The concentration and purity of RNA were evaluated using a UV-spectrophotometer (BioRad, USA) at 260 and 280 nm. The RNA was diluted to 1 μ g/ μ L. Then, 2.5 μ g of RNA was used to synthesize cDNA from each tissue using a PrimeScript[™] first strand cDNA synthesis kit (TaKaRa). Concisely, RNA was incubated with 1 μ L of 50 μ M oligo(dT)₂₀ and 1 μ L of 10 mM dNTPs for 5 min at 65°C. After incubation, 4 μ L of 5 \times PrimeScript[™] buffer, 0.5 μ L of RNase inhibitor (20 U), 1 μ L of PrimeScript[™] RTase (200 U), were added and incubated for 1 h at 42°C. The reaction was terminated by adjusting the temperature to 70°C for 15 min. Finally, synthesized cDNA was diluted 40-fold before storing at -20°C

6.2.4.3 Tissue distribution

Quantitative reverse transcription polymerase chain reaction (qRT-PCR) was used to examine tissue distribution of *RbIRF3* mRNAs in tissues from muscle, intestine, skin, kidney, head kidney, spleen, gill, heart, brain, liver tissues and blood of healthy fish with gene specific primers. qRT-PCR was performed in a 15 μ L reaction volume containing 4 μ L of diluted cDNA, 7.5 μ L of 2 \times SYBR Green Master Mix, 0.6 μ L of each primer (10 pmol/ μ L) and 2.3 μ L of PCR grade water and subjected to the following conditions: one cycle of 95°C for 3 min, amplification for 35 cycles of 95°C for 20 sec, 58°C for 20 sec, 72°C for 30 sec. The baseline was set automatically by the Thermal Cycler Dice™ Real Time System software (version 2). In order to confirm that a single product was amplified by the primer pair used in the reaction, a dissociation curve was generated at the end of the reaction by heating from 60°C to 90°C, with a continuous registration of changes in fluorescent emission intensity. The Ct for the *RbIRF3* (target gene) and *β -actin* (internal control) were determined for each sample. The differences between the target and internal control Ct, called Δ Ct were calculated to normalize the differences in the amount of total cDNA added to each reaction and the efficiency of the RT-PCR. The Δ Ct for each sample was subtracted from Δ Ct of the calibrator and this difference was called $\Delta\Delta$ Ct and the *RbIRF3* gene expression was determined by Livak comparative Ct method. The relative expression level calculated in each tissue was compared with respective expression level in muscle.

6.2.4.4 Temporal *RbIRF3* mRNA expression analysis post immune challenges

qRT-PCR was performed with liver, head kidney tissues and blood cells isolated from poly I:C challenged animals. qRT-PCR conditions were the same as used for tissue distribution profiling. The Δ Ct for each sample was determined by the method described above and subtracted from Δ Ct of the un-injected control and this difference was called $\Delta\Delta$ Ct.

The relative expression of *RbIRF3* was determined by the Livak method. The relative fold change in expression after immune challenges was obtained by comparing the relative expression to corresponding PBS-injected controls. The expression normalized to PBS-injected controls is represented in the figures.

All data have been presented in terms of relative mRNA expressed as means \pm standard deviation (S.D.). All experiments were performed in triplicate. Statistical analysis was performed using un-paired two-tailed Student's t-Test. *P*-values of less than 0.01 were considered to indicate statistical significance.

6.3 Results

6.3.1 Sequence characterization and phylogenetic analysis of RbIRF3

The cDNA sequence obtained from the cDNA library 1884 bp long consisting of ORF of 1386 bp, 5' untranslated region (UTR) of 178 bp and 3' UTR of 320 bp. RbIRF3 cDNA possessed a single mRNA instability motif in its 3' UTR. The ORF encoded a protein of 461 amino acids with molecular mass of 51 kDa with isoelectric point of 4.9. The complete sequence was deposited in GenBank under the accession no KF267453. *In silico* characterization of the RbIRF3 protein revealed the conserved IRF tryptophan pentad repeat DNA-binding domain (DBD) at the N-terminal region, an IRF-associated domain (IAD) and a serine-rich domain at the C-terminal region, similar to the other IRF3 proteins (**Fig. 28**). Pairwise alignment showed that RbIRF3 had the highest identity and similarity of 87 and 92%, respectively with *Dicentrarchus labrax*. The molecular mass of RbIRF3 was also similar to that of *Dicentrarchus labrax*. RbIRF3 share high identity with other teleosts except for zebrafish, with which it shared an identity of 40%. It shares an identity of 29 to 33% with vertebrates other than fish (**Table 15**). Multiple sequence alignment showed revealed high

conservation in the DBD, IAD and SRD, whilst deletions could be found in the middle part of the sequence of mammalian lineage making it diverse (**Fig. 28**).

A phylogenetic tree was reconstructed with members belonging to IRF subfamilies, comprising of IRF 1 to 10. The IRF proteins group into four subfamilies: IRF1, IRF3, IRF4 and IRF5. The constructed tree also showed a similar pattern with four subfamilies forming separate clusters, inside which the fish homologues formed a separate cluster. RbIRF3 was closely associated with fish homologues in the IRF3 subfamily of IRFs. RbRIF3 was found close to the sea bass homologue (**Fig. 29**).

DNA binding domain

RbIRF3 MSHSKPLLIPLWLGQIDSGKYPGVQWITNPERTEFSIPWKHALRODSSDITDILIFKAWAEV 60
SmIRF3 MSYSKPLLIPLWLGQIDSGKYPGVQWITNPEQSEFTVPMKHALRODSSGTDVLIIFKAWAEV 60
DlIRF3 MSHSKPLLIPLWRSHIDSGRYPGVQWITNPERTEFSIPWKHALRODSSDITDILIFKAWAEV 60
MmIRF3 METPKPRILPWLVSQDLDLGQLEGVAVLDESRTFRFRIWKHGLRQDAQMADFQGFQAWAEA 60
BtIRF3 MGTQKPRILPWLISQLDRGELEGVAVLWGESRTFRFRIWKHGLRQDAQQEDFGIFQAWAVA 60
XlIRF3 MGSQKPRIIPWLISQIGNPAYPGLIWMNEEKTRFRIWKHGLRQDRCDADVKIFEGWAV 60
HsIRF3 MGTQKPRILPWLVSQDLDLGQLEGVAVWVNSRTRFRIWKHGLRQDAQQEDFGIFQAWAEA 60

DBD

RbIRF3 SGN---GRAQGEASVTKRNFRSALRAKG-FKLVGDKNDAANPHKVFWRWPKTSPGA--- 113
SmIRF3 SGN---GRAQGDSSVTKRNFRSALRAKG-FKMVDNKNETANPHKVFWRWPEDESASGAKSS 116
DlIRF3 SGN---GRAHGDAVTKRNFRSALRAKG-FKLLSDNKNDAANPHKVFWRWPEDESASGANS 116
MmIRF3 SGAYTPGKDKPDVSTWTKRNFRSALNRKEVLRLAADNSKDPYDPHKVYEFVT----- 111
BtIRF3 SGAYTPGKDKPDLPTWTKRNFRSALNRKEVLRLEADHSKDSQDPHKIYEFVN----- 111
XlIRF3 SGSYDPSKQDPNPAVWTKRNFRSALNRKAGINVMVDKSSSESNPHKVIYEQIG- ISVEGDV 119
HsIRF3 TGAYVPGRDKPDLPTWTKRNFRSALNRKEGLRLEADRSKDHPDHPKVIYEFVN----- 111

IRF- associated domain (IAD)

RbIRF3 AVGGACGGQFAEQFLHTMTKTSEGNFRTOFRISVYRQVGVSEQLVENEAGIRIVYSPE 290
SmIRF3 AAGGACGGQLAEQFLHTVNQTNQDNLKTEFRISVYRQVGVKQELVVNEAGLSLVYRPE 295
DlIRF3 AVGGACDGGFAEQFLDTMNKTRDGDNFKTQFRISVYRQVGVLEQLVENEAGVRLVYSPE 293
MmIRF3 -----NPLKQLLA-----EEQWEFEVTAFYRGRQVFQQTFLFCPGGLR----- 221
BtIRF3 -----NPLKQLLAN-----EEDWEFEVTAFYRGCQVFQQTVFCPGGLR----- 223
XlIRF3 LPAEVATNQSPLOQHITDHFQDRTLRTEFEVTVYRGIIEVSKTLVKNPHGFR----- 277
HsIRF3 -----NPLKRLVLP-----GEEWEFEVTAFYRGRQVFQQTISCEPEGLR----- 227

IAD

RbIRF3 LTG-TVLDPKSGLSVSLPSP-GVMLDRTQANLTQRILDKLGDLVGVSGHVYVYQRRG 348
SmIRF3 LIG-TVLDYESGLTVVSLPSP-GAMLDQTQAKLTQRILDNLGDLVGVSGHVYVYQRRG 353
DlIRF3 LVGTALVDHESGLSLVSLPSP-GAMLDQTQANLTQRILDKLGDLVGVSGHVYVYQRRG 352
MmIRF3 LVGSTA-DMTLPWQPVTLDPDEGFLTDKLVKEVYVGVVQLKGLGNLALWQAGQCLWAQRLG 280
BtIRF3 LVGSEAGDRMLPGQPIRLPDPATSLTDKSVTDYVQVLSCLGGGLALWRAGQWLCAQRLG 283
XlIRF3 ITRKHSPGSLYLDVVLVSP-TMIADQAVVGEIHKLLRNLEEGVLVEVRGGSICGKRQG 336
HsIRF3 LVGSEVGDRTLPGWVPTLDPDGMSTLDRGVMSVVRHVLVSLCLGGGLALWRAGQWLWAQRLG 287

IAD

RbIRF3 EIKAFWSFSKFDKRSR---QPQEISKLPQPLFLFKNFVRGILDFIE--GRDCPPCSLFF 402
SmIRF3 EIKAFWSLSKFDCKS---QPQEISKLPQPLYMFKDFLRGISDFID--GRDCPHCSLFL 407
DlIRF3 ETKAFWSVSKFDKRSR---QPQEISKLHPQPLYMFKDFVVRGIMDFIN--GGDCPPCSLFF 406
MmIRF3 HSHAFWALGELLPPDSGRGPDGEVHKDKDGAVDLRFVADLIAFMEGSGHS-PRYTLWF 339
BtIRF3 HCHVYWAIGEELLPPSCGHKPDGEVPKDREGGVFNLPFITDLITFIEGSRRS-PLYTLWF 342
XlIRF3 KCRAFWSMTEPEIS---QPNQIDKNDYCILHTLQQFVAELTEFIERTKSSPOYHWM 392
HsIRF3 HCHTYWAVSEELLPPNSGHGPDGEVPKDKEGGVFDLGPFIVDLITFIEGSGRS-PRYALWF 346

IAD **Serine rich domain**

RbIRF3 CLGEKWPDPNRPWEKKLITVEVVLTSMELLKNMAVVGGASSLQ-SVELQMSLEEMMELY 461
SmIRF3 CLGEKWPDPNRPWEKKLITVEVVLTSMEILKMAVGGGASSLQ-SVELQMSLEEMMEMC 466
DlIRF3 CLGEKWPDPNRPWEKKLITVEVVLTSMELLKMAVAGGASSLQ-SVELQMSLEEMMELY 465
MmIRF3 CMGEMWPQ--DQPWVKRLVMVKVPTCLKELLEEMAREGGASSLK-TVDLHISNSQIPISLT 396
BtIRF3 CVGQSWPQ--DQPWIKRLVMVKVPMCLRVLVDIARQGGASSLENTVDLHISNSDPLSLT 400
XlIRF3 CLGELWPD--VRPWNKKFMVQIVPVMKLLHDMSYSTGASSLH--SSEINLEISDSLSST 449
HsIRF3 CVGESWPQ--DQPWTKRLVMVKVPTCLRALVEMARVGGASSLLENTVDLHISNSHPLSLT 404

RbIRF3 -----
SmIRF3 -----
DlIRF3 -----
MmIRF3 SDQYKAYLQDLVEDMDFQATGNI 419
BtIRF3 PDQYMACLQDLAEDMDF----- 417
XlIRF3 -NDVMAVLRLELHEMMDFE----- 466
HsIRF3 SDQYKAYLQDLVEGMDFQGGPES 427

Fig. 28. Multiple sequence alignment of RbIRF3 with other homologues.

RbIRF3 is on the top of all sequences. The DNA binding domain (DBD), IRF associated domain (IAD) and serine rich domain are indicated with arrow heads with corresponding names on the top of them. The tryptophan repeats are boxed. The lysine-arginine residues which serve as nuclear localization signal (NLS) in human IRF3 are indicated by red upward facing arrows. The accession numbers of the orthologues are given in Table 14.

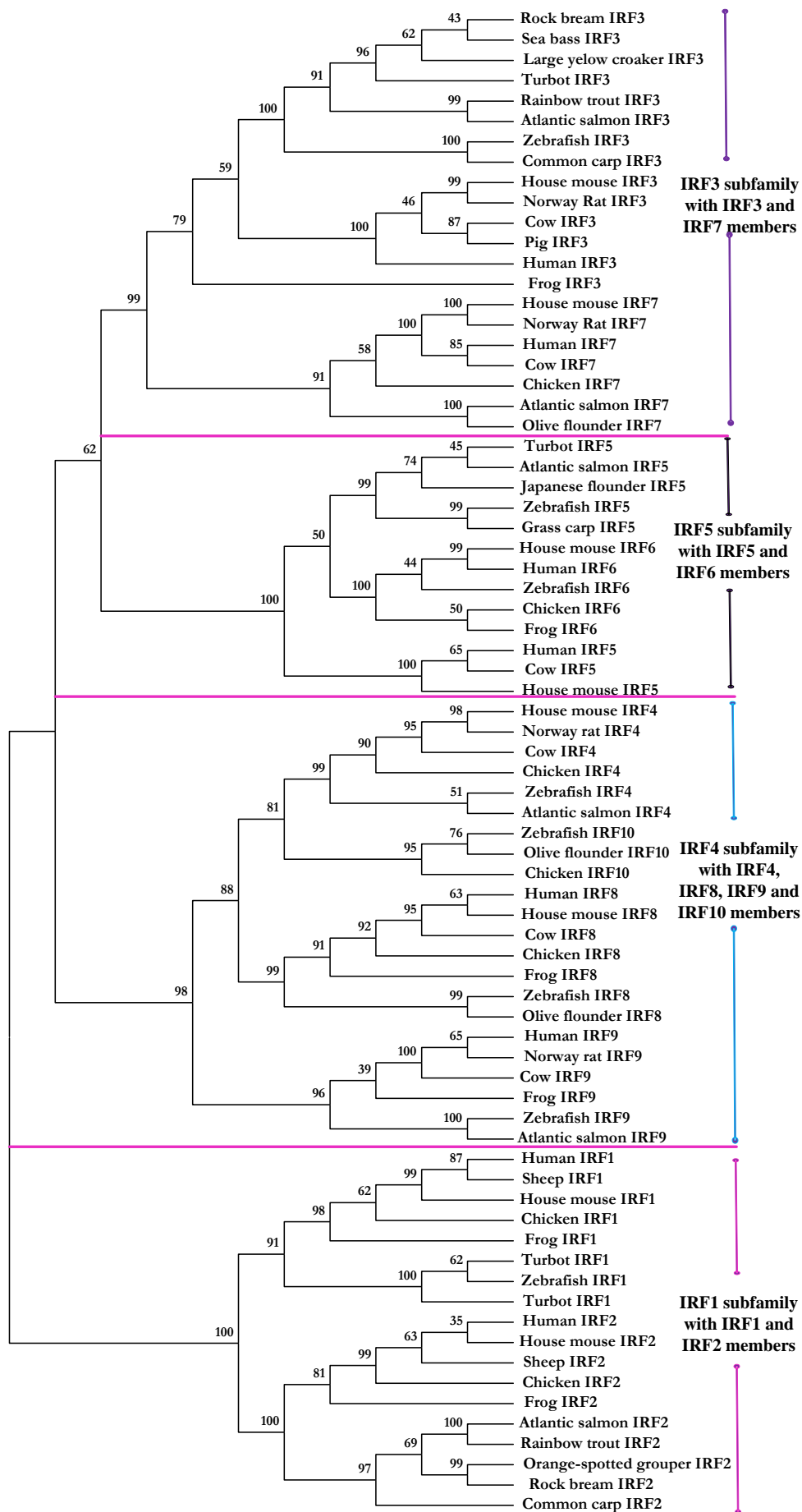


Fig. 29. Phylogenetic analysis of RbIRF3 with IRF family proteins.

Phylogenetic tree was constructed with the homologous sequences aligned using clustalW and applying it to the MEGA5 using minimum evolution method. The accession numbers are tabulated in Table 14..

Table 14. Accession numbers of IRF orthologues obtained from NCBI and GenBank.

| Common name | Gene | Database | Accession No. | Common name | Gene | Database | Accession No. |
|------------------------|------|----------|----------------|-----------------|-------|----------|----------------|
| Sea bass | IRF3 | GenBank | CBN81356 | House mouse | IRF4 | NCBI | NP_038702 |
| Large yellow croaker | IRF3 | GenBank | AFE88606 | Norway rat | IRF4 | NCBI | NP_001099578 |
| Turbot | IRF3 | GenBank | ADQ52415 | Cow | IRF4 | NCBI | NP_001193091 |
| Rainbow trout | IRF3 | NCBI | NP_001244191 | Chicken | IRF4 | NCBI | NP_989630 |
| Zebrafish | IRF3 | NCBI | NP_001137376 | Zebrafish | IRF4 | NCBI | NP_001116182 |
| Atlantic salmon | IRF3 | NCBI | NP_001165753 | Atlantic salmon | IRF4 | NCBI | NP_001133454 |
| Common carp | IRF3 | GenBank | AGC67025 | Zebrafish | IRF10 | NCBI | NP_998044 |
| House mouse | IRF3 | NCBI | NP_058545 | Olive flounder | IRF10 | NCBI | BAI63220 |
| Cow | IRF3 | NCBI | NP_001025016 | Chicken | IRF10 | NCBI | NP_989889 |
| Norway rat | IRF3 | NCBI | NP_001006970 | Human | IRF8 | NCBI | NP_002154 |
| Pig | IRF3 | GenBank | ABY26589 | House mouse | IRF8 | NCBI | NP_032346 |
| Frog | IRF3 | NCBI | NP_001079588 | Cow | IRF8 | NCBI | NP_001077238 |
| Human | IRF3 | NCBI | NP_001562 | Chicken | IRF8 | NCBI | NP_990747 |
| House mouse | IRF7 | GenBank | U73037.1 | Frog | IRF8 | NCBI | NP_001087097 |
| Norway rat | IRF7 | NCBI | NP_001028863 | Zebrafish | IRF8 | NCBI | NP_001002622 |
| Human | IRF7 | GenBank | U73036.1 | Olive flounder | IRF8 | GenBank | AFE18694 |
| Cow | IRF7 | NCBI | NP_001098510 | Human | IRF9 | NCBI | NP_006075 |
| Atlantic salmon | IRF7 | NCBI | NP_001130020 | Norway Rat | IRF9 | NCBI | NP_001012041 |
| Olive flounder | IRF7 | GenBank | ACY69214 | Cow | IRF9 | NCBI | NP_001019677 |
| Turbot | IRF5 | GenBank | JF913460.1 | Frog | IRF9 | NCBI | NP_001084846 |
| Atlantic salmon | IRF5 | NCBI | NP_001133324.1 | Zebrafish | IRF9 | NCBI | NP_991273 |
| Japanese flounder | IRF5 | GenBank | JF312910.1 | Atlantic salmon | IRF9 | NCBI | NP_001167190 |
| Zebrafish | IRF5 | GenBank | EU274624.1 | Human | IRF1 | GenBank | X14454.1 |
| Grass carp | IRF5 | GenBank | FJ556994.1 | Sheep | IRF1 | NCBI | NP_001009751 |
| House mouse | IRF5 | NCBI | NP_036187.1 | House mouse | IRF1 | GenBank | M21065.1 |
| Human | IRF5 | NCBI | NM_001242452.1 | Chicken | IRF1 | GenBank | L39766.1 |
| Cow | IRF6 | NCBI | NP_001070402 | Frog | IRF1 | GenBank | BC075398.1 |
| House mouse | IRF6 | NCBI | NM_016851.2 | Turbot | IRF1 | GenBank | AY962251.1 |
| Human | IRF6 | NCBI | NM_006147.3 | Zebrafish | IRF1 | NCBI | NP_991310 |
| Zebrafish | IRF6 | NCBI | NP_956892.1 | Human | IRF2 | GenBank | X15949.1 |
| Chicken | IRF6 | GenBank | DQ250733.1 | House mouse | IRF2 | NCBI | NP_032417 |
| Frog | IRF6 | GenBank | D86492.1 | Sheep | IRF2 | GenBank | AF228445.1 |
| Orange-spotted grouper | IRF2 | GenBank | ACO81886 | Chicken | IRF2 | NCBI | NP_990527 |
| Common carp | IRF2 | GenBank | AFV99156 | Frog | IRF2 | NCBI | NP_001088726 |
| Rainbow trout | IRF2 | GenBank | AY034055.2 | Atlantic salmon | IRF2 | NCBI | NM_001123615.1 |

Table 15. Pairwise alignment of RbIRF3 with full length protein of IRF3 orthologues.

Identity (I) and similarity (S) percentages were obtained by MatGat.

| Organisms | | I (%) | S (%) | Amino acids | Mass (kDa) | Accession No. |
|------------------------------|----------------------|-------|-------|-------------|------------|---------------|
| <i>Oplegnathus fasciatus</i> | | 100 | 100 | 461 | 51 | KF267453 |
| <i>Dicentrarchus labrax</i> | Sea bass | 87 | 92 | 465 | 51 | CBN81356 |
| <i>Larimichthys crocea</i> | Large yellow croaker | 83 | 89 | 462 | 51 | AFE88606 |
| <i>Scophthalmus maximus</i> | Turbot | 80 | 89 | 466 | 51 | ADQ52415 |
| <i>Oncorhynchus mykiss</i> | Rainbow trout | 63 | 76 | 464 | 52 | NP_001244191 |
| <i>Danio rerio</i> | Zebrafish | 40 | 54 | 426 | 48 | NP_001137376 |
| <i>Cyprinus carpio</i> | Common carp | 40 | 57 | 454 | 51 | AGC67025 |
| <i>Mus musculus</i> | House mouse | 30 | 46 | 419 | 47 | NP_058545 |
| <i>Bos taurus</i> | Cow | 29 | 46 | 417 | 47 | NP_001025016 |
| <i>Sus scrofa</i> | Pig | 30 | 45 | 419 | 47 | ABY26589 |
| <i>Gallus gallus</i> | Chicken | 28 | 41 | 491 | 54 | AAK58583 |
| <i>Xenopus laevis</i> | Frog | 33 | 48 | 466 | 53 | NP_001079588 |
| <i>Homo sapiens</i> | Human | 29 | 43 | 427 | 47 | NP_001562 |

6.3.2 Genomic characterization of *RbIRF3*

The genomic structure of *RbIRF3* derived from the BAC clone revealed 11 exon -10 intron structural organization. *RbIRF3* genome structure was similar to that of large yellow croaker and turbot with 11 exons and 12 introns. The genome structure was not consistent with any of the earlier identified mammalian and a few fish homologues (zebrafish, Fugu). The introns followed different phases in *RbIRF3* genome structure. All intron splice junctions were consistent with GT-AG rule. The exon 1 consisted of untranslated region in its entirety. The translation initiation site was present in the second exon. The *RbIRF3* genome structure was not consistent with the mammalian lineage homologues, in the number of exons and as well as the coding region. Generally, the IRF3 homologues from mammals were shorter than those identified from teleosts. This may be the reason for the shorter genome structure (**Fig.**

30).

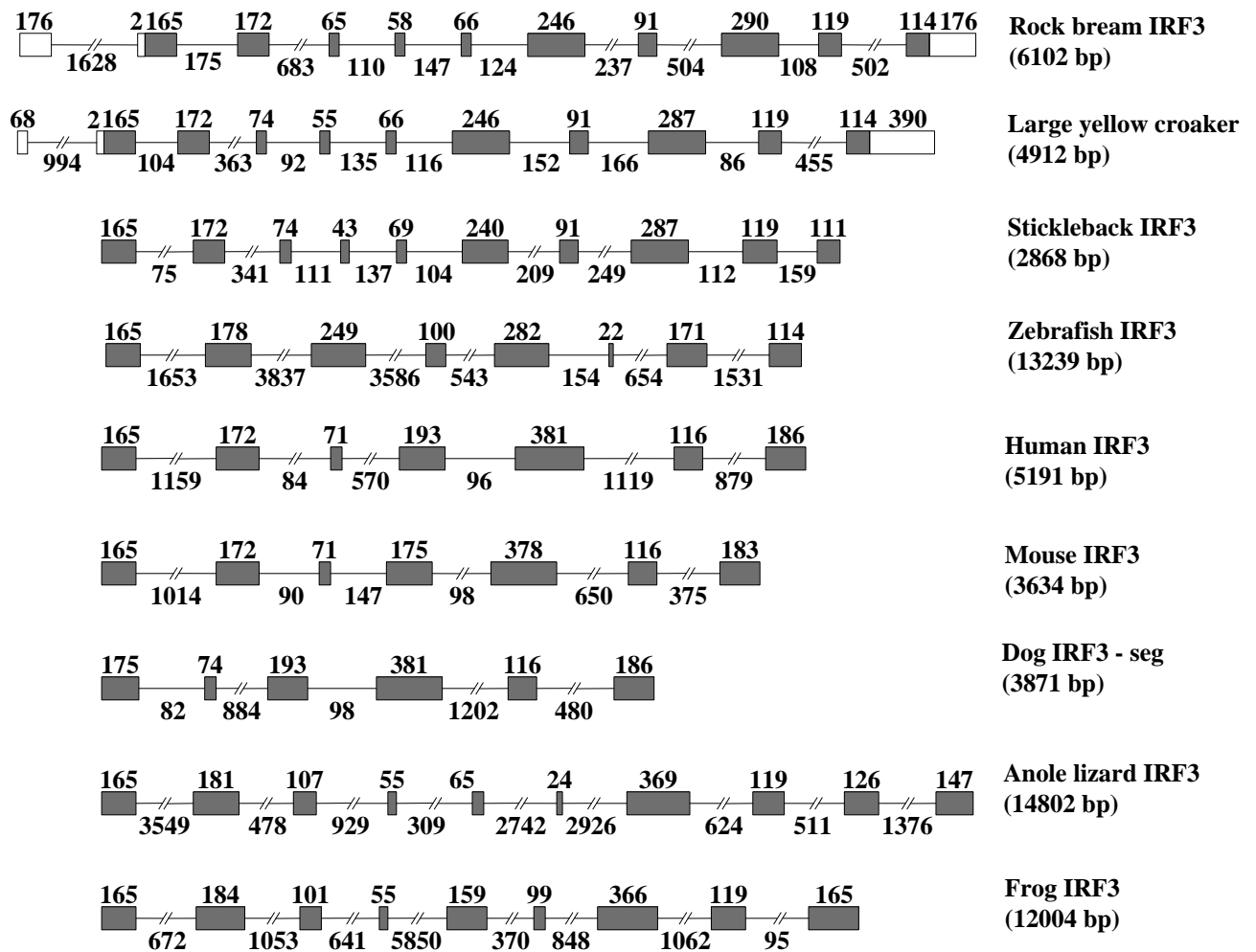


Fig. 30. Genomic structure analysis of *RbIRF3*.

The genome structures of IRF3 homologues were obtained from the previously published article (Huang et al., 2010a). The large yellow croaker genome sequence was obtained from NCBI available under the accession number JQ249912. The coding exons are indicated by shaded boxes while the untranslated regions are indicated by empty boxes. The introns are indicated by lines with the length written below them. The exon sizes are indicated on the top of boxes.

6.3.3 Promoter analysis of *RbIRF3*

In silico promoter analysis of the putative promoter region mapped to various putative transcription factor binding sites. These included several PAMP-associated transcription

factor binding sites like activator protein- 1 and -4 (AP-1 and AP-4), CCAAT-enhancer binding protein (C/EBP), C/EBP - α and - β , hepatic nuclear factor (HNF)-3b, interferon-sensitive response element (ISRE), cAMP response element-binding protein (CREB), and nuclear factor-kappa (NF-kappa), suggesting that these immune-related factors may play a vital role in the regulation of *RbIRF3* expression and function. In addition, other transcription factor binding sites such as those for Lyf-1, HSF, Sp1, Oct-1 Sox-5, E2F, ROR α , AML-1a, GATA-1, and upstream transcription factor (USF) were identified (**Fig. 31**).

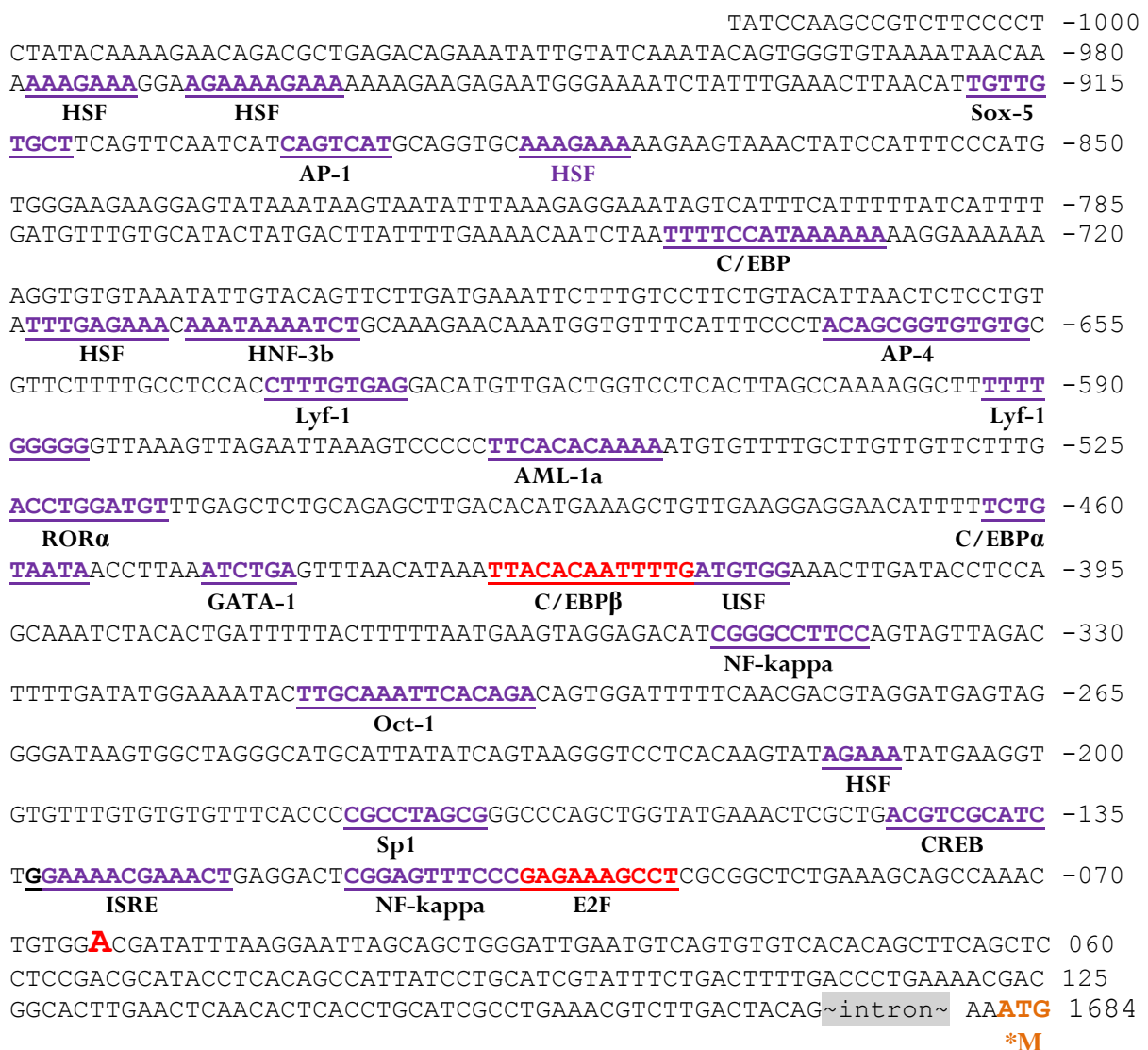


Fig. 31. Promoter analysis of *RbIRF3*.

The transcription factor binding sites are underlined with the corresponding names written below. The transcription initiation site is bold and red. The intron between the 5' UTR and ATG site is shaded. The ATG is orange colored.

6.3.5 Tissue distribution of *RbIRF3*

Tissue distribution profiling of *RbIRF3* was performed in 11 different tissues isolated from healthy rock bream maintained under normal conditions. The *RbIRF3* expression was normalized to the expression of β -actin transcript level and expressed as relative-fold with respect to mRNA level in muscle. The *RbIRF3* expression was ubiquitous and high level of transcripts were observed in liver, with the next level of abundance in skin and blood. Spleen, head kidney, kidney and brain showed relatively similar levels of expression of *RbIRF3* transcripts (Fig. 32).

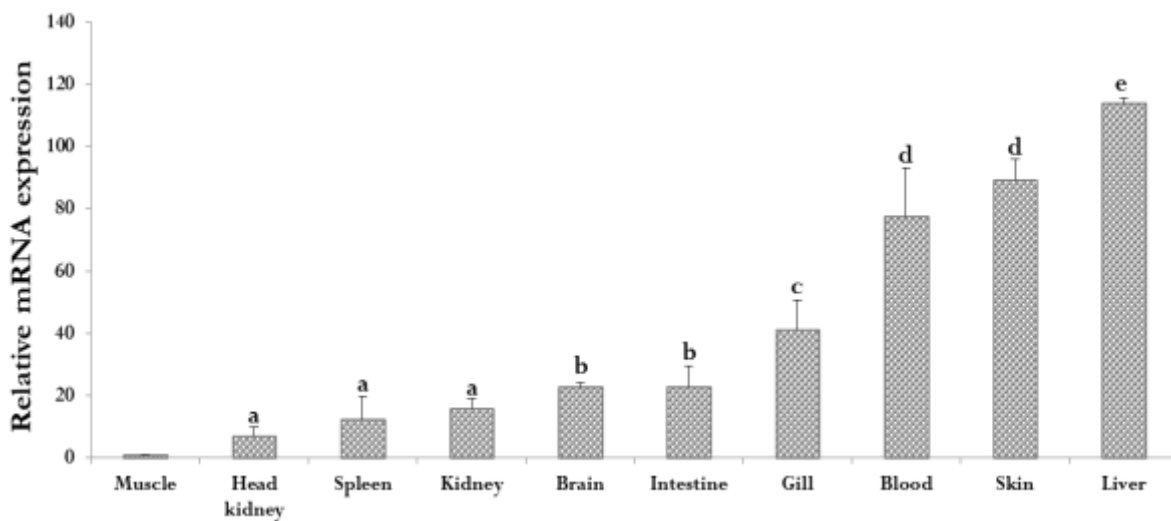


Fig. 32. Tissue distribution analysis of *RbIRF3*.

RbIRF3 tissue-specific expression in muscle, head kidney, brain, skin, kidney, spleen, intestine, gill, liver, heart tissues, and blood collected from unchallenged rock bream was analyzed using quantitative RT-PCR. Relative mRNA expression was calculated using the $2^{-\Delta\Delta Ct}$ method, with β -actin as the invariant control gene. In order to determine the tissue-

specific expression, the relative mRNA level was compared with muscle expression. Data are presented as mean values (n=3) with error bars representing SD. Data shown with “*” indicates significant expression levels at $P<0.01$.

6.3.6 Temporal expression post immune challenges

The kinetic transcriptional pattern of *RbIRF3* was analyzed by RT-PCR from blood, liver and head kidney isolated from rock bream following *in vivo* challenge with poly I:C. Post poly I:C challenge, all three tissues showed variable pattern of expression. Poly I:C altered the *RbIRF3* transcript level to a greater extent. In liver and head kidney, expressional modulation was observed from 3 h to 12 h, with a second elevation at 48 h in liver. In liver, *RbIRF3* expression peaked at 6 h (4-fold), while in head kidney at 3 h (12-fold). In blood, elevation in expression could be observed from 6 h to 24 h with maximum level being at 12 h (16-fold) (Fig. 33).

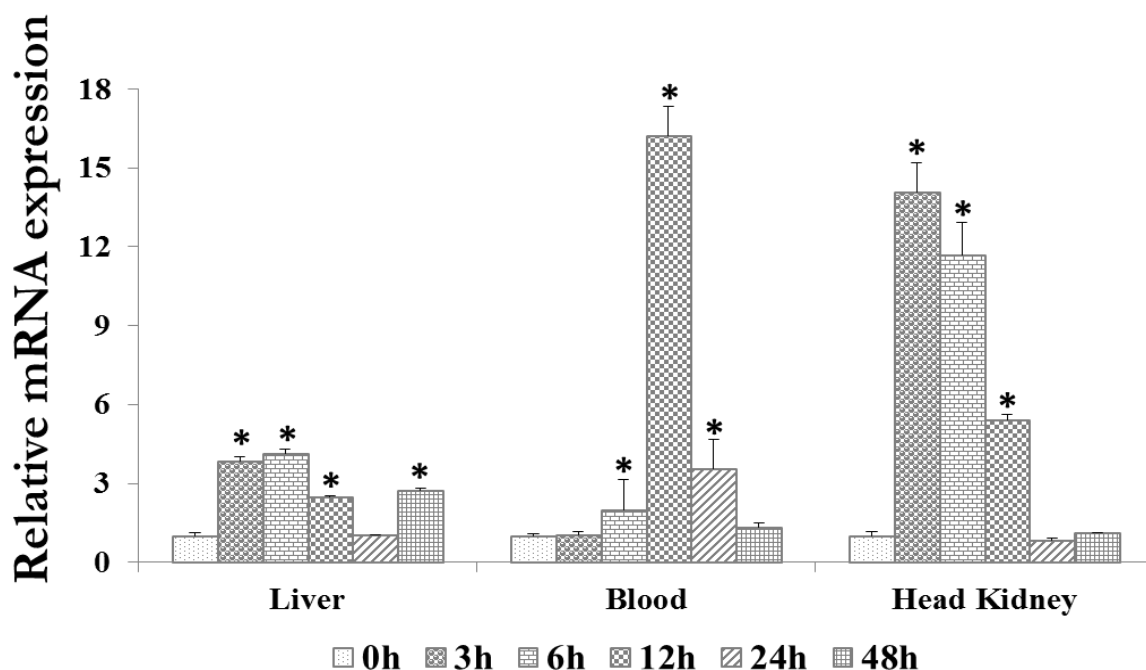


Fig. 33. *RbIRF3* expression analysis after poly I:C challenge.

RbIRF3 expression was analyzed in liver, blood, spleen, gill and head kidney post poly I:C challenge. Relative mRNA expression was calculated by the $2^{-\Delta\Delta Ct}$ method relative to PBS-

injected controls and normalized with the same, with β -actin as the reference gene. Data are presented as mean values (n=3) with error bars representing SD. Data shown with “*” indicates significant expression levels at $P < 0.01$.

6.4 Discussion

Interferon regulatory factors play a pivotal role in the initial induction of IFNs, during infection. IRFs are also involved in cytokine signaling, haemopoietic development and cell growth regulation. In this study, we have identified, characterized, and analyzed the spatial/temporal expression pattern of RbIRF3 from rock bream. *RbIRF3* cDNA was 1884 bp long consisting of ORF of 1386 bp which encoded a protein of 462 amino acids with molecular mass of 51 kDa. The pairwise and multiple sequence alignment showed high identity and conservation, respectively with the other IRF3 homologues. Multiple sequence alignment revealed highly conserved DBD with five tryptophan residues in the N-terminus and IAD in the C-terminus. Unlike the large yellow croaker, RbIRF3 possessed five tryptophan residues in the DBD. Three of the five tryptophan residues are crucial for DNA binding. The C-terminal IAD is significant in activating the double-stranded RNA-activated factor 1 (DRAF1) and defenses against the viral infection, and is also required for the formation of IRF homo/heterodimers and association with other transcription factor, IAD was conserved in RbIRF3 like other fish and vertebrate homologues. Similar to the mammalian, chicken and other fish IRF3 subfamily members, the C-terminal SRD in RbIRF3 was found but shorter (4 serine and no threonine residue) than the human IRF3 which contained 6 Ser and 2 Thr residues. Human IRF3 possesses potential virus-mediated phosphorylation sites in the C-terminal region (Ser 385, 386 [“2 S site”] and Ser 396, 398, 402, 405, and Thr 404 [“5 ST site”]). The phosphorylation of Ser386 in human IRF3 is the critical determinant for its activation, which in rock bream corresponds to Ser 443. Ser444 in RbIRF3 corresponds to Ser 386 in human IRF3. Thus RbIRF3 possessed the 2S site, similar to the human IRF3.

Almost all the Ser residues in the SRD including the SSL motif are phosphoacceptor sites in human IRF7. RbIRF3 also possessed the SSL motif, while trout showed less conservation in the SSL motif (Holland et al., 2008). RbIRF3 lacked the inhibitory domain which is characteristic of the mammalian IRF3. Although two basic residues (lysine-arginine) which serve as nuclear localization signal (NLS) in human IRF3 were found in RbIRF3, no nuclear export signal (NES) and proline rich domain were found in the corresponding positions. RbIRF3 shared high identity and similarity with *Dicentrarchus labrax* and a reasonable identity with other fish homologues including rainbow trout, Japanese flounder, large yellow croaker and turbot. Phylogenetic analysis revealed that RbIRF3 belonged to the IRF3 subfamily clustering with the IRF3 and IRF7 homologues, suggesting the notion that IRFs emerged early in the vertebrate evolution and IRF3 subfamily comprising of IRF3/IRF7 originated from a single ancestral gene. The conserved DBD, IAD, SRD together with the phylogenetic relationship suggests that RbIRF3 is a new member of the IRF3 subfamily, which might play a vital role in immunity, similar to the other homologues.

RbIRF3 genome structure was similar to that of large yellow croaker and turbot with 11 exons and 12 introns. The first exon constituted of UTR in its entirety in both large yellow croaker and rock bream. RbIRF3 gene structure was different from that of other fish like zebrafish and stickleback. The genome length could be attributed both variation in the exon and intron lengths among the species. The putative promoter region and 5' flanking region analysis revealed a number of TFBS, like AP-1, AP-4, AML-1a, C/EBP, CREB which play significant roles in the regulation of immune related genes. Also an ISRE could be found in the close proximity to the transcription initiation site, which suggests its regulation by IFNs. *RbIRF3* gene neither possessed a TATA nor CCAAT box but was GC rich, similar to the human IRF3 promoter (Lowther et al., 1999). The *RbIRF3* promoter possessed Sp1, E2F, HSF, GATA-1, USF and NF-kappa sites similar to the human IRF3 (Ren et al., 2012; Xu et

al., 2010). Mutation and over expression of Sp1 sites in human IRF3 promoter repressed and increased the transcription activity of human IRF3, respectively (Ren et al., 2012). In contrast, mouse IRF3 promoter which showed high homology to the human IRF3 promoter possessed TATA and CCAAT box motifs, suggesting that, at least at the level of transcription initiation, these genes may be differentially regulated. In chicken, poly I:C and IFN-mediated induction is dependent on the NF- κ B binding sites and overlapping ISREs, respectively, present in the IRF3 promoter (May et al., 2000). The mammalian IRF7 promoter also possesses a single NF- κ B binding site and a single ISRE binding the ISGF3 complex (Lu et al., 2000; Lu et al., 2002).

Spatial expression analysis of RbIRF3 showed ubiquitous expression in all the examined tissues. IRF3 was detected in all the examined tissues in large yellow croaker (Yao et al., 2012), rainbow trout (Holland et al., 2008) and Atlantic salmon (Hu et al., 2011b). Constitutive expression of IRF3 was observed in rainbow trout, which did not reveal any transcriptional modulation (Holland et al., 2008). In contrast to the constitutive expression of mammalian and a few fish IRF3, Japanese flounder IRF3 was significantly expressed in the immune tissues but not in brain, gonad, stomach, muscle and skin. Other known fish IRFs including IRF-1, 2, 4, 5 and 8 were ubiquitously expressed in all the tested tissues of healthy fish. IRF4 and 8 from rock bream revealed ubiquitous presence in all the examined tissues (Bathige et al., 2012). IRF3 and IRF7 constitute the IRF3 subfamily of proteins. IRF7 in several fish species were found to be ubiquitously expressed (Holland et al., 2008; Zhang et al., 2003). IRF3 is constitutively expressed and resides in the cytosol in the latent form and undergoes phosphorylation and activation upon viral infection. Constitutively expressed IRF subfamily members are crucial for the early and late phases of IFN induction, post challenges encountered by the host (Honda and Taniguchi, 2006; Honda et al., 2005). RbIRF3's

ubiquitous and constitutive expression in physiologically different tissues suggest that they may involve in a wide range of functions, which in teleosts are yet to be demonstrated.

In order to understand the modulation of *RbIRF3* by immunostimulants, *RbIRF3* transcripts were investigated in blood, liver and head kidney tissues post poly I:C challenge *in vivo*. Our results revealed modulation of the *RbIRF3* transcripts in all the analyzed tissues, suggesting that *RbIRF3* played a crucial role in antiviral defense. Poly I:C is a synthetically-derived mimic of the double-stranded RNA that is present in some viruses and has been employed to understand the modulation of immune related genes in various organisms. Poly I:C is a potent inducer of IRF3 subfamily proteins, IRF3/IRF7. IRF3 expression exhibited different dynamics following poly I:C challenge. In mammals, poly I:C recognition through the TLR and RIF-like receptors leads to the activation of the signaling cascades resulting in the activation of IFN promoter through IRF3, IRF7 and NF- κ B (Kawai and Akira, 2006, 2007; Takeuchi and Akira, 2009). Induction of the IRF3 and IRF7 transcripts were detected in trout cells post poly I:C, type I IFN and IFN γ treatment (Holland et al., 2008). Similarly, elevation in the IRF3 transcripts could be observe din large yellow croaker after poly I:C challenge (Yao et al., 2012), carp (Sun et al., 2010), flounder (Hu et al., 2011b), rainbow trout (Holland et al., 2008) and Atlantic salmon (Bergan et al., 2010). In this study, blood and head kidney, which are major immune organs in fish showed a dramatic change in *RbIRF3* transcript levels, suggesting their active role in antiviral immunity.

The identification of IRFs belonging to different families and understanding their role in the regulation of IFNs in anti-bacterial and -viral defense in fish is of great significance. This study will further the functional roles of the IRF family members in different teleosts and obtain a comparative understanding of mechanism of regulation in mammals.

7.0 References

- Alff, P.J., Sen, N., Gorbunova, E., Gavrilovskaya, I.N., Mackow, E.R., 2008. The NY-1 hantavirus Gn cytoplasmic tail coprecipitates TRAF3 and inhibits cellular interferon responses by disrupting TBK1-TRAF3 complex formation. *Journal of virology* 82, 9115-9122.
- Batbayar, S., Lee, D.-H., Kim, H.-W., 2012. Immunomodulation of Fungal β -Glucan in Host Defense Signaling by Dectin-1. *Biomolecules and Therapeutics* 20, 433-445.
- Bathige, S.D., Whang, I., Umasuthan, N., Lim, B.S., Park, M.A., Kim, E., Park, H.C., Lee, J., 2012. Interferon regulatory factors 4 and 8 in rock bream, *Oplegnathus fasciatus*: structural and expressional evidence for their antimicrobial role in teleosts. *Fish & shellfish immunology* 33, 857-871.
- Baum, A., Garcia-Sastre, A., 2011. Differential recognition of viral RNA by RIG-I. *Virulence* 2, 166-169.
- Belgnaoui, S.M., Paz, S., Hiscott, J., 2011. Orchestrating the interferon antiviral response through the mitochondrial antiviral signaling (MAVS) adapter. *Current opinion in immunology* 23, 564-572.
- Bergan, V., Kileng, O., Sun, B., Robertsen, B., 2010. Regulation and function of interferon regulatory factors of Atlantic salmon. *Molecular immunology* 47, 2005-2014.
- Berke, I.C., Li, Y., Modis, Y., 2013. Structural basis of innate immune recognition of viral RNA. *Cellular microbiology* 15, 386-394.
- Berke, I.C., Modis, Y., 2012. MDA5 cooperatively forms dimers and ATP-sensitive filaments upon binding double-stranded RNA. *The EMBO journal* 31, 1714-1726.
- Berke, I.C., Yu, X., Modis, Y., Egelman, E.H., 2012. MDA5 assembles into a polar helical filament on dsRNA. *Proceedings of the National Academy of Sciences of the United States of America* 109, 18437-18441.
- Biacchesi, S., LeBerre, M., Lamoureux, A., Louise, Y., Lauret, E., Boudinot, P., Bremont, M., 2009. Mitochondrial antiviral signaling protein plays a major role in induction of the fish innate immune response against RNA and DNA viruses. *Journal of virology* 83, 7815-7827.
- Biron, C.A., 1999. Initial and innate responses to viral infections--pattern setting in immunity or disease. *Current opinion in microbiology* 2, 374-381.
- Bondad-Reantaso, M.G., Subasinghe, R.P., Arthur, J.R., Ogawa, K., Chinabut, S., Adlard, R., Tan, Z., Shariff, M., 2005. Disease and health management in Asian aquaculture. *Veterinary parasitology* 132, 249-272.

Bostock, J., McAndrew, B., Richards, R., Jauncey, K., Telfer, T., Lorenzen, K., Little, D., Ross, L., Handisyde, N., Gatward, I., Corner, R., 2010. Aquaculture: global status and trends. *Philosophical Transactions of the Royal Society B: Biological Sciences* 365, 2897-2912.

Boudinot, P., Massin, P., Blanco, M., Riffault, S., Benmansour, A., 1999. *vig-1*, a new fish gene induced by the rhabdovirus glycoprotein, has a virus-induced homologue in humans and shares conserved motifs with the MoeA family. *Journal of virology* 73, 1846-1852.

Bruns, A.M., Horvath, C.M., 2012. Activation of RIG-I-like receptor signal transduction. *Critical reviews in biochemistry and molecular biology* 47, 194-206.

Butchar, J.P., Parsa, K.V., Marsh, C.B., Tridandapani, S., 2006. Negative regulators of toll-like receptor 4-mediated macrophage inflammatory response. *Current pharmaceutical design* 12, 4143-4153.

Campanella, J.J., Bitincka, L., Smalley, J., 2003. MatGAT: an application that generates similarity/identity matrices using protein or DNA sequences. *BMC bioinformatics* 4, 29.

Chang, M., Collet, B., Nie, P., Lester, K., Campbell, S., Secombes, C.J., Zou, J., 2011. Expression and functional characterization of the RIG-I-like receptors MDA5 and LGP2 in Rainbow trout (*Oncorhynchus mykiss*). *Journal of virology* 85, 8403-8412.

Chen, L., Su, J., Yang, C., Peng, L., Wan, Q., Wang, L., 2012. Functional Characterizations of *RIG-I* to GCRV and Viral/Bacterial PAMPs in Grass Carp *Ctenopharyngodon idella*. *PLoS ONE* 7, e42182.

Chi, H., Zhang, Z., Bogwald, J., Zhan, W., Dalmo, R.A., 2011. Cloning, expression analysis and promoter structure of TBK1 (TANK-binding kinase 1) in Atlantic cod (*Gadus morhua* L.). *Fish & shellfish immunology* 30, 1055-1063.

Childs, K., Randall, R., Goodbourn, S., 2012. Paramyxovirus V Proteins Interact with the RNA Helicase LGP2 To Inhibit RIG-I-Dependent Interferon Induction. *Journal of virology* 86, 3411-3421.

Collet, B., Hovens, G.C., Mazzoni, D., Hirono, I., Aoki, T., Secombes, C.J., 2003. Cloning and expression analysis of rainbow trout *Oncorhynchus mykiss* interferon regulatory factor 1 and 2 (IRF-1 and IRF-2). *Developmental and comparative immunology* 27, 111-126.

Crane, M., Hyatt, A., 2011. Viruses of fish: an overview of significant pathogens. *Viruses* 3, 2025-2046.

Cui, S., Eisenacher, K., Kirchhofer, A., Brzozka, K., Lammens, A., Lammens, K., Fujita, T., Conzelmann, K.K., Krug, A., Hopfner, K.P., 2008. The C-terminal regulatory domain is the RNA 5'-triphosphate sensor of RIG-I. *Molecular cell* 29, 169-179.

Cui, Y., Li, M., Walton, K.D., Sun, K., Hanover, J.A., Furth, P.A., Hennighausen, L., 2001. The Stat3/5 locus encodes novel endoplasmic reticulum and helicase-like proteins that are preferentially expressed in normal and neoplastic mammary tissue. *Genomics* 78, 129-134.

Curtis, P.A., Drawbridge, M., Iwamoto, T., Nakai, T., Hedrick, R.P., Gendron, A.P., 2001. Nodavirus infection of juvenile white seabass, *Atractoscion nobilis*, cultured in southern California: first record of viral nervous necrosis (VNN) in North America. *Journal of fish diseases* 24, 263-271.

Das, B.K., Nayak, K.K., Fourrier, M., Collet, B., Snow, M., Ellis, A.E., 2007. Expression of Mx protein in tissues of Atlantic salmon post-smolts – An immunohistochemical study. *Fish & shellfish immunology* 23, 1209-1217.

De Andrea, M., Ravera, R., Gioia, D., Gariglio, M., Landolfo, S., 2002. The interferon system: an overview. *European journal of paediatric neurology : EJPN : official journal of the European Paediatric Neurology Society* 6 Suppl A, A41-46; discussion A55-48.

de Kinkelin, P., Dorson, M., 1973. Interferon production in rainbow trout (*Salmo gairdneri*) experimentally infected with Egtved virus. *The Journal of general virology* 19, 125-127.

Dinarello, C.A., 2007. Historical insights into cytokines. *European journal of immunology* 37 Suppl 1, S34-45.

Diperna, G., 2005. The RNA Helicase Lgp2 is a Negative Regulator of Virus-induced Immune Signaling. Boston University.

Dorson, M., Barde, A., de Kinkelin, P., 1975. Egtved virus induced rainbow trout serum interferon: some physicochemical properties. *Annales de microbiologie* 126, 485-489.

Drutskaya, M.S., Belousov, P.V., Nedospasov, S.A., 2011. Innate mechanisms of viral recognition. *Mol Biol* 45, 5-15.

Du Pasquier, L., 2001. The immune system of invertebrates and vertebrates. *Comparative biochemistry and physiology. Part B, Biochemistry & molecular biology* 129, 1-15.

Eaton, W.D., 1990. Anti-viral activity in four species of salmonids following exposure to poly inosinic:cytidylic acid. *Diseases of aquatic organisms* 9, 193-198.

Eisenacher, K., Krug, A., 2012. Regulation of RLR-mediated innate immune signaling--it is all about keeping the balance. *European journal of cell biology* 91, 36-47.

Eliassen, T.M., Froystad, M.K., Dannevig, B.H., Jankowska, M., Brech, A., Falk, K., Romoren, K., Gjoen, T., 2000. Initial events in infectious salmon anemia virus infection: evidence for the requirement of a low-pH step. *Journal of virology* 74, 218-227.

- Erlandsson, L., Blumenthal, R., Eloranta, M.L., Engel, H., Alm, G., Weiss, S., Leanderson, T., 1998. Interferon-beta is required for interferon-alpha production in mouse fibroblasts. *Current biology* : CB 8, 223-226.
- Essbauer, S., Ahne, W., 2001. Viruses of lower vertebrates. *Journal of veterinary medicine. B, Infectious diseases and veterinary public health* 48, 403-475.
- Ferrero-Miliani, L., Nielsen, O.H., Andersen, P.S., Girardin, S.E., 2007. Chronic inflammation: importance of NOD2 and NALP3 in interleukin-1beta generation. *Clinical and experimental immunology* 147, 227-235.
- Fitzgerald, K.A., McWhirter, S.M., Faia, K.L., Rowe, D.C., Latz, E., Golenbock, D.T., Coyle, A.J., Liao, S.M., Maniatis, T., 2003. IKKepsilon and TBK1 are essential components of the IRF3 signaling pathway. *Nat Immunol* 4, 491-496.
- Foy, E., Li, K., Sumpter, R., Jr., Loo, Y.M., Johnson, C.L., Wang, C., Fish, P.M., Yoneyama, M., Fujita, T., Lemon, S.M., Gale, M., Jr., 2005. Control of antiviral defenses through hepatitis C virus disruption of retinoic acid-inducible gene-I signaling. *Proceedings of the National Academy of Sciences of the United States of America* 102, 2986-2991.
- Gao, B., Jeong, W.I., Tian, Z., 2008. Liver: An organ with predominant innate immunity. *Hepatology* 47, 729-736.
- Gitlin, L., Barchet, W., Gilfillan, S., Cella, M., Beutler, B., Flavell, R.A., Diamond, M.S., Colonna, M., 2006. Essential role of mda-5 in type I IFN responses to polyriboinosinic:polyribocytidylic acid and encephalomyocarditis picornavirus. *Proceedings of the National Academy of Sciences of the United States of America* 103, 8459-8464.
- Goodbourn, S., Didcock, L., Randall, R.E., 2000. Interferons: cell signalling, immune modulation, antiviral response and virus countermeasures. *The Journal of general virology* 81, 2341-2364.
- Hammaker, D., Boyle, D.L., Firestein, G.S., 2012. Synoviocyte innate immune responses: TANK-binding kinase-1 as a potential therapeutic target in rheumatoid arthritis. *Rheumatology* 51, 610-618.
- Hansen, J.D., La Patra, S., 2002. Induction of the rainbow trout MHC class I pathway during acute IHNV infection. *Immunogenetics* 54, 654-661.
- Hayashi, T., Nakamura, T., Takaoka, A., 2011. [Pattern recognition receptors]. *Nihon Rinsho Men'eki Gakkai kaishi = Japanese journal of clinical immunology* 34, 329-345.
- Hemmi, H., Takeuchi, O., Sato, S., Yamamoto, M., Kaisho, T., Sanjo, H., Kawai, T., Hoshino, K., Takeda, K., Akira, S., 2004. The roles of two IkappaB kinase-related kinases in

lipopolysaccharide and double stranded RNA signaling and viral infection. *The Journal of experimental medicine* 199, 1641-1650.

Hikima, J., Yi, M.K., Ohtani, M., Jung, C.Y., Kim, Y.K., Mun, J.Y., Kim, Y.R., Takeyama, H., Aoki, T., Jung, T.S., 2012. LGP2 expression is enhanced by interferon regulatory factor 3 in olive flounder, *Paralichthys olivaceus*. *PLoS One* 7, e51522.

Holland, J.W., Bird, S., Williamson, B., Woudstra, C., Mustafa, A., Wang, T., Zou, J., Blaney, S.C., Collet, B., Secombes, C.J., 2008. Molecular characterization of IRF3 and IRF7 in rainbow trout, *Oncorhynchus mykiss*: Functional analysis and transcriptional modulation. *Molecular immunology* 46, 269-285.

Holland, J.W., Karim, A., Wang, T., Alnabulsi, A., Scott, J., Collet, B., Mughal, M.S., Secombes, C.J., Bird, S., 2010. Molecular cloning and characterization of interferon regulatory factors 4 and 8 (IRF-4 and IRF-8) in rainbow trout, *Oncorhynchus mykiss*. *Fish & shellfish immunology* 29, 157-166.

Honda, K., Takaoka, A., Taniguchi, T., 2006. Type I interferon [corrected] gene induction by the interferon regulatory factor family of transcription factors. *Immunity* 25, 349-360.

Honda, K., Taniguchi, T., 2006. IRFs: master regulators of signalling by Toll-like receptors and cytosolic pattern-recognition receptors. *Nature reviews. Immunology* 6, 644-658.

Honda, K., Yanai, H., Takaoka, A., Taniguchi, T., 2005. Regulation of the type I IFN induction: a current view. *International immunology* 17, 1367-1378.

Hornung, V., Ellegast, J., Kim, S., Brzozka, K., Jung, A., Kato, H., Poeck, H., Akira, S., Conzelmann, K.K., Schlee, M., Endres, S., Hartmann, G., 2006. 5'-Triphosphate RNA is the ligand for RIG-I. *Science* 314, 994-997.

Hou, F., Sun, L., Zheng, H., Skaug, B., Jiang, Q.-X., Chen, Zhijian J., 2011. MAVS Forms Functional Prion-like Aggregates to Activate and Propagate Antiviral Innate Immune Response. *Cell* 146, 448-461.

Hu, G., Xia, J., Lou, H., Liu, Q., Lin, J., Yin, X., Dong, X., 2011a. Cloning and expression analysis of interferon regulatory factor 7 (IRF-7) in turbot, *Scophthalmus maximus*. *Developmental and comparative immunology* 35, 416-420.

Hu, G., Yin, X., Lou, H., Xia, J., Dong, X., Zhang, J., Liu, Q., 2011b. Interferon regulatory factor 3 (IRF-3) in Japanese flounder, *Paralichthys olivaceus*: sequencing, limited tissue distribution, inducible expression and induction of fish type I interferon promoter. *Developmental and comparative immunology* 35, 164-173.

- Hu, G., Yin, X., Xia, J., Dong, X., Zhang, J., Liu, Q., 2010. Molecular cloning and characterization of interferon regulatory factor 7 (IRF-7) in Japanese flounder, *Paralichthys olivaceus*. *Fish & shellfish immunology* 29, 963-971.
- Hu, G.B., Cong, R.S., Fan, T.J., Mei, X.G., 2004. Induction of apoptosis in a flounder gill cell line by lymphocystis disease virus infection. *Journal of fish diseases* 27, 657-662.
- Huang, B., Qi, Z.T., Xu, Z., Nie, P., 2010a. Global characterization of interferon regulatory factor (IRF) genes in vertebrates: glimpse of the diversification in evolution. *BMC immunology* 11, 22.
- Huang, T., Su, J., Heng, J., Dong, J., Zhang, R., Zhu, H., 2010b. Identification and expression profiling analysis of grass carp *Ctenopharyngodon idella* LGP2 cDNA. *Fish & shellfish immunology* 29, 349-355.
- Huang, X., Huang, Y., Cai, J., Wei, S., Ouyang, Z., Qin, Q., 2013. Molecular cloning, expression and functional analysis of ISG15 in orange-spotted grouper, *Epinephelus coioides*. *Fish & shellfish immunology* 34, 1094-1102.
- Ireton, R.C., Gale, M., Jr., 2011. RIG-I like receptors in antiviral immunity and therapeutic applications. *Viruses* 3, 906-919.
- Isaacs, A., Lindenmann, J., 1957. Virus interference. I. The interferon. *Proceedings of the Royal Society of London. Series B, Containing papers of a Biological character. Royal Society* 147, 258-267.
- Isaacs, A., Lindenmann, J., Valentine, R.C., 1957. Virus interference. II. Some properties of interferon. *Proceedings of the Royal Society of London. Series B, Containing papers of a Biological character. Royal Society* 147, 268-273.
- Iwamoto, T., Mise, K., Mori, K., Arimoto, M., Nakai, T., Okuno, T., 2001. Establishment of an infectious RNA transcription system for Striped jack nervous necrosis virus, the type species of the betanodaviruses. *The Journal of general virology* 82, 2653-2662.
- Jacobs, B.L., Langland, J.O., 1996. When two strands are better than one: the mediators and modulators of the cellular responses to double-stranded RNA. *Virology* 219, 339-349.
- Jensen, S., Thomsen, A.R., 2012. Sensing of RNA viruses: a review of innate immune receptors involved in recognizing RNA virus invasion. *Journal of virology* 86, 2900-2910.
- Jia, Y., Song, T., Wei, C., Ni, C., Zheng, Z., Xu, Q., Ma, H., Li, L., Zhang, Y., He, X., Xu, Y., Shi, W., Zhong, H., 2009. Negative regulation of MAVS-mediated innate immune response by PSMA7. *Journal of immunology* 183, 4241-4248.

Jiang, F., Ramanathan, A., Miller, M.T., Tang, G.Q., Gale, M., Jr., Patel, S.S., Marcotrigiano, J., 2011. Structural basis of RNA recognition and activation by innate immune receptor RIG-I. *Nature* 479, 423-427.

Jiang, X., Kinch, L.N., Brautigam, C.A., Chen, X., Du, F., Grishin, N.V., Chen, Z.J., 2012. Ubiquitin-induced oligomerization of the RNA sensors RIG-I and MDA5 activates antiviral innate immune response. *Immunity* 36, 959-973.

Kang, D.C., Gopalkrishnan, R.V., Lin, L., Randolph, A., Valerie, K., Pestka, S., Fisher, P.B., 2004. Expression analysis and genomic characterization of human melanoma differentiation associated gene-5, mda-5: a novel type I interferon-responsive apoptosis-inducing gene. *Oncogene* 23, 1789-1800.

Kang, D.C., Gopalkrishnan, R.V., Wu, Q., Jankowsky, E., Pyle, A.M., Fisher, P.B., 2002. mda-5: An interferon-inducible putative RNA helicase with double-stranded RNA-dependent ATPase activity and melanoma growth-suppressive properties. *Proceedings of the National Academy of Sciences of the United States of America* 99, 637-642.

Kato, H., Sato, S., Yoneyama, M., Yamamoto, M., Uematsu, S., Matsui, K., Tsujimura, T., Takeda, K., Fujita, T., Takeuchi, O., Akira, S., 2005. Cell type-specific involvement of RIG-I in antiviral response. *Immunity* 23, 19-28.

Kato, H., Takeuchi, O., Mikamo-Satoh, E., Hirai, R., Kawai, T., Matsushita, K., Hiiragi, A., Dermody, T.S., Fujita, T., Akira, S., 2008. Length-dependent recognition of double-stranded ribonucleic acids by retinoic acid-inducible gene-I and melanoma differentiation-associated gene 5. *The Journal of experimental medicine* 205, 1601-1610.

Kato, H., Takeuchi, O., Sato, S., Yoneyama, M., Yamamoto, M., Matsui, K., Uematsu, S., Jung, A., Kawai, T., Ishii, K.J., Yamaguchi, O., Otsu, K., Tsujimura, T., Koh, C.S., Reis e Sousa, C., Matsuura, Y., Fujita, T., Akira, S., 2006. Differential roles of MDA5 and RIG-I helicases in the recognition of RNA viruses. *Nature* 441, 101-105.

Kawai, T., Akira, S., 2006. Innate immune recognition of viral infection. *Nat Immunol* 7, 131-137.

Kawai, T., Akira, S., 2007. Signaling to NF-kappaB by Toll-like receptors. *Trends in molecular medicine* 13, 460-469.

Kawai, T., Akira, S., 2010. The role of pattern-recognition receptors in innate immunity: update on Toll-like receptors. *Nat Immunol* 11, 373-384.

Kawai, T., Takahashi, K., Sato, S., Coban, C., Kumar, H., Kato, H., Ishii, K.J., Takeuchi, O., Akira, S., 2005. IPS-1, an adaptor triggering RIG-I- and Mda5-mediated type I interferon induction. *Nat Immunol* 6, 981-988.

- Kielian, M., Jungerwirth, S., 1990. Mechanisms of enveloped virus entry into cells. *Molecular biology & medicine* 7, 17-31.
- Kim, H.J., Kwon, S.R., Lee, E.H., Nam, Y.K., Kim, S.K., Kim, K.H., 2007. Pathogenicity of marine birnavirus (MABV) on fingerlings of rock bream (*Oplegnathus fasciatus*). *Aquaculture* 272, 762-766.
- King, J.A., Snow, M., Smail, D.A., Raynard, R.S., 2001. Distribution of viral haemorrhagic septicaemia virus in wild fish species of the North Sea, north east Atlantic Ocean and Irish Sea. *Diseases of aquatic organisms* 47, 81-86.
- Kocan, R., Bradley, M., Elder, N., Meyers, T., Batts, W., Winton, J., 1997. North American Strain of Viral Hemorrhagic Septicemia Virus is Highly Pathogenic for Laboratory-Reared Pacific Herring. *Journal of Aquatic Animal Health* 9, 279-290.
- Komuro, A., Horvath, C.M., 2006. RNA- and virus-independent inhibition of antiviral signaling by RNA helicase LGP2. *Journal of virology* 80, 12332-12342.
- Kontsek, P., Karayianni-Vasconcelos, G., Kontsekova, E., 2003. The human interferon system: characterization and classification after discovery of novel members. *Acta virologica* 47, 201-215.
- Kowalinski, E., Lunardi, T., McCarthy, Andrew A., Louber, J., Brunel, J., Grigorov, B., Gerlier, D., Cusack, S., 2011. Structural Basis for the Activation of Innate Immune Pattern-Recognition Receptor RIG-I by Viral RNA. *Cell* 147, 423-435.
- Kumagai, Y., Akira, S., 2010. Identification and functions of pattern-recognition receptors. *The Journal of allergy and clinical immunology* 125, 985-992.
- Kumar, H., Kawai, T., Akira, S., 2011. Pathogen recognition by the innate immune system. *International reviews of immunology* 30, 16-34.
- Kumar, H., Kawai, T., Kato, H., Sato, S., Takahashi, K., Coban, C., Yamamoto, M., Uematsu, S., Ishii, K.J., Takeuchi, O., Akira, S., 2006. Essential role of IPS-1 in innate immune responses against RNA viruses. *The Journal of experimental medicine* 203, 1795-1803.
- Kumar, K.P., McBride, K.M., Weaver, B.K., Dingwall, C., Reich, N.C., 2000. Regulated Nuclear-Cytoplasmic Localization of Interferon Regulatory Factor 3, a Subunit of Double-Stranded RNA-Activated Factor 1. *Molecular and cellular biology* 20, 4159-4168.
- L. Tort, J.C.B., S. Mackenzie, 2003. Fish immune system. A crossroads between innate and adaptive responses. *Inmunología* 22, 277-286.
- Lauksund, S., Svingerud, T., Bergan, V., Robertsen, B., 2009. Atlantic salmon IPS-1 mediates induction of IFN α 1 and activation of NF-kappaB and localizes to mitochondria. *Developmental and comparative immunology* 33, 1196-1204.

- Lee, Y.G., Lee, J., Byeon, S.E., Yoo, D.S., Kim, M.H., Lee, S.Y., Cho, J.Y., 2011. Functional role of Akt in macrophage-mediated innate immunity. *Frontiers in bioscience : a journal and virtual library* 16, 517-530.
- Leong, J.C., Trobridge, G.D., Kim, C.H., Johnson, M., Simon, B., 1998. Interferon-inducible Mx proteins in fish. *Immunological reviews* 166, 349-363.
- Leu, J.H., Yan, S.J., Lee, T.F., Chou, C.M., Chen, S.T., Hwang, P.P., Chou, C.K., Huang, C.J., 2000. Complete genomic organization and promoter analysis of the round-spotted pufferfish JAK1, JAK2, JAK3, and TYK2 genes. *DNA and cell biology* 19, 431-446.
- Leung, D.W., Amarasinghe, G.K., 2012. Structural insights into RNA recognition and activation of RIG-I-like receptors. *Current Opinion in Structural Biology* 22, 297-303.
- Li, S., Sun, F., Zhang, Y.-B., Gui, J.-F., Zhang, Q.-Y., 2012. Identification of DreI as an Antiviral Factor Regulated by RLR Signaling Pathway. *PLoS ONE* 7, e32427.
- Li, X., Lu, C., Stewart, M., Xu, H., Strong, R.K., Igumenova, T., Li, P., 2009a. Structural basis of double-stranded RNA recognition by the RIG-I like receptor MDA5. *Archives of biochemistry and biophysics* 488, 23-33.
- Li, X., Ranjith-Kumar, C.T., Brooks, M.T., Dharmiah, S., Herr, A.B., Kao, C., Li, P., 2009b. The RIG-I-like receptor LGP2 recognizes the termini of double-stranded RNA. *The Journal of biological chemistry* 284, 13881-13891.
- Lin, C.H., Christopher John, J.A., Lin, C.H., Chang, C.Y., 2006. Inhibition of nervous necrosis virus propagation by fish Mx proteins. *Biochemical and biophysical research communications* 351, 534-539.
- Lin, R., Heylbroeck, C., Pitha, P.M., Hiscott, J., 1998. Virus-dependent phosphorylation of the IRF-3 transcription factor regulates nuclear translocation, transactivation potential, and proteasome-mediated degradation. *Molecular and cellular biology* 18, 2986-2996.
- Lin, R., Mamane, Y., Hiscott, J., 1999. Structural and Functional Analysis of Interferon Regulatory Factor 3: Localization of the Transactivation and Autoinhibitory Domains. *Molecular and cellular biology* 19, 2465-2474.
- Loo, Y.M., Fornek, J., Crochet, N., Bajwa, G., Perwitasari, O., Martinez-Sobrido, L., Akira, S., Gill, M.A., Garcia-Sastre, A., Katze, M.G., Gale, M., Jr., 2008. Distinct RIG-I and MDA5 signaling by RNA viruses in innate immunity. *Journal of virology* 82, 335-345.
- Loo, Y.M., Gale, M., Jr., 2011. Immune signaling by RIG-I-like receptors. *Immunity* 34, 680-692.
- Lowther, W.J., Moore, P.A., Carter, K.C., Pitha, P.M., 1999. Cloning and functional analysis of the human IRF-3 promoter. *DNA and cell biology* 18, 685-692.

- Lu, R., Au, W.C., Yeow, W.S., Hageman, N., Pitha, P.M., 2000. Regulation of the promoter activity of interferon regulatory factor-7 gene. Activation by interferon and silencing by hypermethylation. *The Journal of biological chemistry* 275, 31805-31812.
- Lu, R., Moore, P.A., Pitha, P.M., 2002. Stimulation of IRF-7 gene expression by tumor necrosis factor alpha: requirement for NFkappa B transcription factor and gene accessibility. *The Journal of biological chemistry* 277, 16592-16598.
- Luo, D., Ding, S.C., Vela, A., Kohlway, A., Lindenbach, B.D., Pyle, A.M., 2011. Structural insights into RNA recognition by RIG-I. *Cell* 147, 409-422.
- Ma, Y., Jin, H., Valyi-Nagy, T., Cao, Y., Yan, Z., He, B., 2012. Inhibition of TANK binding kinase 1 by herpes simplex virus 1 facilitates productive infection. *Journal of virology* 86, 2188-2196.
- Marchlik, E., Thakker, P., Carlson, T., Jiang, Z., Ryan, M., Marusic, S., Goutagny, N., Kuang, W., Askew, G.R., Roberts, V., Benoit, S., Zhou, T., Ling, V., Pfeifer, R., Stedman, N., Fitzgerald, K.A., Lin, L.L., Hall, J.P., 2010. Mice lacking Tbk1 activity exhibit immune cell infiltrates in multiple tissues and increased susceptibility to LPS-induced lethality. *Journal of leukocyte biology* 88, 1171-1180.
- Matsui, K., Kumagai, Y., Kato, H., Sato, S., Kawagoe, T., Uematsu, S., Takeuchi, O., Akira, S., 2006. Cutting edge: Role of TANK-binding kinase 1 and inducible I kappa B kinase in IFN responses against viruses in innate immune cells. *Journal of immunology* 177, 5785-5789.
- May, D.L., Grant, C.E., Deeley, R.G., 2000. Cloning and promoter analysis of the chicken interferon regulatory factor-3 gene. *DNA and cell biology* 19, 555-566.
- McCartney, S.A., Thackray, L.B., Gitlin, L., Gilfillan, S., Virgin, H.W., Colonna, M., 2008. MDA-5 recognition of a murine norovirus. *PLoS Pathog* 4, e1000108.
- Medzhitov, R., 2001. Toll-like receptors and innate immunity. *Nature reviews. Immunology* 1, 135-145.
- Meyers, T.R., Short, S., Lipson, K., 1999. Isolation of the North American strain of viral hemorrhagic septicemia virus (VHSV) associated with epizootic mortality in two new host species of Alaskan marine fish. *Diseases of aquatic organisms* 38, 81-86.
- Meylan, E., Curran, J., Hofmann, K., Moradpour, D., Binder, M., Bartenschlager, R., Tschopp, J., 2005. Cardif is an adaptor protein in the RIG-I antiviral pathway and is targeted by hepatitis C virus. *Nature* 437, 1167-1172.
- Moresco, E.M., Vine, D.L., Beutler, B., 2011. Prion-like behavior of MAVS in RIG-I signaling. *Cell research* 21, 1643-1645.

- Mortensen, H.F., Heuer, O.E., Lorenzen, N., Otte, L., Olesen, N.J., 1999. Isolation of viral haemorrhagic septicaemia virus (VHSV) from wild marine fish species in the Baltic Sea, Kattegat, Skagerrak and the North Sea. *Virus research* 63, 95-106.
- Munday, T.N.a.B.L., 1997. Special topic review: Nodaviruses as pathogens in larval and juvenile marine finfish. *World Journal of Microbiology & Biotechnology* 13, 375-381.
- Nakashima, M., Kinoshita, M., Nakashima, H., Habu, Y., Miyazaki, H., Shono, S., Hiroi, S., Shinomiya, N., Nakanishi, K., Seki, S., 2012. Pivotal Advance: Characterization of mouse liver phagocytic B cells in innate immunity. *Journal of leukocyte biology* 91, 537-546.
- Nousiainen, L., Sillanpää, M., Jiang, M., Thompson, J., Taipale, J., Julkunen, I., 2013. Human kinome analysis reveals novel kinases contributing to virus infection and retinoic-acid inducible gene I-induced type I and type III IFN gene expression. *Innate Immunity*.
- O'Farrell, C., Vaghefi, N., Cantonnet, M., Buteau, B., Boudinot, P., Benmansour, A., 2002. Survey of transcript expression in rainbow trout leukocytes reveals a major contribution of interferon-responsive genes in the early response to a rhabdovirus infection. *Journal of virology* 76, 8040-8049.
- Ohtani, M., Hikima, J.-i., Kondo, H., Hirono, I., Jung, T.-S., Aoki, T., 2010. Evolutional Conservation of Molecular Structure and Antiviral Function of a Viral RNA Receptor, LGP2, in Japanese Flounder, *Paralichthys olivaceus*. *The Journal of Immunology* 185, 7507-7517.
- Ohtani, M., Hikima, J., Kondo, H., Hirono, I., Jung, T.S., Aoki, T., 2011. Characterization and antiviral function of a cytosolic sensor gene, MDA5, in Japanese flounder, *Paralichthys olivaceus*. *Developmental and comparative immunology* 35, 554-562.
- Onoguchi, K., Onomoto, K., Takamatsu, S., Jogi, M., Takemura, A., Morimoto, S., Julkunen, I., Namiki, H., Yoneyama, M., Fujita, T., 2010. Virus-infection or 5'ppp-RNA activates antiviral signal through redistribution of IPS-1 mediated by MFN1. *PLoS Pathog* 6, e1001012.
- Otsuka, M., Kato, N., Moriyama, M., Taniguchi, H., Wang, Y., Dharel, N., Kawabe, T., Omata, M., 2005. Interaction between the HCV NS3 protein and the host TBK1 protein leads to inhibition of cellular antiviral responses. *Hepatology* 41, 1004-1012.
- Palti, Y., 2011. Toll-like receptors in bony fish: from genomics to function. *Developmental and comparative immunology* 35, 1263-1272.
- Park, E.M., Kang, J.H., Seo, J.S., Kim, G., Chung, J., Choi, T.J., 2008. Molecular cloning and expression analysis of the STAT1 gene from olive flounder, *Paralichthys olivaceus*. *BMC immunology* 9, 31.
- Park, S.I., 2009. Disease Control in Korean Aquaculture. *Fish Pathology* 44, 19-23.

- Peisley, A., Lin, C., Wu, B., Orme-Johnson, M., Liu, M., Walz, T., Hur, S., 2011. Cooperative assembly and dynamic disassembly of MDA5 filaments for viral dsRNA recognition. *Proceedings of the National Academy of Sciences*.
- Perry, A.K., Chow, E.K., Goodnough, J.B., Yeh, W.C., Cheng, G., 2004. Differential requirement for TANK-binding kinase-1 in type I interferon responses to toll-like receptor activation and viral infection. *The Journal of experimental medicine* 199, 1651-1658.
- Pestka, S., Krause, C.D., Walter, M.R., 2004. Interferons, interferon-like cytokines, and their receptors. *Immunological reviews* 202, 8-32.
- Peters, R.T., Liao, S.M., Maniatis, T., 2000. IKKepsilon is part of a novel PMA-inducible IkappaB kinase complex. *Molecular cell* 5, 513-522.
- Peters, R.T., Maniatis, T., 2001. A new family of IKK-related kinases may function as I kappa B kinase kinases. *Biochimica et biophysica acta* 1471, M57-62.
- Pichlmair, A., Reis e Sousa, C., 2007. Innate Recognition of Viruses. *Immunity* 27, 370-383.
- Pichlmair, A., Schulz, O., Tan, C.P., Naslund, T.I., Liljestrom, P., Weber, F., Reis e Sousa, C., 2006. RIG-I-mediated antiviral responses to single-stranded RNA bearing 5'-phosphates. *Science* 314, 997-1001.
- Pines, J., 1994. Protein kinases and cell cycle control. *Seminars in cell biology* 5, 399-408.
- Platanias, L.C., 2005. Mechanisms of type-I- and type-II-interferon-mediated signalling. *Nature reviews. Immunology* 5, 375-386.
- Pomerantz, J.L., Baltimore, D., 1999. NF-kappaB activation by a signaling complex containing TRAF2, TANK and TBK1, a novel IKK-related kinase. *The EMBO journal* 18, 6694-6704.
- Purcell, M.K., Smith, K.D., Hood, L., Winton, J.R., Roach, J.C., 2006. Conservation of Toll-Like Receptor Signaling Pathways in Teleost Fish. *Comparative biochemistry and physiology. Part D, Genomics & proteomics* 1, 77-88.
- Qureshi, N., Vogel, S.N., Van Way, C., 3rd, Papasian, C.J., Qureshi, A.A., Morrison, D.C., 2005. The proteasome: a central regulator of inflammation and macrophage function. *Immunologic research* 31, 243-260.
- Rathinam, V.A., Fitzgerald, K.A., 2011. Cytosolic surveillance and antiviral immunity. *Current opinion in virology* 1, 455-462.
- Rebl, A., Goldammer, T., Seyfert, H.-M., 2010a. Toll-like receptor signaling in bony fish. *Veterinary immunology and immunopathology* 134, 139-150.
- Rebl, A., Goldammer, T., Seyfert, H.M., 2010b. Toll-like receptor signaling in bony fish. *Veterinary immunology and immunopathology* 134, 139-150.

Ren, W., Zhu, L.H., Xu, H.G., Jin, R., Zhou, G.P., 2012. Characterization of a spliced variant of human IRF-3 promoter and its regulation by the transcription factor Sp1. *Molecular biology reports* 39, 6987-6993.

Richardson, M.P., Tay, B.H., Goh, B.Y., Venkatesh, B., Brenner, S., 2001. Molecular cloning and genomic structure of a gene encoding interferon regulatory factor in the pufferfish (*Fugu rubripes*). *Mar Biotechnol (NY)* 3, 145-151.

Rimstad, E., 2011. Examples of emerging virus diseases in salmonid aquaculture. *Aquaculture Research* 42, 86-89.

Rise, M.L., Hall, J., Rise, M., Hori, T., Kurt Gamperl, A., Kimball, J., Hubert, S., Bowman, S., Johnson, S.C., 2008. Functional genomic analysis of the response of Atlantic cod (*Gadus morhua*) spleen to the viral mimic polyriboinosinic polyribocytidylic acid (pIC). *Developmental & Comparative Immunology* 32, 916-931.

Robertsen, B., 2006. The interferon system of teleost fish. *Fish & shellfish immunology* 20, 172-191.

Rosenstiel, P., Till, A., Schreiber, S., 2007. NOD-like receptors and human diseases. *Microbes and infection / Institut Pasteur* 9, 648-657.

Rothenburg, S., Deigendesch, N., Dittmar, K., Koch-Nolte, F., Haag, F., Lowenhaupt, K., Rich, A., 2005. A PKR-like eukaryotic initiation factor 2alpha kinase from zebrafish contains Z-DNA binding domains instead of dsRNA binding domains. *Proceedings of the National Academy of Sciences of the United States of America* 102, 1602-1607.

Rothenfusser, S., Goutagny, N., DiPerna, G., Gong, M., Monks, B.G., Schoenemeyer, A., Yamamoto, M., Akira, S., Fitzgerald, K.A., 2005. The RNA helicase Lgp2 inhibits TLR-independent sensing of viral replication by retinoic acid-inducible gene-I. *Journal of immunology* 175, 5260-5268.

Saha, S.K., Pietras, E.M., He, J.Q., Kang, J.R., Liu, S.Y., Oganessian, G., Shahangian, A., Zarnegar, B., Shiba, T.L., Wang, Y., Cheng, G., 2006. Regulation of antiviral responses by a direct and specific interaction between TRAF3 and Cardif. *The EMBO journal* 25, 3257-3263.

Sasai, M., Tatematsu, M., Oshiumi, H., Funami, K., Matsumoto, M., Hatakeyama, S., Seya, T., 2010. Direct binding of TRAF2 and TRAF6 to TICAM-1/TRIF adaptor participates in activation of the Toll-like receptor 3/4 pathway. *Molecular immunology* 47, 1283-1291.

Sato, M., Suemori, H., Hata, N., Asagiri, M., Ogasawara, K., Nakao, K., Nakaya, T., Katsuki, M., Noguchi, S., Tanaka, N., Taniguchi, T., 2000. Distinct and essential roles of transcription factors IRF-3 and IRF-7 in response to viruses for IFN-alpha/beta gene induction. *Immunity* 13, 539-548.

Satoh, T., Kato, H., Kumagai, Y., Yoneyama, M., Sato, S., Matsushita, K., Tsujimura, T., Fujita, T., Akira, S., Takeuchi, O., 2010. LGP2 is a positive regulator of RIG-I- and MDA5-mediated antiviral responses. *Proceedings of the National Academy of Sciences of the United States of America* 107, 1512-1517.

Schmidt, A., Rothenfusser, S., Hopfner, K.P., 2012. Sensing of viral nucleic acids by RIG-I: from translocation to translation. *European journal of cell biology* 91, 78-85.

Schultz, U., Kaspers, B., Staeheli, P., 2004. The interferon system of non-mammalian vertebrates. *Developmental & Comparative Immunology* 28, 499-508.

Seki, S., Nakashima, H., Kinoshita, M., 2012. The Liver as a Pivotal Innate Immune Organ. *Immuno-Gastroenterology* 1, 76-89.

Sen, G.C., 2000. Novel functions of interferon-induced proteins. *Semin Cancer Biol* 10, 93-101.

Seppola, M., Johnsen, H., Mennen, S., Myrnes, B., Tveiten, H., 2009. Maternal transfer and transcriptional onset of immune genes during ontogenesis in Atlantic cod. *Developmental and comparative immunology* 33, 1205-1211.

Seth, R.B., Sun, L., Ea, C.-K., Chen, Z.J., 2005a. Identification and Characterization of MAVS, a Mitochondrial Antiviral Signaling Protein that Activates NF- κ B and IRF3. *Cell* 122, 669-682.

Seth, R.B., Sun, L., Ea, C.K., Chen, Z.J., 2005b. Identification and characterization of MAVS, a mitochondrial antiviral signaling protein that activates NF-kappaB and IRF 3. *Cell* 122, 669-682.

Sharma, S., tenOever, B.R., Grandvaux, N., Zhou, G.P., Lin, R., Hiscott, J., 2003. Triggering the interferon antiviral response through an IKK-related pathway. *Science* 300, 1148-1151.

Shimada, T., Kawai, T., Takeda, K., Matsumoto, M., Inoue, J., Tatsumi, Y., Kanamaru, A., Akira, S., 1999. IKK-i, a novel lipopolysaccharide-inducible kinase that is related to IkappaB kinases. *International immunology* 11, 1357-1362.

Simora, R.M., Ohtani, M., Hikima, J., Kondo, H., Hirono, I., Jung, T.S., Aoki, T., 2010. Molecular cloning and antiviral activity of IFN-beta promoter stimulator-1 (IPS-1) gene in Japanese flounder, *Paralichthys olivaceus*. *Fish & shellfish immunology* 29, 979-986.

Siren, J., Imaizumi, T., Sarkar, D., Pietila, T., Noah, D.L., Lin, R., Hiscott, J., Krug, R.M., Fisher, P.B., Julkunen, I., Matikainen, S., 2006. Retinoic acid inducible gene-I and mda-5 are involved in influenza A virus-induced expression of antiviral cytokines. *Microbes and infection / Institut Pasteur* 8, 2013-2020.

Solis, M., Romieu-Mourez, R., Goubau, D., Grandvaux, N., Mesplede, T., Julkunen, I., Nardin, A., Salcedo, M., Hiscott, J., 2007. Involvement of TBK1 and IKKepsilon in lipopolysaccharide-induced activation of the interferon response in primary human macrophages. *European journal of immunology* 37, 528-539.

Stark, G.R., Kerr, I.M., Williams, B.R., Silverman, R.H., Schreiber, R.D., 1998. How cells respond to interferons. *Annual review of biochemistry* 67, 227-264.

Stewart C. Johnson, J.W.T., Sandra Bravo, Kazuya Nagasawa, and Zbigniew, Kabata, 2004. A Review of the Impact of Parasitic Copepods on Marine Aquaculture. *Zoological Studies* 43, 229-243.

Su, J., Huang, T., Dong, J., Heng, J., Zhang, R., Peng, L., 2010. Molecular cloning and immune responsive expression of MDA5 gene, a pivotal member of the RLR gene family from grass carp *Ctenopharyngodon idella*. *Fish & shellfish immunology* 28, 712-718.

Su, J., Huang, T., Yang, C., Zhang, R., 2011. Molecular cloning, characterization and expression analysis of interferon-beta promoter stimulator 1 (IPS-1) gene from grass carp *Ctenopharyngodon idella*. *Fish & shellfish immunology* 30, 317-323.

Su, Z.Z., Sarkar, D., Emdad, L., Barral, P.M., Fisher, P.B., 2007. Central role of interferon regulatory factor-1 (IRF-1) in controlling retinoic acid inducible gene-I (RIG-I) expression. *Journal of cellular physiology* 213, 502-510.

Sun, F., Zhang, Y.B., Liu, T.K., Gan, L., Yu, F.F., Liu, Y., Gui, J.F., 2010. Characterization of fish IRF3 as an IFN-inducible protein reveals evolving regulation of IFN response in vertebrates. *Journal of immunology* 185, 7573-7582.

Sun, Q., Sun, L., Liu, H.H., Chen, X., Seth, R.B., Forman, J., Chen, Z.J., 2006. The specific and essential role of MAVS in antiviral innate immune responses. *Immunity* 24, 633-642.

Suzuki, Y., Yasuike, M., Kondo, H., Aoki, T., Hirono, I., 2011. Molecular cloning and expression analysis of interferon regulatory factor 10 (IRF10) in Japanese flounder, *Paralichthys olivaceus*. *Fish & shellfish immunology* 30, 67-76.

Takahasi, K., Kumeta, H., Tsuduki, N., Narita, R., Shigemoto, T., Hirai, R., Yoneyama, M., Horiuchi, M., Ogura, K., Fujita, T., Inagaki, F., 2009a. Solution structures of cytosolic RNA sensor MDA5 and LGP2 C-terminal domains: identification of the RNA recognition loop in RIG-I-like receptors. *The Journal of biological chemistry* 284, 17465-17474.

Takahasi, K., Kumeta, H., Tsuduki, N., Narita, R., Shigemoto, T., Hirai, R., Yoneyama, M., Horiuchi, M., Ogura, K., Fujita, T., Inagaki, F., 2009b. Solution Structures of Cytosolic RNA Sensor MDA5 and LGP2 C-terminal Domains: IDENTIFICATION OF THE RNA

RECOGNITION LOOP IN RIG-I-LIKE RECEPTORS. *Journal of Biological Chemistry* 284, 17465-17474.

Takaoka, A., Yanai, H., 2006. Interferon signalling network in innate defence. *Cellular microbiology* 8, 907-922.

Takashi Aoki, T.T., Mudjekeewis D. Santos, H.K., Hirono, a.I., 2008. Molecular Innate Immunity in Teleost Fish: Review and Future Perspectives. *Fisheries for Global Welfare and Environment, 5th World Fisheries Congress*, 263-276.

Takeuchi, O., Akira, S., 2008. MDA5/RIG-I and virus recognition. *Current opinion in immunology* 20, 17-22.

Takeuchi, O., Akira, S., 2009. Innate immunity to virus infection. *Immunological reviews* 227, 75-86.

Tamura, K., Peterson, D., Peterson, N., Stecher, G., Nei, M., Kumar, S., 2011. MEGA5: molecular evolutionary genetics analysis using maximum likelihood, evolutionary distance, and maximum parsimony methods. *Molecular biology and evolution* 28, 2731-2739.

Tang, E.D., Wang, C.Y., 2009. MAVS self-association mediates antiviral innate immune signaling. *Journal of virology* 83, 3420-3428.

Thompson, A.J., Locarnini, S.A., 2007. Toll-like receptors, RIG-I-like RNA helicases and the antiviral innate immune response. *Immunology and cell biology* 85, 435-445.

Thompson, J.D., Higgins, D.G., Gibson, T.J., 1994. CLUSTAL W: improving the sensitivity of progressive multiple sequence alignment through sequence weighting, position-specific gap penalties and weight matrix choice. *Nucleic acids research* 22, 4673-4680.

Tojima, Y., Fujimoto, A., Delhase, M., Chen, Y., Hatakeyama, S., Nakayama, K.-i., Kaneko, Y., Nimura, Y., Motoyama, N., Ikeda, K., Karin, M., Nakanishi, M., 2000. NAK is an I[κ]B kinase-activating kinase. *Nature* 404, 778-782.

Toranzo, A.E., Magariños, B., Romalde, J.L., 2005. A review of the main bacterial fish diseases in mariculture systems. *Aquaculture* 246, 37-61.

Venkataraman, T., Valdes, M., Elsby, R., Kakuta, S., Caceres, G., Saijo, S., Iwakura, Y., Barber, G.N., 2007. Loss of DExD/H box RNA helicase LGP2 manifests disparate antiviral responses. *Journal of immunology* 178, 6444-6455.

Verrier, E.R., Langevin, C., Benmansour, A., Boudinot, P., 2011. Early antiviral response and virus-induced genes in fish. *Developmental and comparative immunology* 35, 1204-1214.

Vitour, D., Meurs, E.F., 2007. Regulation of interferon production by RIG-I and LGP2: a lesson in self-control. *Science's STKE : signal transduction knowledge environment* 2007, pe20.

- Walker, P.J., Winton, J.R., 2010. Emerging viral diseases of fish and shrimp. *Veterinary research* 41, 51.
- Wan, Q., Wicramaarachchi, W.D., Whang, I., Lim, B.S., Oh, M.J., Jung, S.J., Kim, H.C., Yeo, S.Y., Lee, J., 2012. Molecular cloning and functional characterization of two duplicated two-cysteine containing type I interferon genes in rock bream *Oplegnathus fasciatus*. *Fish & shellfish immunology* 33, 886-898.
- Wan, X., Chen, X., 2008. Molecular characterization and expression analysis of interferon-inducible protein 56 gene in large yellow croaker *Pseudosciaena crocea*. *Journal of Experimental Marine Biology and Ecology* 364, 91-98.
- Wang, L., Su, J., Yang, C., Wan, Q., Peng, L., 2012. Genomic organization, promoter activity of grass carp MDA5 and the association of its polymorphisms with susceptibility/resistance to grass carp reovirus. *Molecular immunology* 50, 236-243.
- Weissmann, C., Weber, H., 1986. The Interferon Genes, in: Waldo, E.C., Klivle, M. (Eds.), *Progress in Nucleic Acid Research and Molecular Biology*. Academic Press, pp. 251-300.
- Wheelan, S.J., Church, D.M., Ostell, J.M., 2001. Spidey: a tool for mRNA-to-genomic alignments. *Genome research* 11, 1952-1957.
- Xiang, Z., Qi, L., Chen, W., Dong, C., Liu, Z., Liu, D., Huang, M., Li, W., Yang, G., Weng, S., He, J., 2011. Characterization of a TnMAVS protein from *Tetraodon nigroviridis*. *Developmental and comparative immunology* 35, 1103-1115.
- Xie, X.H., Zang, N., Li, S.M., Wang, L.J., Deng, Y., He, Y., Yang, X.Q., Liu, E.M., 2012. Resveratrol Inhibits respiratory syncytial virus-induced IL-6 production, decreases viral replication, and downregulates TRIF expression in airway epithelial cells. *Inflammation* 35, 1392-1401.
- Xu, H.G., Ren, W., Lu, C., Zhou, G.P., 2010. Characterization of the human IRF-3 promoter and its regulation by the transcription factor E2F1. *Molecular biology reports* 37, 3073-3080.
- Xu, L.G., Wang, Y.Y., Han, K.J., Li, L.Y., Zhai, Z., Shu, H.B., 2005. VISA is an adapter protein required for virus-triggered IFN-beta signaling. *Molecular cell* 19, 727-740.
- Yan, N., Chen, Z.J., 2012. Intrinsic antiviral immunity. *Nat Immunol* 13, 214-222.
- Yao, C.-L., Huang, X.-N., Fan, Z., Kong, P., Wang, Z.-Y., 2012. Cloning and expression analysis of interferon regulatory factor (IRF) 3 and 7 in large yellow croaker, *Larimichthys crocea*. *Fish & shellfish immunology* 32, 869-878.
- Yasuike, M., Kondo, H., Hirono, I., Aoki, T., 2011. Identification and characterization of Japanese flounder, *Paralichthys olivaceus* interferon-stimulated gene 15 (Jf-ISG15). *Comparative immunology, microbiology and infectious diseases* 34, 83-91.

- Yokota, S., Okabayashi, T., Fujii, N., 2010. The battle between virus and host: modulation of Toll-like receptor signaling pathways by virus infection. *Mediators of inflammation* 2010, 184328.
- Yoneyama, M., Fujita, T., 2007a. Function of RIG-I-like receptors in antiviral innate immunity. *The Journal of biological chemistry* 282, 15315-15318.
- Yoneyama, M., Fujita, T., 2007b. Function of RIG-I-like Receptors in Antiviral Innate Immunity. *Journal of Biological Chemistry* 282, 15315-15318.
- Yoneyama, M., Fujita, T., 2010. Recognition of viral nucleic acids in innate immunity. *Reviews in medical virology* 20, 4-22.
- Yoneyama, M., Kikuchi, M., Matsumoto, K., Imaizumi, T., Miyagishi, M., Taira, K., Foy, E., Loo, Y.M., Gale, M., Jr., Akira, S., Yonehara, S., Kato, A., Fujita, T., 2005. Shared and unique functions of the DExD/H-box helicases RIG-I, MDA5, and LGP2 in antiviral innate immunity. *Journal of immunology* 175, 2851-2858.
- Yoneyama, M., Kikuchi, M., Natsukawa, T., Shinobu, N., Imaizumi, T., Miyagishi, M., Taira, K., Akira, S., Fujita, T., 2004. The RNA helicase RIG-I has an essential function in double-stranded RNA-induced innate antiviral responses. *Nat Immunol* 5, 730-737.
- Yu, T., Shim, J., Yang, Y., Byeon, S.E., Kim, J.H., Rho, H.S., Park, H., Sung, G.H., Kim, T.W., Rhee, M.H., Cho, J.Y., 2012a. 3-(4-(tert-Octyl)phenoxy)propane-1,2-diol suppresses inflammatory responses via inhibition of multiple kinases. *Biochem Pharmacol* 83, 1540-1551.
- Yu, T., Yi, Y.-S., Yang, Y., Oh, J., Jeong, D., Cho, J.Y., 2012b. The Pivotal Role of TBK1 in Inflammatory Responses Mediated by Macrophages. *Mediators of inflammation* 2012, 8.
- Zemirli, N., Arnoult, D., 2012. Mitochondrial anti-viral immunity. *The international journal of biochemistry & cell biology* 44, 1473-1476.
- Zenke, K., Kim, K.H., 2009. Molecular cloning and expression analysis of three Mx isoforms of rock bream, *Oplegnathus fasciatus*. *Fish & shellfish immunology* 26, 599-605.
- Zhang, L., Daly, R.J., 2012. Targeting the Human Kinome for Cancer Therapy: Current Perspectives. *17*, 233-246.
- Zhang, Y., Gui, J., 2004. Molecular characterization and IFN signal pathway analysis of *Carassius auratus* CaSTAT1 identified from the cultured cells in response to virus infection. *Developmental and comparative immunology* 28, 211-227.
- Zhang, Y.B., Gui, J.F., 2012. Molecular regulation of interferon antiviral response in fish. *Developmental and comparative immunology* 38, 193-202.

- Zhang, Y.B., Hu, C.Y., Zhang, J., Huang, G.P., Wei, L.H., Zhang, Q.Y., Gui, J.F., 2003. Molecular cloning and characterization of crucian carp (*Carassius auratus* L.) interferon regulatory factor 7. *Fish & shellfish immunology* 15, 453-466.
- Zhang, Y.B., Wang, Y.L., Gui, J.F., 2007. Identification and characterization of two homologues of interferon-stimulated gene ISG15 in crucian carp. *Fish & shellfish immunology* 23, 52-61.
- Zou, J., Bird, S., Secombes, C., 2010. Antiviral sensing in teleost fish. *Current pharmaceutical design* 16, 4185-4193.
- Zou, J., Chang, M., Nie, P., Secombes, C.J., 2009. Origin and evolution of the RIG-I like RNA helicase gene family. *BMC evolutionary biology* 9, 85.
- Zou, J., Secombes, C.J., 2011. Teleost fish interferons and their role in immunity. *Developmental and comparative immunology* 35, 1376-1387.